Università degli studi di Pavia

Dipartimento di Biologia e Biotecnologie "*L. Spallanzani*"

The global transcriptional regulator CodY controls virulence in Group B *Streptococcus*

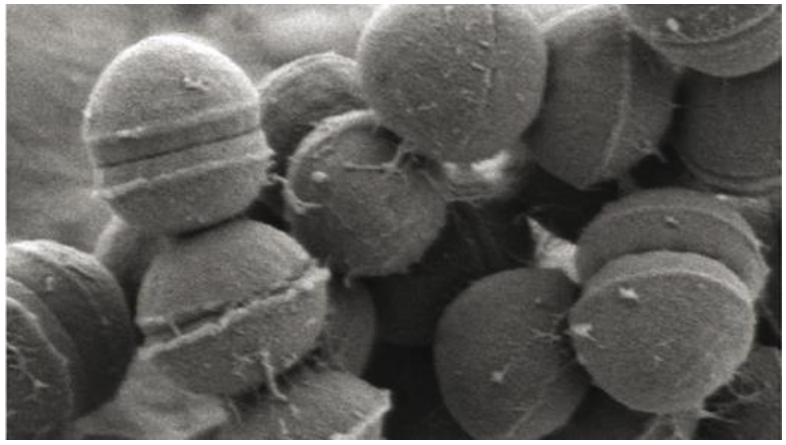

Angelica Pellegrini

Dottorato di Ricerca in
Genetica, Biologia Molecolare e Cellulare
XXXV Ciclo – A.A. 2019-2022

Università degli studi di Pavia

Dipartimento di Biologia e Biotecnologie "*L. Spallanzani*"

The global transcriptional regulator CodY controls virulence in Group B *Streptococcus*

Angelica Pellegrini

Supervised by:

Dr. Giulia Barbieri and Prof. Silvia Buroni

Dottorato di Ricerca in
Genetica, Biologia Molecolare e Cellulare
XXXV Ciclo – A.A. 2019-2022

Cover image: Electron microscopy imaging of Group B *Streptococcus*
(Caliot *et al,* 2012)

Table of Contents

Abstract

CodY is a highly conserved global transcriptional regulator of metabolism in low-G+C Gram-positive bacteria. As its activity is dependent on its interaction with branched-chain amino acids (BCAAs) and GTP (except for *Lactococcus* and *Streptococcus* species), this regulator controls gene expression in response to the nutritional status of the cell. In pathogens, CodY links nutrient availability with the concerted regulation of metabolism and virulence.

In this study, we investigated the role of CodY in *Streptococcus agalactiae*, a harmless colonizer of the intestinal and urogenital tracts of healthy adults that is responsible of severe, invasive infections in neonates and immunocompromised subjects. Adaptation to the different environments encountered during colonization and infection is essential to the success of *S. agalactiae* as a commensal and as an opportunistic pathogen. However, to date, there is still a great lack of information on how this bacterium integrates the diverse environmental signals and orchestrates the different regulatory pathways to rapidly adapt to distinct human host niches and control its switch from commensal to pathogen.

Here, a *codY* deletion derivative (Δ*codY*) of the hypervirulent *S. agalactiae* strain BM110 was prepared. The mutant strain displayed decreased bacterial virulence in different murine models of infection. The reduced lethality observed *in vivo* was related to a decreased ability of the Δ*codY* strain to disseminate in blood and to distant organs of infected mice. *In vitro* investigation of virulence-related characteristics revealed that several traits linked to the ability to colonize the host were affected in the Δ*codY* strain, including its ability to adhere to and invade human epithelial cells, bind to plasma and extracellular matrix proteins and form biofilm.

A transcriptomic analysis showed that CodY controls about 13% of the *S. agalactiae* genome, with genes encoding functions related to amino acid transport and metabolism, adhesion, DNA replication, recombination, and repair being subjected to the highest level of regulation. The regulatory activity of CodY was demonstrated to be dependent on the presence of BCAAs, whose intracellular abundance is influenced by CodY-mediated regulation of genes encoding BCAAs transport systems. The list of genes under CodY control includes *srr2*, encoding a virulence factor known to be negatively regulated by the two-component system CovRS, the master regulator of virulence. We showed that CodY is a direct repressor of *srr2* and provided preliminary results suggesting a potential interplay of CodY and CovR in the regulation of *srr2*.

The obtained results show that CodY is a global regulator of metabolism and virulence in *S. agalactiae*. The activity of this factor appears to be coordinated with the regulatory action of CovRS, highlighting the existence of interlinked regulatory

pathways governing *S. agalactiae* virulence and gene expression. Dissection of the molecular mechanisms governing *S. agalactiae* transition from harmless to potent pathogen could set the basis for the development of new therapeutic strategies.

Abbreviations

EOD	Early onset disease
LOD	Late onset disease
IAP	Intrapartum antibiotic prophylaxis
AMR	Antimicrobial resistance
CPS	Capsular polysaccharide
ST	Sequence type
CC	Clonal complex
BCAA	Branched chain amino acid
ILV	Isoleucine, leucine, valine
CDM	Chemically defined medium
CWA	Cell-wall anchored (protein)
ECM	Extra-cellular matrix
TCS	Two-component system
THY	Todd-Hewitt Yeast extract (medium)
EMSA	Electrophoretic Mobility Shift Assay
ELISA	Enzyme-Linked Immuno-Sorbent Assay
CFU	Colony forming units
TSS	Transcription start site
FAM	6-carboxyfluorescein

1. Introduction

Streptococci (*Streptococcus*, from the Greek words "strepto", a chain and "coccus" a berry) were first described in 1874 by the Austrian surgeon Dr. Theodor Billroth, who reported the presence of small organisms, either isolated or arranged in chains of two to twenty, found in wound infections. Streptococci entered formally to history in 1879, when Louis Pasteur isolated the microorganism from the uterus and blood of women with puerperal fever and demonstrated that *Streptococcus* was the etiological agent of the disease causing the highest mortality rates of women and newborns at that time. The genus *Streptococcus* comprises more than 100 different species, that are commonly classified according to two main criteria: the composition of surface antigens, through which the species are divided into groups A-X; their haemolytic patterns, established by using blood agar plates to differentiate them into alpha, beta and gamma classes (Ferretti and Köhler, 2016).

1.1 *Streptococcus agalactiae*

Streptococcus agalactiae is an encapsulated, Gram-positive, beta-haemolytic, multi-host microorganism (Verani *et al*, 2010). This specie was first described in 1887 as a bacterium infecting the udders of cattle, causing mastitis, a disease that led to a strong decrease in milk production, from where the name "*agalactiae*" came (from the Greek: a-, no; galactos, milk). This species is also defined as Group B *Streptococcus*, or GBS, based on the Lancefield classification, that takes into account a specific peptidoglycan-anchored antigen, the Group B carbohydrate (GBC). *S. agalactiae* commonly colonizes the gastrointestinal and urogenital tracts of healthy adults (Perani *et al*, 2010). As a part of the urogenital microbiota of approximately 10-30% of pregnant women, this opportunistic pathogen can be transmitted to the newborn through *in utero* ascending infections or during labour through aspiration of contaminated amniotic or vaginal fluids (Shabayeck *et al*, 2018). In addition, during the last decades, *S. agalactiae* invasive disease has spread among adults as well (Trollfors *et al*, 2022).

1.1.1 Epidemiology of *S. agalactiae*

S. agalactiae vaginal colonization in pregnant mothers represents the most important risk factor both for the mother, that can experience symptoms ranging from mild urinary tract infections to sepsis, and for the newborn, that can develop severe invasive diseases. Two forms of *S. agalactiae* disease exist in neonates: the early onset disease (EOD), which occurs within 7 days from birth, and the late onset disease (LOD), that develops within three months of life (Dhudasia *et al*, 2021). EOD occurs due to vertical transmission, when newborns are exposed to *S. agalactiae in utero* or

during labour, through aspiration or swallowing of contaminated fluids while passing through the birth canal. EOD is typically associated with manifestations such as bacteremia or pneumonia, while less commonly it manifests with meningitis, bone, joint and soft tissue infections. On the other hand, LOD is generally acquired by horizontal transmission, and it is associated with meningitis as the most typical manifestation of the disease, even though it may present as bacteremia, pneumonia or urinary tract infection as well (Berardi *et al*, 2013). *S. agalactiae* neonatal disease accounts for 392.000 cases, 91.000 deaths and 37.000 cases of children that survive with neurodevelopmental impairment worldwide each year (Gonçalves *et al,* 2022).

Beyond maternal-foetal disease, *S. agalactiae* has emerged as a pathogen causing invasive diseases in non-pregnant adults as well. Adults commonly at risk are elderly, immunocompromised individuals and subjects with underlying medical conditions such as diabetes mellitus, cancer, obesity and cardiovascular disease. The most common manifestations of *S. agalactiae* illness in non-pregnant adults are skin and soft tissue infections, urinary tract infections, pneumonia, sepsis, endocarditis and meningitis (Graux *et al*, 2021).

1.1.2 Antibiotic treatment and evolution of antimicrobial resistance in *S. agalactiae*

As a primary approach for *S. agalactiae* disease prevention in neonates, Centers for Disease Control and Prevention recommend maternal intrapartum antibiotic prophylaxis (IAP) through the administration of intravenous penicillin or ampicillin. In case of allergy to these antibiotics, cefazolin or clindamycin can be administered. Vancomycin intravenous administration remains the only validated alternative to be considered in case of penicillin allergy and no bacterial response to the other treatments (ACOG, 2020).

Administration of IAP has led to a strong decrease of EOD, from an incidence of 1.8 newborns per 1,000 live births in the 1990s to 0.23 newborns per 1,000 live births in 2015 (Nanduri *et al*, 2019). Despite that, LOD incidence has not been influenced by IAP, remaining unaltered with 0.3 cases per 1,000 live births (Creti *et al*, 2021). Although since the implementation of IAP *S. agalactiae* has remained susceptible to penicillins and first-generation cephalosporins, isolates with increasing penicillin minimum inhibitory concentrations (MICs) have recently been reported in Japan, in the US and Canada. This poses a threat to the advances made in disease prevention and treatment (Jones *et al,* 2022).

As a versatile multi-host pathogen, *S. agalactiae* is a cause of infectious diseases also among food-producing animals, including cattles, fishes, and camels. Both evolutionary and epidemiological studies report cases of *S. agalactiae* transmission between humans and animals, in both directions and via multiple routes (Botelho *et al,* 2018). This represents a concerning threat in terms of antimicrobial resistance (AMR). Different hosts are exposed to different antimicrobial agents. Hence, *S. agalactiae* acquirement of AMR in one host might lead to host-species jumping of

lineages and subsequent transmission in another host. The misuse and overuse of antimicrobials contribute to resistance selection and clonal spread of antimicrobial-resistant lineages across species, and to the final horizontal transmission of resistance determinants (Oliveira *et al*, 2022). Human *S. agalactiae* strains presenting additional AMR markers other than low susceptibility to penicillin emerged recently. For example, human *S. agalactiae* strains non-susceptible to lincosamide and macrolide antibiotics have significantly increased in the recent years, with around half of human *S. agalactiae* isolates being resistant to macrolide in the US. Lastly, the emergence of clindamycin and erythromycin resistant *S. agalactiae* strains has markedly increased in the recent years as well (Oliveira *et al*, 2022).

The increasing prevalence of AMR in bacterial pathogens constitutes a global concern since it has an impact on humans, animals and environment. In a multi-host pathogen as *S. agalactiae*, AMR occurrence might be independent among *S. agalactiae* strains from human and animal hosts. AMR may be mostly driven by a combination of horizontal gene transfer and clonal expansion, amongst the major forces driving *S. agalactiae* genome plasticity and evolution (Pinto *et al*, 2014).

1.1.3 A vaccine against *S. agalactiae*

IAP cannot represent the solution to *S. agalactiae* infections for several reasons: screening and IAP in high-income countries have drastically reduced the incidence of EOD, but LOD incidence remains unaltered; in addition, low- and middle- income countries cannot implement IAP as a routine practice; moreover, IAP negatively influences the microbiota of neonates, besides promoting the risk of development of *S. agalactiae* resistant strains (Creti *et al,* 2017).

A suitable vaccine against this pathogen given to pregnant women could drastically decrease *S. agalactiae* caused diseases, preventing 231,000 infant and maternal *S. agalactiae* cases, 41,000 stillbirths and 66,000 child deaths annually. Up to date no approved vaccine exists against *S. agalactiae.* As a matter of fact, the World Health Organization (WHO) has identified the development of a maternal *S. agalactiae* vaccine as a key priority (Seale *et al*, 2019).

The most recent advances to this purpose come from Minervax: the company has recently developed a prototype subunit vaccine GBS-NN that has reached a phase I study, conducted on 240 vaccinated adult healthy women, that displayed good safety and immunogenicity profiles (Pawlowski *et al*, 2022). This candidate vaccine consists of a fusion protein composed of the N-terminal domains of two *S. agalactiae* proteins belonging to the alpha-like protein (Alp) family, AlphaC (aC) and Rib (Fischer *et al,* 2021). Rib and aC have been selected as candidates for the vaccine development since they are the most common variants of Alp proteins among *S. agalactiae* strains. In a more recent investigation, it has been observed that the vaccination with GBS-NN results in IgG and IgA responses against both homotypic and heterotypic Alp-Ns, even though the heterotypic responses rely on a pre-existing immunity. Importantly, the vaccine confers enhanced ability to prevent bacterial

invasion of cervical epithelial cells. Interestingly, the authors noted that IgG of both Alp-N specificities is still detectable in neonatal blood up to 2 months after birth (Pawlowski *et al*, 2022). Further phase II and III studies will be performed to investigate the efficacy of this promising vaccine.

1.1.4 *S. agalactiae* classification

S. agalactiae strains can be clustered according to different classification techniques. One classification approach for *S. agalactiae* isolates relies on capsular polysaccharide (CPS) typing. Ten different serotype variants (i.e., Ia, Ib, II, III, IV, V, VI, VII, VIII, and IX) have been described. CPS typing is the common technique used in routine clinical laboratories to identify circulating *S. agalactiae* isolates. CPS types differ in their disease-causing abilities (Sheppard *et al*, 2016). In particular, CPS types Ia, Ib, II, III, and V are associated with the 96% and 88% of cases of neonatal and adult invasive *S. agalactiae* infections, respectively; the majority of LOD and a conspicuous proportion of EOD are instead associated with CPS type III (Bellais *et al*, 2012).

Although CPS typing has been one of the mainstays in the descriptive epidemiology of *S. agalactiae*, different DNA-based techniques have been developed for a deeper characterization of *S. agalactiae* population diversity. They include pulsed-field electrophoresis (PFGE), microarrays and high-throughput sequencing and multilocus sequence typing (MLST) (Bellais *et al*, 2012). In particular, MLST is a method for *S. agalactiae* classification developed by Jones and colleagues by using seven defined housekeeping genes (*adhP, atr, glcK, glnA, pheS, sdhA,* and *tkt*) (Jones *et al*, 2003). Allelic variations among these genes determine different sequence types (STs). STs can be then clustered into clonal complexes (CCs), that collect members with maximum one allelic difference from other members of the cluster. Figure 1 represents schematically how different serotypes are distributed among STs, in turn grouped in CCs (Furfaro *et al*, 2018). MLST is a technique particularly suitable for epidemiological studies since it provides data easily comparable between laboratories. MLST and capsular serotyping of *S. agalactiae* strains isolated from different countries have shown that human carriage and clinical isolates prevalence varies over time and by geographic locations. Several epidemiological studies conducted by DNA-based techniques have pinpointed that *S. agalactiae* capsular type III strains belonging to the ST17 are strongly associated with neonatal meningitis, for this reason they have been historically designated as “hypervirulent” (Jones *et al* 2003).

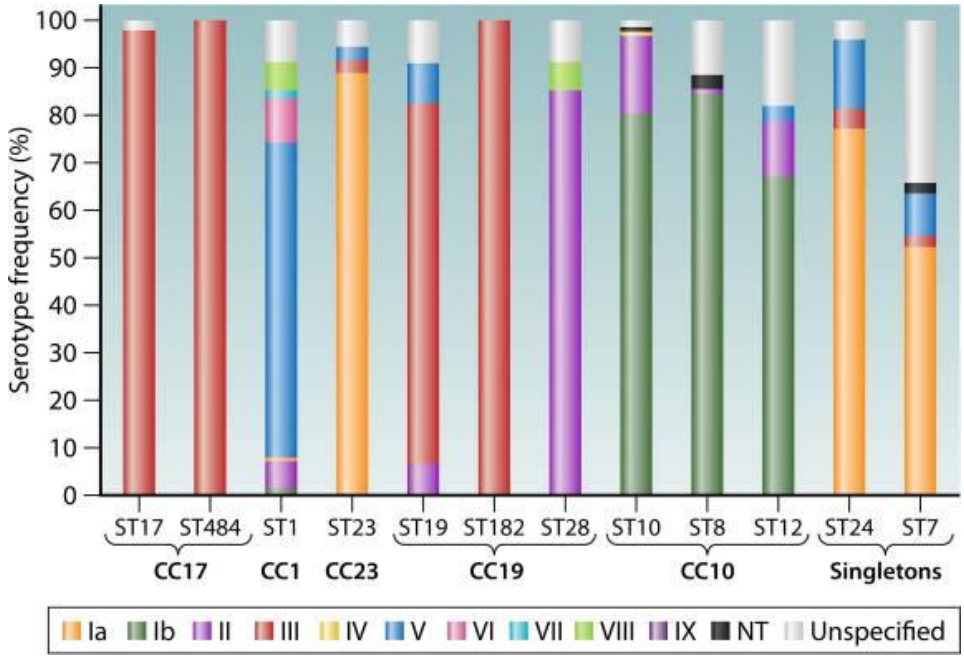

Figure 1. Serotype distribution within each sequence type, according to the public MLST database for *S. agalactiae*, comprising the 12 most represented STs within the database, as well as their corresponding CCs (Furfaro *et al,* 2018).

1.1.5 *S. agalactiae* genome structure

The *S. agalactiae* genome has a median total length of 2.08 Mb and a median GC content of 35.4%. The global gene repertoire of a bacterial species constitutes its pan-genome, that comprises the core genome, or the number of genes present in every strain of that species. The *S. agalactiae* core genome represents only a small fraction of the pan-genome, as this one is vast because new genes are constantly added to the gene pool of the species any time a new strain is sequenced. The essence of the species is strongly linked to the core genome, that comprises genes involved in housekeeping functions, cell envelope, regulatory functions, transport and binding proteins. On the other hand, the dispensable genome comprises genes mostly associated with mobile and extrachromosomal elements. According to the work of Lannes-Costa *et al* (2020) who performed a comparative genomic analysis of 109 *S. agalactiae* strains, *S. agalactiae* contains one of the smallest core genomes (14%) described in the literature, compared to other pathogenic bacterial species, such as *Pseudomonas syringae* with 64% of core genome, *Streptococcus pneumoniae* (74%) and *Listeria monocytogenes* (80%), suggesting a high genetic variability of *S. agalactiae* (Lannes-Costa *et al*, 2020).

Pathogenicity Islands (PAIs) are genetic elements present in the chromosomes of a large number of bacterial pathogens. PAIs contain several virulence genes grouped in blocks, normally absent in non-pathogenic strains of the same or closely related species, that play important roles in the bacterial pathogenicity. From the work of Lannes-Costa, the presence of 10 PAIs, corresponding to the 15% of the genome, was predicted in *S. agalactiae*. Interestingly, two PAIs (SagPAI_2 and 5) in ST-17 strains were highly conserved among the capsular type III strains analysed, and their presence seemed to be related to the presence of an integrase. Both the two PAIs presented ABC transporters genes essential for cell viability, virulence, nutrition, acquisition and for the export of other substances, including capsular polysaccharides and hemolysin (He *et al*., 2017). The mobile genetic elements and the genes they carry play an important role in the hypervirulence and plasticity of ST-17 lineage.

1.1.6 *S. agalactiae* metabolism

During invasive infections, *S. agalactiae* colonizes several sites in the host with varying oxygen abundance, ranging from atmospheric oxygen levels to near anaerobiosis (Johri *et al*, 2003). Moreover, reactive oxygen species (ROS) are generated by macrophages or neutrophils as part of the host defence mechanisms, thus, the ability of the bacterium to survive in the host might be strongly influenced by the bacterial ability to adapt to or eliminate oxygen, and to deal with ROS (Yamamoto *et al*, 2006). *S. agalactiae* is a facultative anaerobe bacterium. Under anaerobic growth conditions, *S. agalactiae* must grow strictly by fermentation. When the bacterium is in growth conditions of rapid sugar metabolism and constant NADH production, NAD is regenerated by converting pyruvate to lactate via lactate dehydrogenase (homolactic fermentation). Despite its capacity for fermentative metabolism, *S. agalactiae* can perform aerobic respiration upon addiction of external sources of heme and quinone in presence of oxygen (Yamamoto *et al*, 2006). Bacteria usually have a branched respiratory chain with multiple dehydrogenases and terminal oxygen reductases. According to the work of Lencina *et al* (2018), *S. agalactiae* utilizes only one type 2 NADH dehydrogenase (NDH-2) and one cytochrome bd quinol oxidase as a terminal oxydoreductase to perform respiration (Lencina *et al*, 2018). NADH-dependent respiration is fundamental for the pathogen to maintain NADH/NAD redox balance in the cell, optimize ATP production, and oxygen toleration (Lencina *et al*, 2018). Importantly, respiration metabolism confers *S. agalactiae* the ability to eliminate oxygen from its environment. This process could facilitate *S. agalactiae* dissemination and virulence by promoting bacterial survival in blood (Yamamoto *et al*, 2006).

Bacteria sense a wide range of physical and chemical signals in the environment and use this information to adapt and promote their growth and survival. Among others, amino acids are important factors for host-pathogen interactions (Ren *et al*, 2018). *S. agalactiae* is known to require a great number of amino acids for its growth. Analyses of the genome sequence reveal that in *S. agalactiae*, as in *Streptococcus pyogenes* and in *S. pneumoniae,* the tricarboxylic acid (TCA) cycle is completely missing, thus the bacterium is unable to synthesize the precursors of most amino

acids. The only biosynthetic pathways present are the ones for alanine, serine, glycine, glutamine, aspartate, asparagine and threonine. Most importantly, *S. agalactiae* lacks the genes for the *de novo* synthesis of the branched-chain-amino acids (BCAA). BCAAs (isoleucine, leucine and valine) are small nonpolar amino acids, endowed with branched alkyl side chains that confer hydrophobicity. BCAAs are a quantitatively important group of amino acids in bacterial proteins. Moreover, they are fundamental for the synthesis of branched-chain fatty acids (BCFA), the predominant fatty acids in the membranes of Gram-positive bacteria (Kaiser and Heinrichs, 2018). Being auxotrophic for most amino acids, *S. agalactiae* imports them from exogenous sources thanks to different ABC transporters and permeases. In addition, *S. agalactiae* possesses peptidases that, through peptides degradation, provide another precious source of amino acids.

1.1.7 *S. agalactiae* colonization of mucosal surfaces and translocation through host cellular barriers

S. agalactiae expresses an armamentarium of virulence factors fundamental for bacterial participation to several pathogenic processes, such as colonization of host surfaces and translocation through host cellular barriers, bacterial evasion of the immune system and activation of inflammatory response, and biofilm formation (Spellerberg, 2000).

Bacterial adhesion to host-cell surfaces constitutes the first crucial step for *S. agalactiae* mucosal colonization and invasion of the host. *S. agalactiae* adhesion and invasion of a great number of host cells has been reported, including vaginal epithelial cells, lung epithelial and endothelial cells and blood brain barrier cells (BBB, a single layer of micro-vascular endothelial cells) (Rajagopal, 2009). As indicated in Figure 2, *S. agalactiae* intracellular uptake involves activation of cytoskeletal rearrangements in the host cell. Pathogens at the cell surface manipulate the Rho family GTPases, small signalling molecules present in the eukaryotic cytosol, to trigger downstream cytoskeletal rearrangement (Dumenil and Nassif, 2005). *S. agalactiae*-host initial interactions involve bacterial binding to proteins of the extracellular matrix (ECM) and serum proteins, such as fibrinogen, plasminogen, vitronectin, fibronectin, laminin, with subsequent interactions with host-cell surface integrins and facilitated entry into the host cell (Maisey *et al*, 2008, a).

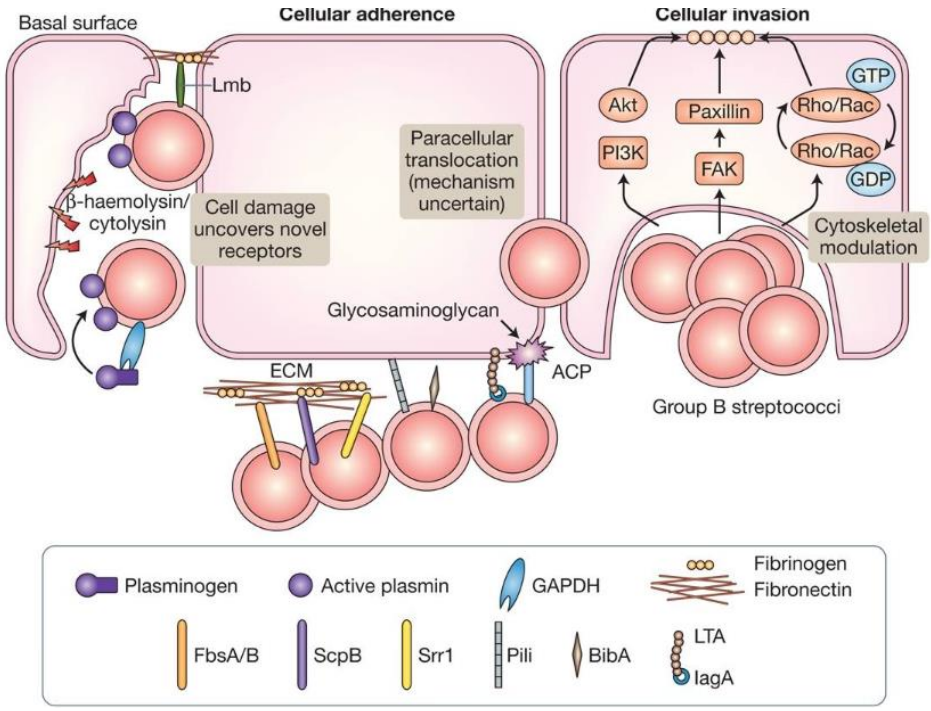

Figure 2. Mechanisms of *S. agalactiae* cellular adhesion and invasion (Maisey *et al*, 2008, a).

Surface-associated protein families are the principal factors that mediate *S. agalactiae* adherence to ECM and host cell surfaces (Pietrocola *et al*, 2018). As a general structure, the cell-wall anchored (CWA) proteins comprise different domains. The N-terminal signal sequence directs the protein translocation to the cytoplasmic membrane, where it will be removed at the moment of the secretion. The C-terminus displays the sorting signal that comprises a conserved sorting motif (LPXTG, Leu-Pro-Thr-Gly). Moreover, CWA proteins contain a hydrophobic transmembrane segment and a positively charged cytosolic terminal tail. The central moiety of CWA proteins comprises domains directly involved in several functional activities, such as binding of ECM-proteins. Comparative genomic analyses of *S. agalactiae* genome from different strains predict the presence of up to 35 distinct CWA protein encoding genes (Tettelin *et al*, 2002). Nevertheless, there is variability of CWA proteins from strain to strain and depending on bacterial growth phase or conditions as well.

1.1.7.1 Fibrinogen-binding adhesins

Fibrinogen is a soluble plasma glycoprotein and a component of the ECM, composed of two sets of disulfide-bridged Aα-, Bβ-, and γ-chains (Figure 3) (Pietrocola *et al*, 2018). *S. agalactiae* displays several CWA proteins involved in fibrinogen binding:

the fibrinogen-binding surface (Fbs) proteins FbsA, FbsB and FbsC, and the serine-rich repeat (Srr) proteins Srr1 and Srr2.

1.1.7.1.1 Fbs proteins

Through fibrinogen binding, FbsA plays a crucial role in promoting bacterial adhesion to both epithelial and human brain microvascular endothelial cells (hBMEC) (Schubert *et al*, 2004, Tenenbaum *et al*, 2005). Nonetheless, Pietrocola *et al* (2005) observed that FbsA binding to fibrinogen promotes a fibrinogen-dependent aggregation of platelets, therewith this interaction could play a role in *S. agalactiae*-triggered cardiovascular diseases such as endocarditis (Pietrocola *et al*, 2005).

FbsB is an excreted protein involved in bacterial invasion of epithelial cells, promoting bacterial dissemination in the host (Gutekunst *et al*, 2004).

FbsC is the protein most recently identified as involved in fibrinogen binding, preferentially interacting with the Bβ chain of fibrinogen. This protein contributes to *S. agalactiae* adhesion and invasion of epithelial cells as well (Buscetta *et al*, 2014).

1.1.7.1.2 Srr proteins

Concerning the Srr proteins, the binding of Srr1 to fibrinogen has been deeply investigated and it occurs through direct binding of Srr1 to the Aa chain of fibrinogen. This interaction confers *S. agalactiae* the ability to bind to several types of human epithelial cell lines and to endothelial hBMEC as well (Seo *et al*, 2012).

Expressed only by ST-17 strains, Srr2 is mutually exclusive with the Srr1 adhesin expressed by non ST-17 strains. As for Srr1, Srr2 binds to the Aα chain of fibrinogen but compared to Srr1, Srr2 has a greater binding affinity to fibrinogen. Increased fibrinogen binding by Srr2 could confer a competitive advantage to ST-17 strains in the vaginal niche and promote at the same time binding to epithelial and endothelial cells in invasive niches. Srr2 enhances the bacterial capacity to cross the intestinal barrier in the neonatal gastrointestinal tract (Seo *et al*, 2013). Additionally, in a recent investigation, Srr2 role in mediating *S. agalactiae* invasion of BBB has been better elucidated. The adhesin harbours two distinct binding motifs that are exploited to interact with the $\alpha_v\beta_3$ integrin. Moreover, Srr2 displays other two motifs required for direct binding to the $\alpha_5\beta_1$ integrin. Interestingly, $\alpha_5\beta_1$ and $\alpha_v\beta_3$ integrins are host receptors for fibrinogen on endothelial cells, and they are overexpressed during the postnatal period in brain vessels. Integrin recognition is important for the bacterium from a pathophysiological point of view, as it promotes bacterial internalization into the host cell. It has been demonstrated that Srr2-integrins interaction is essential for *S. agalactiae* to adhere to and invade brain endothelial cells and contributes to meningitis development *in vivo*. Up to date it is still not clear how Srr2 recognition and binding to integrins enables bacterial entry into the brain (Deshayes de Cambronne *et al*, 2021).

The redundancy of different adhesins involved in the binding of the same ligand may allow *S. agalactiae* to bind to different sites of a molecule, thereby promoting stronger interactions (Brochet *et al*, 2008). Nonetheless, protein redundancy could help the bacterium to maintain its fitness in case of loss of function mutations that might affect a specific adhesin, whose role could be then compensated by the activity of another protein (Pietrocola *et al*, 2018).

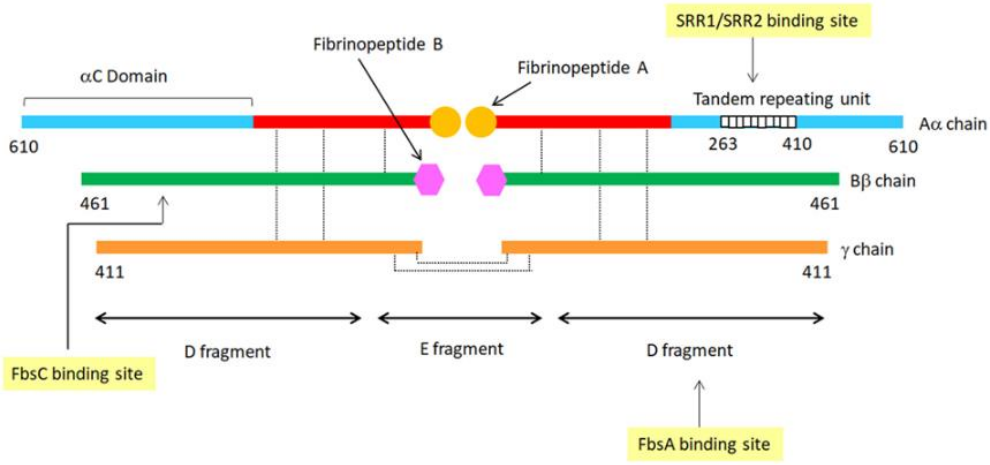

Figure 3. Fibrinogen structure and binding sites on fibrinogen chains for CWA proteins of *S. agalactiae* (Pietrocola *et al*, 2018).

1.1.7.2 Plasminogen-binding adhesins

It has been recently evidenced that Srr2 is a multiligand protein: beside being involved in fibrinogen binding, it binds plasminogen as well. This binding increases *S. agalactiae* surface proteolytic activity, thus favouring the crossing of the BBB and subsequent contribution to the establishment of meningitis (Six *et al*, 2015, Magalhães *et al*, 2013). As for fibrinogen binding, *S. agalactiae* binding to plasminogen is mediated by different CWA proteins.

In addition to Srr2, the plasminogen-binding surface protein P (PbsP) binds plasminogen, promoting bacterial invasion of brain endothelial cells *in vitro* and of the central nervous system *in vivo* (Buscetta *et al*, 2016). PbsP is expressed in mostly all *S. agalactiae* strains and its interaction with plasminogen leads to plasminogen activation to plasmin, allowing *S. agalactiae* migration through endothelial barriers (Magalhães *et al*, 2013). PbsP is a multiligand protein as it is also able to interact with the multifunctional glycoprotein vitronectin, present both as a component of the ECM and as a plasma protein. Binding of PbsP to vitronectin constitutes a molecular bridge for the bacterium to interact with the ECM integrins and promote bacterial invasion of the host epithelial mucosal cells (De Gaetano *et al*, 2018).

1.1.7.3 Fibronectin-binding adhesins

Fibronectin is a large dimeric glycoprotein present both in plasma and on the surface of the ECM (Pietrocola *et al*, 2018). As for other ECM components, fibronectin is targeted by bacteria to adhere to and invade host cells. It has been reported that *S. agalactiae* does not bind to soluble fibronectin, but only to adsorbed fibronectin (Hull *et al*, 2007). Since soluble fibronectin acts as an opsonin in the body, this behaviour could be explained as a trick to evade the host immune system. *S. agalactiae* interaction with fibronectin is mediated by the streptococcal fibronectin binding protein A (SfbA). This interaction is relevant for bacterial invasion of the BBB. Indeed, infection with *S. agalactiae* mutant strains lacking *sfbA* results in reduced bacterial penetration of the BBB and subsequent reduced meningeal inflammation in mice, suggesting a crucial role of SfbA in the development of meningitis *in vivo* (Mu *et al*, 2014).

1.1.7.4 Laminin-binding proteins

Laminins are a family of glycoproteins present on the surface of the ECM of the host. Almost all human-colonizing *S. agalactiae* strains express a CWA lipoprotein involved in binding to laminin: the laminin-binding protein (Lmb). Lmb-laminin interaction plays a role in promoting bacterial colonization of the host. It has been shown that the Lmb protein promotes invasion of human brain microvascular endothelial cells (Tenenbaum *et al*, 2017).

1.1.7.5 Pili

Pili are long, filamentous, multimeric macromolecules found on the surface of bacteria. The pilus is composed of three structural subunits: PilA is the pilus associated adhesin located along the pilus backbone, PilB is the major component of the pilus, and PilC is an accessory protein mainly localized at the base of the pilus (Dramsi *et al*, 2006). There are three distinct pilus islands (PIs), PI-1, PI-2a, and PI-2b, that encode structurally different pili in *S. agalactiae* (Rosini *et al*, 2006). Several studies have reported the importance of the pilus in promoting *S. agalactiae* colonization and pathogenesis. Besides being involved in *S. agalactiae* adhesion to human pulmonary epithelial cells (Krishnan *et al*, 2007), the pilus plays a role in bacterial adhesion to and invasion of brain endothelial cells. In particular, the PilA component promotes initial adhesion of the bacterium to the brain endothelium, while the PilB subunit does not seem to be involved in bacterial adhesion, but it confers invasive abilities to the bacterium (Maisey *et al*, 2007). Lastly, an alternative route of bacterial infection described for *S. agalactiae* consists in bacterial traversing of epithelial monolayer through association with intercellular junctions, without the disruption of the epithelium. To this regard, according to the work of Pezzicoli (2008), the pilus backbone appears to be involved in the bacterial ability to transcytose through different human epithelial cell lines, such as cervical, lung and colon carcinoma cells (Pezzicoli *et al*, 2008).

1.1.7.6 HvgA protein

The hypervirulent GBS adhesin (HvgA) is a surface anchored protein, expressed only in ST17 isolates (Pietrocola *et al*, 2018), that represents an allelic variant of the BibA protein present in non-CC17 strains. Described as a major determinant of *S. agalactiae* hypervirulence in neonates, HvgA promotes *S. agalactiae* adhesion to epithelial and endothelial cells of the intestinal and blood brain barriers respectively, which are typical *S. agalactiae* targets during LOD infections. The work of Tazi (2010) shows that HvgA plays a crucial role in mediating *S. agalactiae* invasion of the central nervous system and development of meningitis *in vivo*, as it confers to the bacterium an increased ability to translocate through the BBB (Tazi *et al*, 2010).

1.1.7.7 Alpha-C protein

Alpha-like proteins are a family of proteins present in nearly all *S. agalactiae* isolates. The role of the alpha-C protein (ACP) in bacterial pathogenesis has been investigated. It has been observed that this protein does not affect bacterial binding but promotes bacterial internalization into cervical epithelial cells (Bolduc *et al*, 2002). ACP binds to several cell receptors, such as α1β1-integrin, or heparin and epithelial cell associated glycosaminoglycans. The latter interaction promotes bacterial internalization through Rho GTPase-dependent actin rearrangements, allowing bacterial entrance in the eukaryotic cell cytosol (Baron *et al*, 2004).

1.1.7.8 β-hemolysin/cytolysin

Also known as CylE, the β-hemolysin/cytolysin (β-h/c) is a surface-associated toxin, that plays a role in promoting injury in a wide range of eukaryotic cell types, such as lung epithelial, lung microvascular endothelial and hBMEC cell lines. *S. agalactiae* mutants deficient for β-h/c display reduced virulence in several animal models of infection, including sepsis, pneumonia and arthritis (Rajagopal, 2009). Doran *et al* (2003) have reported that the β-hemolysin plays a role in development of meningitis *in vivo*. Mice infected with mutants lacking β-h/c displayed decreased mortality rates and reduced brain bacterial load compared to mice infected with wild-type *S. agalactiae* strains (Doran *et al*, 2003). β-h/c biosynthesis is associated to the production of an orange pigment, a rhamnopolyene with 12 unsaturated bonds, that acts as a defence mechanism to quench ROS. *S. agalactiae* pigment is a major virulence factor, as it promotes bacterial crossing of the human placenta and invasion of the amniotic cavity, enabling bacterial dissemination in the host and consequent injury of the fetus (Whidbey *et al*, 2013).

1.1.8 *S. agalactiae* evasion of immunological clearance

Once it crosses the initial host barriers to disseminate into deeper tissues or to reach the bloodstream, *S. agalactiae* triggers a complex immunological response in the host that involves phagocytic cells, such as neutrophils and macrophages. Specific antibodies or serum complement factors fundamental for *S. agalactiae* opsonization

are deficient in newborns. As a consequence, the bacterium displays an increased ability to resist to opsonophagocytosis or neutralise the bactericidal activities of neutrophils and macrophages in these hosts (Maisey *et al*, 2008, a). In addition, *S. agalactiae* secretes several virulence factors that interfere with innate immune clearance mechanisms.

One way through which the innate immune system quickly detects microorganisms is the complement system, that consists in a series of enzymatic reactions. *S. agalactiae* interferes with the complement system mostly through the capsular polysaccharide (CPS). The CPS is the main defence factor that protects *S. agalactiae* against opsonophagocytic killing. The terminal sialic acid (Sia) present in this thick component prevents surface deposition of opsonically active complement C3 on the bacterial surface, providing antiphagocytic protection (Marques *et al*, 1992). Moreover, Sia is a component of the surface of vertebrate cells as well, hence, the Sia on the surface of *S. agalactiae* mimics the host cells, avoiding immune detection (Korir *et al*, 2017). Together with the CPS, several surface components of *S. agalactiae* interfere with the complement cascade and prevent bacterial opsonophagocytosis, as reported in Figure 4.

BibA, for example, is an immunogenic adhesin of *S. agalactiae* that binds specifically to the human C4-binding protein, a component of the classic complement pathway. Through this binding, *S. agalactiae* can resist opsonophagocytic killing by neutrophils (Santi *et al*, 2007).

The complement-interfering protein (CIP) is a secreted protein that binds the complement inhibitor factor H to the surface of the microorganism, preventing C3b deposition and subsequent opsonophagocytosis. Moreover, the CIP is able to reduce classical and lectin complement pathway activation through binding of the C4b factor, inhibiting its interaction with the C2 component (Pietrocola *et al*, 2016).

ScpB is a serine-protease, C5a peptidase, that proteolytically cleaves the complement-activated chemoattractant C5a and prevents the recruitment of inflammatory cells (Cheng *et al*, 2002). This protein has also been shown to mediate bacterial binding to immobilized fibronectin (Beckmann *et al*, 2002).

CspA is a cell surface protein able to cleave fibrinogen, leading to fibrinogen polymerization, subsequent aggregation of *S. agalactiae* and coating of the bacterial surface with fibrin. Bacterial coating with fibrin reduces the access of opsonins to the surface and prevents opsonophagocytosis. In addition, CspA is also able to cleave and inactivate chemokines that recruit neutrophils to infection sites (Bryan and Shelver, 2009).

The β-antigen is an important virulence factor for *S. agalactiae* resistance to the host immune system. Also called IgA Fc-receptor protein, the β-antigen binds IgA to the bacterial surface, consequently blocking the binding of other opsonizing antibodies and inhibiting phagocytosis (Madoff *et al*, 1994). More recently, it was reported that

the β-antigen binds human factor H, preventing phagocytosis as well (Jarva *et al,* 2004).

Neutrophil extracellular traps (NETs) are structures made of DNA and antimicrobial peptides produced by neutrophils in response to invading bacteria to ensnare and eliminate bacteria during an infection. *S. agalactiae* nuclease A (NucA) is an extracellular nuclease, which degrades the DNA in the NETs to allow *S. agalactiae* escape (Derré-Bobillot *et al*, 2013).

Through binding to the human sialic acid-binding immunoglobulin-like lectin 5 (Siglec-5), a leukocyte cell-surface receptor, the aforementioned β-antigen promotes not only impaired oxidative burst, but also decreased production of NETs by the host, improving bacterial survival in the host (Carlin *et al*, 2009).

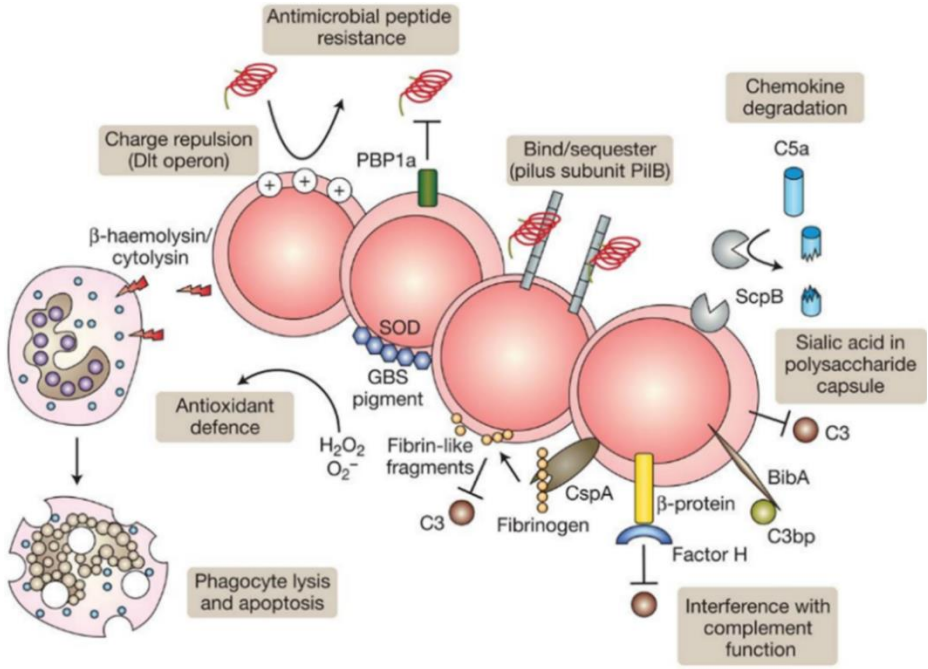

Figure 4. Mechanisms of *S. agalactiae* immune evasion (Maisey *et al*, 2008, a).

Despite *S. agalactiae* ability to prevent immune detection and phagocytosis, the bacterium is phagocytosed and killed by phagocytic cells in presence of serotype-specific antibodies. On the other hand, *S. agalactiae* is able to induce apoptosis in the macrophages and has evolved mechanisms to survive in the host as well.

For example, after invading the host, *S. agalactiae* secretes a hyaluronidase, HylB, that degrades a component of the extracellular matrix, the hyaluronan HA, inhibiting proinflammatory cytokine expression and promoting bacterial dissemination. Interestingly, HylB plays also a role in enhancing bacterial survival inside macrophages, allowing the use of HA as a carbon source in the host (Wang *et al*, 2014). Moreover, once phagocytosed, the bacterium is exposed to a harsh environment comprising ROS and antimicrobial peptides (AMPs). For what concerns oxidative damage, *S. agalactiae* is able to inactivate ROS produced by the host through the use of superoxide dismutase (SodA), which converts superoxide into oxygen and hydrogen peroxide. Protection from oxidative damage is also conferred by the orange carotenoid pigment produced by the beta-hemolysin/cytolysin. Moreover, *S. agalactiae* can inhibit ROS formation to protect itself from oxidative stress and low pH through production of glutathione.

Concerning bacterial resistance to AMPs, *S. agalactiae* can increase the number of D-alanine residues in lipoteichoic acids, a process regulated by the *dlt* operon, preventing AMPs crossing of the bacterial cell (Korir *et al*, 2017). In addition, bacterial resistance to AMPs is also mediated by pili. The previously mentioned pilus protein subunit PilB confers bacterial resistance to AMPs, promoting intracellular survival in murine macrophages and human neutrophils (Maisey *et al*, 2008, b).

Lastly, other than mediating binding to both fibrinogen and plasminogen, the Srr2 protein has also been shown to play a role in increasing phagocytic uptake and intracellular survival in macrophages and neutrophils (Six *et al*, 2015). Even though this function seems counterproductive, the protein could instead use this trick to enhance bacterial survival inside macrophages and at the same time promote its dissemination (Korir *et al*, 2017).

1.1.9 Activation of inflammatory response

Once overcome epithelial barriers' protections and immunological clearance, *S. agalactiae* can establish an infection, eliciting a strong inflammatory response in the host. Proinflammatory cytokines are produced by the host cells, including TNF and interleukin-6 (IL-6), but cytokine responses vary among strains. Strains belonging to the ST-17 and ST-19 lineages are associated to higher levels of TNF, IL-6, and IL-8 compared to other strains (Maisey *et al*, 2008, a). In an attempt to identify the *S. agalactiae* components that trigger host inflammatory response, it has been observed that the peptidoglycan is among the strongest stimulators of cytokine release from monocytes (Vallejo *et al*, 1996).

Toll-like receptors (TLRs) are a class of recognition receptors that play a role in warning the immune system about the presence of microbial infections. Neonatal macrophages produce high levels of proinflammatory cytokines such as IL-6, upon stimulation through TLRs 1, 2, and 4. However, compared to murine adult ones, neonatal macrophages display reduced expression levels of TLRs. Additionally, newborns display much less pulmonary macrophages than adults (even though their

number increases in about 24 to 48 h after birth). This condition prevents newborns' ability to quickly fight the infection, leading to development of EOD (Lund *et al*, 2020).

1.1.10 Biofilm

Bacterial ability to adhere and colonize different host niches facilitates cellular aggregation and formation of biofilms, sessile communities fundamental for bacterial persistence and establishment of chronic infections. The extracellular matrix of polysaccharides, proteins and DNA confers protection from recognition by the immune system (Shabayek and Spellerberg, 2018). Type IIa pili and the CPS have been reported to be key surface factors involved in development of biofilm for *S. agalactiae*. More precisely, it has been observed that PilA and PilB, but not PilC subunit, are fundamental for the biofilm formation (Konto-Ghiorghi *et al*, 2009), while CPS requirement has been demonstrated in presence of human plasma (Xia *et al*, 2015).

Environmental conditions are essential to prevent or promote development of bacterial biofilms. To this regard, since *S. agalactiae* is a common colonizer of the vagina, a host niche with an acidic pH is expected to be the ideal environment for bacterial colonization. According to preliminary analyses, *S. agalactiae* displays increased adherence to vaginal epithelial cells under acidic pH conditions compared to neutral pH (Zawaneh *et al*, 1979). In accordance with this early investigation, several studies reported that *S. agalactiae* biofilm production by isolates collected from pregnant women is increased when the bacterium is grown under acidic pH (4.5), compared to a neutral pH (7). This enhanced biofilm formation at vaginal pH could confer a potential advantage in colonizing vagina and increase the risk of vaginosis and neonatal infections (Ho *et al*, 2013).

Contradictory data are available concerning *S. agalactiae* ST-17 strains classification as weak or strong biofilm formers. As reported in figure 5, according to the work of D'urzo *et al* (2014), that performed an analysis working under acidic pH conditions, most of the strong biofilm formers belong to the serotype III, ST-17 lineage (D'urzo *et al*, 2014). On the contrary, Parker *et al* (2016) reported that invasive isolates belonging to the ST-17 and ST-19 lineages tend to form weak biofilms compared to strains associated to asymptomatic colonization of the host (Parker *et al*, 2016). It is possible to speculate that the difference in the result may rely on the different setup of the experiment performed to test the biofilm formation. What is proven to be crucial for *S. agalactiae* biofilm formation is the low pH and the presence of plasma, environmental factors fundamental to regulate the expression of bacterial surface-associated structures involved in biofilm formation.

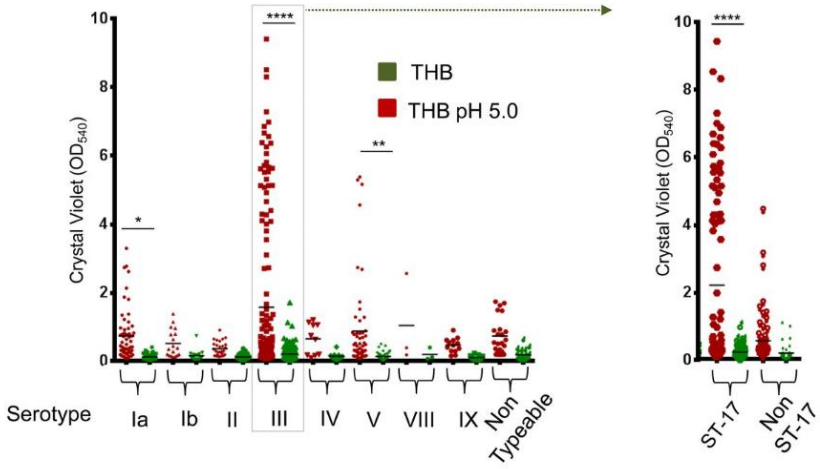

Figure 5. Effects of an acidic pH on *S. agalactiae* biofilm formation of 366 bacterial clinical isolates of eight different serotypes and nontypeable strains (D'urzo *et al*, 2014).

1.1.11 *S. agalactiae* dual personality: from asymptomatic colonizer to potent pathogen

The principal niche where *S. agalactiae* resides as an asymptomatic colonizer is the rectovaginal tract of females (Armistead *et al*, 2019). Interestingly, only a small fraction of colonized people develops *S. agalactiae* invasive disease, suggesting a potential role of host-specific factors in determining an individual's susceptibility to invasive disease. The bacterium possesses a great number of factors that promote host colonization, evasion of the immune system and dissemination in unprotected niches such as neonates. *S. agalactiae* expression of virulence factors is tightly regulated by signal transduction systems. These regulatory systems sense the signals encountered by the bacterium in the diverse host environments and consequently coordinate transcriptional responses to mediate bacterial adaptation. The mechanisms used by *S. agalactiae* to tightly regulate the expression of virulence factors remain largely unknown (Armistead *et al*, 2019).

1.1.11.1 Two-component signal transduction systems

An important class of signal transduction systems evolved by bacteria to sense and respond to the environmental changes are the so-called two-component systems (TCS). As indicated by the name, TCS comprise two constituents: a membrane-associated sensor histidine kinase and a cognate response regulator, that usually displays DNA-binding abilities. Upon sensing of an external specific signal, the histidine kinase phosphorylates the response regulator, thus causing a conformational change that will alter its binding affinity for target DNA sequences. Whole genomic analysis has revealed that *S. agalactiae* encodes up to 22 TCS, but the role of only

few of them has been investigated and partially elucidated (Figure 6) (Thomas and Cook, 2020).

1.1.11.1.1 CovR/CovS: the master regulator of virulence

Also known as CsrRS, CovRS is the most studied TCS of *S. agalactiae*. CovRS is a global regulator, controlling the expression of more than 100 genes, many of which are involved in virulence. Lamy *et al* (2004) reported that a Δ*covRS* mutant of *S. agalactiae* grown in rich Todd-Hewitt (TH) medium formed orange pigmented clumps. Given the association between β-h/c toxin expression and pigment production, the authors tested the haemolytic activity of the mutant pigmented strains and observed, as expected, that the Δ*covRS* mutant displayed an hyperhaemolytic phenotype compared to the wild-type strains when streaked on blood agar plates. The phenotypes observed were in accord with the expression profiling analysis conducted by the authors. The *cyl* operon, encoding three major virulence factors, the β-h/c toxin, the *bibA* gene, and the PI-1 pili operon, displayed increased expression levels in Δ*covSR* mutants compared to wild-type strains. In addition, *covRS* deletion caused a 5- to 20-fold increase in bacterial adhesion to human epithelial cells compared to wild-type strains. On the other hand, mutant strains displayed decreased survival rates compared to wild-type strains in neonate mice, demonstrating that this TCS is essential for bacterial virulence. Several virulence factors are controlled by the CovRS system. Among phenotypes associated to *S. agalactiae* virulence, canonical antimicrobial peptide (CAMP) factor is a toxin encoded by the *cfb* gene, that increases the β-hemolysin activity of *Staphylococcus aureus*. CAMP factor test revealed a decrease in CAMP activity in Δ*covSR* strains compared to wild-type strains. This result was in line with the observed decreased expression of the *cfb* gene. Additionally, decreased CPS levels were observed in Δ*covSR* mutants compared to wild-type strains. This phenotype could be explained by gene expression analysis as well. Mutant strains displayed a slight repression of the *cps* operon, encoding genes for capsular polysaccharide, compared to WT strains (Lamy *et al*, 2004). All these analyses confirm the essentiality of CovRS for *S. agalactiae* virulence.

CovR activity is modulated by CovS, which acts both as a kinase and a phosphatase at the level of a conserved aspartate residue (Asp53) of CovR. The equilibrium between the opposite enzymatic activities of CovS depends on its interaction with the *S. agalactiae* membrane protein Abx1. This protein is able to inhibit the CovRS signaling by antagonizing CovS, interfering with regulation of *S. agalactiae* virulence. Modulation of *abx1* expression affects direct targets of CovR, such as hemolysin/pigment production, expression of the adhesin BibA and the CAMP factor (Firon *et al*, 2013).

The TCS CovSR is embedded in an extremely complex regulatory network that involves several regulatory proteins. In addition to Abx1, the eukaryotic-type serine/threonine kinase Stk1 controls *S. agalactiae* virulence indirectly, via CovR. Stk1 phosphorylates CovR at the level of threonine 65 (Lin *et al*, 2009). CovR phosphorylation at the level of Thr65 is mutually exclusive respect to Asp53 residue

phosphorylation. Hence, Thr65 phosphorylation of CovR diminishes its activation at the conserved Asp53 residue, reducing CovR ability to bind DNA and to control gene expression in *S. agalactiae* (Rajagopal *et al*, 2006).

An additional layer of regulation resides in pH-dependent transcriptional changes. For a successful colonization of the host, *S. agalactiae* must quickly adapt to changes in environmental pH, by activation of cellular processes such as transcription of genes involved in transport and metabolism. Santi *et al* (2009) demonstrated that CovRS mediates bacterial adaptation during the transition from acidic to neutral pH (e.g., from the vagina to a more basic environment such as neonate lungs), by up-regulating the expression of several virulence determinants. The authors hypothesized that an acidic pH might induce an autokinase activity of the CovS cytoplasmic domain, with a subsequent phosphotransfer to the CovR regulator, thereby increasing its activity as a transcriptional regulator. This means that in case of switch to a neutral pH, the autokinase activity of CovS would not be stimulated, leaving CovR unphosphorylated and inactive (Santi *et al,* 2009).

All these studies investigated the role of CovR in *S. agalactiae* strains belonging to non-CC17 lineages. The architecture of the CovR network in *S. agalactiae* has been recently furtherly explored in BM110, a strain belonging to the hypervirulent lineage ST-17 (Mazzuoli *et al,* 2021). Two different mutants were prepared to define the transcriptional changes induced by CovR inactivation in BM110: a Δ*covR* mutant presenting an in-frame deletion of *covR* and a CovRD53A mutant, in which the conserved aspartic acid residue at position 53 was substituted with an Alanine, preventing CovR phosphorylation. In addition to virulence genes previously shown to be controlled by CovR, including *fbsA*, *fbsB*, *pbsP*, the C5a peptidase *scpB* and the secreted *nucA* endonuclease, two ST-17 specific virulence factors, named *hvgA* and *srr2,* were identified as direct targets of CovR-regulation. Interestingly, while several genes displayed similar expression patterns in the two strains, other genes showed strain-specific expression patterns. For example, the operon encoding for Srr2 was differentially expressed only in the *ΔcovR* mutant, but not in the D53A mutant strain, compared to the wild-type strain (Mazzuoli *et al,* 2021). A hypothesis to explain this result is that regulation of *srr2* transcription might involve an activator that would outcompete the binding of the non-phosphorylated CovR form, with a lower affinity for DNA compared to the phosphorylated form.

Another interesting analysis performed in the work of Mazzuoli *et al* (2021) regards the investigation of the plasticity of CovR regulatory network among *S. agalactiae* strains. The authors conducted a parallel RNA-Seq analysis in two different *S. agalactiae* strains, BM110 and NEM316 (a strain belonging to the ST-III type), to quantify the specificities of CovR regulation between them. A striking difference between the WT strains was observed, with 172 increased or 60 decreased genes ($|Log2\ FC| > 1$; adjusted p-value < 0.005) in NEM316 compared to BM110, respectively. The transcriptional profiles of CovRD53A mutants in BM110 and NEM316 were globally similar, with strain-specific sets of genes differentially expressed. Moreover, the ChIP-seq analysis revealed a global difference in the CovR

ability to bind chromosomal DNA between strains, that leads to strain-specific CovR regulation (Mazzuoli *et al*, 2021).

1.1.11.1.2 The regulator of fibrinogen- binding RgfAC

RgfAC is a TCS of *S. agalactiae* that plays a role in virulence regulation. Encoded by the operon *rgfBDAC*, this TCS is composed of RgfC, the sensor kinase, and RgfA, the response regulator. RgfAC was discovered in 2002, when it was demonstrated that mutant strains lacking the response regulator displayed increased expression levels of the C5a peptidase *scpB* gene (Spellerberg *et al*, 2002). Later on, it has been demonstrated that this TCS modulates the expression of two fibrinogen binding proteins, acting as a repressor of FbsA and an activator of FbsB. Further experiments conducted with *fbsA* and *fbsB* mutant strains revealed that FbsB plays a greater role compared to FbsA in human fibrinogen binding ability in CC17 *S. agalactiae* strains (Al safadi *et al*, 2011). This result explains why mutant strains lacking RgfAC, displaying decreased levels of FbsB, showed a reduced bacterial binding to fibrinogen even in presence of *fbsA* upregulation (Spellerberg *et al,* 2002). I*n vivo* analysis showed that mutant strains depleted for the response regulator were hypervirulent in a murine model of systemic infection. This result is consistent with the upregulation of the virulence factors FbsA and C5a peptidase observed in absence of RgfAC regulation. All these data suggest a role for RgfAC in promoting a colonization versus a virulent phenotype (Faralla *et al*, 2014, Thomas and Cook, 2020).

1.1.11.1.3 CiarH and antimicrobial-peptide resistance

CiaRH (CiaH, the sensor histidine kinase, and CiaR, the response regulator) is a TCS of *S. agalactiae* encoded by a locus that is homologous to the CiaRH TCS present in other streptococcal pathogens. Successful establishment of meningitis resides in bacterial ability to maintain high levels of bacteremia in terms of magnitude and duration into the host; thus, before entering the central nervous system, *S. agalactiae* must resist to the attack of neutrophils and macrophages. Experiments conducted on human neutrophils and murine macrophages infected with wild-type or Δ*ciaR* mutant strains revealed that wild-type strain displayed increased survival rates compared to Δ*ciaR* strains. This result revealed that CiaRH is involved in promoting bacterial survival in phagocytic cells (Quach *et al*, 2009). Survival of Δ*ciaR* strains is decreased compared to WT strains in hBMEC cells as well. Lastly, CiaRH confers *S. agalactiae* resistance against antimicrobial peptides (Quach *et al*, 2009). Despite being part of the innate immune response of the host, antimicrobial peptides called cathelicidins are naturally occurring antibiotics whose expression is induced in epithelial cells, neutrophils, and macrophages. It is possible that CiaRH promotes bacterial survival both in endothelial cells and in macrophages thanks to the increased resistance to these AMPs conferred to the bacterium.

1.1.11.1.4 DltRS and regulation of d-alanylation of LTA

DltRS is a TCS encoded by two operons, comprising six genes (*dltA, dltB, dltC*, *dltD, dltR and dltS*), that are transcribed from two different promoters, one upstream of the *dltABCD* operon, and the other one upstream of the two additional genes *dltRS,* in turn located upstream of the *dltABCD* operon. The *dltABCD* operon catalyzes the incorporation of d-alanine residues into the lipoteichoic acid (LTA) anchored to the bacterial membrane. D-Ala incorporated in the cell wall of Gram-positive microorganisms confers protection to the bacterial cell-wall from external stresses, such as antibiotics, via a simple mechanism: upon d-alanylation of LTA, its net charge is reduced, thus cells will be less electronegative and consequently will bind with a lower efficiency to cationic molecules such as AMPs (Thomas and Cook, 2020). As soon as the amount of d-Ala incorporated decreases, the DltRS system will upregulate the *dltABCD* operon expression, in order to guarantee constant physiological levels of cell-wall d-alanylation and maintain *S. agalactiae* fitness (Poyart *et al*, 2001).

1.1.11.1.5 BgrRS

The BgrRS system is encoded by the *brg* operon, located in a putative pathogenicity island near the *bac* gene, that encodes the β-antigen. This TCS regulates the β-antigen expression: it has been observed that strains lacking BgrR display strongly decreased expression levels of β-antigen expression, and that this leads to a consequent reduction of virulence in a murine intraperitoneal model of infection. Notably, in absence of BgrS, BgrR maintains its ability to upregulate *bac* gene expression. As observed for other transcriptional regulators, this suggests a potential crosstalk between BgrR and other sensor kinases (Rozhdestvenskaya *et al*, 2010).

1.1.11.1.6 The HssRS sensor of heme

Heme is both an important iron source and metabolic cofactor for bacteria. *S. agalactiae* does not carry the genes encoding enzymes for heme biosynthesis, thus it must import heme from the external environment. In order to avoid heme toxicity in the cell, bacteria possess the heme-regulated transport efflux system, HrtBA. The HssRS system is able to sense the presence of heme and consequently upregulates the expression of HrtBA, preventing toxicity (Thomas and Cook, 2020).

1.1.11.1.7 SaeRS regulator of adhesion to the host

The SaeRS system was identified as a TCS of *S. agalactiae* highly upregulated during *in vivo* growth in the vaginal tract (Cook *et al,* 2018). SaeRS plays a crucial role in promoting bacterial invasion of the CNS, as it upregulates the gene encoding the PbsP adhesin involved in *S. agalactiae* invasion of the BBB. Other than *pbsP*, SaeRS TCS upregulates other factors through which it promotes host colonization (Cook *et al,* 2018). Very recently, it has been demonstrated that SaeRS upregulates the group B *streptococcus* vaginal adherence protein (BvaP). BvaP promotes bacterial adhesion

to ECM components and to vaginal epithelial cells *in vitro*. Moreover, this protein is required for vaginal colonization *in vivo* as well (Thomas and Cook, 2022). According to Cook *et al* (2018), upon sensing the presence of a signal (hypothetically a small heat-labile peptide) in murine vaginal lavage fluid, SaeRS is activated and induces transcriptional changes that promote host colonization (Cook *et al,* 2018).

1.1.11.1.8 Regulation of Carbon metabolite and virulence by FspSR

The FpsR system composed of the fructose-6-phosphate (Fru-6-P) sensor histidine kinase and its cognate response regulator plays a role in monitoring and responding to nutrients availability. Experiments conducted on Δ*fspR* mutant cells grown on Fru-6-P as a carbon source displayed impaired growth rates compared to wild-type cells. Additionally, in presence of Fru-6-P, induction of both *fspSR* and the neighboring phosphotransferase system (PTS) operon were observed in the wild-type strain, suggesting that Fru-6-P is a signal sensed by FspSR to upregulate that PTS operon (Faralla *et al*, 2014). Moreover, in a murine model of vaginal colonization Δ*fspR* strain was significantly less persistent than the wild-type strain in the vaginal tract, indicating its involvement in mucosal colonization (Thomas and Cook, 2020).

1.1.11.1.9 LiaSR Lipid II-interacting antibiotics

Highly conserved in Gram-positive organisms, LiaSR is a TCS generally involved in sensing and responding to agents that disrupt cell envelope, such as antimicrobials and antibiotics like Lipid II-interacting antibiotics. In *S. agalactiae* the expression of *liaSR* is concomitant to the expression of *liaF*, a gene encoding a membrane protein that negatively regulates the LiaSR system. This TCS is able to sense disruptions in cell wall integrity and to regulate the response to disrupting agents by positively regulating the expression of several genes involved in cell wall synthesis (Klinzing *et al*, 2013).

1.1.11.1.10 Nisin and bacitracin resistance regulation: NsrRK/BceRS

BceRS (or NsrRK) is another TCS involved in bacterial resistance against antibiotics, such as nisin and bacitracin. BceRS upregulates the expression of *Sa*NSR, a nisin resistance protein and the expression of *nsrFP*, an efflux pump for AMPs. The *nsrFP* and *sa*NSR genes are encoded by the same operon, whose expression is upregulated by BceRS. This TCS is also involved in promoting biofilm formation and survival in the host (Yang *et al*, 2019).

1.1.11.1.11 Regulation of pathogenesis and host colonization: LtdRS

The LtdRS TCS was recently shown to be involved in vaginal colonization and development of meningitis. It has been observed that infection of human cerebral

microvascular endothelial cells (hCMEC) with the Δ*ltdR* mutant strain led to increased secretion of inflammatory cytokines; moreover, this outcome was concomitant with a Δ*ltdR* increased invasion of hCMEC and penetration of the BBB in a murine model of meningitis. These data indicate that LtdRS plays an important role in the pathogenesis of *S. agalactiae* meningitis. Given the increased invasiveness and decreased ability to colonize the mucosa of Δ*ltdR* mutant compared to wild-type strains, LtdRS potentially promotes colonization and suppresses pathogenesis of *S. agalactiae* (Deng *et al*, 2018).

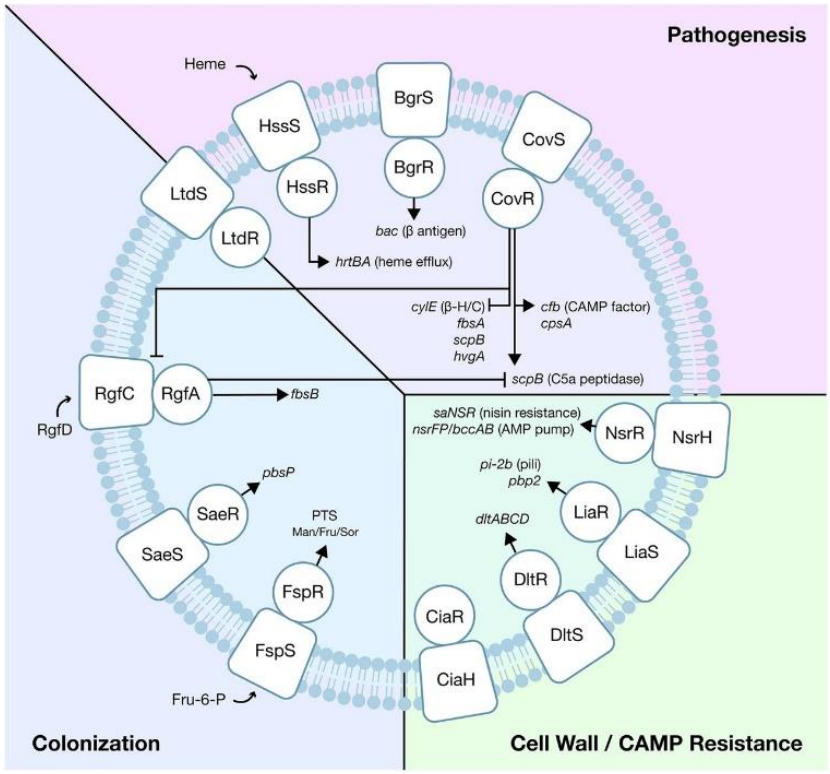

Figure 6. Two-component systems of *S. agalactiae* (Thomas and Cook, 2020).

1.1.11.1.12 One-component systems

In addition to TCS, *S. agalactiae* encodes several one-component systems involved in bacterial fitness and transition from commensal to pathogen. The transcriptional regulator MtaR plays a role in *S. agalactiae* interaction with fibrinogen. MtaR acts in fact as a repressor of *fbsB* and as an activator of *cspA* (Bryan *et al*, 2008). RogB is a transcriptional regulator involved in upregulation of *fbsA*, whose expression is controlled by several regulatory systems on the basis of the genetic background of

the bacterial strain (Gutekunst *et al*, 2003). The regulator of virulence RovS is a one-component transcriptional regulator involved in *S. agalactiae* virulence. Increased expression levels of *fbsA* detected in Δ*rovS* strains reveal that RovS acts as a repressor of *fbsA*. This regulation is a probable explanation to the observed increased adhesion to epithelial cells by Δ*rovS* compared to wild-type strains. Moreover, RovS stimulates the expression of *cyl* operon and of the *sodA* gene, directly controlling the expression of these genes (Samen *et al,* 2006). Finally, the recently characterized Catabolite control protein A (CcpA) is a regulator of genes involved in carbon metabolism, that controls 13.5% of *S. agalactiae* genome. The majority of genes under CcpA control are involved in acidic and oxidative stress resistance and confer to the bacterium the ability to survive in macrophages (Roux *et al*, 2022).

1.1.11.1.13 Exploring novel transcriptional regulators governing the switch of *S. agalactiae* from harmless commensal to invading pathogen

S. agalactiae has two major lifestyles: it can exist as an innocuous commensal in the gut or genital tract of healthy adults, or it can cause severe diseases and invade host tissues of neonates, pregnant women and fragile subjects (Shabayek and Spellerberg, 2018). The ability to switch between these two lifestyles is determined by environmental cues, such as pH, the presence of nutrients or host signals. These signals are perceived by a variety of regulators that orchestrate global responses, thus allowing *S. agalactiae* to adapt to different host niches and to coordinate metabolic and virulence pathways. As described above, the role of several two-component and one-component systems has been deeply studied (Thomas and Cook, 2020). However, the signals controlling their activity as well as the role of many regulators remains to be determined.

In all low G+C Gram-positive bacteria, the global transcriptional regulator CodY allows the concerted regulation of metabolic pathways in response to the nutritional status of the cell. Its role in the control of gene expression has been deeply investigated in *Bacillus subtilis*, the model organism of Gram-positive bacteria. In the years, it became evident that, in pathogens, this regulator plays a key role coordinating metabolism and virulence (Brinsmade, 2017). Depending on the species, CodY can activate or repress virulence, either directly or indirectly. Despite its role has been previously investigated in several streptococcal species, its function in *S. agalactiae* has not been studied so far.

In the following paragraphs, the role of CodY in *B. subtilis* and in Gram-positive pathogens will be described.

1.2 The global regulator CodY

1.2.1 Structure and *modus operandi* of CodY in *B. subtilis*

CodY is a global transcriptional regulator originally discovered in *Bacillus subtilis* as a repressor of the dipeptide transport operon (*dpp*) during the exponential growth phase in rich medium (Slack *et al*, 1995). Further studies revealed that CodY plays a wider role in *B. subtilis*, controlling the expression of more than 200 genes involved in cellular adaptation to nutrient conditions (Brinsmade *et al,* 2014). This transcriptional regulator is highly conserved and ubiquitous in low-G+C Gram-positive bacteria, such as staphylococci, streptococci, bacilli, clostridi*,* where it acts as a global regulator of metabolism. Importantly, in pathogens, CodY links nutrient availability and cell metabolism with the expression of virulence genes (Brinsmade, 2017).

The DNA binding ability, and therefore the regulatory function of CodY is activated upon binding to two different cofactors, GTP and branched-chain amino acids (BCAAs). As the abundance of these effectors reflects the energetic and metabolic status of the cell, CodY controls gene expression in response to nutritional availability. Interestingly, while BCAAs are universal CodY cofactors (Guédon *et al*, 2001; Brinsmade *et al*, 2017), GTP is not involved in CodY regulation in the genera *Streptococcus* and *Lactococcus* (Hendriksen *et al,* 2008; Petranovic *et al*, 2004). CodY binding to its cofactors is selective, occurs in the millimolar concentration range and leads to protein conformational changes that increase the affinity for its target sites on the DNA (Levdikov *et al*, 2006). Crystallization studies revealed that CodY from *B. subtilis* is a dimer of 29 KDa that displays an N-terminal cofactor binding domain, belonging to the GAF domain family, highly conserved in signalling and sensory proteins, and a C-terminal domain for DNA binding, that belongs to the winged helix-turn-helix (HTH) domain family (Levdikov *et al*, 2017).

CodY binds to a conserved 15 nucleotides consensus sequence (CodY motif), AATTTTCWGAAAATT (“W” stands for adenine or thymine), identified for the first time in *Lactococcus lactis* (den Hengst *et al*, 2005) and later shown to be conserved in all the species in which CodY was described. CodY affinity for DNA varies among its different target sites. That is, given a determined level of CodY active molecules, not all CodY targets are regulated to the same extent. Hence, as the abundance of intracellular BCAAs and GTP drops, the fraction of active CodY molecules in the cell is gradually reduced and CodY-mediated regulation of gene expression is progressively relieved (Brinsmade, 2017).

In *B. subtilis* CodY acts mostly as a repressor of stationary phase genes involved in amino acid and purine biosynthesis, nutrient transport, catabolism, motility, competence and sporulation. In addition, it acts as an activator of carbon overflow pathways (Brinsmade *et al*, 2014). When the cell is in a condition of high nutrients

availability, high levels of intracellular BCAAs determine a high number of CodY active molecules. In this case, genes which are normally under positive regulation of CodY will be highly expressed, while genes under CodY negative regulation will be expressed at a very low level. CodY can act as negative regulator in two different ways: it can compete with the RNA polymerase or with a positive regulator for binding to the promoter; it can act through a roadblock mechanism by binding within the coding sequence of the target gene and forcing a premature termination of transcription (Belitsky and Sonenshein, 2011). On the other hand, CodY can activate transcription by stabilizing the binding of the RNA polymerase to the promoters (Shivers *et al,* 2006). Importantly, genome-wide studies performed in *B. subtilis* revealed that CodY can also regulate gene expression indirectly by controlling the expression of other transcriptional regulators (Brinsmade *et al,* 2014).

When intracellular levels of BCAAs are sufficient to support growth, bacteria repress BCAA biosynthesis. In *S. aureus*, as in *B. subtilis*, the BCAA biosynthetic genes are repressed by CodY. An interesting finding was that, even though CodY binds all three BCAAs *in vitro*, its activity in regulating expression of BCAAs is predominantly regulated by isoleucine availability during growth (Kaiser *et al*, 2018). Reduced availability of CodY cofactors in the medium, such as during stationary phase of growth, will lead to a progressive decrease in the number of CodY active molecules. That is, genes normally repressed by CodY will be progressively de-repressed. On the other hand, CodY activated genes that are instead upregulated during active growth in rich medium, will be expressed only at low levels in case of depletion of CodY cofactors. In this way, CodY decreased affinity for DNA binding will determine a hierarchical modulation of gene expression, with the prioritization of determinate metabolic pathways ahead of others (Brinsmade *et al,* 2014). Bacteria use CodY to prioritize gene expression and critical metabolic pathways ahead of others, to guarantee a hierarchical expression of genes and pathways at varying extents of nutrient limitation, in order to reconfigure genetic circuits to survive or thrive in the dynamic environments they inhabit.

Several studies aimed at characterizing CodY targets in *B. subtilis* have revealed that changes in CodY activity mediated by changes in medium composition led to varying extents of gene expression mediated by CodY (Brinsmade and Sonenshein, 2011). Belitsky and Sonenshein have reported how CodY activity does not only depend on varying intracellular pools of its effectors. A genome-wide *in vitro* binding analysis conducted by the authors allowed the identification of all CodY-binding sites in the *B. subtilis* genome. Moreover, the experiment revealed the relative binding strengths for those sites, demonstrating that CodY affinity for DNA is different among the various target sites. The threshold concentration of activated CodY that regulates a gene is specific for that gene and determination of such thresholds can be very complex (Belitsky and Sonenshein, 2013). A genome-wide profiling of transcript abundances in strains producing mutant CodY proteins of *B. subtilis* have allowed the identification of genes that are turned on or off at different levels of CodY activity. These analyses have provided a framework for determining the bacterium's strategy for altering the activities of multiple metabolic pathways when faced with changing

levels of nutrient availability. In particular, the authors have pinpointed how, if a gene has a second regulator whose role is to interfere with CodY binding, a relatively strong CodY-binding site might not have *in vivo* the same relative effectiveness observed *in vitro* (Brinsmade *et al,* 2014*)*. Together these findings confirm the complexity of CodY-mediaded regulation of gene expression.

1.2.2 Interactions of CodY with other global regulators for the control of metabolism in *B. subtilis*

CodY-mediated regulation of gene expression in *B. subtilis* has been widely investigated. This transcription factor acts in combination with other global regulators to control cellular metabolism in response to diverse intracellular metabolites that signal the environmental conditions of the cell.

When growing in a glucose-rich medium*, B. subtilis* is able to metabolize a large proportion of it to obtain pyruvate and acetyl CoA, that will be in turn converted to fermentation products (i.e., lactate, acetate and acetoin) and excreted in the extracellular environment. During this process of glycolysis and production of fermentation products, the energy is stored as ATP. As soon as glucose is consumed, the fermentation products are taken up from the environment and used for central metabolism through their entry in the citric acid cycle. In this scenario, a crucial role is played by CcpA, a regulator that controls carbon metabolism in many Gram-positive bacteria. Upon activation by fructose-1-6-bisphosphate (FBP), an intermediate of glycolysis, CcpA promotes the expression of genes required for the synthesis of fermentation products. When the cell is in nutrient rich conditions, in presence of high levels of BCAAs and GTP, CodY promotes the synthesis of lactate and acetoate as well. Hence, if glucose is available, CodY and CcpA cooperate together to activate the carbon-flow (Figure 7).

When active, CcpA and CodY act also as repressors of the enzymes involved in the re-utilization of acetoin and acetate: once extruded into the extracellular environment, these fermentation products enter the citric acid cycle, if the enzymes involved in their re-utilization are not repressed (Figure 7). Together these two regulators control pyruvate conversion to fermentation products based on few metabolites: FBP, BCAAs and GTP (Sonenshein, 2007).

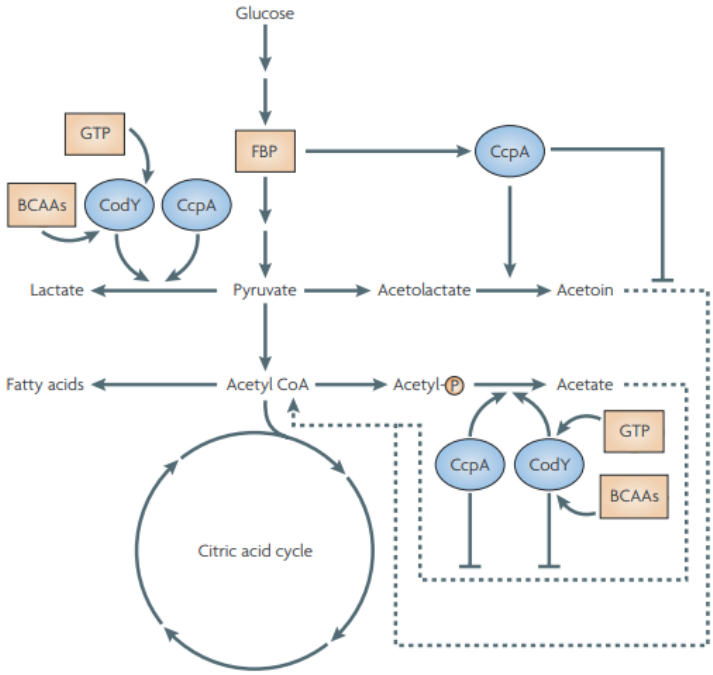

Figure 7. Interplay of the global regulators CcpA and CodY in carbon overflow metabolism in *B. subtilis (*Sonenshein, 2007).

Despite interacting at the level of regulation of carbon overflow pathways, CodY and CcpA control also the regulation of the synthesis of BCAAs together with a third transcription factor, TnrA. BCAAs play a multifaceted role in bacterial fitness and the level of their synthesis depends on the availability of metabolites linked to central metabolism such as pyruvate, acetyl-CoA and oxoalacetate. The BCAAs biosynthetic pathway provides also intermediates for pantothenate and BCFAs, the main constituents of Gram-positive bacterial membranes (Kaiser and Heinrichs, 2018). The *B. subtilis ilv-leu* operon comprises seven genes (*ilvBHC* and *leuABCD*) necessary for BCAAs biosynthesis. CodY, CcpA and TnrA participate in the regulation of the *ilv-leu* operon in a very well-orchestrated way.

When BCAAs are supplied from a nitrogen-rich medium, CcpA promotes *ilv-leu* expression to make the cell synthesize more BCAAs for rapid cell growth. CcpA-mediated stimulation of expression of genes for BCAAs biosynthesis promotes CodY activation. CodY in turn exerts a negative regulation on BCAAs synthesis, counteracting the positive regulation CcpA-dependent (Figure 8). This mechanism allows the cell to prevent an excess of BCAA synthesis, maintaining their level in appropriate concentrations *in vivo*. By mediating the creation of different steady-state levels of BCAA biosynthesis, under different conditions of nutrient availability, CcpA determines the extent to which CodY is active, thereby determining the impact

of CodY on the many genes that it controls. This means that CcpA not only regulates its own target genes, but also CodY target genes. Together with CcpA and CodY, also TnrA regulates BCAA biosynthesis, but this regulator is only active when nitrogen is limiting. Under this condition, TnrA acts as a repressor of BCAAs biosynthesis (Figure 8). Thus, if carbon is in excess and nitrogen is lacking, TnrA will partially counterbalance the effect of CcpA on BCAA biosynthesis. In this way, TnrA will decrease CodY activity as a repressor of amino-acid utilization pathways, adjusting the amounts of BCAAs in response to a poor nitrogen supply (Tojo *et al*, 2005). Globally, we can conclude that CodY and TnrA counteract the positive regulation of CcpA, according to nitrogen availability on the medium.

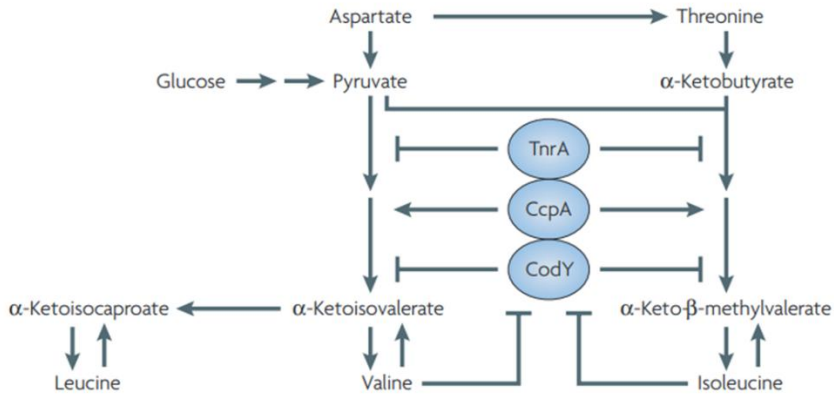

Figure 8. Interplay of CodY, CcpA and TnrA in the regulation of BCAAs biosynthetic pathway (Sonenshein, 2007).

It is important to interrogate gene expression at intermediate levels of activity in order to unravel complex regulatory mechanisms that couldn't be revealed if considering that CodY is just active or inactive. An example is the CodY-mediated regulation of *braB*, a gene encoding a BCAA permease. Regulation of *braB* is subject to a complex regulation by which CodY acts both as a direct repressor and as an indirect positive regulator. The positive regulation of CodY is mediated by repression of *scoC*, a gene encoding a second repressor of *braB*. In this scenario, *braB* expression occurs only under particular conditions, such as during growth in a BCAAs poor medium, in which CodY activity is low enough to prevent repression of *braB*, but high enough to maintain sufficient repression of *scoC.* Depending on the respective affinity of CodY and ScoC for their different targets, the action of one regulator may have a greater effect than the other or, as in the case of *braB*, balance each other almost perfectly (Belitsky *et al*, 2015, a). CodY control of ScoC creates a regulatory cascade that allows to maintain or increase repression of certain genes under conditions in

which CodY is no more active. As ScoC and CodY share a number of direct targets, this feed-forward regulatory loop occurs at different promoters.

Oligopeptide permeases are other targets of complex transcriptional regulation mediated by CodY and ScoC. Both the regulatory proteins act as negative regulators of the *opp* operon. Moreover, CodY serves as indirect positive regulator of the ScoC-repressed *opp* operon (Belitsky *et al*, 2015, b). The combined actions of CodY and ScoC serve to maintain *opp* repressed even when one of the regulators is not active.

An additional layer of complexity is given by TnrA. When CodY is inactive, under conditions of nitrogen limitations, TnrA acts as a positive regulator of the *opp* operon via interference with ScoC action (Fisher, 1999). Hence, the presence of CodY and ScoC in the same cell allows different kinds of outcomes when CodY loses activity because of nutrient exhaustion. Genes controlled negatively and directly by both CodY and ScoC can have varying responses depending on the concentrations of the active forms of the proteins needed to bind to the regulatory regions of the genes in question and the strength of the corresponding binding sites.

B. subtilis displays two major exoproteases, AprE and NprE, important enzymes involved in several functions, such as degrading extracellular proteins to provide amino acids for growth. Interestingly, regulation of expression of their genes *aprE* and *nprE* is subject to complex interplay of multiple transcription factors, such as AbrB, DegU, ScoC, and SinR. Barbieri *et al* (2016) have demonstrated a simultaneous regulation by CodY and ScoC. More precisely, both CodY and ScoC repress *aprE* and *nprE* transcription. Moreover, even though *scoC* expression increases when CodY is inactive, the authors have observed that the loss of CodY-mediated repression is compensated by a stronger ScoC-mediated repression of the proteases. Hence, in order to observe the strong negative role of CodY in *aprE* and *nprE* regulation, ScoC must be absent or inactive (Barbieri *et al*, 2016). Regulation of metabolism, BCAAs uptake and biosynthesis, oligopeptide transport and protein degradation mediated by different regulators reflects the importance of a tight interconnection of signals in order to guarantee bacterial fitness.

1.2.3 Intersection of CodY with the stringent response

When nutrient levels decrease, bacteria are able to activate a stress response system that allows them to survive under harsh conditions. The stringent response involves the synthesis of pppGpp, subsequently hydrolysed to ppGpp. Bacterial (p)ppGpp synthesis is fundamental for bacterial fitness, survival and adaption. Alarmons such as ppGpp generally repress rRNA synthesis, reducing protein translation. In addition, (p)ppGpp synthesis is involved in several physiological changes such as gene activation/repression or protein translation. In most firmicutes, alarmones are synthetised by RelA (or RSH), which has synthesis and hydrolysis activities, RelQ and RelP, small proteins which have only the synthase domain. In *B. subtilis*, RSH is the major (p)ppGpp synthase that displays the highest activity in response to amino acid deprivation. The synthesis of alarmones requires the consumption of GTP and

ATP. Under nutrient rich conditions there are high levels of GTP and BCAAs. Through binding of its cofactors, CodY binds DNA and inhibits RNA-polymerase activity, exerting its role as transcriptional regulator. As soon as the cell undergoes nutrient limitation, the RSH enzyme becomes activated. At this point, sythesis of (p)ppGpp leads to a decrease of the GTP pool and therefore to a release of CodY from DNA. Hence, genes involved in adaptation to nutrient deficiency that were previously repressed, can now be expressed (Figure 9) (Geiger and Wolz, 2014).

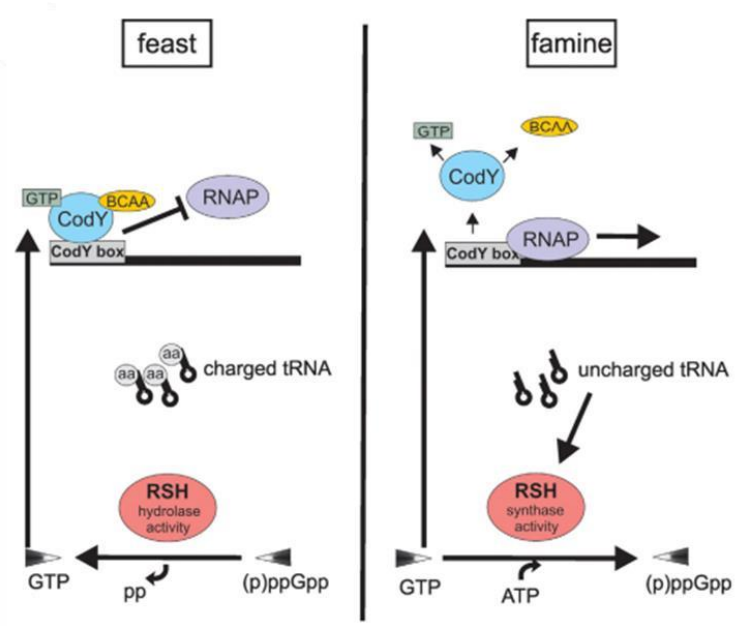

Figure 9. Scheme of the intersection of CodY and the stringent response in *B. subtilis* (Geiger and Wolz, 2014).

1.2.4 CodY as a link between metabolism and virulence in pathogens

In pathogens, CodY constitutes an important link between regulation of metabolism and pathogenesis, acting either as an activator or a repressor of virulence gene expression depending on the bacterium.

1.2.4.1 Staphylococcus aureus

Staphylococcus aureus is a pathogen that colonizes the nares of healthy individuals but can lead to severe infectious diseases ranging from skin lesions to pneumonia, sepsis and endocarditis. Several studies revealed that CodY is a global regulator of gene expression in *S. aureus,* as its regulon comprises about 200 genes. Among the

several gene targets of CodY, the majority of them encode proteins that control metabolic pathways. CodY also represses many *S. aureus* virulence genes during *in vitro* growth (Pohl *et al*, 2009, Majerczyk *et al,* 2010). Montgomery *et al* reported how, in absence of *codY*, *S. aureus* becomes hypervirulent in murine skin and pneumonia infection models. The increased virulence displayed in the deletion mutant is given by an increased expression of several virulence factors (Montgomery *et al*, 2012). Experiments conducted with *S. aureus* Δ*codY* strains revealed that CodY acts as a repressor of haemolytic activity, as it represses the hemolytic alpha-toxin (*hla*). Moreover, CodY is involved in repression of biofilm formation, as *codY* deletion mutants displayed a reduced biofilm biomass. CodY-mediated repression of biofilm occurs through CodY negative regulation of the *ica* operon, that controls the expression of the PIA protein involved in biofilm formation (Majerczyk *et al,* 2008). Among CodY-controlled virulence genes, *sodA* and *katA*, encoding respectively a superoxide dismutase and catalase, emerged among genes under direct control of CodY (Majerczyk *et al,* 2010).

Figure 10 schematically shows how CodY governs bacterial transition from a commensal to virulent pathogen. From the bacterium's perspective, as long as *S. aureus* grows in an environment rich of nutrients at the beginning of the host colonization site, the cells grow without the need to turn on virulence genes. Genes that promote colonization, such as *fnbA* and *spa*, encoding for adhesive proteins, will be therefore upregulated. However, as soon as nutrients become limiting, these genes are no more expressed, preventing adhesion but promoting dissemination. At this point, *S. aureus* promotes expression of genes encoding for lipases, proteases and hyaluronidases, whose products will re-establish nutrient availability by damaging host cells. As soon as nutrients are depleted, CodY sequentially loses repression and turns on genes required for transporting preformed compounds, *de novo* synthesis of amino acids and virulence factors (Waters *et al*, 2016). Hence, *S. aureus* uses CodY to keep virulence gene expression shut off until a nutrient limitation threshold has been reached. Thus, BCAAs and GTP depletion can be indicators of *S. aureus* transition from a commensal lifestyle to an invasive, pathogenic lifestyle.

CodY regulation of virulence occurs both directly and indirectly. *S. aureus* CodY co-regulates virulence in conjunction with other regulators of virulence, the Agr quorum sensing system and the SaeRS two-component system. In particular, CodY represses the TCS accessory gene regulator (*agr*), well characterized for being involved in the synthesis of several *S. aureus* virulence factors, such as polysaccharide intercellular adhesin (PIA) or the delta-toxin hemolysin. Majerczyk *et al* discovered that nearly half of the genes repressed by CodY are not its direct targets but are overexpressed in absence of *codY* due to derepression of the *agr* locus (Majerczyk *et al*, 2010). CodY's role in repressing *agr* has important effects on regulation of virulence. The effector of the Agr system RNAIII inhibits translation of the repressor of toxins (Rot). Hence, as nutrients availability drops, so does CodY activity. As a result, the *agr* locus is derepressed and RNAIII synthesis increases, leading to a drop of Rot abundance. Additionally, Majerczyk *et al* (2010) identified *saeRS,* encoding the SaeRS two-component system (TCS), to be regulated by CodY. The *sae* locus

consists of four genes (*saeP, saeQ, saeR, and saeS*), whose expression is driven by two promoters: a constitutive promoter (P3) and an autoregulated promoter (P1). P3 promotes transcription of *saeR* and *saeS*, encoding proteins required for sensing and response to changes in environmental conditions. SaeR in turn activates P1 through protein phosphorylation. CodY regulation of *saeRS* occurs through direct repression of *sae* expression by binding the upstream region of the *sae* P1 promoter. This binding hinders SaeR binding to the P1 promoter (Pendleton *et al*, 2022). Importance of CodY-mediated regulation of *saeRS* resides *nuc*, a gene encoding a thermonuclease. This factor is directly controlled by SaeRS and is at the same time a CodY-regulated virulence factor. Waters *et al* (2016) have observed that CodY represses the expression and production of the thermonuclease during rapid, exponential growth, and this graded regulation is dependent on the Sae TCS (Waters *et al,* 2016).

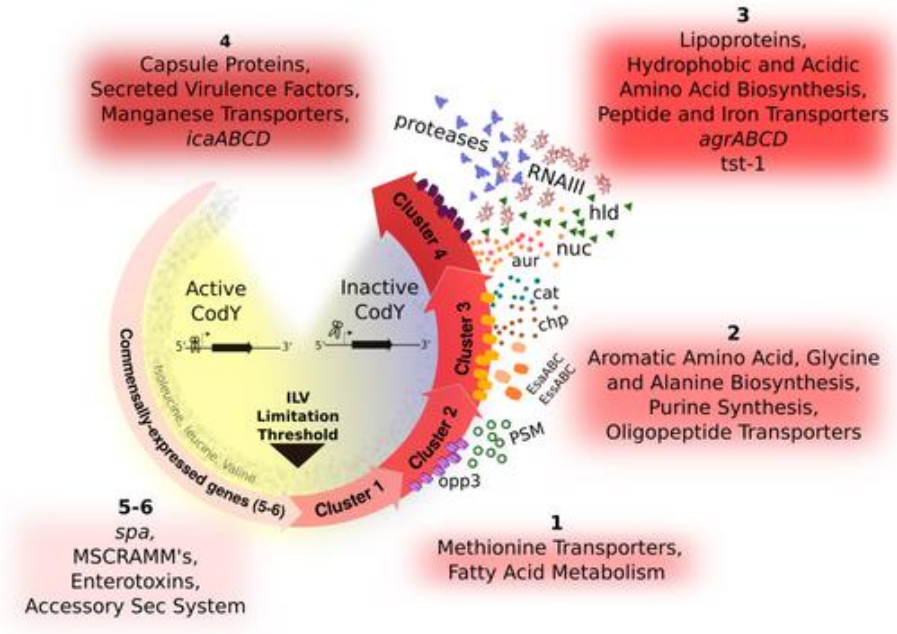

Figure 10. Model for CodY regulatory role in bacterial transition from commensal to virulent pathogen (Waters *et al*, 2016).

1.2.4.2 Clostridium difficile

Clostridium difficile is a Gram-positive bacterium that colonizes the intestine. *C. difficile* encodes two large toxins, TcdA and TcdB, which are essential for virulence. Dineen *et al* (2010) demonstrated that, upon binding to GTP and BCAAs, CodY

controls either directly or indirectly the expression of around 150 genes in *C. difficile*, acting mostly as a repressor of gene expression. CodY controlled targets include genes involved in amino acid biosynthesis, nutrient transport, fermentation pathways. Moreover, CodY negatively controls the expression of several virulence factors, such as membrane components and surface proteins (Dineen *et al*, 2010). Together with the transcriptional regulator CcpA, CodY controls the expression of genes encoding toxins TcdA and TcdB. TcdR is the major sigma factor for toxin gene transcription necessary for high expression levels of toxin genes (*tcdA* and *tcdB*) (Figure 11). CcpA and CodY respond independently to different nutritional signals, and both bind upstream and repress the *tcdR* gene (Figure 11). In particular, CodY regulates toxin gene expression by binding to the *tcdR* promoter region at three different locations with varying affinities, with two of the binding sites overlapping with sigma factor-binding regions (Bouillaut *et al*, 2015).

Another critical trait governing *C. difficile* pathogenesis is the spore formation. Being a strict anaerobe, sporulation in *C. difficile* is an obliged process that allows the bacterium to effectively persist and spread in the aerobic environment outside the host. It has been recently reported that CodY plays a role in controlling *C. difficile* sporulation. The list of genes controlled by CodY comprises genes involved in sporulation initiation, including *spo0A, rapA, rapC, rapE, sinI/R, sigH,* and *kinB.* Moreover, CodY acts as a repressor of the *opp* oligopeptide transporter operon which was demonstrated to inhibit the initiation of sporulation in *C. difficile*. By importing peptides, and therefore by increasing the availability of BCAAs, OppA can modulate CodY activity and CodY-mediated repression of sporulation. Nawrocki *et al* (2016) also reported that CodY acts as a repressor of sporulation by controlling directly and indirectly the expression of the sporulation regulator gene *sinR* (Nawrocki *et al*, 2016). More precisely, CodY binds directly upstream the *sinR* coding region, and β-galactosidase assays reported an increase in *sinR* expression levels in *codY*-null mutant strains compared to wild-type strains. However, despite these observations, researchers have observed that alleviation of CodY repression at stationary phase is not sufficient to increase transcription from the *sin* promoter. This outcome is due to other factors, CcpA and SigD, involved in *sinR* repression together with CodY (Nawrocki *et al*, 2016).

Spore formation and toxin production are critical for *C. difficile* pathogenesis. RstA is a conserved *C. difficile* regulator, that promotes sporulation initiation and directly represses toxin expression by binding upstream the *tcdR* coding region. Edwards *et al* (2020) have reported that RstA-mediated regulation of both sporulation and toxin production is species-specific. As a matter of fact, several point mutations have been detected within the *tcdR* promoter region among various strains, many of which overlap the RstA and CodY binding sites. These mutations affect RstA- and CodY-mediated repression. At the same time, since these regulators respond to different cofactors, their repression prevents a full *tcdR* transcription, unless DNA binding is relieved by both regulators (Edwards *et al*, 2020).

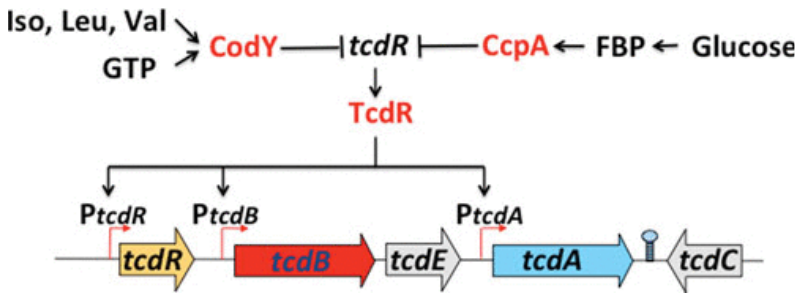

Figure 11. Synergistic repression of *C. difficile* toxin synthesis by CodY and CcpA (Richardson *et al,* 2015).

1.2.4.3 CodY as positive regulator of virulence: *Lysteria monocytogenes* and *Bacillus anthracis*

In *Bacillus anthracis*, the eziological agent of the anthrax disease, and *Listeria monocytogenes* CodY plays a fundamental role as an indirect activator of virulence gene expression.

L. monocytogenes is a firmicute that causes listeriosis, a foodborn disease. Biswas *et al* (2020) identified all CodY-binding regions in *L. monocytogenes in vitro* through an *in vitro* DNA affinity purification coupled with parallel sequencing (IDAP-Seq). The analysis conducted with varying concentrations of CodY allowed the identification of all the relative binding strength for each potential target site (Biswas *et al,* 2020). As a facultative intracellular pathogen, *L. monocytogenes* displays virulence factors mostly involved in host cell invasion, intracellular replication and bacterial spread in the host. These factors are positively regulated by the master activator of virulence, PrfA. As demonstrated by Lobel *et al* (2015), CodY directly activates *prfA* expression by binding a sequence located within the 5' coding region. Interestingly, ChIP assay in combination with RT-qPCR analysis revealed that CodY bound *prfA* region preferably during growth in presence of low BCAAs levels. Ligand-limited CodY appears to activate *prfA* transcription, leading to induction of virulence (Lobel *et al*, 2015). Low concentration of BCAAs in the environment constitutes the major metabolic signal that contributes to consistent virulence genes expression. Through this elegant mechanism, *L. monocytogenes* can respond to a drop in BCAA availability, as during invasion of host cells, releasing repression of several pathways, such as BCAA biosynthesis, promoting growth and survival (Lobel *et al*, 2015).

Brenner *et al* (2018) discovered that isoleucine deficiency in the environment constitutes a signal for virulence gene activation. In particular, they demonstrated that a ribosome-mediated attenuator Rli60 controls *leucine* gene transcription in a BCAA-dependent manner, limiting BCAAs synthesis. As isoleucine is also the input signal

of CodY, Rli60 impacts CodY activity as well. In this way, BCAAs biosynthesis is regulated at two different levels, the first involving CodY repression under nutrient rich conditions, the second through Rli60 mediated attenuation of BCAAs biosynthesis under poor BCAA conditions (Brenner *et al,* 2018).

Among factors that inhibit mammalian cell invasion in *L. monocytogenes*, high c-di-GMP levels play a robust role, as high levels of c-di-GMP lead to suppression of *prfA* gene expression, and so to repression of virulence. Elbakush *et al* (2018) identified CodY as a c-di-GMP-sensitive component. In particular, they observed that decreased CodY activity leads to a signal transduction cascade that results in lower expression levels of *codY* and *prfA*. This in turn leads to reduced production of virulence factors, such as proteins involved in invasion, particularly InlA. Additionally, CodY perceives c-di-GMP levels changes indirectly, through a process that is not clear yet (Elbakush *et al*, 2018).

Regarding *B. anthracis*, the pathogenicity of this bacterium is principally due to two key virulence factors, the anthrax toxins and a weakly immunogenic poly-γ-D-glutamic acid capsule. Toxins and proteins for the synthesis of the capsule are encoded by the pXO1 and pXO2 separate extrachromosomal plasmids, respectively. The pXO1 plasmid encodes also the major regulator of virulence genes, the anthrax toxin activator (AtxA) protein. AtxA controls the expression of hundreds of genes, but most importantly, it positively regulates the expression of toxin components and of the capsule activator genes (Fouet, 2010). van Schaik *et al* (2009) demonstrated that AtxA is directly controlled by CodY. CodY acts as a positive regulator of virulence in *B. anthracis*, as it promotes AtxA cellular accumulation acting at a post-translational level (van Schaik *et al*, 2009). Very recently, Gangwal *et al* (2022) have elucidated a possible mechanism through which CodY controls AtxA expression. They have demonstrated that CodY is a substrate of the serine/threonine phosphatase PrpN and the serine/threonine kinase PrkC. CodY phosphorylation constitutes a regulatory switch in the synthesis of virulence factors. When CodY is dephosphorylated by PrpN, it binds the *atxA* promoter, and AtxA expression is in turn activated, favouring virulence. On the other hand, CodY phosphorylation abolishes its DNA binding ability to the *atxA* promoter region, as a consequence AtxA is downregulated and so do anthrax toxin synthesis (Gangwal *et al*, 2022).

1.2.4.4 CodY in streptococci

Streptococcus pyogenes (group A streptococcus, GAS) is one of the most common bacterial pathogens infecting humans. In *S. pyogenes*, CodY controls the expression of 17% of genes in the chromosome, including genes involved in the response to nutritional stress, genes encoding for other transcriptional regulators, transporters, and metabolic enzyme genes, similarly to what commonly observed in Gram-positive bacteria (Kreth *et al*, 2011). However, CodY-regulated virulence genes remain highly organism specific. These include genes encoding exoproteins, such as DNases, a protease and hyaluronidase. All together these factors influence host-pathogen interactions, for instance alleviating bacterial starvation. Proteases degrade several

extracellular matrix proteins, promoting bacterial dissemination to nutrient rich environments. Secreted nucleases instead can promote bacterial dissemination by degrading nucleic acids present in neutrophil extracellular NETs. Experiments conducted culturing cells in a chemically defined medium report that *S. pyogenes* CodY promotes biofilm formation, as a Δ*codY* mutant formed less biofilm biomass compared to a wild-type strain. No difference in biofilm formation was observed when both strains were cultured in rich TH medium. These results suggest that CodY plays a minor role in influencing biofilm formation of *S. pyogenes*. This influence might be due to changes in extracellular nuclease activity, that could promote biofilm dispersal (McDowell *et al*, 2012).

By influencing the expression of other transcriptional regulators, including Mga and the two-component regulatory system CovRS, CodY affects the expression of many virulence genes. As described above, CovRS controls 15% of the bacterial genome and directly regulates, mainly as a repressor, the expression of major virulence factors (Graham *et al*, 2002). By repressing *covRS* expression, CodY acts as an activator of different virulence genes (*slo, hasA, nga*) and exerts a counteractive balancing of CovRS activity according to the nutritional status of the cell. At the same time, CodY-mediated activation of the pleiotropic virulence gene activator Mga results in the enhanced expression of a broad range of virulence factor genes required for host colonization and evasion of the host immune system *(scpA, sof* and *scl*) (Kreth *et al*, 2011).

Development of virulence requires a careful balance between consume of energy for virulence factors production and energy consumption for adaptation to a constantly changing environment. It is fundamental to finely coordinate external environmental signals with gene expression response that best suits a particular infection site. This sets a point on how focusing on the effect of solely one regulator per time might miss the chance to discover crucial steps in virulence development (Kreth *et al*, 2011).

Streptococcus pneumoniae is a human pathogen that colonises asymptomatically the nasopharynx but can cause diseases such as pneumonia or meningitis. Investigation of the pneumococcal CodY regulon revealed that CodY predominantly controls genes and operons involved in BCAA metabolism and general amino acid metabolism, such as the *ilv* operon (*ilvBNC*) and the genes *ilvA* and *ilvE*, that emerged as strongly upregulated in a Δ*codY* mutant. The glutamate dehydrogenase *gdhA* is a gene controlled by multiple regulators: CodY acts as its repressor but at the same time, the expression of this gene is also regulated by the nitrogen regulatory protein GlnR, suggesting a central role of GdhA in pneumococcal nitrogen metabolism. Furthermore, Hendriksen *et al* (2008) have demonstrated that CodY is involved in promoting bacterial colonization of the nasopharynx *in vitro*, as Δ*codY* mutants displayed decreased adherence to epithelial cells compared to wild-type strains (Hendriksen *et al,* 2008). It is important to underline that, recently, it has been demonstrated that CodY is an essential protein of *S. pneumoniae*, as it controls genes/functions crucial for the bacterium. Analysis of the *codY*-null mutant strain used in the work of Hendriksen *et al* (2008) revealed that this mutant contained

additional suppressor mutations. For this reason, data previously obtained by Hendriksen cannot be attributed solely to *codY* deletion, but they might be due to the effect of other mutations compensating for CodY deletion (Caymaris *et al*, 2010).

Streptococcus suis is a prevalent pathogen and an important zoonotic agent in swine. The capsule rich in sialic acid (Sia) plays a central role in its virulence, as it confers antiphagocytic properties to the bacterium. The virulence of *S. suis* is also associated with the pathogen-host interaction. Investigation on *S. suis* serotype 2 reported that CodY strongly modulates global gene expression, targeting especially genes involved in metabolism and virulence. A *codY* mutation strongly decreased the capsule thickness in *S. suis* 2 during both exponential phase and stationary phase; moreover, *codY* mutation decreased the Sia synthesis in capsule. As the Sia promotes bacterial adhesion to host cells, the reduced capsule biomass could at least partially explain the attenuated adherence and invasion ability of the mutant strain to host cells compared to wild-type strains (Feng *et al*, 2016).

2. Aim of the work

The opportunistic pathogen *Streptococcus agalactiae* is a commensal of the urogenital and gastrointestinal tracts of almost a third of the healthy population. This bacterium, however, is able to cause invasive infections in newborns and immunocompromised patients (Shabayek and Spellerberg, 2018). During infection, the ability of *S. agalactiae* to invade different host niches depends on its capacity to adapt to various environmental conditions. This versatility is possible thanks to the concerted activity of several transcriptional regulators that, upon sensing external environmental signals, respond by controlling the expression of factors involved in nutrient acquisition, immune evasion and adhesion to the host tissues. To date, the regulatory mechanisms governing *S. agalactiae* switching from a harmless commensal to an invasive pathogen are still not completely understood.

The aim of this work was to investigate whether the transcriptional regulator CodY plays a role in controlling and coordinating metabolism and virulence in *S. agalactiae*. CodY is a global regulator of gene expression highly conserved in low-G+C Gram-positive bacteria. Since its affinity for DNA is increased by its interaction with GTP and branched chain amino acids (BCAAs), the variety of metabolic genes that are under its control are regulated according to the nutritional status of the cell. In pathogens, CodY coordinates metabolism and virulence in a species-specific manner by directly and indirectly controlling genes involved in bacterial pathogenesis (Brinsmade, 2017). Despite the role of CodY in governing bacterial virulence has previously been studied in several bacterial species, including Streptococci, its role in *S. agalactiae* has never been investigated to date.

In *Streptococcus suis* and *Streptococcus salivarius*, for example, CodY was shown to be essential for virulence (Feng *et al,* 2016; Geng *et al*, 2018). In this work, with the aim to investigate whether CodY plays a role in *S. agalactiae* virulence, the ability of the *codY* deletion mutant to cause infection in several murine infection models resembling neonatal infection, sepsis and meningitis was tested. Moreover, virulence-related characteristics of the mutant strains associated to its ability to colonize the host were assessed *in vitro*. These included its ability of adhere and invade epithelial cell monolayers, bind extracellular matrix and plasma components and form biofilms.

To decipher the regulatory role of CodY in *S. agalactiae*, in this work the entire *S. agalactiae* CodY regulon was identified. To this purpose, a transcriptomic analysis of a marker-less, *codY* deletion mutant of the hypervirulent *S. agalactiae* strain BM110 was performed. As CodY can control gene expression through direct and indirect activity, the mechanisms of CodY-mediated regulation at specific target

genes playing relevant roles in bacterial metabolism and virulence was investigated. To this goal, gel-shift and β-galactosidase assays were performed to evaluate direct interaction between CodY and the regulatory region of controlled genes. Importantly, the effects of BCAAs availability on the regulatory activity of *CodY* was investigated since in all the species in which this protein has been described so far, its regulatory ability has been demonstrated to be dependent on the availability of BCAAs. As the abundance of these universal cofactors varies, the fraction of CodY active molecules changes accordingly, thus creating a hierarchy in gene expression which depends on the relative affinity of CodY for its targets.

In *Staphylococcus aureus*, for example, when the bacterium encounters limiting amounts of BCAAs at the infection site, CodY-mediated regulation is relieved even at sites that are bound with very high affinity, thus leading to the activation of CodY-repressed virulence genes and to the consequent trigger of bacterial virulence (Brinsmade, 2017). Hence, nutrients availability is perceived by the cell as a key signal for regulation of virulence and the cascade of gene regulation that is initiated in response to decreased availability of BCAAs is controlled by CodY. On these premises, as *S. agalactiae* displays auxotrophy for BCAAs and relies on their uptake from the extracellular environment for survival, the regulatory mechanisms controlling the expression of BCAAs and oligopeptide transporters in this bacterium were subjected to careful analysis. This is particularly relevant if we consider that, during growth in amniotic fluid, *S. agalactiae* encounters low concentrations of BCAAs (Mesavage *et al*, 1985). Gene-expression analyses highlighted that in this environment *codY* expression is strongly downregulated, while genes encoding BCAA transporters are overexpressed (Sitkiewicz *et al,* 2009).

Global responses, like the regulation of metabolism and virulence, require the interplay of different regulatory networks. CodY activity is exerted in coordination with other transcriptional regulators: many targets of CodY-mediated regulation are controlled also by other factors and CodY is able to control the activity of other regulators by acting both at transcriptional and post-transcriptional level (Belitsky *et al,* 2015; Pendleton *et al*, 2022). In particular, CodY-mediated regulation of virulence is often a result on indirect regulation through regulation of the levels of key virulence regulators. For instance, in *Streptococcus pyogenes*, by repressing the expression of the genes encoding the CovRS two-component system, CodY counteracts the activity of this master regulator of virulence, acting as an indirect activator of the ability of the bacterium to cause disease (Kreth *et al*, 2011). Here, preliminary investigations of the potential interplay of CodY and CovR in the regulation of gene expression in *S. agalactiae* were performed.

3. Materials and methods

3.1 Bacterial strains, plasmids and culture conditions

Bacterial strains and plasmids used in this work are listed in Tables 1 and 2.

TABLE 1. Bacterial strains used in this study

S. agalactiae			
Strain	**Relevant Genotype**	**Plasmid**	**Source or Reference**
BM110	Serotype III, ST-17, human hypervirulent clinical isolate		Tazi *et al,* 2010
Δ*codY*	BM110 carrying in-frame *codY* deletion		This study
BM1102	BM110	pTCVΩP_{tet}	This study
BM1104	BM110*codY*	pTCVΩP_{tet}	This study
BM1105	BM110*codY*	pTCVΩP_{tet}_*codY*	This study
BM1106	BM110	pTCV-*lacZ_livK*p_{220}	This study
BM1107	BM110*codY*	pTCV-*lacZ_livK*p_{220}	This study
BM1108	BM110	pTCV-*lacZ_srr2*p_{615}	This study
BM1109	BM110*codY*	pTCV-*lacZ_srr2*p_{615}	This study
BM1110	BM110	pTCV-*lacZ_srr2*p_{398}	This study
BM1111	BM110*codY*	pTCV-*lacZ_srr2*p_{398}	This study
BM1114	BM110	pTCV-*lacZ_livK*$p1_{220}$	This study
BM1115	BM110*codY*	pTCV-*lacZ _livK*$p1_{220}$	This study
BM1116	BM110	pTCV-*lacZ _srr2*$p1_{615}$	This study
BM1117	BM110*codY*	pTCV-*lacZ _srr2*$p1_{615}$	This study
BM1118	BM110	pTCV-*lacZ _srr2*$p2_{615}$	This study
BM1119	BM110*codY*	pTCV-*lacZ _srr2*$p2_{615}$	This study
BM1120	BM110	pTCV-*lacZ* _srr2$p1,2_{615}$	This study
BM1121	BM110*codY*	pTCV-*lacZ _srr2*$p1,2_{615}$	This study
BM1124	BM110	pTCV-*lacZ _srr2*$p3_{615}$	This study
BM1125	BM110*codY*	pTCV-*lacZ _srr2*$p3_{615}$	This study
BM1128	BM110 *ΔcovR*		This study
BM1129	BM110 *ΔcodY ΔcovR*		This study

BM1130	BM110 *ΔcovR*	pTCV-*lacZ _srr2*p$_{398}$	This study
BM1131	BM110 *ΔcodY ΔcovR*	pTCV-*lacZ _srr2*p$_{398}$	This study
BM1134	BM110 *ΔcovR*	pTCV-*lacZ _srr2*p$_{615}$	This study
BM1135	BM110 *ΔcodY ΔcovR*	pTCV-*lacZ _srr2*p$_{615}$	This study
BM1144	BM110 *Δsrr2*		This study
BM1145	BM110 *ΔcodY Δsrr2*		This study
BM1150	BM110	pTCV-*lacZ _brnQ*p	This study
BM1151	BM110*codY*	pTCV-*lacZ _brnQ*p	This study
BM1152	BM110	pTCV-*lacZ _brnQ*p1	This study
BM1153	BM110*codY*	pTCV-*lacZ _brnQ*p1	This study
BM1164	BM110	pTCV-*lacZ _srr2*p$_{371}$	This study
BM1165	BM110*codY*	pTCV-*lacZ _srr2*p$_{371}$	This study
BM1166	BM110 *ΔcovR*	pTCV-*lacZ _srr2*p$_{371}$	This study
BM1167	BM110 *ΔcodY ΔcovR*	pTCV-*lacZ _srr2*p$_{371}$	This study
BM1182	BM110	pTCV-*lacZ _srr2*p3$_{371}$	This study
BM1183	BM110*codY*	pTCV-*lacZ _srr2*p3$_{371}$	This study
BM1184	BM110 *ΔcovR*	pTCV-*lacZ _srr2*p3$_{371}$	This study
BM1185	BM110 *ΔcodY ΔcovR*	pTCV-*lacZ _srr2*p3$_{371}$	This study
E. coli			
Strain	**Genotype**		**Source or Reference**
XL-1 Blue	*recA1 endA1 gyrA96 thi-1 hsdR17 supE44 relA1 lac [F′proAB lacI^{q} ZΔM15 Tn10 (Tet^{r})]*		Agilent
BL21(DE3)	*B F– ompT gal dcm lon hsdSB(rB–mB–) λ (DE3 [lacI lacUV5-T7p07 ind1 sam7 nin5]) [malB+]K-12(λS)*		

TABLE 2. List of plasmids used in this study

Plasmid	**Resistance**	**Relevant properties**	**Source or Reference**
pG1	Erythromycin	This plasmid contains a temperature sensitive origin of replication for *S. agalactiae* and a ColE1 origin of replication for *E. coli*.	(Devaux *et al,* 2018)
pG1-Δ*codY*	Erythromycin	pG1 carrying the *codY* deletion cassette.	This study
pTCVΩP_{tet}	Kanamycin/ Erythromycin	GBS expression vector carrying a constitutive P_{tet} promoter	(Firon *et al*, 2013)
pTCVΩP_{tet}_*codY*	Kanamycin/ Erythromycin	pTCVΩP_{tet} containing the full length *codY* ORF cloned between the *Bam*HI/*Pst*I restriction sites.	This study
pTCV-*lacZ*	Kanamycin/ Erythromycin	Vector for the construction of transcriptional fusions to β-galactosidase in Gram-positive bacteria.	(Poyart and Trieu-Cuot, 1997)
pTCV-*lacZ_livK*p$_{220}$	Kanamycin/ Erythromycin	pTCV-*lacZ* carrying a 220 bp sequence which comprises the regulatory region of the *livK* gene cloned between the *Eco*RI/*Bam*HI restriction sites of the plasmid.	This study
pTCV-*lacZ_livK*p1$_{220}$	Kanamycin/ Erythromycin	pTCV-*lacZ_livK*p$_{220}$ carrying a double nucleotide substitution in one of the two CodY motifs located upstream of *livK*.	This study
pTCV-*lacZ_brnQ*p	Kanamycin/ Erythromycin	pTCV-*lacZ* carrying a 250 bp sequence which comprises the regulatory region of the *brnQ* gene cloned between the *Eco*RI/*Bam*HI restriction sites of the plasmid.	This study
PTCV-*lacZ_brnQ*p1	Kanamycin/ Erythromycin	pTCV-*lacZ_brnQ*p carrying a double nucleotide substitution mutation in the CodY motif located upstream of *brnQ*.	This study
pTCV-*lacZ_srr2*p$_{398}$	Kanamycin/ Erythromycin	pTCV-*lacZ* carrying a 398 bp sequence, spanning from position -115 to +283 with respect to the *srr2* transcription start site, comprising the downstream putative CodY binding motif, cloned between the	This study

		*Eco*RI/*Bam*HI restriction sites of the plasmid.	
pTCV-*lacZ_srr2*p$_{615}$	Kanamycin/ Erythromycin	pTCV-*lacZ* carrying a 615 bp sequence which comprises the regulatory region of the *srr2* gene, spanning from position −332 to +283 with respect to the *srr2* transcription start site, cloned between the *Eco*RI/*Bam*HI restriction sites of the plasmid.	This study
pTCV-*lacZ_srr2*p1$_{615}$	Kanamycin/ Erythromycin	pTCV-*lacZ_srr2*p$_{615}$ carrying the p1 double nucleotide substitution mutation in the downstream CodY binding motif located upstream of *srr2*.	This study
pTCV-*lacZ_srr2*p2$_{615}$	Kanamycin/ Erythromycin	pTCV-*lacZ_srr2*p$_{615}$ carrying a the p2 double nucleotide substitution mutation in the upstream CodY binding motif located upstream of *srr2*.	This study
pTCV-*lacZ_srr2*p1,2$_{615}$	Kanamycin/ Erythromycin	pTCV-*lacZ_srr2*p$_{615}$ carrying the p1 and p2 mutations in the downstream and upstream CodY binding motifs.	This study
pTCV-*lacZ_srr2*p3$_{615}$	Kanamycin/ Erythromycin	pTCV-*lacZ_srr2*p$_{615}$ carrying a triple nucleotide substitution mutation in the upstream CodY binding motif located upstream of *srr2*.	This study
pTCV-*lacZ_srr2*p$_{371}$	Kanamycin/ Erythromycin	pTCV-*lacZ* carrying a 371 bp sequence, spanning from position -115 to +283 with respect to the *srr2* transcription start site, cloned between the *Eco*RI/*Bam*HI restriction sites of the plasmid.	This study
pTCV-*lacZ_srr2*p3$_{371}$	Kanamycin/ Erythromycin	pTCV-*lacZ_srr2*p3$_{371}$ carrying a triple nucleotide substitution mutation the CodY motif located upstream of *srr2*.	This study
pET28a	Kanamycin		Novagen
pET28a-*codY*	Kanamycin	pET28a carrying the full length *codY* ORF.	This study

Streptococcus agalactiae was cultured in Todd Hewitt (TH, Difco Laboratories) supplemented with 5 g/liter of yeast extract (THY) or in chemically defined medium (CDM, Table 3) (Willet and Morse, 1966) at 37°C, 5% CO_2, under steady state conditions. CDM composition is reported in Table 3. All components were purchased from Sigma (St. Louis, USA).

Escherichia coli XL-1 Blue was used for cloning experiments and isolation of plasmids. *E. coli* BL21(DE3) was used for protein expression. *E. coli* strains were cultured in Luria Bertani (LB) broth at 37°C with vigorous shaking (200 rpm).

Media were solidified with 1.6 % agar. Antibiotics were used at the following concentrations: for *E. coli*, kanamycin 50 µg/ml; erythromycin 150 µg/ml; for *S. agalactiae*: kanamycin 1 mg/ml; erythromycin 10 µg/ml.

Table 3. Chemically defined medium composition

Component	**Concentration**
Fe $(NO_3)_3 \cdot 9H_2O$	2.5 mM
$FeSO_4 \cdot 7H_2O$	18 mM
$MgSO_4 \cdot 7H_20$	3 mM
$MnSO_4 \cdot H_2O$	0.03 mM
$NaC_2H_3O_2 \cdot 3H_20$	33 mM
$CaCl_2$	46 µM
L-cysteine HCl	40 µM
NaHCO	30 mM
glucose	10 g/l
Phosphate stock (10 X)	
K_2HPO_4	11 mM
KH_2PO_4	74 mM
$NaH_2PO_4 \cdot H_2O$	0.6 M
$Na_2HPO_4 \cdot 7H_2O$	1.3 M
Bases stock (100 X)	
Adenine	2 mg/ml
Guanine hydrochloryde	2 mg/ml
Uracil	2 mg/ml
Aminoacids stock (50 X)	
DL-alanine	5 g/L
L-arginine	5 g/L
L-aspartic acid	5 g/L
L-asparagine	5 g/L
L-cystine	2.5 g/L
L-glutamic acid	5 g/L
L-glutamine	10 g/L
Glycine	5 g/L
L-histidine	5 g/L
L-lysine	5 g/L
L-methionine	5 g/L
L-phenylalanine	5 g/L
L-proline	5 g/L
L-serine	5 g/L
Hydroxy-L-proline	5 g/L
L-serine	5 g/L

L-threonine	10 g/L
L-tryptophan	5 g/L
L-tyrosine	5 g/L
Vitamins stock (1000 X)	
p-aminobenzoic acid	0.2 mg/ml
Biotin	0.2 mg/ml
Folic acid	0.16 mg/ml
Niacinamide	0.2 mg/ml
b-nicotinamide adenine dinucleotide phosphate	0.5 mg/ml
Pantothenate calcium salt	0.4 mg/ml
Pyridoxal	0.2 mg/ml
Pyridoxamine dihydrochloride	0.2 mg/ml
Riboflavin	0.4 mg/ml
Thiamine hydrochloryde	0.2 mg/ml
Vitamin B12	0.02 g/ml

L-isoleucine, L-leucine and L-valine were prepared separately as a 5 g/L stock solution and added to CDM medium at proper concentrations.

Table 4. List of primers used in this work

Name	Sequence (5'-3')
Primers used for qRT-PCR	
braBF	TCTGGTGCTATCGCTACATTTC
braBR	CCCACCGTCTATTGGAGTATTG
brnQF	TGTGCCTAGTAGGAGGGTAATA
brnQR	TTCCACCAGCATTAGGTGTAG
GBS_livK_F	CTCCGCTGGTGATACTGATTT
GBS_livK_R	CGGTATAGTAACCTGGCATCAC
NEM_gyrA_F	AAAGGGTCGTGGTGGTAAAG
GBS_gyrA_R	TAATCGTCACTAAGCGTGCTAATG
Primers used for *lacZ* transcriptional fusions	
livKp220F	CAAAATAGATATGAACAAATGAATTCGATATTGATC AGGATTTTGTTGGA
livKp220R	GTGTATCAACAAGCTGGGGATCCCGCTCCTAAACTA AGTCTCTTTTCCA
srr2p398	CAAAATAGATATGAACAAATGAATTCCAATAGTAG CGAAGAAGAACACTATG
srr2p615	CAAAATAGATATGAACAAATGAATTCGTCATGTCTC TAAATACCCCTAGT
brnQpF	CAAAATAGATATGAACAAATGAATTCGTGGCAAAT GGATCAATTATTGG
brnQpR	TAGTGTATCAACAAGCTGGGGATCCCGTTAAAAAG CCTTTTTTTACC
srr2pR	GTGTATCAACAAGCTGGGGATCCGTTTCCAAACTGC TTTTTTAACAT
srr2p371R	GTGTATCAACAAGCTGGGGATCCGCTTCTTTCTAAT CTAAATAAGGTG
Internal mutagenic primers for *lacZ* transcriptional fusions	
livKp1F	CAATTTAAAAACTATTGACAATATTCTCCTAATTCT GTATTATTTTAGTTAC
livKp1R	GTAACTAAAATAATACAGAATTAGGAGAATATTGT CAATAGTTTTTAAATTG
brnQp1F	GAATAGTTGGAAAATTATCCAAATGACCTAGAATT
brnQp1R	AATTCTAGGTCATTTGGATAATTTTCCAACTATTC
srr2p1F	GCAATAGTTGATTTAATTTTCACCAGAGAGGAAGAA TTGTTTATTGTAGC
srr2p1R	GCTACAATAAACAATTCTTCCTCTCTGGTGAAAATT AAATCAACTATTGC
srr2p2F	CTAATTTTATATTTTTTATAATTTACTCCAAATTAAC ATATAATGATGATAGTG
srr2p2R	CACTATCATCATTATATGTTAATTTGGAGTAAATTA TAAAAAATATAAAATTAG
srr2p3F	CTAATTTTATATTTTTTATAATTTAGTCCAAATTAAC ATATAATGATGATAGTG

srr2p3R	CACTATCATCATTATATGTTAATTTGGACTAAATTATAAAAAATATAAAATTAG
Primers used for fragments labeling	
Vlac1-FAM	GTTGAATAACACTTATTCCTATC
Vlac2-FAM	CTTCCACAGTAGTTCACCACC
Primers used for *S. agalactiae* Δ*codY* construction	
BM_codYFusR	CGCAAAACATACAAAGGATGAAGGAATCATAGCATGGGACTGGGAGTAGC
BM_codYFusF	GCTACTCCCAGTCCCATGCTATGAtTCCTTCATCCTTTGTATGTTTTGCG
pG1R	GAATTCGTAATCATGGTCATAG
pG1F	GAGCTCGGTACCCGGGGA
pG1_codYUpF	ATGACCATGATTACGAATTCGTTAGCTAACATGAGGCTG
pG1_BM_codYDwR	GATCCCCGGGTACCGAGCTCCATTTAAGCTGGCTACAGC
COH1_1525FUp	GCTGGACACGGCTTTTATGATTACG
COH1_1527RDw	CCCAATTGCTTCTATTGCAGAGG
M13For	TTGTAAAACGACGGCCAGT
M13Rev	CAGGAAACAGCTATGACC
Primers used for *covR* in-frame deletion in *S. agalactiae* genome	
pG1covRUpF	CACATAGCCCATTCCGCGGTCCAATCCTTCACGACCG
pG1covRUpR	GGAAACAGCTATGACCATGATTACGAATTCCTTCGTGTTCTGGCAGCTGA
pG1covRDwF	GCATGCCTGCAGGTCGACTCTAGAGGATCCCCTTCCATATCTGCAACTTTAGAG
pG1covRDwR	CGGTCGTGAAGGATTGGACCGCGGAATGGGCTATGTG
Primers used for *srr2* in-frame deletion in *S. agalactiae* genome	
pG1srr2UpF	CTGAAGCCGAGTTATCACCTGTCATAACACTTTTGACCCAGTG
pG1srr2UpR	GGAAACAGCTATGACCATGATTACGAATTCGAGAGCGGCTATTTATTTTTAG
pG1srr2DwF	GCATGCCTGCAGGTCGACTCTAGAGGATCCGAAACACCATATGCTTGTATAAC
pG1srr2DwR	CACTGGGTCAAAAGTGTTATGACAGGTGATAACTCGGCTTCAG
Primers used for *codY* complementation	
pTCV_codYF_Bam	TGATGGATCCCGCAAAACATACAAAGGATGAAGGAA
pTCV_codYR_Pst	TGATCTGCAGGCTACTCCCAGTCCCATGCTATGA
Primers used for *codY* cloning in pET28a	
pET_GBS_codYF	AGCAAATGGGTCGCGGATCCATGCCGAATTTATTAGAAAAAAC
pET_GBS_codYR	TGTCGACGGAGCTCGAATTCTTAATTATATTCTTTTAATTTGTCAAAAATACC

3.2 Growth curves

Overnight cultures of *S. agalactiae* strains grown in THY medium were diluted to a starting OD_{600} of 0.05 in the same medium. Every 30 minutes, the OD_{600} was monitored using a spectrophotometer and dilutions of the bacterial cultures were plated on THY agar plates for CFU counting. Growth curves were performed in biological triplicate. For bacterial cultures in CDM, overnight cultures of *S. agalactiae* strains grown in THY medium were firstly diluted to an initial OD_{600} of 0.05 in THY medium. Once bacteria reached the exponential phase of growth (OD_{600}= 0.5), cultures were centrifuged at 4000 rpm for 10', washed with PBS and resuspended in CDM at an initial OD_{600} of 0.05. Bacterial growth was followed every 30 minutes by monitoring the OD_{600} of the culture.

3.3 Strains construction

Chromosomal DNA of *S. agalactiae* BM110 strain was purified with DNeasy Blood and Tissue kit (Qiagen) and used as template in PCR reactions. All oligonucleotides used in this study are listed in Table 4. Analytical PCRs were performed using DreamTaq DNA polymerase (ThermoFisher Scientific). In preparative PCRs for cloning, a high-fidelity pfu polymerase was employed (Phusion DNA polymerase, ThermoFisher Scientific).

To construct a marker-less *codY* deletion mutant of *S. agalactiae* BM110, two DNA regions upstream and downstream of the targeted gene were amplified and fused by overlap extension PCR. The upstream fragment was amplified using primers pG1_codYUpF and BM_codYFusR, the downstream fragment was amplified with oligonucleotides pG1_BM_codYDwR and BM_codYFusF. The fusion product was obtained through overlap extension PCR performed using pG1_codYUpF and pG1_BM_codYDwR primers (Table 4). The ends of the resulting fragment were complementary to the regions upstream of the *Eco*RI site and downstream of the *Bam*HI site of the pG1 plasmid, respectively. The temperature-sensitive pG1 plasmid (Devaux *et al*, 2018) was amplified with the divergent oligonucleotides pG1R and pG1F. The resulting fragments, displaying overlapping regions, were joined by Gibson assembly (NEBuilder HiFi DNA Assembly Cloning Kit, New England Biolabs) reaction. Two µl of the reaction mixture were used for *E. coli* XL-1 Blue electroporation. Recombinant clones were screened by colony PCR using primers M13For and M13Rev which anneal on pG1 plasmid 51 bp upstream and 26 bp downstream of the fragment insertion site (Table 4). The obtained pG1-Δ*codY* plasmid was verified by sequencing and used for electroporation of *S. agalactiae* BM110 (Table 2). Transformants were selected by growing on TH agar plates containing erythromycin at 30°C. Plasmid integration into the bacterial genome was mediated by isolating transformants on TH agar plates containing erythromycin (Ery) at 37°C. Integrants were further isolated to single colonies, on the same selective medium, and incubated at 37°C. Plasmid excision was favored by growing cells 30°C in TH without erythromycin. After five subsequent passages of culture in the same

conditions, aliquotes were plated on TH agar plates. Ery sensitive clones were selected and used as template in colony PCRs aimed at determining whether plasmid excision led to a "back-to-wild-type" phenotype or to the excision of the desired sequence. The in-frame *codY* deletion was confirmed on genomic DNA by PCR (primers COH1_1525FUp and COH1_1527RDw) and sequencing. The resulting strain was named Δ*codY* (Table 1).

For complementation of *codY* deletion, the *codY* gene was amplified with oligonucleotides pTCV_codYF_Bam and pTCV_codYR_Pst. The obtained fragment was cloned between the *Bam*HI and *Pst*I sites of the pTCVΩPtet vector (Buscetta *et al*, 2016). The resulting pTCVΩPtet_*codY* plasmid was verified by sequencing and used to electroporate the Δ*codY* strain, obtaining BM1105 (Table 1). Two control strains, BM1102 and BM1104, were prepared by electroporation of the empty pTCVΩPtet plasmid into wild-type and Δ*codY* strains, respectively (Table 1). Transformants were selected on TH agar plates supplemented with kanamycin.

The pG1-Δ*covR* vector was prepared to insert an in-frame deletion of *covR* (deleted region length: 537 bp, nucleotides from 1,603,597 to 1,604,133 on the BM110 genome, Accession: NZ_LT714196.1). Genomic regions located upstream and downstream of the *covR* target sequence were amplified using primers pG1covRUpR x pG1covRUpF (513 bp) and pG1covRDwF x pG1covRDwFR (483 bp), respectively (Table 4). The obtained fragments were inserted by Gibson Assembly in the pG1 plasmid previously digested with *Eco*RI and *Bam*HI restriction enzymes. The pG1-Δ*covR* plasmid (Table 2) was obtained after electroporation of *E. coli* XL-1 Blue cells with 2 µl of the Gibson reaction mixture and selection of recombinant clones by colony PCR (M13For and M13Rev primers) and sequencing. The pG1-Δ*covR* plasmid was introduced by electroporation in the wild-type and Δ*codY S. agalactiae* strains. Plasmid integration and excision events were performed as previously described for the preparation of the Δ*codY* strain. Derivatives of the WT and Δ*codY* strains carrying the in-frame *covR* deletion were confirmed by sequencing and named BM1128 (*S. agalactiae* carrying *covR* deletion) and BM1129 (Δ*codY* strain carrying *covR* deletion) (Table 1).

The pG1-Δ*srr2* vector was prepared by Gibson assembly to insert an in-frame deletion of *srr2* in the wild-type and Δ*codY* strains (deleted region length: 3429 bp, nucleotides from 1,376,970 to 1,373,542 on the BM110 genome, Accession: NZ_LT714196.1). Genomic regions located upstream and downstream of *srr2*, were amplified by PCR using primers pG1srr2UpF x pG1srr2UpR (717 bp) and pG1srr2DwF x pG1srr2DwR (567 bp), respectively (Table 4). Upstream and downstream *srr2* regions were fused to the pG1 plasmid previously digested with *Eco*RI and *Bam*HI restriction enzymes. The pG1-Δ*srr2* (Table 2) plasmid was obtained after electroporation of *E. coli* XL-1 Blue cells with 2 µl of the Gibson reaction mixture and selection of recombinant clones by colony PCR (M13For and M13Rev primers) and sequencing. Strains with the resulting in-frame *srr2* deletion,

obtained through allelic replacement after plasmid integration and excision, were confirmed by sequencing of the region encompassing the *srr2* gene and named BM1144 (*S. agalactiae* carrying *srr2* deletion) and BM1145 (Δ*codY* strain carrying *srr2* deletion) (Table 1).

3.4 Time-Lapse Microscopy and Single-Cell Image Analysis

Agarose pads were spotted with 5 µl of a 1:10 dilution of *S. agalactiae* cell cultures collected at mid-log phase of growth (OD_{600} 0.5 in THY medium), flipped and transferred to an imaging dish sealed with parafilm (Young *et al,* 2011). Time-lapse imaging was performed using a Leica DMi8 widefield microscope, equipped with a 100× oil immersion objective (Leica HC PL Fluotar 100×/1.32 OIL PH3), a Leica DFC9000 sCMOS camera and driven by Leica LASX software. Experiments were conducted using an environmental microscope incubator set at 37°C and bacteria were imaged in phase contrast, every 5-min up to 6 h. Manual segmentation of individual cells and analysis of image stacks were performed using the ImageJ 1.52a software, as previously described (Manina *et al*, 2015). Data were analysed using Prism 9.

3.5 Mouse Infection Models

For the neonatal model of infection, 48-h-old mice of both sexes were inoculated subcutaneously with 8×10^4 CFU of the wild-type or the Δ*codY* strain, as previously described (Biondo *et al*, 2014). Mice that started displaying clear signs of disease, such as diffuse redness spreading from the inoculation site, were humanely euthanized. In the adult model of *S. agalactiae* sepsis, 8-week-old female mice were inoculated intraperitoneally with 5×10^8 CFU of the wild-type or the Δ*codY* cells, as previously described (Biondo *et al,* 2014). Lastly, in the meningitis model of infection, 8-week-old female mice were inoculated intravenously 1×10^9 CFU of WT or the Δ*codY* strain, as previously described (Lentini *et al,* 2018). Mice showing signs of irreversible disease, such as inactivity, prolonged hunching, or neurological symptoms were humanely euthanized. For bacterial burden determination in organs of infected mice, animals were euthanized at 16 h after challenge and bacterial burden was determined in organ homogenates, as previously described (Famà *et al,* 2020).

3.6 *In vivo* and *in vitro* Cytokine Induction

Eight weeks old female mice were infected intraperitoneally with 1×10^9 CFU of the wild-type or the Δ*codY* strain. Mice were treated at 30 min post-challenge with penicillin (500 IU i.p.) in order to prevent bacterial overgrowth. Peritoneal lavage fluids were collected at the indicated times and analyzed for cytokine levels as previously described (Mohammadi *et al*, 2016). For *in vitro* cytokine induction, bone marrow-derived macrophages were obtained from 8-week-old female mice and

cultured in the presence of M-CSF (macrophage colony-stimulating factor) as previously described (Lentini *et al*., 2021). Macrophage cultures were then stimulated for 1 h with *S. agalactiae* grown to the late exponential phase at the indicated multiplicities of infection (MOI). Cultures were then treated with penicillin and gentamycin (100 IU and 50 µg/ml) to kill extracellular bacteria and supernatants were collected 18 h after culture, as previously described (Lentini *et al.,* 2021). Cytokine levels were measured in peritoneal lavage fluid samples or culture supernatants by ELISA, using Mouse TNF-alpha DuoSet ELISA DY410, Mouse IL-1 beta/IL-1F2 DuoSet ELISA DY401, Mouse CXCL2/MIP-2 DuoSet ELISA DY452, Mouse CXCL1/KC DuoSet ELISA DY453 (R&D Systems).

3.7 RNA-sequencing and analysis

For RNA-sequencing and analysis, total RNA was extracted from wild-type and Δ*codY* strains during exponential phase of growth in THY medium. Samples of each strain were collected from four independent growth experiments, each performed in the same condition. RNA samples were treated with Turbo DNAseI (Life technologies) and QIAseq FastSelect –5S/16S/23S Kit (QIAGEN) for DNA and rRNA depletion, respectively. RNA was sequenced using Illumina sequencing technology (BMR-Genomics, Padova). For RNA-Seq data analysis, raw reads were quality checked using FASTQC1 and processed by Trimmomatic (Bolger *et al,* 2014) to trim the adaptor sequences and remove low-quality reads. Clean reads were mapped onto the reference genome of *S. agalactiae* BM110 (Accession: NZ_LT714196.1) using Bowtie2 (Langmead, 2010). To quantify the known transcripts, the alignment results were input into featureCounts (Liao *et al,* 2014). Lastly, the R package DESeq2 (Love *et al*, 2014) was used to test for differential expression. Genes were defined as differentially expressed using the following criteria: $|\text{Log2 Fold Change}| \geq 1$ and adjusted p-value FDR < 0.05. Prediction of orthologous groups was performed using COGnitor (Tatusov, 2000).

3.8 RNA preparation and quantitative real-time-PCR (qRT-PCR)

S. agalactiae total RNA extraction was performed using the Quick-RNA Fungal/Bacterial Miniprep Kit (Zymo Research) as described in the instructions provided by the manufacturer. Total RNA was isolated from *S. agalactiae* wild-type and Δ*codY* cells collected during the exponential phase of growth (OD_{600} of 0.4-06) in THY medium or in CDM medium supplemented with Isoleucine, Leucine and Valine amino acids (50 or 1500 mM). Traces of genomic DNA were removed from samples using the Turbo DNA-free DNase treatment and removal kit (Ambion). For qRT-PCR analysis, samples were collected from two independent growth experiments. Reverse transcription and quantitative real-time PCR were performed in a single step using the iTaq Universal SYBR Green One-Step Kit (Bio-Rad). The

reactions were performed in 20 µl volumes using 4 ng of DNase I treated RNA, according to the manufacturer's protocol. All reactions were carried out on three replicates. The analysis on cDNA was carried out using 400 nM primers relative to the *livK*, *braB* and *brnQ* coding sequences (Table 4). RNA was retrotranscribed at 50°C for 10 min and the reaction mixture was then incubated at 95°C for 1 min followed by 35 amplification cycles with 95°C for 10 sec and 55°C for 30 sec. No-template controls were run on each plate for each assay, and specificity of each amplification product was verified using melting curve analysis. Standard curves were generated from serial dilutions of RNA. All reactions proceeded within 90% to 110% efficiency. The expression of target genes was normalized using the housekeeping *gyrA* gene as reference.

3.9 Mammalian Cell cultures and epithelial adhesion and invasion assays

A549 cells and HeLa cells were routinely grown in 75 cm^2 flasks in Dulbecco's modified Eagle's medium (DMEM) supplemented with 10% fetal bovine serum (FBS) at 37°C in 5% CO_2. For bacterial adhesion and invasion assays, cells were seeded at 2 x 10^5 cell density per well in 24-well tissue culture plates and cultured in DMEM without antibiotics. Monolayers were used after 24 hours of incubation.

Bacteria grown for 16 h under at 37°C, 5% CO_2 in THY medium were diluted to an initial OD_{600} of 0.05 and grown to exponential phase (OD_{600}=0.4-0.6) before being collected by centrifugation (4400 rpm, 10 min), washed with Phosphate Buffered Saline (PBS) and resuspended in DMEM containing 10% FBS. Confluent cell monolayers were then washed once with PBS and infected with bacteria at a multiplicity of infection (MOI) of 10 bacteria per cell. To determine the total number of associated CFU (both adherent and internalized), after two hours of incubation at 37°C and 5% CO_2, the culture medium was removed, cells were washed three times with PBS and lysed with 0.1% ice-cold Tryton X-100 solution by repeated pipetting. Serial dilutions of the epithelial cell lysates were plated onto TH agar plates and adhesion levels were determined the following day by counting bacterial CFU. Percent of adhesion of each strain was calculated as follows: (number of CFUs on plate)/(number of CFUs of initial inoculum) × 100. Percentage of adhesion was normalized to the wild-type strain, set at 100%. To enumerate internalized bacteria, before cell lysis, the monolayers were further incubated for 2 h in medium supplemented with penicillin and streptomycin to kill extracellular bacteria. Bacterial invasion was calculated as: recovered CFU/initial inoculum CFU × 100. Percentage of invasion was normalized to the wild-type strain, set at 100%.

3.10 Biofilm formation assay

Bacterial biofilm formation was evaluated by Crystal Violet (CV) assay on polystyrene microtiter plates and through confocal microscopy analysis. For bacterial biofilm formation assays, a 1:20 dilution of an overnight culture grown in TH broth supplemented with 1% glucose and the appropriate antibiotic was used to inoculate (100 µl/well) a 96-well Tissue Culture Treated plate (16 technical replicates per strain). After 6 hours of incubation at 37°C, 5% CO_2, non-adherent bacteria were removed by washing with PBS and fresh medium was added. The plate was further incubated at 37°C with 5% CO_2 for additional 19 hours. Cell growth was quantified by reading the absorbance at OD_{600} with a plate reader. Wells were washed twice with PBS and attached cells were fixed with 100 µl methanol for 15 minutes. Wells were then air dried for 10 minutes and bacteria were fixed with 100 µl of 0.1% CV dissolved in water for 20 minutes. Wells were washed three times with PBS and cell bound CV was dissolved in 150 µl acetic acid (33%). Biofilm growth was evaluated by reading absorbance at 600 nm and normalizing the obtained value to the OD_{600} of the culture in the well.

For confocal microscopy analysis of biofilms, bacterial overnight cultures in TH broth supplemented with 1% glucose and the appropriate antibiotic were diluted in the same medium to an OD_{600} 0.05 (about 1×10^7 CFU/mL) and added to a four-well Nunc Lab-Tek II Chambered Coverglass. Non-adherent cells were removed after 6 h. After overnight growth, biofilms were washed twice with PBS and stained with 5 µM Syto 9 (Invitrogen). Cells were imaged with a Leica TCS SP8 confocal microscope equipped with a Leica DMi8 inverted microscope, a tunable excitation laser source (White Light Laser, Leica Microsystems, Germany), and driven by Leica Application Suite X, ver. 3.5.6.21594, using a 63× oil immersion objective (Leica HC PL APO CS2 63X/1.40). Images were acquired using a 488 nm laser line as an excitation source, and the fluorescence emitted was collected in a 500–540 nm range for Syto 9 as previously described (Trespidi *et al*, 2020). Biofilm images visualization and analysis was performed using ImageJ. Biofilm parameters were measured using the COMSTAT 2 software (Heydorn *et al,* 2000). All confocal scanning laser microscopy experiments were performed three times and standard deviations were measured.

3.11 Construction of pTCV-*lacZ* transcriptional fusions and β-galactosidase assays

Amplified fragments corresponding to *livK, brnQ* or *srr2* regulatory regions to be tested for CodY-binding and regulation were cloned by Gibson assembly between the *Eco*RI and *Bam*HI restriction sites of pTCV-*lacZ* plasmid (kind gift of Arnaud Firon, Institute Pasteur, France) (Table 2), carrying a spoVG RBS upstream of the promoter-less *lacZ* gene.

To investigate the contribution of specific nucleotides to CodY-binding and regulation, site-directed mutagenesis was performed by Gibson assembly. In the first step, the 5' part of the sequence to be mutagenized was amplified by using the forward primer used for cloning and a mutagenic, reverse oligonucleotide (Table 4). A product containing the 3' part of the regulatory region was similarly synthesized by using a forward mutagenic oligonucleotide and the reverse oligonucleotide used for cloning (Table 4). The two mutagenized, partially overlapping PCR products and the *Eco*RI/*Bam*HI digested pTCV-*lacZ* plasmid were then fused by Gibson using the NEBuilder HiFi DNA Assembly Cloning Kit (New England Biolabs).

For β-galactosidase assays, cells were harvested at different time points during exponential growth. Frozen pellets were resuspended in ice-cold Z-buffer (60 mM $Na_2HPO_4xH_2O$, 40 mM $NaH_2PO_4xH_2O$, 10 mM KCl, 1 mM $MgSO_4x7H_2O$, 50 mM 2-mercaptoethanol pH=7) and permeabilized with 0.5% (v/v) toluene and 4.5% (v/v) ethanol. β-galactosidase activity was assayed at 28°C using o-nitrophenyl-beta-D-galactopyranoside (ONPG) as substrate. Reaction was stopped with 1M Na_2CO_3. β-galactosidase activity was expressed in Miller Units and calculated as follows: (10^3 x (OD_{420} of the reaction mixture - 1.75 OD_{550} of the reaction mixture)) divided by (time of the reaction (min) x OD_{600} of the culture at the moment of harvesting x volume of the cell extract collected).

3.12 Purification of CodY

The *codY* CDS was amplified using pET_GBS_codYF and pET_GBS_codYR primers (Table 4) and inserted by Gibson assembly between the *Eco*RI and *Bam*HI restriction sites of the pET28a plasmid. The CodY protein with an N-terminal 6X-His tag was produced in in *E. coli* BL21(DE3) cells. Overnight starter culture was diluted 1:100 in LB medium containing Kanamycin (50 µg/ml) and incubated at 37°C with vigorous shaking until the culture reached an exponential phase (OD_{600} of 0.4-0.6). Iso-propyl 1-thio-β-D-galactopyranoside (IPTG) (0.5 mM) was added to the culture to induce recombinant protein expression. Bacterial cells were harvested by centrifugation after o/n growth at 28°C. Pellets were resuspended in lysis buffer (50 mM NaH_2PO_4, 300 mM NaCl, 1 mM PMSF, 20 µg DNase) and cells were lysed by repeated cycles of freezing with liquid nitrogen and defrosting with warm water. After removal of cell debris by centrifugation, CodY recombinant protein was purified from the supernatant by Ni2+-affinity chromatography using a HiTrap chelating column. Protein purity of 98% was estimated by SDS-PAGE and Coomassie Brilliant Blue Staining and protein concentration was measured by Bradford protein assay (Bio-Rad).

3.13 Electrophoretic Mobility Shift Assays (EMSA)

To be used as probes in gel-shift experiments, PCR products containing the regulatory region of the *livK, brnQ* or *srr2* genes were amplified using the appropriate pTCV-*lacZ* derivative plasmid as template and the 5'FAM labeled, vector specific primers Vlac1-FAM and Vlac2-FAM (Table 4).

EMSA assays were performed as previously described (Barbieri *et al*, 2015). Briefly, FAM-labeled promoter fragments (20 nM) were incubated with increasing concentrations of CodY in a CodY-binding buffer (20 mM Tris-Cl pH 8.0, 50 mM KCl, 2 mM $MgCl_2$, 5% glycerol 0.05%, Nonidet P-40, 25 μg/ml sonicated salmon sperm DNA, 0.5 mM EDTA, 1 mM DTT, 10 mM ILV). After 30 minutes of incubation at room temperature, samples were separated on 5% non-denaturing Tris-Glycine polyacrylamide gels. When indicated, BCAAs were added to the final concentration of 10 mM in the CodY-binding reaction mixture. Ten mM each of BCAAs were added to the 5% non-denaturing Tris-Glycine polyacrylamide gel and electrophoresis buffer as well.

For competitive or non-competitive assays, CodY incubation with FAM-labeled *livK* promoter fragment was performed in presence of non-labeled *livK* promoter fragment or non-labeled non-specific PCR fragment.

3.14 Enzyme-Linked Immuno-Sorbent Assay (ELISA) for *S. agalactiae* binding of host-cell proteins

To test *S. agalactiae* binding of fibrinogen, fibronectin or plasminogen host proteins, microtiter wells were coated overnight with increasing concentration of proteins at 4°C. The plates were washed three times with PBS. To block free protein binding sites, the wells were treated for 1 h at 22°C with BSA (2%, v/v) in PBS. The plates were then incubated for 1 h at 37°C with 100 μl/well of exponential-phase cells at a final OD_{600} of 1 in PBS. Bound bacteria were detected with rabbit anti-*S. agalactiae* IgG, followed by goat HRP-conjugated anti-rabbit IgG diluted 1:1000. After washing, o-phenylenediamine dihydrochloride was added, and the absorbance at 490 nm was determined using an ELISA plate reader (Bio-Rad, CA USA).

4. Results

4.1 Deletion of *codY* does not affect *S. agalactiae* growth *in vitro*

To study the role of CodY in *S. agalactiae*, a *codY* deletion mutant (Δ*codY*) was prepared in the hypervirulent CC17 wild-type strain BM110 (WT). The mutant was constructed by introduction of a marker-free, in-frame deletion of the *codY* gene by allelic replacement. Using the genome of BM110 as a template, the upstream and downstream DNA regions flanking the *codY* gene were amplified by PCR before being fused by overlapping PCR and cloned into the temperature sensitive pG1 vector to produce the pG1-Δ*codY* plasmid (See paragraph 3.3). BM110 cells were electroporated and pG1-Δ*codY* integration and excision events were performed as previously described (See paragraph 3.3) (Biswas *et al*, 1993). The marker-less deletion of *codY* was confirmed by sequencing.

The growth characteristics of the resulting Δ*codY* mutant in rich THY liquid medium were evaluated. Deletion of *codY* did not affect bacterial growth, as no defects were observed when comparing the growth curves of the WT and Δ*codY* strains (Fig. 12 A). When investigating the phenotypic properties of the Δ*codY* mutant through time-lapse microscopy analysis, we observed that it displayed a 10% decrease in bacterial cell size (Fig. 12 B) and formed smaller colonies compared with the WT strain (Fig. 12 C and D).

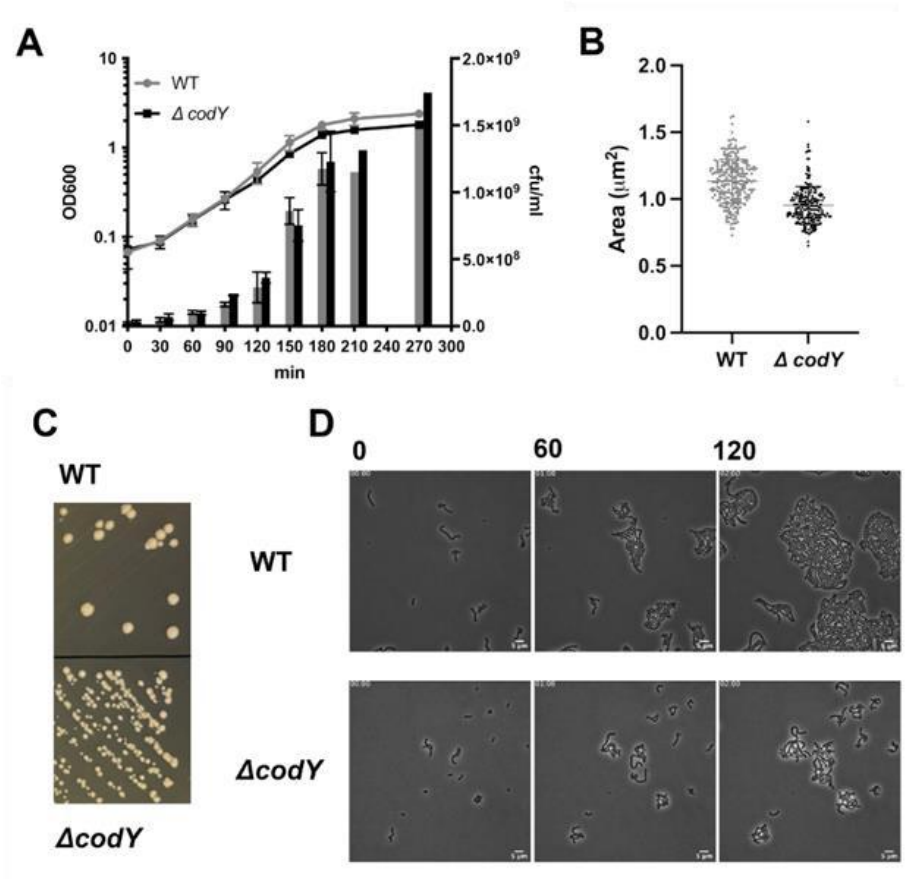

Figure 12. Deletion of *codY* does not alter *S. agalactiae* growth in liquid medium. A) Growth curves of the BM110 strain (WT) and of the *codY*-null mutant strain (Δ*codY*) in THY rich medium, evaluated as absorbance at OD_{600} (left axis) and cfu/ml (right axis) measured over time. Data are the average ± SD of two independent experiments. B) Single cell area measurements (μm^2) of 50 cells of each strain. Presented data refer to two independent experiments. Statistically significant differences are indicated (Welch's t-test). C) Colonies of the WT and Δ*codY* strains grown on THY agar plates. D) Contrast-phase image stacks of BM110 and Δ*codY* cells during time-lapse microscopy (0, 60, 120 minutes). Scale bar is 5 μm.

4.2 Investigating the role of CodY in *S. agalactiae* virulence *in vivo*

4.2.1 Deletion of *codY* decreases *S. agalactiae* virulence in mice

In order to investigate whether CodY plays a role in the pathogenicity of *S. agalactiae*, *in vivo* experiments were performed using several murine models of infection.

To mimick neonatal sepsis, neonate mice were injected subcutaneously with *S. agalactiae*. In this model, bacteria replicate at the inoculation site and spread systemically to blood and distant organs. Newborn mice infected with the WT strain displayed typical symptoms of irreversible infection within 24 h after the injection and were humanely euthanized. In contrast, nearly all neonates infected with the Δ*codY* strain survived and remained healthy until the end of the experiment (Figure 13 A). To determine whether the decreased lethality induced by the Δ*codY* mutant was associated with an impaired ability of the strain to invade and grow in the organs and tissues of newborn mice, bacterial counts were performed. As shown in Figures 13 B, C, D, blood, brain, and liver of mice infected with WT *S. agalactiae*, collected 14 h after infection, contained a consistent bacterial load, while the amounts of viable bacteria in the organs of mice infected with the *codY*-null strain were much lower or absent. The results indicate that *codY* deletion significantly impaired bacterial ability to replicate locally *in vivo* and to spread hematogenously to distal organs.

Considering the increasing number of cases of *S. agalactiae* diseases reported among adults, the data obtained in newborn mice were tested and confirmed in an adult model of infection as well. As already observed for neonate mice, adult mice intraperitoneally injected with the WT strain succumbed to overwhelming infection, while animals infected with the *codY*-null strain survived and remained healthy (Figure 13 E). Even in this model of infection, the bacterial burden detected in the organs of mice infected with the *codY*-null strain was consistently lower compared to that of WT strain (Figure 13 F-I).

Since *S. agalactiae* strains belonging to the hypervirulent CC17 lineage are associated to increased levels of meningitis development, a meningoencephalitis model of infection was created by intravenous injection of bacteria in mice. This model allowed to evaluate whether CodY is involved in *S. agalactiae* ability to cross the blood-brain barrier. The results revealed that in absence of *codY*, bacteria display a strongly decreased ability to persist in the blood and to cause lethal meningitis (Figures 13 J-L).

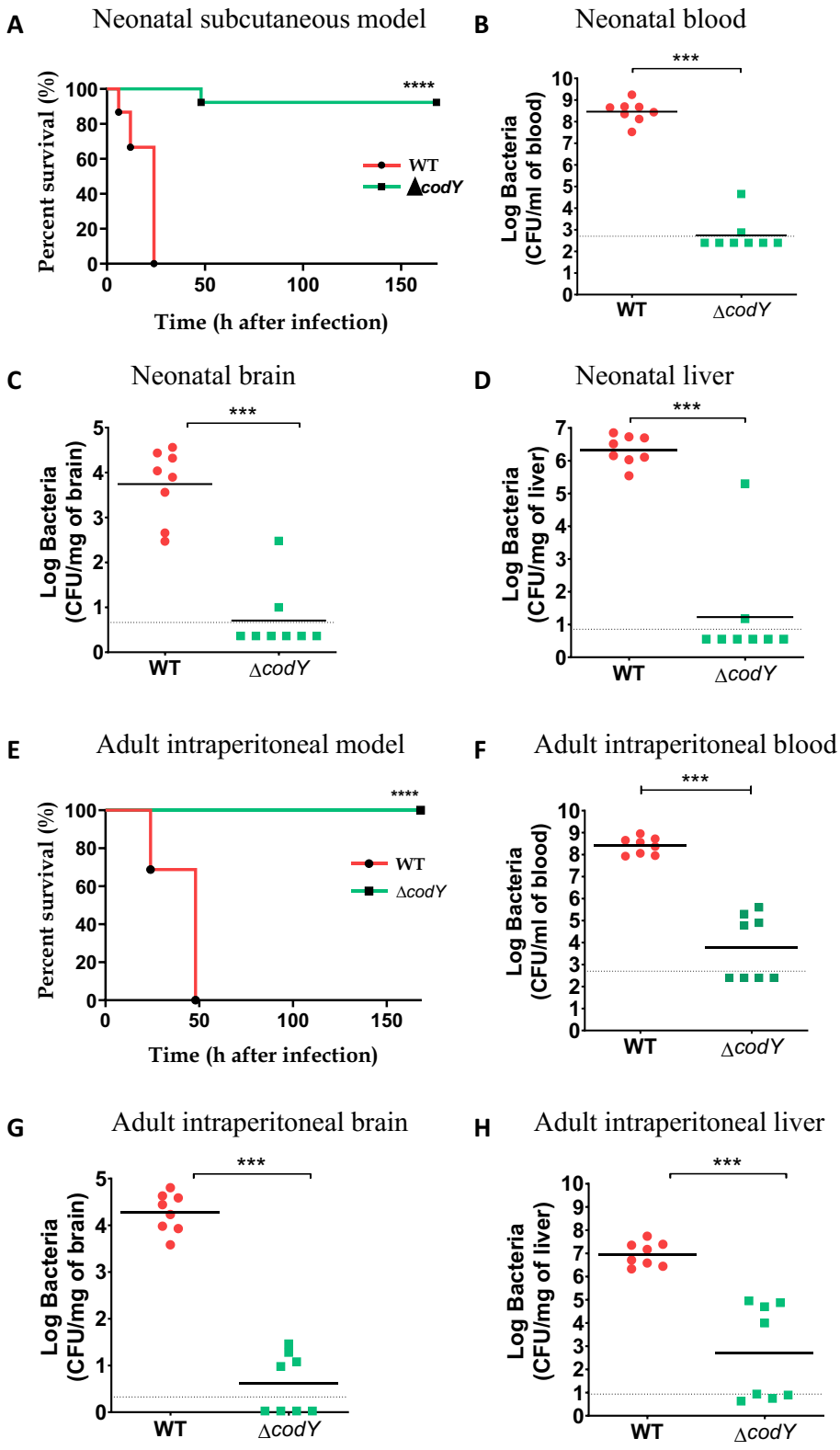
A
Neonatal subcutaneous model
Percent survival (%)
Time (h after infection)
WT
ΔcodY
****
B
Neonatal blood
Log Bacteria (CFU/ml of blood)
***
C
Neonatal brain
Log Bacteria (CFU/mg of brain)
D
Neonatal liver
Log Bacteria (CFU/mg of liver)
E
Adult intraperitoneal model
F
Adult intraperitoneal blood
G
Adult intraperitoneal brain
H
Adult intraperitoneal liver

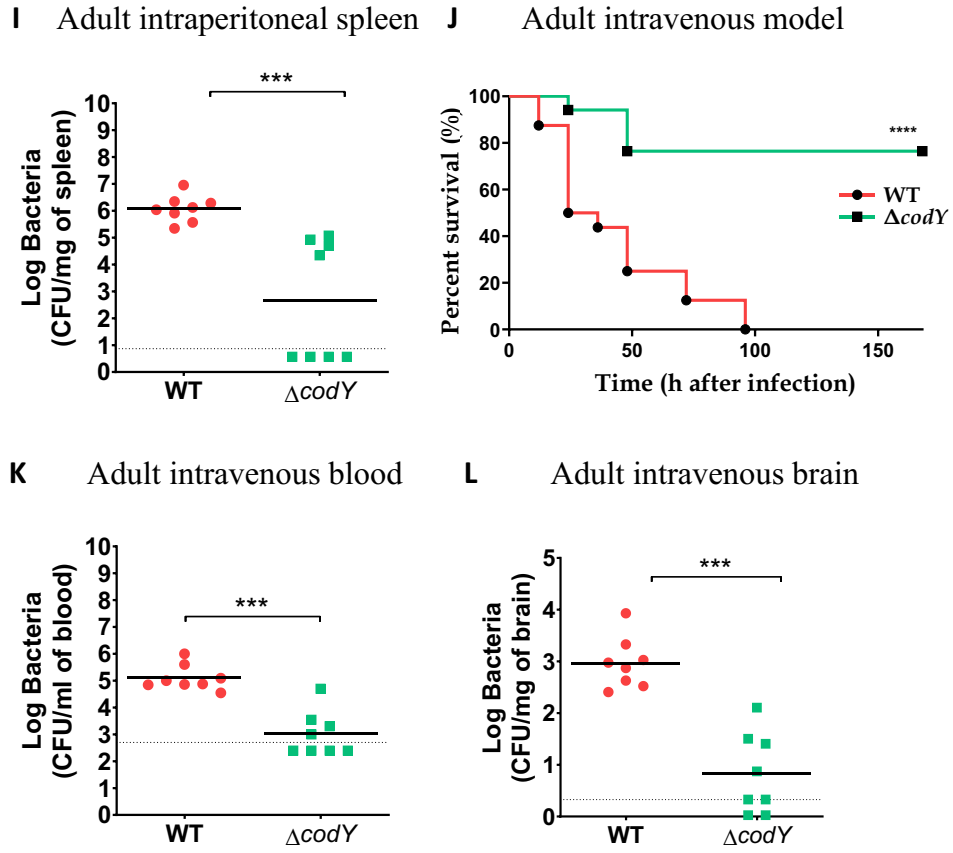

Figure 13. CodY is fundamental for *S. agalactiae* to establish the infection in neonatal and adult mice. A) Lethality of newborn mice (8 per group) infected subcutaneously with 8 × 10^4 CFU of the WT strain or the Δc*odY* mutant. B, C, D) Bacterial burden in the indicated organs of newborn mice infected in the same experimental condition as in panel (A); horizontal bars indicate mean log CFU values. E) Lethality of adult mice (8 per group) infected intraperitoneally (IP) with 5 × 10^8 of the WT strain or Δ*codY* mutant. F, G, H, I) Bacterial burden in the indicated organs of adult mice infected in the same experimental condition as in panel (E); horizontal bars indicate mean log CFU values. J) Lethality of adult mice (8 per group) infected intravenously (IV) with 1 × 10^9 CFU. K, L) Bacterial burden in the indicated organs of adult mice infected in the same experimental condition as in panel (I); horizontal bars indicate mean log CFU values. ***p < 0.001; ****p < 0.0001 by the Kaplan Meier (panels A, E, I) or Mann Whitney test (panels B, C, D, F, G, H, J-L).

4.2.2 CodY does not alter host cytokine production against *S. agalactiae*

After establishment of an infection, bacteria stimulate host cells to release a variety of pro-inflammatory cytokines that can induce cytokine networks or alter the existing ones (Wilson *et al*, 1998). We investigated whether the reduced *in vivo* virulence of the Δ*codY* strain could be related to an altered release of pro-inflammatory cytokines in the host. To this purpose, we used a sepsis model of infection in which mice were injected intraperitoneally with $1x10^9$ CFU of the WT or *codY*-null mutant strains. At different time points after the injection, peritoneal lavage fluid samples were collected and cytokine levels were measured. Penicillin was administered 30 min post-challenge in order to avoid bacterial overgrowth. The levels of different cytokines (TNF-α, IL-1β, Cxcl1, and Cxcl2) detected in the peritoneal lavage fluid increased rapidly and reached peak levels 3 h after bacterial infection. No differences were detected in the levels of cytokines released after infection with the WT and Δ*codY* strains (Figure 14 A-D). In addition, TNF-α or IL-1β levels were quantified in the culture supernatant of peritoneal macrophages stimulated with the two strains. Also in this case, the WT and Δ*codY* strain induced similar levels of both cytokines (Figure 14 E, F).

Taken together, the increase in mice survival rates and the reduced bacterial burden in the organs of animals infected with the *codY*-null mutant indicate that CodY is essential for *in vivo* growth and virulence of *S. agalactiae*. Nonetheless, the observed reduced virulence in the absence of CodY is not due to an alteration in cytokine levels produced by the host, as revealed by the similar cytokine response elicited after infection with the WT and Δ*codY* strains.

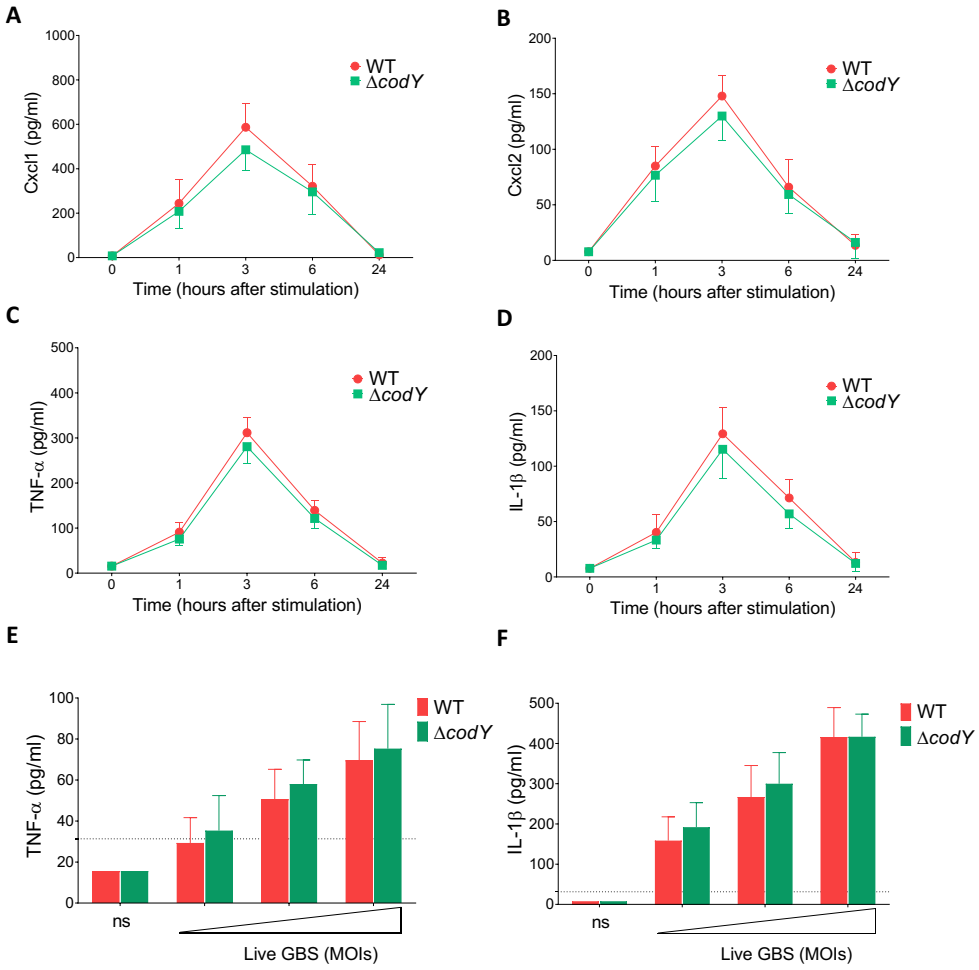

Figure 14. **Deletion of *codY* does not alter host cytokine production *in vivo* and *in vitro*.** A-D) Cxcl1, Cxcl2, TNF-α and IL-1β, levels detected in peritoneal lavage fluid samples collected at the indicated times after infection. E, F) TNF-α or IL-1β levels measured in the supernatants of macrophages stimulated with increasing doses of live bacteria (ns, non-stimulated, 3, 6 or 12 multiplicity of infection or MOI). Dashed lines indicate the detection limit of the tests. Values are the average ± SD of three independent experiments, each performed in duplicate.

4.3 CodY controls *S. agalactiae* virulence-related characteristics *in vitro*

4.3.1 *S. agalactiae* adhesion and invasion ability are altered in the absence of CodY

Adhesion to host cells and tissue invasion are two crucial steps for initiation of host colonization. By using two different epithelial cell lines, i.e. the adenocarcinoma human alveolar basal epithelial cell line A549 and the human adenocarcinoma cervical epithelial cell line HeLa, we evaluated the effect of *codY* deletion on the adhesion and invasion ability of *S. agalactiae* to mammalian cells.

The absence of CodY caused a significant reduction in the ability of *S. agalactiae* to adhere to both cell lines (Figure 15 A and C). On the contrary, *codY* deletion led to a significant increase in the capacity to invade both cell lines compared with WT (Figure 15 B and D). Complementation of *codY* deletion by plasmid-mediated expression of *codY* under the control of the constitutive Ptet promoter restored the adhesion and invasion abilities to levels similar to the WT strain (Figure 15 A-D).

These results suggest that the *codY* mutation could decrease the virulence of *S. agalactiae* by affecting its ability to colonize the host, thus preventing the establishment of a successful infection. On the other hand, the increased invasion ability could be due to the specific overexpression of factors involved in bacterial invasion of the host cells as a consequence of *codY* deletion.

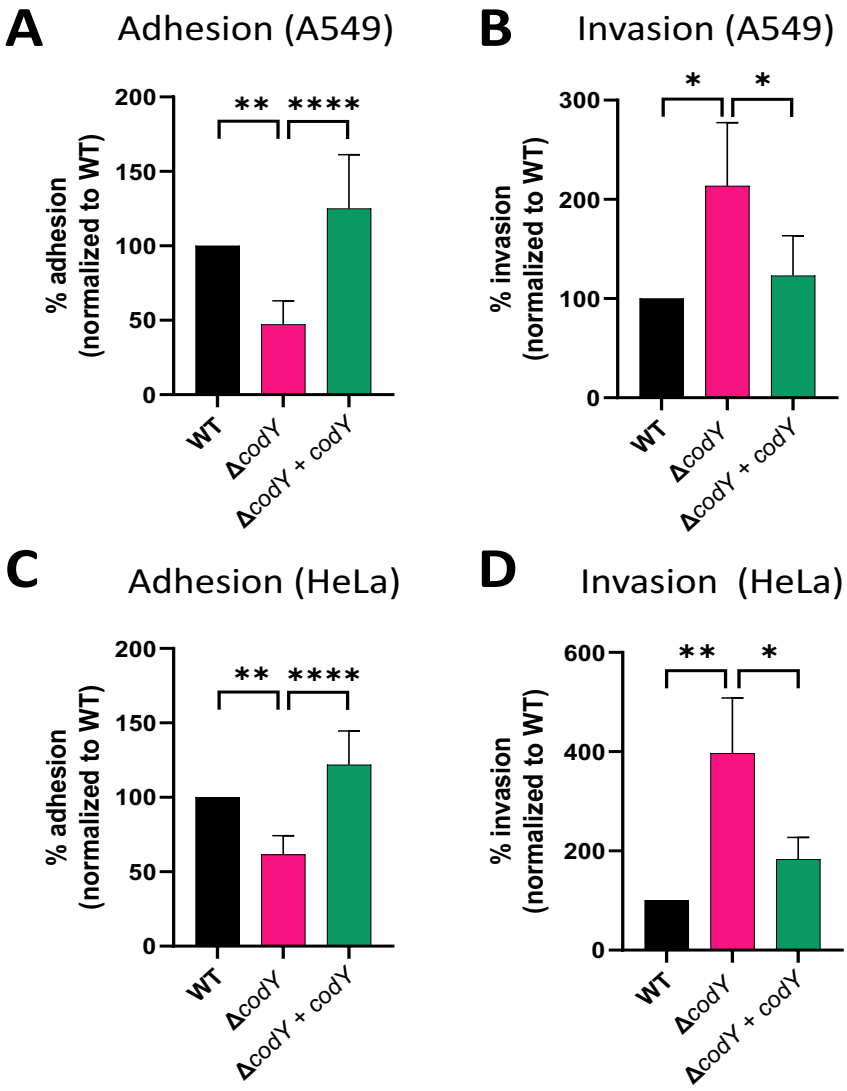

Figure 15. Deletion of *codY* decreases adhesion and increases invasion ability of *S. agalactiae*. Cell adhesion and invasion was quantified using A549 and HeLa immortalized cell lines. The WT and the Δ*codY* mutant strains carry the empty vector pTCVΩPtet, the Δ*codY*+*codY* strain contains the complementing vector pTCVΩPtet_codY. The percent of adhesion and invasion of each strain was calculated relative to the initial inoculum and was normalized to the adhesion or invasion of the WT strain, set as 100%. Represented data are the average ± SD of six independent experiments, each performed in duplicate. Statistically significant differences are indicated (One-way ANOVA). *$p < 0.05$, **$p < 0.01$, ****$p < 0.0001$.

4.3.2 CodY affects biofilm formation in *S. agalactiae*

To investigate the potential role of CodY in the ability of *S. agalactiae* to form biofilms, crystal violet staining (Figure 16 A) and confocal laser scanning microscopy analysis (Figure 16 B) were performed. Biofilm formed by the WT strain consisted of a very weak biomass. On the contrary, the *codY*-null mutant strain formed a thick and compact biofilm able to completely cover the surface of the well and of the chambered coverglass (Figure B-D). Complementation of the *codY* deletion decreased the biofilm-forming ability to levels similar to the WT strain (Figure 16 A–D).

To further investigate the characteristics of the biofilm formed by *S. agalactiae*, eradication experiments were performed using Proteinase K and DNase I. As reported in figure 16 A, the biofilms formed by the WT and *codY*-complemented strains were strongly eradicated both by proteinase K and DNase I treatment. Interestingly, the biofilm formed by the *codY*-null mutant was strongly eradicated only when treated with proteinase K (Figure 16 A). On the contrary, DNAse I was less effective against the biofilm biomass, as only a slight biofilm eradication was observed after DNAseI digestion (Figure 16 A). This result suggests that increased biofilm levels in the Δ*codY* strain could be due to overexpression of extracellular proteins involved in biofilm formation.

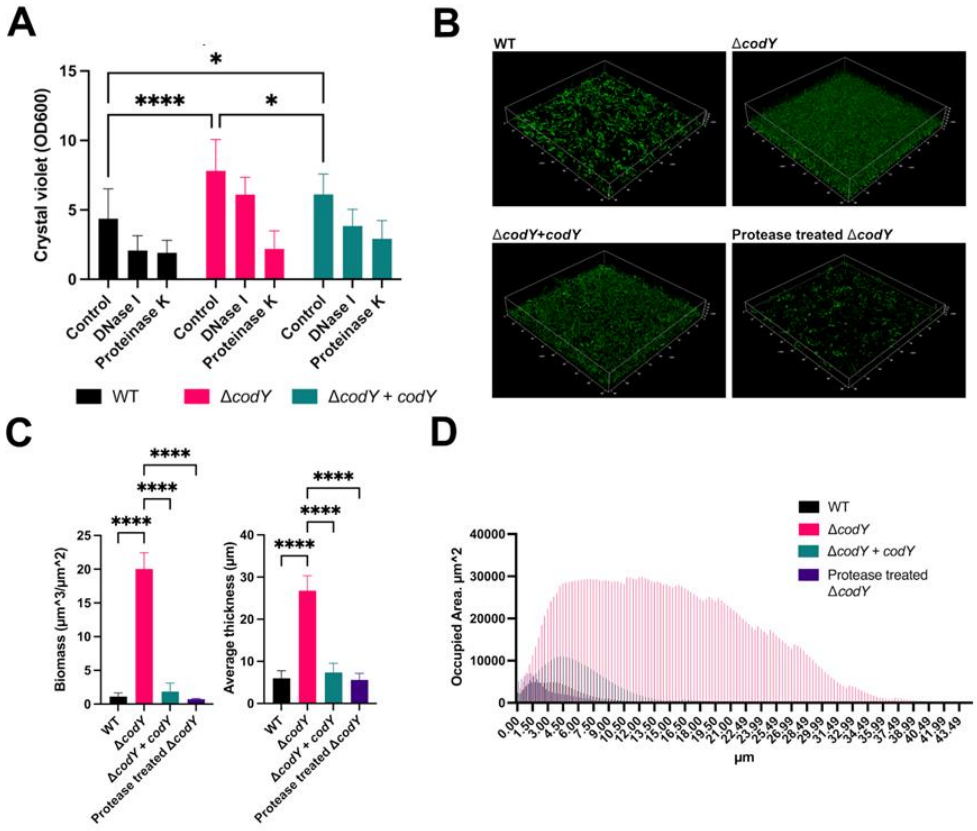

Figure 16. CodY inhibits biofilm formation. A) Crystal violet staining was used to measure biofilm biomass formed after static culture for 19 h. The WT and the Δ*codY* strain contain the empty vector pTCVΩPtet or the complementing vector pTCVΩPtet_codY (+ *codY*). The nature of the biofilm matrix was investigated by digesting eDNA and extracellular proteins as biofilm structural components by individual treatments with DNase I and proteinase K, respectively. Represented data are the average ± SD of two independent experiments, each performed in 8 replicates. Statistically significant differences are reported (two-way ANOVA). B) WT, Δ*codY* and Δ*codY* + *codY* strains' biofilm images obtained through confocal laser scanning microscope. Cells were by grown in static culture for 19 h in Nunc™ Lab-Tek™ II Chambered Coverglass. The effect of treatment with proteinase K on the Δ*codY* biofilm is reported. C, D) Analysis of biofilm properties by COMSTAT 2. Measures of total biomass, average thickness C) and % of the area occupied by biofilm distribution D). Data are the average ± SD of the results from three independent replicates. *p < 0.05, ****p < 0.0001 (one-way ANOVA test).

4.4 Characterization of the CodY regulon of *S. agalactiae*

4.4.1 CodY is a global regulator of gene expression of *S. agalactiae*

To define the transcriptional response associated with *codY* deletion in the BM110 strain, an RNA-Seq analysis was performed on WT and Δ*codY* cells collected during exponential growth phase in rich THY medium. Under these conditions, CodY activity is expected to be maximal. The results obtained from the transcriptional analysis demonstrate that CodY plays a global regulatory role in *S. agalactiae* (Figure 17). Out of 2,128 genes examined, 277 genes were differentially expressed at least two-fold (adjusted p-value < 0.05) in the Δ*codY* strain (Supplementary Datasets 1A–C; Pellegrini *et al,* 2022). In particular, 256 genes were up-regulated (Supplementary Dataset 1B; Pellegrini *et al,* 2022), and 21 genes were down-regulated (Supplementary Dataset 1C; Pellegrini *et al,* 2022) in the mutant strain. This result reveals that CodY acts mainly as a negative regulator of gene expression in *S. agalactiae* (Figure 17). Interestingly, around 55% (140/256) of the over-expressed genes were clustered in four prophages. Notably, fold changes associated to genes negatively regulated were higher than those associated to genes positively regulated.

The FIMO Motif Search Tool (Grant *et al*, 2011) was used to scan the genome of BM110 for sequences matching the conserved AATTTTCWGAAAATT CodY binding motif. Using a p-value lower than 0.0001, 101 matches were obtained in the genomic regions located upstream of the genes' coding sequences. Eighteen of the genes differentially expressed in the Δ*codY* strain presented at least one sequence resembling the CodY motif located in proximity of the coding sequence (Supplementary Datasets 1A–D and Supplementary Table; Pellegrini *et al,* 2022). This suggests that these genes could be potential targets of direct regulation by CodY.

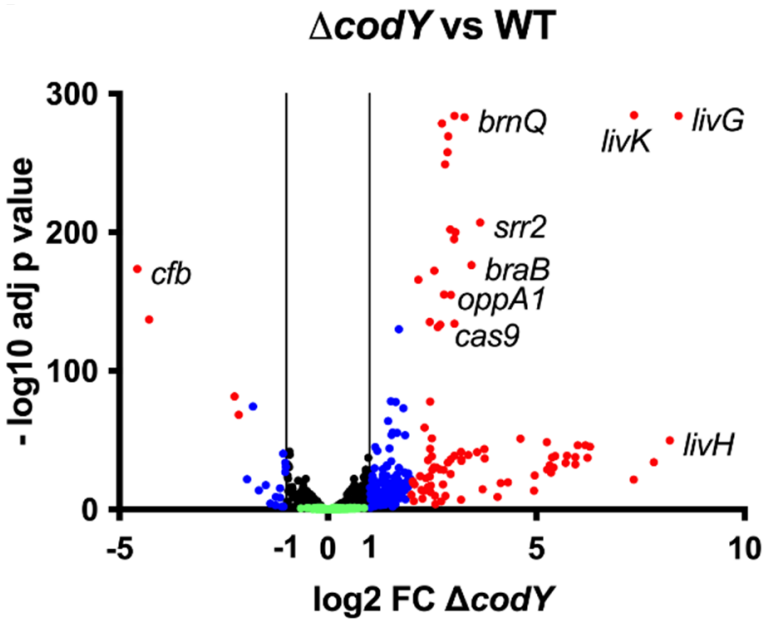

Figure 17. CodY is a global regulator of gene expression in *S. agalactiae*. Volcano plot representative of the transcriptome of Δ*codY* cells compared to WT cells. Cells were collected at mid-exponential phase in THY medium. Each dot represents a gene with its log2 fold change and adjusted p-value calculated from four independent replicates. Genes showing a significant differential expression in the Δ*codY* strain (adjusted p-value < 0.05) are represented in blue (–2 ≤ log2FC ≤ –1 or 1 ≤ log2FC ≤ 2) and red (log2FC < –2 or log2FC > 2) according to their fold change relative to the WT strain. Genes whose expression is not affected by *codY* deletion are represented by black dots (–1 < log2FC < 1; adjusted p-value < 0.05). Green dots indicate non-significant differentially transcribed genes (adjusted p-value > 0.05).

4.4.2 COGs classification reveals gene categories majorly controlled by CodY

Among the differentially expressed genes, 98 targets of CodY-mediated regulation showed at least a four-fold change in their levels in the mutant strain compared to the WT (in particular, 94 genes were up-regulated and 4 down-regulated) (Supplementary Datasets 1D, E; Pellegrini *et al,* 2022). Classification of the proteins encoded by these genes by Cluster of Orthologous Genes (COGs) analysis clustered them into seventeen functional categories (Figure 18), (Supplementary Dataset 2, Pellegrini *et al,* 2022). These included "amino acid transport and metabolism", "cell wall/membrane/envelope biogenesis", and "mobilome: prophages, transposons" among the most represented categories.

Specifically, targets of CodY repression (Supplementary Dataset 1D; Pellegrini *et al,* 2022), included genes encoding BCAAs transporters (*braB, brnQ*, all the genes belonging to the *livK-G* operon), the (oligo)peptide permease OppA1-F, adhesins, serine peptidases anchored to the cell wall through the LPxTG motif, as well as proteins involved in DNA replication, recombination, and repair (Figure 17). Interestingly, genes encoding the CRISPR-Cas system proteins Cas9, Cas1, Cas2, and Csn2 were among the ones more intensely up-regulated in the deletion mutant. This suggests a role of CodY in modulating the expression of this defense system. Another interesting cluster of differentially expressed genes regards the operon encoding the CC17-specific multifaceted virulence factor Srr2, which was over-expressed in the absence of CodY. This operon contains genes encoding the accessory secretion system SecA2/SecY2 and glycosyltransferases GtfA, GtfB. The latter are necessary for glycosylation and subsequent secretion of the Srr2 protein. On the contrary, the gene encoding the CAMP factor pore-forming toxin Cfb was under positive regulation of CodY (Figure 17, Supplementary Dataset 1E; Pellegrini *et al,* 2022).

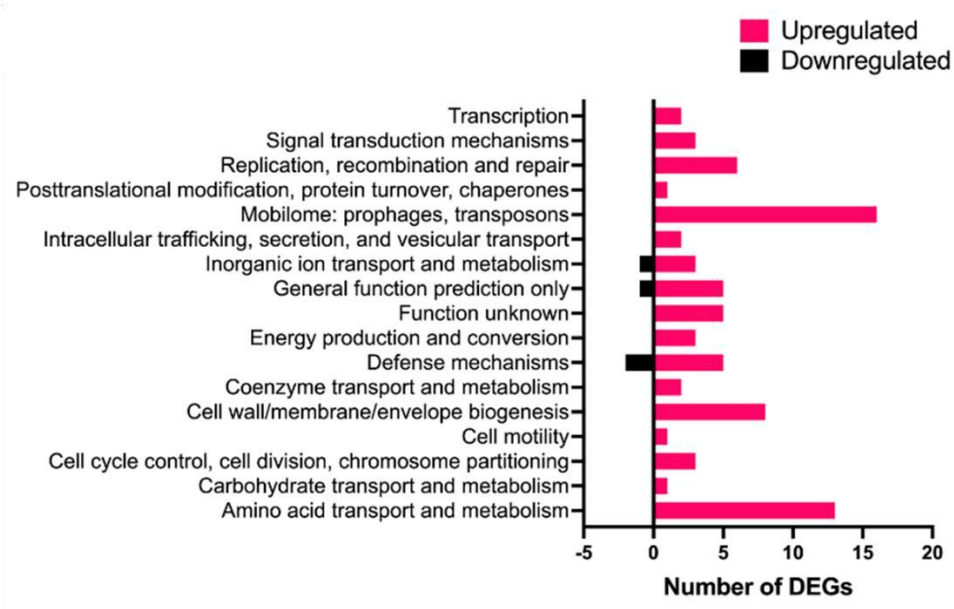

Figure 18. **CodY controls several *S. agalactiae* genes, grouped in 17 functional categories.** Cluster of Orthologous Genes (COGs) associated to downregulated and upregulated genes, whose expression was affected by *codY* deletion at least four-fold.

4.5 Investigation of CodY-mediated regulatory mechanisms

4.5.1 CodY activity is enhanced by branched-chain amino acid availability

In all the species in which it has been described so far, the global regulator CodY is activated by BCAAs. Therefore, the expression of CodY-regulated genes is expected to be dependent on the availability of these amino acids. The transcript levels of three targets of CodY-regulation were investigated by qRT-PCR on RNA extracted from cells grown in a chemically defined medium (CDM) supplemented with high (1500 μM) or low (50 μM) BCAAs concentrations. Worthy of note, genes encoding for the precursors of most amino acids, BCAAs included, are missing in *S. agalactiae* (Glaser *et al*, 2002), hence BCAAs cannot be omitted completely from the growth medium.

The WT and Δ*codY* strains displayed similar growth kinetics under both conditions tested, with an approximate two-fold increase in their doubling time compared to growth in rich THY medium (Figure 19 B). The qRT-PCR analysis was conducted on genes encoding three different BCAAs transporters: *livK*, the first gene on the *livK-G* operon, *brnQ* and *braB*. All of them were identified through RNA-Seq analysis (Figure 17), (Supplementary Dataset 1D; Pellegrini *et al,* 2022), and qRT-PCR (Figure 19 A) as negatively regulated by CodY during growth in rich THY medium. When low levels of BCAAs were present in the growth medium, transcript levels of all three genes increased in the WT strain compared to conditions of high BCAAs availability. On the contrary, gene expression was not affected by BCAAs levels in the Δ*codY* mutant (Figure 19 C). In this strain, all genes were further and significantly over-expressed compared to the WT strain under both conditions tested. Nevertheless, the extent of this overexpression was gene-specific: higher for *livK* (82-fold and 11-fold increase in CDM + 1500 μM and in CDM + 50 μM ILV, respectively) and lower for *braB* (3.4-fold and 2.3-fold increase in CDM + 1500 μM and in CDM + 50 μM ILV, respectively) and *brnQ* (4.8-fold and 2.8-fold increase in CDM + 1500 μM and in CDM + 50 μM ILV, respectively) (Figure 19 C). The results obtained for the WT strain suggest that, as the levels of BCAAs decrease, the expression of CodY-repressed genes increases in a gene-specific manner (Figure 19 C). Hence, CodY regulatory role is strongly dependent on BCAA availability.

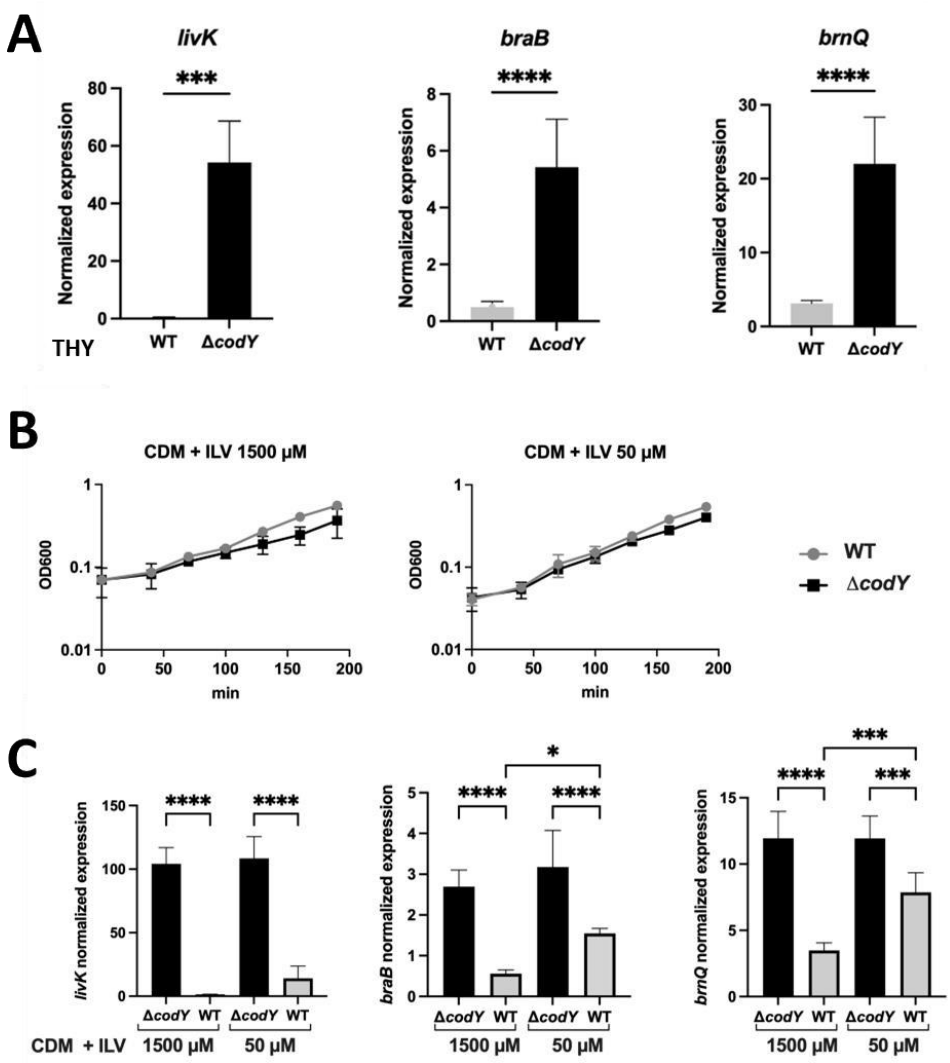

Figure 19. CodY-mediated repression of three BCAAs transporters is dependent on BCAAs availability. A) qRT-PCR analysis of *livK*, *braB* and *brnQ* expression in the WT (grey) and Δ*codY* mutant (black) strains during exponential growth in rich medium THY. Gene expression is normalized to the expression of the housekeeping *gyrA* gene. Asterisks denote statistically significant differences as assessed by t-test analysis. ***p < 0.001, ****p < 0.0001. B) Growth curves of WT (gray) and Δ*codY* strain (black) in CDM supplemented with high (1500 µM) and low (50 µM) ILV concentrations. Reported absorbance data at OD_{600} are the average ± SD of two independent experiments. C) qRT-PCR analysis of *livK*, *braB*, and *brnQ* in the WT and Δ*codY* strains grown in CDM supplemented with high or low ILV concentrations. Gene expression is normalized to the expression of the housekeeping *gyrA* gene. Asterisks indicate statistically significant differences. *p < 0.05, ***p < 0.001, ****p < 0.0001. (One-way ANOVA analysis).

4.6 CodY regulates directly two branched-chain amino acid transporters

4.6.1 CodY-mediated regulation of the *livK-G* operon

The mechanism of CodY-mediated regulation of the *livK-G* operon, encoding an ABC-type BCAAs transporter, was investigated. Two putative CodY-binding motifs were identified by FIMO analysis upstream of the *livK* gene. These sequences are located at positions from −64 to −50 and from −31 to −17 with respect to the transcription start site of *livK* (Mazzuoli *et al*, 2021) and show three and two mismatches to the CodY consensus sequence, respectively (Figure 20).

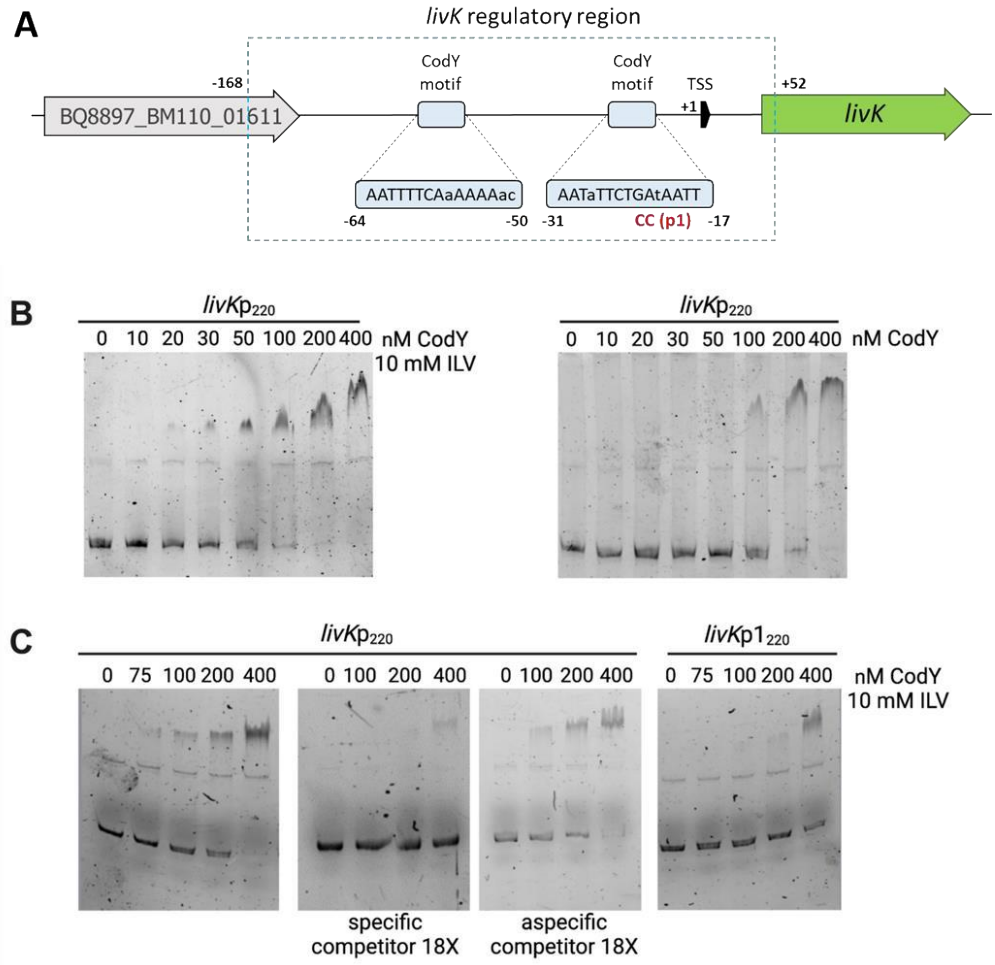

Figure 20. CodY binds directly to the *livK* regulatory region. A) Schematic structure of the *livK* regulatory region. The dashed line box comprises the sequence of the *livK* regulatory region included in the *livK*p$_{220}$-*lacZ* fusion. Coordinates are reported with respect to the

transcription start site (Mazzuoli *et al*, 2021). Sequences of the two CodY-binding motifs are reported. Mismatches with respect to the CodY consensus sequence are reported in lowercase. The mutated nucleotides (p1) are indicated in red below the sequence. B) Electrophoretic mobility shift assays (EMSA) for investigation of CodY binding to the *livK* regulatory region. CodY and the WT *livK*p$_{220}$ fragment were incubated in the presence or absence of 10 mM of isoleucine, leucine, and valine (ILV). The BCAAs were included in the reaction mixture, in the non-denaturing polyacrylamide gel and in the electrophoresis buffer as well. C) EMSA performed to compare CodY binding to the WT *livK*p$_{220}$ and mutated *livK*p1$_{220}$ fragments. Specificity of binding was evaluated by performing the experiment with the WT fragment in presence or absence of a specific (unlabeled *livK*p$_{220}$ fragment) or non-specific competitor. DNA-Protein mixtures were separated on 5% non-denaturing gel in presence of 10 mM ILV.

The ability of CodY to bind the *livK* promoter was investigated by electrophoretic-mobility shift assay (EMSA). The assay was performed with a 6-carboxyfluorescein (FAM) labeled fragment encompassing the *livK* regulatory region from position −168 to +52 with respect to the transcription start site of the gene (Figure 20 A). Labeled DNA was incubated with increasing concentrations of purified CodY in the presence or absence of 10 mM BCAAs (ILV). CodY bound the *livK* fragment with an apparent equilibrium dissociation constant (KD) of ≈50 nM (here, KD indicates the concentration of CodY required to shift 50% of DNA fragments under conditions of vast protein excess over DNA) in the presence of BCAAs (Figure 20 B). Affinity of CodY for the *livK* regulatory region decreased significantly (KD ≈150 nM) when ILV were omitted from the binding mixture, suggesting that BCAAs enhance CodY ability to bind DNA. Specificity of CodY binding was assessed by competitive and non-competitive binding assays in the presence of ILV and 18-fold excess of unlabeled specific or non-specific competitor DNA, respectively (Figure 20 C).

To assess the ability of CodY to regulate *livK* expression, a *lacZ* transcriptional fusion (*livK*p$_{220}$-*lacZ*) comprising the entire intergenic region upstream of *livK*, from position −168 to +52 with respect to the *livK* transcription start site, was constructed using the pTCV-*lacZ* plasmid (Poyart and Trieu-Cuot, 1997). To prepare the pTCV-*lacZ_livK*p$_{220}$ plasmid (Table 2), a 269 bp fragment comprising the regulatory region and the first 27 nucleotides of the *livK* gene was amplified with primers livKp220F and livKp220R using the BM110 chromosomal DNA as template (Table 4). Expression levels of the fusion were investigated during the exponential phase of growth in THY medium, i.e. under conditions of maximal CodY activity. Expression of the *livK*p$_{220}$-*lacZ* fusion was about 400-fold higher in the Δ*codY* mutant compared to the WT strain (Table 5). To prove that the observed effects of CodY on *livK* expression are direct and mediated by its binding to the *in silico* identified putative CodY binding motifs, a two-nucleotide substitution mutation was introduced within the site located immediately upstream of *livK* (*livK*p1$_{220}$-*lacZ*), at positions −22 and −23 with respect to the transcription start site of the gene. To create

pTCV*lacZ_livK*p1$_{220}$ (Table 2), a 196 bp product containing the 5′ part of the *livK* regulatory region was amplified by using oligonucleotides livKp220F and mutagenic oligonucleotide livKp1R. A 125 bp fragment comprising the 3′ part of the regulatory region and the first 27 bp of the *livK* coding sequence was synthesized by using mutagenic oligonucleotide livKp1F and livKp220R as reverse primer (Table 4). Interestingly, the p1 mutation strongly reduced the affinity of CodY for the *livK* regulatory region as observed by EMSA assay (Figure 20 C). The reduced affinity led to a complete loss of CodY's ability to repress *livK* expression (Table 5).

Table 5. Expression of *livK*$_p$-*lacZ* fusions

Strain	Relevant genotype	Fusion type	β-galactosidase activity *	
			Miller Units ± SD	Repression Ratio **
BM1106	WT	*livKp*$_{220}$-*lacZ*	0.47 ± 0.07	393.62
BM1107	Δ*codY*		185 ± 19.02	
BM1114	WT	*livKp1*$_{220}$-*lacZ*	157.6 ± 0.35	1.03
BM1115	Δ*codY*		161.9 ± 6.86	

* β-galactosidase activity is reported in Miller Units. Data are the average ± SD of two independent experiments, each performed in duplicate.

** The repression ratio is the ratio of expression values for the corresponding fusions in the *codY* null mutant and in the wild-type strain.

4.6.2 CodY-mediated regulation of the *brnQ* gene

RNA-Seq and qRT-PCR analyses of *brnQ* expression during growth in rich THY medium revealed a 9,8- and 6.8-fold increase, respectively, in the expression of this gene in the Δ*codY* strain compared to the WT (Supplementary Dataset 1D and Figure 19 A; Pellegrini *et al,* 2022). No putative CodY binding motifs were identified upstream of *brnQ* by *in-silico* analysis of the BM110 genome using the FIMO Motif Search Tool (Grant *et al*, 2011). However, one putative CodY binding motif could be identified by manual analysis. The identified sequence showed four mismatches to the consensus one and was identified at positions from −53 to −39 with respect to the transcription start site of *brnQ* (Mazzuoli *et al*, 2021) (Figure 21 A).

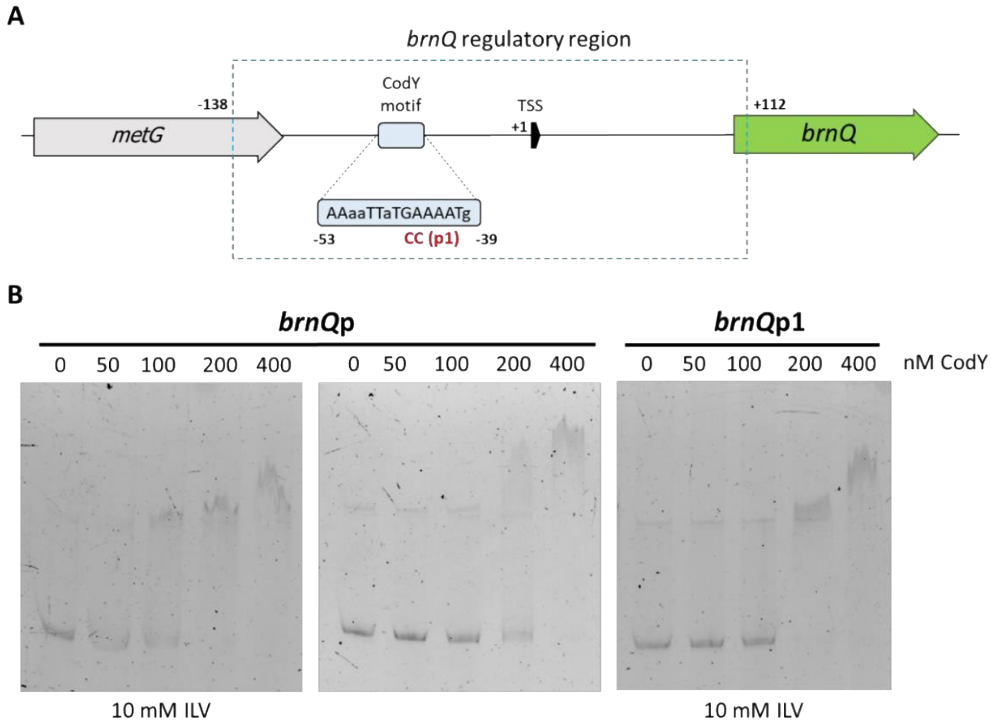

Figure 21. CodY binds directly the *brnQ* regulatory region. A) Schematic structure of the *brnQ* regulatory region. The dashed line box comprises the sequence of the *brnQ* regulatory region comprised within the *brnQ*p-*lacZ* fusion. Coordinates are reported with respect to the transcription start site (Mazzuoli *et al*, 2021). The sequence of CodY-binding motif is reported. Mismatches with respect to the CodY consensus sequence are reported in lowercase. The mutated nucleotides (p1) are indicated in red below the sequence. B) EMSA for investigation of CodY binding to the *brnQ* regulatory region. CodY and the WT *brnQ*p fragment were incubated in the presence (first panel) or absence (second panel) of 10 mM of ILV. BCAAs were included in the reaction mixture, in the non-denaturing polyacrylamide gel and in the electrophoresis buffer as well. The third panel shows EMSA performed to evaluate

CodY binding to the mutated *brnQ*p fragment. DNA-Protein mixtures were separated on 5% non-denaturing gel in presence of 10 mM ILV.

An EMSA was performed to investigate the ability of CodY to bind the *brnQ* promoter. A 6-carboxyfluorescein (FAM) labeled fragment encompassing the *brnQ* regulatory region from position -138 to +112 with respect to the transcription start site of the gene (Figure 21 A) was incubated with increasing concentrations of purified CodY in presence or absence of 10 mM BCAAs. CodY bound the *brnQ* fragment with an apparent KD of ≈75 nM in the presence of BCAAs (Figure 21 B). In the absence of BCAAs, CodY affinity for the *brnQ* regulatory region decreased significantly (KD ≈200 nM).

The ability of CodY to regulate *brnQ* expression was tested using a *lacZ* transcriptional fusion (*brnQ*p-*lacZ*), including the region spanning from position -138 to +112 with respect to the *brnQ* transcription start site. To prepare the pTCV-*lacZ_brnQ*p plasmid (Table 2), a 297 bp fragment comprising the regulatory region and the first 28 nucleotides of the *brnQ* gene was amplified with primers brnQpF and brnQpR using the BM110 chromosomal DNA as template (Table 4). Expression of the *brnQ*p-*lacZ* fusion during the exponential phase of growth in THY medium was about 12-fold higher in the Δ*codY* strain than in the WT strain (Table 6).

A two-nucleotide substitution mutation was introduced in the putative CodY-binding site at positions −45 and −44 with respect to the *brnQ* transcription start site (*brnQ*p1-*lacZ*). To create pTCV*lacZ_brnQ*p1 (Table 2), a 136 bp product containing the 5′ part of the *brnQ* regulatory region was amplified by using oligonucleotides brnQpF and mutagenic oligonucleotide brnQp1R. A 196 bp fragment comprising the 3′ part of the regulatory region and the first 28 bp of the *brnQ* coding sequence was synthesized by using mutagenic oligonucleotide brnQp1F and brnQpR as reverse primer (Table 4). The introduced mutation was aimed at decreasing the similarity of the motif to the CodY-binding consensus sequence, thus reducing its ability to control gene expression. Introduction of the p1 mutation strongly reduced the affinity of CodY for the *brnQ* regulatory region (KD ≈200 nM) (Figure 21 B) and abolished the ability of CodY to repress *brnQ* expression (Table 6).

Table 6. Expression of *brnQ*p-*lacZ* fusions

Strain	Relevant genotype	Fusion type	β-galactosidase activity *	
			Miller Units ± SD	Repression Ratio**
BM1150	BM110	*brnQ*p-*lacZ*	4,30 ± 0,44	12,23
BM1151	BM110*codY*		52,57 ± 6,29	
BM1152	BM110	*brnQ*p1-*lacZ*	64,46 ± 4,42	0,89
BM1153	BM110*codY*		57,35 ± 21,85	

* β-galactosidase activity is reported in Miller Units. Data are the average ± SD of two independent experiments, each performed in duplicate.

** The repression ratio is the ratio of expression values for the corresponding fusions in the *codY* null mutant and in the wild-type strain.

4.7 Complex regulation of the *S. agalactiae* major virulence factor Srr2

4.7.1 CodY contributes directly to repression of *srr2*

The mechanism of CodY-mediated regulation of the *srr2* gene, encoding a major virulence factor of *S. agalactiae*, was investigated. Two putative CodY-binding motifs were identified by FIMO analysis upstream of this gene. The two sites are located at positions from −163 to −148 and from +51 to +66 with respect to the transcription start site of *srr2* and show two and three mismatches to the consensus sequence, respectively (Mazzuoli *et al*, 2021), (Figure 22 A).

A fragment encompassing the *srr2* regulatory region from position −332 to +283 with respect to the transcription start site of the gene (*srr2*p_{615}, Figure 22 B) was amplified using FAM labeled primers. Labeled DNA was used in an EMSA experiment performed using purified CodY in the presence of 10 mM ILV. CodY bound the *srr2* fragment with an apparent equilibrium dissociation constant (KD) of ≈100 nM (Figure 22 C). A *lacZ* transcriptional fusion (*srr2*p_{615}-*lacZ*) including the same regulatory region was constructed using the pTCV-*lacZ* plasmid (Poyart and Trieu-Cuot, 1997). To prepare the pTCV-*lacZ_srr2*p_{615} plasmid (Table 2), a 664 bp fragment comprising the *srr2* regulatory region and the first 24 nucleotides of the

srr2 gene was amplified with primers srr2p615 and srr2pR using the BM110 chromosomal DNA as template (Table 4). β-Galactosidase activity of strains carrying the *srr2*p$_{615}$-*lacZ* fusion was analyzed during the exponential phase of growth in THY medium, under conditions of maximal CodY activity. Expression of the fusion during the exponential phase of growth was about 20-fold higher in the *codY*-null mutant than in the WT strain (Figure 22 and Table 7). This result is in line with data previously obtained by RNA-Seq analysis (Supplementary Dataset 1D; Pellegrini *et al,* 2022), which reported a 13-fold increase in *srr2* expression in the Δ*codY* strain compared to the WT. Moreover, the result obtained demonstrates that the region used in the creation of the transcriptional fusion is sufficient for CodY-mediated control of *srr2* expression.

To prove that the observed effects of CodY on *srr2* expression are the result of direct binding, we introduced three different two-nucleotide substitution mutations within the downstream (p1) and/or upstream (p2 and p3) putative CodY-binding sites (Figure 22 A). To create the pTCV*lacZ_srr2*p1$_{615}$, pTCV*lacZ_srr2*p2$_{615}$ and pTCV*lacZ_srr2*p3$_{615}$ plasmids (Table 2), the BM110 chromosomal DNA was used as template to amplify the 5′ part of the *srr2* regulatory region using srr2p615 as forward primer and the mutagenic oligonucleotides srr2p1R, srr2p2R and srr2p3R as reverse primers, respectively. The 3′ part of the regulatory region and the first 24 bp of the *srr2* coding sequence was synthesized by using oligonucleotides srr2pR and the internal, mutagenic oligonucleotides srr2p1F, srr2p2F and srr2p3F respectively (Table 4). The pTCV*lacZ_srr2*p1,2$_{615}$ (Table 2) plasmid, carrying both p1 and p2 mutations was created by following the same procedure used for the preparation of pTCV*lacZ_srr2*p2$_{615}$, using pTCV*lacZ_srr2*p1$_{615}$ as DNA template.

The introduced mutations were designed with the aim to decrease the sequence similarity to the CodY-binding consensus sequence. The p1 mutation, introduced at the level of the putative CodY-binding site located immediately upstream the *srr2* coding region, did not affect the ability of CodY to repress *srr2* expression (Table 7). On the contrary, the p2 and p3 mutation, introduced at the level of the upstream CodY binding motif, strongly reduced the ability of CodY to repress the *srr2* promoter (Table 7). This suggests that CodY binding to the upstream motif is necessary for a full repression of the fusion.

To further investigate the role of the two CodY binding motifs in CodY-mediated regulation of *srr2*, two *lacZ* transcriptional fusions of the *srr2* regulatory region were prepared, each containing one of the two putative CodY binding motifs.

The fusion spanning from position -115 to +283 with respect to the *srr2* transcription start site was named *srr2*p$_{398}$-*lacZ.* To prepare the pTCV-*lacZ_srr2*p$_{398}$ plasmid (Table 2), a 447 bp fragment comprising part of the *srr2* regulatory region and the first 24 nucleotides of the *srr2* gene was amplified with primers srr2p398 and srr2pR

using the BM110 chromosomal DNA as template. The *srr2*p$_{398}$ fragment, encompassing only the downstream binding motif, was amplified with FAM labeled primers using pTCV-*lacZ_srr2*p$_{398}$ as template. An EMSA experiment performed in presence of 10 mM ILV revealed that the fragment was bound by CodY with an apparent equilibrium dissociation constant (KD) of ≈400 nM. As this concentration is higher than the one found in physiological conditions, the downstream binding motif does not appear to be involved in CodY-mediated regulation of *srr2* (Figure 22 D). This result was indeed furtherly confirmed by β-galactosidase assay. As reported in Table 7, analysis of the expression of the *srr2*p$_{398}$-*lacZ* fusion revealed a less than 2-fold repression in the *codY*-null mutant strain, BM1111, than in the WT strain, BM1110.

The fusion from position -332 to +39 with respect to the *srr2* transcription start site was named *srr2*p$_{371}$-*lacZ* (Figure 22 B). To prepare the pTCV-*lacZ_srr2*p$_{371}$ plasmid (Table 2), a 420 bp fragment comprising part of the *srr2* regulatory region was amplified with primers srr2p371R and srr2p615 using the pTCV-*lacZ_srr2*p$_{615}$ as template (Table 4). EMSA analysis performed in presence of 10 mM ILV and FAM-labeled *srr2*p$_{371}$ fragment, comprising the upstream binding motif only, revealed that CodY bound this region with an apparent equilibrium dissociation constant (KD) of ≈100 nM (Figure 22 E), similarly to what observed for the complete regulatory region of *srr2* (Figure 22 C). Moreover, expression of the *srr2*p$_{371}$-*lacZ* fusion was about 4-fold higher in the *codY*-null mutant strain, BM1165, than in the WT strain, BM1164 (Table 7).

CodY's ability to repress the *srr2* promoter was completely abolished by introduction of the p3 mutation in the *srr2*p$_{371}$-*lacZ* fusion (Table 7). These evidences therefore suggest that CodY-mediated repression of *srr2* expression appears to be mediated mainly by CodY binding at the upstream binding motif.

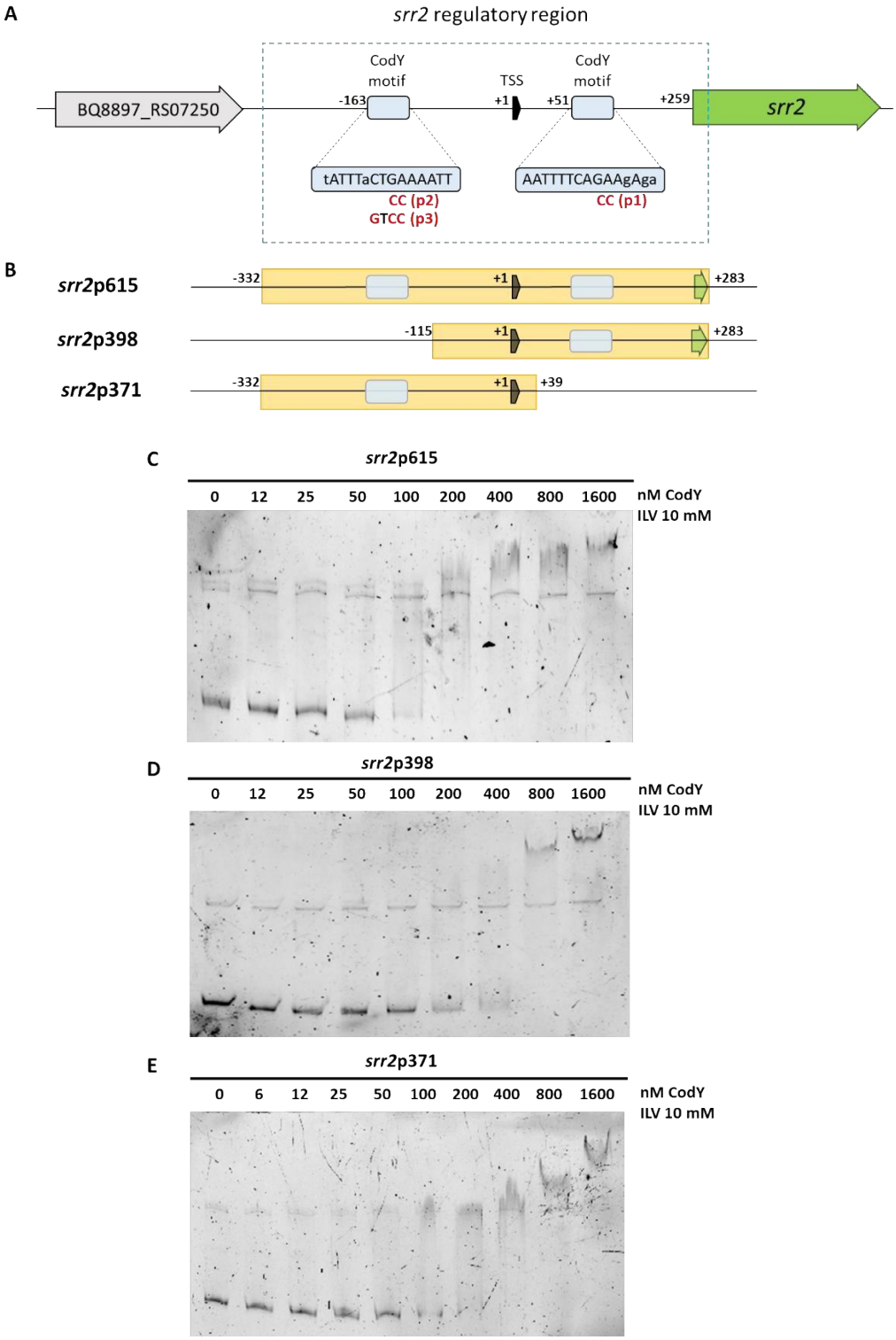
A
srr2 regulatory region
CodY motif
TSS
CodY motif
BQ8897_RS07250
-163
+1
+51
+259
srr2
tATTTaCTGAAAATT
CC (p2)
GTCC (p3)
AATTTTCAGAAgAga
CC (p1)
B
srr2p615
-332
+1
+283
srr2p398
-115
+1
+283
srr2p371
-332
+1
+39
C
srr2p615
0 12 25 50 100 200 400 800 1600
nM CodY
ILV 10 mM
D
srr2p398
0 12 25 50 100 200 400 800 1600
nM CodY
ILV 10 mM
E
srr2p371
0 6 12 25 50 100 200 400 800 1600
nM CodY
ILV 10 mM

Figure 22. CodY binds directly to the *srr2* regulatory region. A) Schematic structure of the *srr2* regulatory region. Coordinates are reported with respect to the transcription start site (Mazzuoli *et al*, 2021). Sequences of the two CodY-binding motifs are reported. Mismatches with respect to the CodY consensus sequence are reported in lowercase. The mutated nucleotides (p1, p2, p3) are indicated in red below the sequence. B) Schematic maps of the *srr2* fragments used to construct *lacZ* fusions or in EMSA experiments. The coordinates indicate the boundaries of different fusions with respect to the *srr2* transcription start site. The location of the transcription start site (TSS) is indicated in black. C-D-E) EMSA for investigation of CodY binding to the *srr2*p$_{615}$, *srr2*p$_{398}$ *and srr2*p$_{371}$ fragments. Labeled DNA fragments were incubated with increasing amounts of purified CodY in the presence of 10 mM each of BCAAs ILV. DNA-Protein mixtures were separated on 5% non-denaturing gel in presence of 10 mM ILV.

4.7.2 CodY- and CovR- mediated regulation of the *srr2* gene

The *srr2* operon has been recently reported to be directly repressed by CovR, the response regulator of the two-component system CovRS. Consequently, we decided to investigate the existance of a possible interplay between CodY and CovRS in the regulation of *srr2* expression. To this purpose, two derivative strains of BM110 were prepared by introducing an in-frame deletion of the *covR* gene in the WT strain and in the Δ*codY* strain, thus obtaining the strains Δ*covR* and Δ*covR*/Δ*codY*, respectively. The obtained strains were electroporated with the pTCV-*lacZ* derivative plasmid carrying different regions of the *srr2* regulatory sequence (See paragraph 3.3). As reported in Table 3, expression of the *srr2*p$_{615}$-*lacZ* fusion increased about 40-fold in the *covR* background (BM1134) compared to the WT background. This result suggests that CovR might play a major role as a negative regulator of *srr2* compared to CodY. According to the work of Mazzuoli *et al* (2021), the Δ*covR* strain displayed a 12-fold increase of *srr2* expression levels compared to WT strain (Mazzuoli *et al*, 2021). Interestingly, expression levels of the *srr2*p615-*lacZ* fusion in the *covR/codY* double mutant (BM1135) were similar to the ones observed in the single *codY* mutant (Table 7). In the absence of CodY, CovR is unable to repress *srr2*: the ratio between the β-galactosidase activities of the Δ*codY* Δ*covR* / Δ*codY* strains is in fact equal to 1. Similarly, in the absence of CovR, the repressive capacity of CodY is also reduced (Δ*codY* Δ*covR* / Δ*covR*, Table 7). Together these results indicate that when one of the two repressors is absent, the repressory activity of both regulators is abolished.

The *srr2*p$_{398}$-*lacZ* and *srr2*p$_{371}$-*lacZ* fusions were tested in the Δ*covR* and Δ*covR*/Δ*codY* strains, in order to test whether the two different regions are involved in CovR-mediated regulation of *srr2* expression. Deletion of *covR* led to a 2-fold derepression of *srr2*p$_{398}$-*lacZ* and a 5.8-fold derepression of *srr2*p$_{371}$-*lacZ* fusions, compared to the WT strain (Table 7). Moreover, expression of both fusions in the Δ*covR*/Δ*codY* double mutant strain remained unchanged compared to the expression

levels obtained in the single Δ*covR* or Δ*codY* mutant strains (Table 7). Together these data suggest that, when individually analyzed, the regions comprised by the two fragmentsare not sufficient for an efficient CovR-mediated repression of *srr2* expression. The limited repression exerted by CovR at the level of the *srr2*p_{371}-*lacZ* fusion was completely abolished upon introduction of the p3 mutation (Table 7). Taken together, these results confirm that both CodY and CovR are strong repressors of the *srr2* gene, but that binding of both of them is needed for an efficient repression of this gene.

Table 7. Expression of *srr2*p-*lacZ* fusions

Strain	Relevant genotype	Fusion type	β-galactosidase activity *		
			Miller Units ± SD	Repression ratio	
				codY/codY+ fold regulation	*covR/covR+* fold regulation
BM1108	BM110	*srr2*p$_{615}$-*lacZ*	5,24 ± 1,4	18,3	39,6
BM1109	BM110*codY*		96,11 ± 16,57		1,2
BM1134	BM110*covR*		207,4 ± 33,23	0,6	
BM1135	BM110*codY/covR*		119,1 ± 27,47		
BM1116	BM110	*srr2*p1$_{615}$-*lacZ*	4,04 ± 0,80	28,4	
BM1117	BM110*codY*		114,8 ± 16,32		
BM1118	BM110	*srr2*p2$_{615}$-*lacZ*	44,87 ± 14,26	2,7	
BM1119	BM110*codY*		120,2 ± 21,71		
BM1120	BM110	*srr2*p1,2$_{615}$-*lacZ*	30,55 ± 7,13	3,3	
BM1121	BM110*codY*		101,9 ± 6,09		
BM1124	BM110	*srr2*p3$_{615}$-*lacZ*	73,83 ± 4,49	2,1	
BM1125	BM110*codY*		156,3 ± 19,19		
BM1110	BM110	*srr2*p$_{398}$-*lacZ*	138 ± 17,7	1,5	2,0
BM1111	BM110*codY*		206,1 ± 24,01		0,8
BM1130	BM110*covR*		273,3 ± 19,92	0,6	
BM1131	BM110*codY/covR*		160,8 ± 29,53		
BM1164	BM110	*srr2*p$_{371}$-*lacZ*	29,11 ± 1,34	4,2	5,8
BM1165	BM110*codY*		123,1 ± 0,31		0,8
BM1166	BM110*covR*		169,2 ± 2,70	0,6	
BM1167	BM110*codY/covR*		99,68 ± 14,59		
BM1182	BM110	*srr2*p3$_{371}$-*lacZ*	84,51 ± 2,85	1,3	1,8
BM1183	BM110*codY*		111,1 ± 10,83		0,7
BM1184	BM110*covR*		154 ± 11,53	0,5	
BM1185	BM110*codY/covR*		79,24 ± 1,13		

* β-galactosidase activity is reported in Miller Units. Data are the average ± SD of two independent experiments, each performed in duplicate.

4.8 Investigating the effect of *srr2* over-expression on the Δ*codY*- altered virulence characteristics

4.8.1 CodY-modulated overexpression of *srr2* mediates *S. agalactiae* adhesion to host proteins

Bacterial binding to plasma and extracellular-matrix proteins represents an important molecular escamotage for bacterial pathogenesis. This interaction can promote bacterial evasion of the immune system, adhesion and eventual invasion of host cells. For this reason, the role of CodY in controlling the ability of *S. agalactiae* to bind to several human proteins was evaluated. Binding of the WT and *codY* mutant strains to fibrinogen, fibronectin and plasminogen was assessed by enzyme-linked immunosorbent assay (ELISA). A slight increase in binding to plasminogen was observed for the *codY*-null mutant compared to the WT strain, however the difference in binding levels was not statistically significant (Figure 23 A). On the contrary, deletion of *codY* led to a significant increase in bacterial binding to fibrinogen and fibronectin with respect to the WT strain. In particular, the higher adhesion to fibronectin of the mutant strain compared to the WT strain was displayed at high substrate concentrations (Figure 23 C), while the increased capability of the mutant strain to adhere to fibrinogen was displayed even at very low concentrations of substrate immobilized in the assay (Figure 23 B). Given the fact that several studies have demonstrated that Srr2 is involved in bacterial binding to both plasminogen and fibrinogen (Six *et al*, 2015), we tested whether the increased adhesion to these proteins by the *codY* deletion mutant was mediated by Srr2 overexpression. An in-frame, marker-less deletion of the *srr2* gene was created in the WT and in the Δ*codY* strains, thus obtaining the strains Δ*srr2* and Δ*srr2*/Δ*codY,* respectively. The ELISA assay performed with the WT, Δ*codY,* Δ*srr2* and Δ*srr2*/Δ*codY* strains revealed that lack of Srr2 results in a strong impairment in bacterial binding to both fibrinogen and fibronectin, regardless of the presence of CodY. Overexpression of Srr2 could therefore be responsible for the increase in Δ*codY* binding to these two host proteins (Figure 23 B and C). On the other hand, binding to plasminogen was not affected by *srr2* deletion, neither in presence nor in absence of CodY (Figure 23 A).

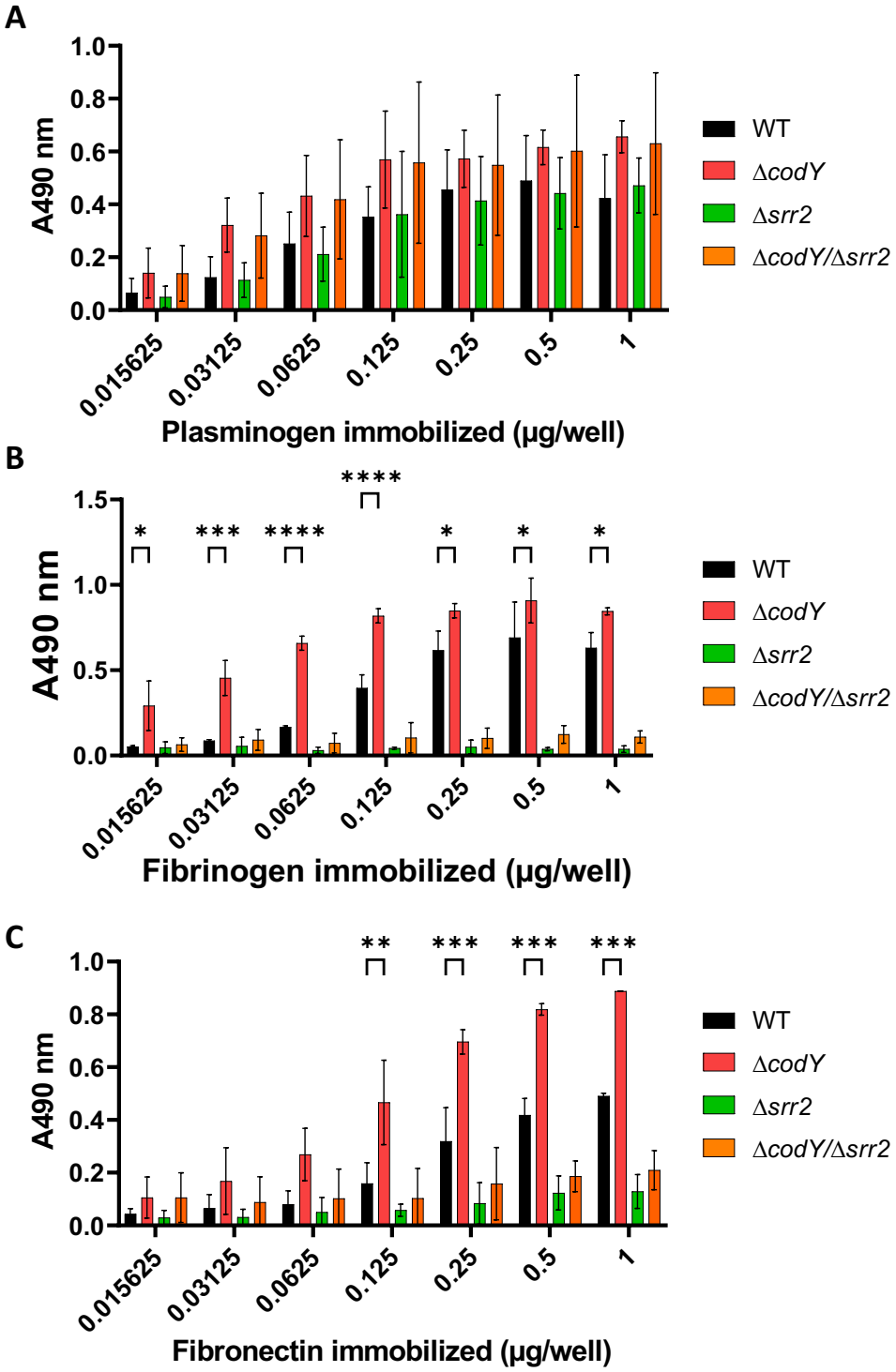
A
A490 nm
1.0
0.8
0.6
0.4
0.2
0.0
0.015625
0.03125
0.0625
0.125
0.25
0.5
1
Plasminogen immobilized (µg/well)
WT
ΔcodY
Δsrr2
ΔcodY/Δsrr2
B
A490 nm
1.5
1.0
0.5
0.0
****
*
***
****
*
*
*
0.015625
0.03125
0.0625
0.125
0.25
0.5
1
Fibrinogen immobilized (µg/well)
WT
ΔcodY
Δsrr2
ΔcodY/Δsrr2
C
A490 nm
1.0
0.8
0.6
0.4
0.2
0.0
**
***
***
***
0.015625
0.03125
0.0625
0.125
0.25
0.5
1
Fibronectin immobilized (µg/well)
WT
ΔcodY
Δsrr2
ΔcodY/Δsrr2

Figure 23. Over-expression of *srr2* influences Δ*codY* binding to host proteins. *S. agalactiae* WT, Δ*codY*, Δ*srr2*, Δ*codY*/Δ*srr2* strains binding to plasma and matrix components were evaluated through ELISA assay. Increasing concentration of proteins were immobilized on the surface of microtiter wells and then incubated with bacterial cells from each strain collected during exponential phase of growth in rich THY medium. Bound bacteria were detected with rabbit anti-*S. agalactiae* IgG, followed by goat HRP-conjugated anti-rabbit IgG. The figures are representative of 2 independent experiments, each performed in duplicate. Statistically significant differences are indicated (2way ANOVA test; **, $P < 0.01$; ***, $P < 0.001$, ****, $P < 0.0001$).

4.8.2 Overespression of *srr2* in Δ*codY* strain is not the cause of the increased biofilm formation

As reported in paragraph 4.3.2, *codY* deletion results in an increased biofilm forming ability of *S. agalactiae*. In an attempt to test whether *srr2* overexpression could be involved in the increase in biofilm biomass in the *codY*-null mutant, we compared the biofilm forming ability of the WT, Δ*codY,* Δ*srr2* and Δ*srr2*/Δ*codY* strains. As reported in Figure 24, deletion of *srr2* led to a slight, but not significant decrease in biofilm levels compared to the WT strain. Moreover, the double mutant strain maintained a significant increased biofilm forming ability compared to the *srr2* mutant strain, suggesting that other factors under control of CodY must be the cause of the increased biofilm biomass in the mutant strain. A slightly significant decrease in biofilm levels of the double mutant strain was obtained with respect to the Δ*codY* strain, however WT/Δ*srr2* and Δ*codY*/(Δ*srr2*/Δ*codY)* ratio of biofilm formed were identical (1.4 ratio). Together these results suggest that *srr2* overexpression could play a role, but is not the main factor involved in Δ*codY* increased biofilm forming ability.

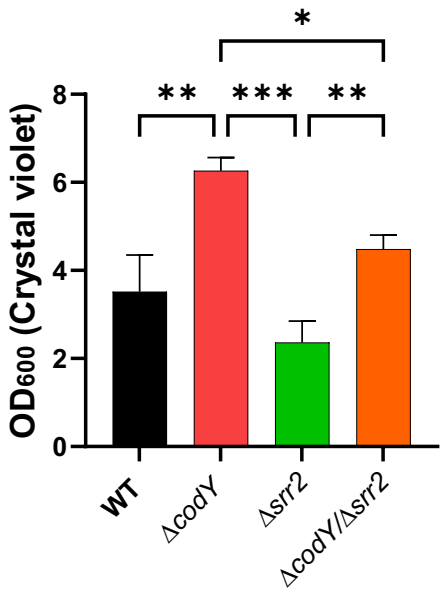

Figure 24. Over-expression of *srr2* in *S. agalactiae* Δ*codY* is not the only cause of increased formation of biofilm. Crystal violet staining was used to measure biofilm biomass formed after static culture for 19 h. Represented data are the average ± SD of three independent experiments, each performed in 8 replicates. Statistically significant differences are reported (Ordinary one-way ANOVA).

5. Discussion and future perspectives

In this study we investigated the role of the global transcriptional regulator CodY in *Streptococcus agalactiae*. In low-G+C Gram-positive bacteria, this highly conserved protein regulates the expression of metabolic pathways according to nutrient availability. In pathogens CodY coordinates metabolism with virulence in a species-specific manner, acting as a repressor or activator of virulence (Brinsmade, 2017). The role of CodY has been previously investigated in several streptococcal species, including *Streptococcus suis, Streptococcus pyogenes, Streptococcus salivarius* (Feng *et al*, 2016; Kreth *et al*, 2011; Majerczyk *et al*, 2008). The analysis conducted in this study aimed at investigating whether CodY controls metabolism and virulence in *S. agalactiae.*

A *codY* deletion mutant was created from the BM110 strain, a hypervirulent strain causative of meningitis in newborns. The resulting strain showed no growth defects under the conditions tested (rich THY medium and chemically defined medium supplemented with high or low branched-chain-amino acids, BCAAs), confirming that *codY* is not essential for *S. agalactiae* growth in laboratory media (Hooven *et al*, 2016). However, morphological observations and confocal microscopy analysis revealed that the deletion mutant formed smaller colonies and displayed a reduced cell size compared to the wild-type strain. This phenotype has been previously observed in other bacterial species in which *codY*-null mutants have been created, including *S. salivarius* (Geng *et al,* 2018) and *S. aureus* (Majerczyk *et al*, 2008).

Analysis conducted on different murine models of infection showed that in *S. agalactiae codY* is necessary for growth *in vivo*. Mutant strains were not able to cause infection and displayed a decreased ability to disseminate in blood and to distant organs in all the infection models investigated. Mice infection with the wild-type and mutant strains elicited a similar cytokine response in the host. Therefore, the reduced virulence of the mutant could be attributed to pleiotropic effects of the *codY* deletion on bacterial physiology and virulence-related characteristics, rather than to an altered immune response of the host.

Adhesion to host tissues represents the first step in bacterial colonization. Deletion of *codY* decreased *S. agalactiae* ability to bind to human epithelial cells *in vitro*. However, the *codY*-null mutant strain displayed increased invasion rates compared to the wild-type strain. Interestingly, preliminary data collected by our collaborator Dr. Brandon Kim (University of Alabama, USA) suggest that the adhesive and invasive characteristics of the mutant strain depend on the type of cell used in the assay. Indeed, when brain microvascular endothelial-like cells obtained through differentiation of induced pluripotent stem-cells were used to test the adhesive and invasive capacities of the Δ*codY* strain, an increased ability to adhere to and invade

host cells was observed compared to the wild-type strain (Brandon Kim's personal communication, manuscript in preparation).

Strong biofilm formation is a common phenotype among *S. agalactiae* strains able to asymptomatically colonize the host. On the contrary, strains associated to a more invasive phenotype (e.g., strains belonging to the CC17 clonal complex) are classified as weak biofilms formers (Parker *et al*, 2016). Deletion of *codY* results in an increased ability of the mutant to form biofilms whose extracellular matrix is enriched in extracellular proteins.

Genes encoding proteins involved in cell wall and membrane biogenesis represent a group of targets subjected to the highest level of CodY-mediated regulation. This group includes proteins anchored to the cell-wall through the LPxTG motif, like the CC17 specific adhesin Srr2. To investigate whether the increased biofilm biomass formed by CodY could be due to overexpression of *srr2* in the *codY* deletion mutant, we conducted biofilm formation assays employing single *srr2* and double *srr2/codY* deletion mutant strains. No significant difference in the biofilm formed by the wild-type and the Δ*srr2* strain could be appreciated. Moreover, the double mutant strain maintained an increased biofilm forming ability compared to the single Δ*srr2* strain. Increased abundance of Srr2 on the surface of the Δ*codY* strain is therefore not involved in its increased ability to form biofilm. We hypothesize that other surface proteins controlled by CodY could be responsible for the observed biofilm forming capacity of the mutant strain.

Srr2 is a key virulence factor that supports the ability of *S. agalactiae* to cross the developing neonatal gastrointestinal epithelium and to adhere to and invade cerebral endothelial cells, thus leading to invasive infections and meningitis in neonates (Deshayes de Cambronne *et al*, 2021).

We demonstrated that CodY is a direct repressor of the *srr2* gene. Two putative CodY binding motifs located upstream of the *srr2* coding region were identified. EMSA analyses and β-galactosidase assays showed that CodY regulation of *srr2* is mostly mediated by CodY binding at the level of the upstream CodY binding site, located at position -163 with respect to the *srr2* transcription start site. It will be important to carry out DNA footprinting experiments to determine the exact site recognized by CodY. Interestingly, CodY binding sites are usually located close to the transcription start site of its target genes or within their coding sequence (Belitsky and Sonenshein, 2013). Therefore, the location of the *srr2* main CodY binding motif is peculiar.

A transcriptomic analysis was recently performed to determine the regulon of the master regulator of virulence CovR in *S. agalactiae* (Mazzuoli *et al*, 2021). Interestingly, comparative transcriptomic analysis revealed an overlap between CodY-mediated gene regulation and genes directly regulated by the master regulator of virulence CovR. The *srr2* operon is included in the group of genes that are directly

repressed by both CodY and CovR (Mazzuoli *et al,* 2021). Importantly, Mazzuoli *et al* (2021) observed that *srr2* expression increased in a *covR*-deletion mutant compared to a wild-type mutant strain. However, *srr2* expression was not affected in a mutant in which CovR was mutagenized in order to prevent its phosphorylation and consequent activation. This result suggested the presence of other regulators involved in control of *srr2* expression. To investigate whether CodY co-operates with CovR in the regulation of *srr2* expression, β-galactosidase analyses were conducted. Preliminary evidence suggests that both transcriptional repressors are needed for an efficient repression of *srr2*. Ongoing studies will further investigate the interplay between CodY and CovR, in order to define the mechanisms behind the concerted regulation of *S. agalactiae* virulence.

These evidences suggest that these two global regulators may coordinate their activities to control virulence. It is worthy of note that in *S. pyogenes*, CodY and CovRS coordinate the bacterial transcriptional network in opposite ways, with CodY stimulating and CovR repressing a consistent portion of the core genome, including several virulence factors. In particular, *S. pyogenes* CodY represses *covR* expression, allowing to counterbalance CovRS activity according to the nutritional status of the cell (Kreth *et al*, 2011). Differently from *S. pyogenes*, *S. agalactiae* CodY and CovRS do not control each other's transcription, adding a layer of complexity to the regulation of virulence and metabolism in *S. agalactiae*.

The adhesin Srr2 mediates *S. agalactiae* adhesion to the plasma and extracellular matrix components fibrinogen and plasminogen. Bacterial adhesion to fibrinogen is essential for early colonization of host tissues and organs (Six *et al*, 2015). We investigated whether *srr2* upregulation mediated by *codY* deletion affects the bacterial ability to bind fibrinogen, fibronectin and plasminogen. The Δ*codY* strain displayed an increased binding ability to fibrinogen and fibronectin compared to the wild-type strain. Deletion of *srr2* in both wild-type and Δ*codY* strains led to a complete loss of the binding ability to these two proteins, indicating that the CodY-mediated increase in *srr2* expression could play a role in the increased ability of the mutant strain to bind fibrinogen and fibronectin. This result suggests the existence of a yet to be defined interaction between Srr2 and fibronectin. The possible interaction between the two proteins will be furtherly investigated *in vitro,* using recombinant wild-type or mutated Srr2 domains. We did not observe any significant difference in binding to plasminogen between the wild-type and Δ*codY* strains. Previous studies had reported that deletion of *srr2* leads to a decreased binding to plasminogen compared to wild-type strains (Six *et al*, 2015). Interestingly, we observed no difference in plasminogen-binding in the presence or absence of *srr2* in both wild-type and *codY*-null mutant strains. One possible explanation for this result could reside in the different experimental procedures employed: Six *et al* (2015) detected bacterial binding to plasminogen through crystal violet assay which, in our hands,

does not provide an ideal method to detect *S. agalactiae*. For this reason, our ELISA assays were performed using an antibody specific for *S. agalactiae* strains.

According to the transcriptomic analysis conducted on wild-type and *codY*-null mutant cells, CodY is a global regulator of gene expression in *S. agalactiae*. In addition to genes involved in cell-wall biosynthesis, targets subjected to the highest level of CodY regulation include genes involved in oligopeptides and amino acid uptake. In different Gram-positive pathogens, including *S. agalactiae*, systems for peptide uptake are important for nutrient acquisition and virulence. In *S. agalactiae*, mutant strains lacking oligopeptide permeases genes displayed decreased adhesion rates to the plasma proteins fibrinogen and fibronectin and to host cells. This negatively interferes with the bacterial ability to colonize the host and therefore leads to a decreased ability to establish an infection. This result suggests that oligopeptide permeases promote virulence in *S. agalactiae* (Samen *et al,* 2004). The genome of *S. agalactiae* does not include genes required for the biosynthesis of precursors of most amino acids, BCAAs included. For this reason, this bacterium relies on transporters and peptidases for amino acids metabolism (Milligan *et al,* 1978). Here, we demonstrated that CodY acts as a direct, negative regulator of at least two BCAAs transporters encoded by the *livK-G* operon and by the *brnQ* gene, respectively.

BCAAs are not only fundamental for protein synthesis but they are also intermediates required for the production of branched chain fatty acids, the major constituents of bacterial membranes. In addition, BCAAs are universal cofactors of CodY. As demonstrated in *Bacillus subtilis* and *Staphylococcus aureus,* a decrease in BCAAs abundance leads to a reduction in the fraction of CodY active molecules. Therefore, as the levels of BCAAs decrease, only targets with higher affinity for CodY will remain under CodY-mediated regulation. The final result is a hierarchical regulation of gene expression depending on the DNA-binding affinity of the regulator for its target genes (Brinsmade *et al,* 2014).

Here, we demonstrated that the activity of *S. agalactiae* CodY is dependent on its interaction with BCAAs. CodY mediated repression of genes involved in amino acid uptake *(livK, braB, brnQ*) decreases under conditions of low BCAAs availability. Moreover, as assessed by gel-shift assays, the DNA binding ability of CodY to its target sequences is increased in the presence of BCAAs. Therefore, as the abundance of BCAAs decreases, CodY-mediated regulation of target genes is relieved. As a consequence, genes encoding BCAAs transporters will be activated when ILV concentrations will be limiting. CodY therefore controls the intracellular levels of BCAAs by regulating the expression of BCAAs transporters.

In accordance with these observations, our analysis revealed that, under conditions of low BCAAs concentrations, the expression of CodY repressed genes was relieved to a different extent depending on the analyzed target. For instance, *livK* expression

was maintained at very low levels even when BCAAs were present in low concentrations, suggesting that CodY is a strong repressor of this gene. On the other hand, CodY-mediated *brnQ* repression decreases to a major extent in presence of low BCAA concentrations.

BCAAs concentrations change in the different host environments that the bacterium encounters during infection. Amniotic fluid represents an example of host niche with low amounts of amino acids (Mesavage *et al*, 1985). Because of its auxotrophy for several amino acids, *S. agalactiae* relies on its capacity to take up exogenous oligopeptides to grow in this environment. Several genes (*oppA1-F* and *livK* operons*, braB, brnQ*, BQ8897_RS10635) involved in peptide and amino acid transport and metabolism, upregulated in the *codY*-null mutant strain, were reported to be upregulated during bacterial growth in amniotic fluid. Overexpression of these genes was concomitant with an 11-fold reduction in the expression of the *codY* gene itself, during growth in amniotic fluid compared to a rich laboratory medium (Sitkiewicz *et al*, 2009). It is possible to hypothesize that the reduced levels of this repressor could explain the overexpression of peptides and amino acids transport systems in amniotic fluid.

By controlling the intracellular levels of components that are essential for cell survival and that act as signals of environmental conditions, amino acid and oligopeptide transporters play an important role in the regulation of bacterial gene expression. In *S. aureus* it has been recently demonstrated that deletion of an isoleucine transporter is associated to increased virulence. *In vivo* experiments showed that mice infected with bacteria lacking the isoleucine transporter displayed decreased bacterial burden in organs compared to mice infected with wild-type strains (Kaiser *et al,* 2015). The authors hypothesized that, as mediators of intracellular levels of CodY co-factors, BCAA transporters might be involved in modulation of CodY-regulation of virulence genes and in turn of *S. aureus* pathogenicity. In *Bacillus anthracis,* CodY acts as a positive regulator of virulence. Dutta *et al* (2022) demonstrated that BCAA transport plays a crucial role for virulence in this species, as deletion of a BCAA transporter resulted in decreased virulence in a mouse model for anthrax. By hindering BCAA uptake through deletion of BCAA transporters, CodY cofactors levels are reduced intracellularly, and in turn CodY promotion of virulence decreases. The authors observed that no single BCAA transporter is fundamental, but that the presence of at least one of them is essential for bacterial survival, even though *B. anthracis* displays genes for BCAAs biosynthesis (Dutta *et al*, 2022). Redundancy among BCAA transporters has been reported for several species. The analysis of the genome of *S. agalactiae* strain BM110 predicts the presence of at least four BCAA transporters (one BCAA-ABC transporter encoded by the *livKG* operon; two single gene-encoded permeases similar to the *S. aureus* BCAA-transporters BrnQ1 and BraB; iii) two genes organized in a dicistronic operon and corresponding to the *azlCD* genes of *B. subtilis*). We

demonstrated that CodY is a direct repressor of at least two of them (*livK-G* and *brnQ*) in rich medium.

Future analysis will be performed to investigate the importance of BCAA transporters in *S. agalactiae*. The creation of deletion mutants for different BCAAs transporters could help in assessing the importance of one or more of them in controlling the intracellular levels of these amino acids. This could in turn give new insights for understanding how the bacterium modulates CodY activity and virulence and, possibly, help in the design of new therapeutic strategies. Modulating *S. agalactiae* ability to uptake BCAAs from the external environment could affect CodY activity and in turn reduce bacterial virulence, possibly.

The lack of an effective vaccine against *S. agalactiae* represents a serious threat and requires a major effort to find new alternative therapeutic options for the treatment of *S. agalactiae* infections. Up to date, even though clinical trials for the formulation of potential vaccine candidates are ongoing, no licensed drugs have been produced yet. To this purpose, it is fundamental to focus the research on the molecular mechanisms that govern *S. agalactiae* infections. Our future goals aim at dissecting how CodY activity is coordinated within the network of regulators that control *S. agalactiae* adaptation to changing host niches and virulence. This will allow deciphering the signals that govern host-pathogen interaction during colonization and infection. In addition, we are going to investigate how *S. agalactiae* CodY exerts hierarchical expression of genes belonging to its regulatory network. It is important to understand how CodY integrates central metabolic pathways with virulence gene expression upon changing levels of BCAAs availability. This will help to understand whether BCAAs transporters could be exploited as targets for the development of a therapeutic strategy.

6. References

- Al Safadi, R., Mereghetti, L., Salloum, M., Lartigue, M. F., Virlogeux-Payant, I., Quentin, R., & Rosenau, A. (2011). Two-component system RgfA/C activates the fbsB gene encoding major fibrinogen-binding protein in highly virulent CC17 clone group B *Streptococcus*. *PloS One*, 6(2), e14658. https://doi.org/10.1371/journal.pone.0014658
- Armistead, B., Oler, E., Adams Waldorf, K., & Rajagopal, L. (2019). The Double Life of Group B *Streptococcus*: Asymptomatic Colonizer and Potent Pathogen. *Journal of Molecular Biology*, *431*(16), 2914–2931. https://doi.org/10.1016/j.jmb.2019.01.035
- Barbieri, G., Albertini, A. M., Ferrari, E., Sonenshein, A. L., & Belitsky, B. R. (2016). Interplay of CodY and ScoC in the Regulation of Major Extracellular Protease Genes of *Bacillus subtilis*. *Journal of Bacteriology*, 198(6), 907–920. https://doi.org/10.1128/JB.00894-15
- Barbieri, G., Voigt, B., Albrecht, D., Hecker, M., Albertini, A. M., Sonenshein, A. L., Ferrari, E., & Belitsky, B. R. (2015). CodY regulates expression of the *Bacillus subtilis* extracellular proteases Vpr and Mpr. *Journal of Bacteriology*, 197(8), 1423–1432. https://doi.org/10.1128/JB.02588-14
- Baron, M. J., Bolduc, G. R., Goldberg, M. B., Aupérin, T. C., & Madoff, L. C. (2004). Alpha C protein of group B *Streptococcus* binds host cell surface glycosaminoglycan and enters cells by an actin-dependent mechanism. *The Journal of Biological Chemistry*, 279(23), 24714–24723. https://doi.org/10.1074/jbc.M402164200
- Beckmann, C., Waggoner, J. D., Harris, T. O., Tamura, G. S., & Rubens, C. E. (2002). Identification of novel adhesins from Group B *streptococci* by use of phage display reveals that C5a peptidase mediates fibronectin binding. *Infection and Immunity*, 70(6), 2869–2876. https://doi.org/10.1128/IAI.70.6.2869-2876.2002
- Belitsky, B. R., & Sonenshein, A. L. (2011). Roadblock repression of transcription by *Bacillus subtilis* CodY. *Journal of Molecular Biology,* 411(4), 729–743. https://doi.org/10.1016/j.jmb.2011.06.012
- Belitsky, B. R., & Sonenshein, A. L. (2013). Genome-wide identification of *Bacillus subtilis* CodY-binding sites at single-nucleotide resolution. *Proceedings of the National Academy of Sciences of the United States of America,* 110(17), 7026–7031. https://doi.org/10.1073/pnas.1300428110
- Belitsky, B. R., Barbieri, G., Albertini, A. M., Ferrari, E., Strauch, M. A., & Sonenshein, A. L. (2015). Interactive regulation by the *Bacillus subtilis* global regulators CodY and ScoC. *Molecular Microbiology*, 97(4), 698–716. https://doi.org/10.1111/mmi.13056 (b)
- Belitsky, B. R., Brinsmade, S. R., & Sonenshein, A. L. (2015). Intermediate Levels of *Bacillus subtilis* CodY Activity Are Required for Derepression of

the Branched-Chain Amino Acid Permease, BraB. *PLoS Genetics*, 11(10), e1005600. https://doi.org/10.1371/journal.pgen.1005600 (a)

- Bellais, S., Six, A., Fouet, A., Longo, M., Dmytruk, N., Glaser, P., Trieu-Cuot, P., & Poyart, C. (2012). Capsular switching in group B *Streptococcus* CC17 hypervirulent clone: a future challenge for polysaccharide vaccine development. *The Journal of Infectious Diseases,* 206(11), 1745–1752. https://doi.org/10.1093/infdis/jis605
- Berardi, A., Rossi, C., Lugli, L., Creti, R., Bacchi Reggiani, M. L., Lanari, M., Memo, L., Pedna, M. F., Venturelli, C., Perrone, E., Ciccia, M., Tridapalli, E., Piepoli, M., Contiero, R., Ferrari, F., & GBS Prevention Working Group, Emilia-Romagna (2013). Group B *Streptococcus* late-onset disease: 2003-2010. *Pediatrics*, 131(2), e361–e368. https://doi.org/10.1542/peds.2012-1231
- Biondo, C., Mancuso, G., Midiri, A., Signorino, G., Domina, M., Lanza Cariccio, V., Venza, M., Venza, I., Teti, G., & Beninati, C. (2014). Essential role of interleukin-1 signaling in host defenses against group B *streptococcus*. *mBio*, *5*(5), e01428-14. https://doi.org/10.1128/mBio.01428-14
- Biswas, I., Gruss, A., Ehrlich, S. D., & Maguin, E. (1993). High-efficiency gene inactivation and replacement system for gram-positive bacteria. *Journal of Bacteriology*, *175*(11), 3628–3635. https://doi.org/10.1128/jb.175.11.3628-3635.1993
- Biswas, R., Sonenshein, A. L., & Belitsky, B. R. (2020). Genome-wide identification of *Listeria monocytogenes* CodY-binding sites. *Molecular Microbiology,* 113(4), 841–858. https://doi.org/10.1111/mmi.14449Bolduc, G. R., Baron, M. J., Gravekamp, C., Lachenauer, C. S., & Madoff, L. C. (2002). The alpha C protein mediates internalization of group B *Streptococcus* within human cervical epithelial cells. *Cellular Microbiology*, 4(11), 751–758. https://doi.org/10.1046/j.1462-5822.2002.00227.x
- Bolger, A. M., Lohse, M., & Usadel, B. (2014). Trimmomatic: a flexible trimmer for Illumina sequence data. *Bioinformatics (Oxford, England)*, *30*(15), 2114–2120. https://doi.org/10.1093/bioinformatics/btu170
- Botelho, A., Ferreira, A., Fracalanzza, S., Teixeira, L. M., & Pinto, T. (2018). A Perspective on the Potential Zoonotic Role of *Streptococcus agalactiae*: Searching for a Missing Link in Alternative Transmission Routes. *Frontiers in Microbiology*, 9, 608. https://doi.org/10.3389/fmicb.2018.00608
- Bouillaut, L., Dubois, T., Sonenshein, A. L., & Dupuy, B. (2015). Integration of metabolism and virulence in *Clostridium difficile*. *Research in Microbiology*, 166(4), 375–383. https://doi.org/10.1016/j.resmic.2014.10.002
- Brenner, M., Lobel, L., Borovok, I., Sigal, N., & Herskovits, A. A. (2018). Controlled branched-chain amino acids auxotrophy in *Listeria monocytogenes* allows isoleucine to serve as a host signal and virulence effector. *PLoS Genetics*, 14(3), e1007283. https://doi.org/10.1371/journal.pgen.1007283

- Brinsmade S. R. (2017). CodY, a master integrator of metabolism and virulence in Gram-positive bacteria. *Current Genetics*, *63*(3), 417–425. https://doi.org/10.1007/s00294-016-0656-5
- Brinsmade, S. R., & Sonenshein, A. L. (2011). Dissecting complex metabolic integration provides direct genetic evidence for CodY activation by guanine nucleotides. *Journal of Bacteriology*, 193(20), 5637–5648. https://doi.org/10.1128/JB.05510-11
- Brinsmade, S. R., Alexander, E. L., Livny, J., Stettner, A. I., Segrè, D., Rhee, K. Y., & Sonenshein, A. L. (2014). Hierarchical expression of genes controlled by the *Bacillus subtilis* global regulatory protein CodY. *Proceedings of the National Academy of Sciences of the United States of America*, *111*(22), 8227–8232. https://doi.org/10.1073/pnas.1321308111
- Brochet, M., Rusniok, C., Couvé, E., Dramsi, S., Poyart, C., Trieu-Cuot, P., Kunst, F., & Glaser, P. (2008). Shaping a bacterial genome by large chromosomal replacements, the evolutionary history of *Streptococcus agalactiae*. *Proceedings of the National Academy of Sciences of the United States of America*, 105(41), 15961–15966. https://doi.org/10.1073/pnas.0803654105
- Bryan, J. D., & Shelver, D. W. (2009). *Streptococcus agalactiae* CspA is a serine protease that inactivates chemokines. *Journal of Bacteriology*, 191(6), 1847–1854. https://doi.org/10.1128/JB.01124-08
- Bryan, J. D., Liles, R., Cvek, U., Trutschl, M., & Shelver, D. (2008). Global transcriptional profiling reveals *Streptococcus agalactiae* genes controlled by the MtaR transcription factor. *BMC Genomics,* 9, 607. https://doi.org/10.1186/1471-2164-9-607
- Buscetta, M., Firon, A., Pietrocola, G., Biondo, C., Mancuso, G., Midiri, A., Romeo, L., Galbo, R., Venza, M., Venza, I., Kaminski, P. A., Gominet, M., Teti, G., Speziale, P., Trieu-Cuot, P., & Beninati, C. (2016). PbsP, a cell wall-anchored protein that binds plasminogen to promote hematogenous dissemination of group B *Streptococcus*. *Molecular Microbiology*, 101(1), 27–41. https://doi.org/10.1111/mmi.13357
- Buscetta, M., Papasergi, S., Firon, A., Pietrocola, G., Biondo, C., Mancuso, G., Midiri, A., Romeo, L., Teti, G., Speziale, P., Trieu-Cuot, P., & Beninati, C. (2014). FbsC, a novel fibrinogen-binding protein, promotes *Streptococcus agalactiae*-host cell interactions. *The Journal of Biological Chemistry*, 289(30), 21003–21015. https://doi.org/10.1074/jbc.M114.553073
- Caliot, É., Dramsi, S., Chapot-Chartier, M. P., Courtin, P., Kulakauskas, S., Péchoux, C., Trieu-Cuot, P., & Mistou, M. Y. (2012). Role of the Group B antigen of *Streptococcus agalactiae*: a peptidoglycan-anchored polysaccharide involved in cell wall biogenesis. *PLoS pathogens*, *8*(6), e1002756. https://doi.org/10.1371/journal.ppat.1002756
- Carlin, A. F., Chang, Y. C., Areschoug, T., Lindahl, G., Hurtado-Ziola, N., King, C. C., Varki, A., & Nizet, V. (2009). Group B *Streptococcus* suppression of phagocyte functions by protein-mediated engagement of human Siglec-5. *The Journal of Experimental Medicine*, 206(8), 1691–1699. https://doi.org/10.1084/jem.20090691

- Caymaris, S., Bootsma, H. J., Martin, B., Hermans, P. W., Prudhomme, M., & Claverys, J. P. (2010). The global nutritional regulator CodY is an essential protein in the human pathogen *Streptococcus pneumoniae*. *Molecular Microbiology,* 78(2), 344–360. https://doi.org/10.1111/j.1365-2958.2010.07339.x
- Cheng, Q., Stafslien, D., Purushothaman, S. S., & Cleary, P. (2002). The group B streptococcal C5a peptidase is both a specific protease and an invasin. *Infection and Immunity*, 70(5), 2408–2413. https://doi.org/10.1128/IAI.70.5.2408-2413.2002
- Cook, L., Hu, H., Maienschein-Cline, M., & Federle, M. J. (2018). A Vaginal Tract Signal Detected by the Group B *Streptococcus* SaeRS System Elicits Transcriptomic Changes and Enhances Murine Colonization. *Infection and Immunity*, 86(4), e00762-17. https://doi.org/10.1128/IAI.00762-17
- Creti, R., Imperi, M., Berardi, A., Lindh, E., Alfarone, G., Pataracchia, M., Recchia, S., & The Italian Network On Neonatal And Infant Gbs Infections (2021). Invasive Group B Streptococcal Disease in Neonates and Infants, Italy, Years 2015-2019. *Microorganisms*, 9(12), 2579. https://doi.org/10.3390/microorganisms9122579
- Creti, R., Imperi, M., Berardi, A., Pataracchia, M., Recchia, S., Alfarone, G., Baldassarri, L., & Italian Neonatal GBS Infections Working Group (2017). Neonatal Group B *Streptococcus* Infections: Prevention Strategies, Clinical and Microbiologic Characteristics in 7 Years of Surveillance. *The Pediatric Infectious Disease Journal*, *36*(3), 256–262. https://doi.org/10.1097/INF.0000000000001414
- De Gaetano, G. V., Pietrocola, G., Romeo, L., Galbo, R., Lentini, G., Giardina, M., Biondo, C., Midiri, A., Mancuso, G., Venza, M., Venza, I., Firon, A., Trieu-Cuot, P., Teti, G., Speziale, P., & Beninati, C. (2018). The *Streptococcus agalactiae* cell wall-anchored protein PbsP mediates adhesion to and invasion of epithelial cells by exploiting the host vitronectin/αv integrin axis. *Molecular Microbiology*, 110(1), 82–94. https://doi.org/10.1111/mmi.14084
- den Hengst, C. D., van Hijum, S. A., Geurts, J. M., Nauta, A., Kok, J., & Kuipers, O. P. (2005). The *Lactococcus lactis* CodY regulon: identification of a conserved cis-regulatory element. *The Journal of Biological Chemistry*, 280(40), 34332–34342. https://doi.org/10.1074/jbc.M502349200
- Deng, L., Mu, R., Weston, T. A., Spencer, B. L., Liles, R. P., & Doran, K. S. (2018). Characterization of a Two-Component System Transcriptional Regulator, LtdR, That Impacts Group B Streptococcal Colonization and Disease. *Infection and Immunity*, 86(7), e00822-17. https://doi.org/10.1128/IAI.00822-17
- Derré-Bobillot, A., Cortes-Perez, N. G., Yamamoto, Y., Kharrat, P., Couvé, E., Da Cunha, V., Decker, P., Boissier, M. C., Escartin, F., Cesselin, B., Langella, P., Bermúdez-Humarán, L. G., & Gaudu, P. (2013). Nuclease A (Gbs0661), an extracellular nuclease of *Streptococcus agalactiae*, attacks the neutrophil extracellular traps and is needed for full virulence. *Molecular Microbiology*, 89(3), 518–531. https://doi.org/10.1111/mmi.12295

- Deshayes de Cambronne, R., Fouet, A., Picart, A., Bourrel, A. S., Anjou, C., Bouvier, G., Candeias, C., Bouaboud, A., Costa, L., Boulay, A. C., Cohen-Salmon, M., Plu, I., Rambaud, C., Faurobert, E., Albigès-Rizo, C., Tazi, A., Poyart, C., & Guignot, J. (2021). CC17 group B *Streptococcus* exploits integrins for neonatal meningitis development. *The Journal of Clinical Investigation,* 131(5), e136737. https://doi.org/10.1172/JCI136737
- Devaux, L., Sleiman, D., Mazzuoli, M. V., Gominet, M., Lanotte, P., Trieu-Cuot, P., Kaminski, P. A., & Firon, A. (2018). Cyclic di-AMP regulation of osmotic homeostasis is essential in Group B *Streptococcus*. *PLoS Genetics*, 14(4), e1007342. https://doi.org/10.1371/journal.pgen.1007342
- Dhudasia, M. B., Flannery, D. D., Pfeifer, M. R., & Puopolo, K. M. (2021). Updated Guidance: Prevention and Management of Perinatal Group B *Streptococcus* Infection. *NeoReviews*, 22(3), e177–e188. https://doi.org/10.1542/neo.22-3-e177
- Dineen, S. S., McBride, S. M., & Sonenshein, A. L. (2010). Integration of metabolism and virulence by *Clostridium difficile* CodY. *Journal of Bacteriology,* 192(20), 5350–5362. https://doi.org/10.1128/JB.00341-10
- Doran, K. S., Liu, G. Y., & Nizet, V. (2003). Group B streptococcal beta-hemolysin/cytolysin activates neutrophil signaling pathways in brain endothelium and contributes to development of meningitis. *The Journal of Clinical Investigation,* 112(5), 736–744. https://doi.org/10.1172/JCI17335
- Dramsi, S., Caliot, E., Bonne, I., Guadagnini, S., Prévost, M. C., Kojadinovic, M., Lalioui, L., Poyart, C., & Trieu-Cuot, P. (2006). Assembly and role of pili in group B streptococci. *Molecular Microbiology*, 60(6), 1401–1413. https://doi.org/10.1111/j.1365-2958.2006.05190.x
- Duménil, G., & Nassif, X. (2005). Extracellular bacterial pathogens and small GTPases of the Rho family: an unexpected combination. *Current topics in Microbiology and Immunology,* 291, 11–28. https://doi.org/10.1007/3-540-27511-8_2
- D'Urzo, N., Martinelli, M., Pezzicoli, A., De Cesare, V., Pinto, V., Margarit, I., Telford, J. L., Maione, D., & Members of the DEVANI Study Group (2014). Acidic pH strongly enhances in vitro biofilm formation by a subset of hypervirulent ST-17 *Streptococcus* agalactiae strains. *Applied and Environmental Microbiology*, 80(7), 2176–2185. https://doi.org/10.1128/AEM.03627-13
- Dutta, S., Corsi, I. D., Bier, N., & Koehler, T. M. (2022). BrnQ-Type Branched-Chain Amino Acid Transporters Influence *Bacillus anthracis* Growth and Virulence. *mBio*, 13(1), e0364021. Advance online publication. https://doi.org/10.1128/mbio.03640-21
- Edwards, A. N., Krall, E. G., & McBride, S. M. (2020). Strain-Dependent RstA Regulation of Clostridioides difficile Toxin Production and Sporulation. *Journal of Bacteriology*, 202(2), e00586-19. https://doi.org/10.1128/JB.00586-19
- Elbakush, A. M., Miller, K. W., & Gomelsky, M. (2018). CodY-Mediated c-di-GMP-Dependent Inhibition of Mammalian Cell Invasion in *Listeria*

monocytogenes. Journal of Bacteriology, 200(5), e00457-17. https://doi.org/10.1128/JB.00457-17

- Famà, A., Midiri, A., Mancuso, G., Biondo, C., Lentini, G., Galbo, R., Giardina, M. M., De Gaetano, G. V., Romeo, L., Teti, G., & Beninati, C. (2020). Nucleic Acid-Sensing Toll-Like Receptors Play a Dominant Role in Innate Immune Recognition of Pneumococci. *mBio*, *11*(2), e00415-20. https://doi.org/10.1128/mBio.00415-20
- Faralla, C., Metruccio, M. M., De Chiara, M., Mu, R., Patras, K. A., Muzzi, A., Grandi, G., Margarit, I., Doran, K. S., & Janulczyk, R. (2014). Analysis of two-component systems in group B *Streptococcus* shows that RgfAC and the novel FspSR modulate virulence and bacterial fitness. *mBio*, 5(3), e00870-14. https://doi.org/10.1128/mBio.00870-14
- Feng, L., Zhu, J., Chang, H., Gao, X., Gao, C., Wei, X., Yuan, F., & Bei, W. (2016). The CodY regulator is essential for virulence in *Streptococcus suis* serotype 2. *Scientific Reports*, 6, 21241. https://doi.org/10.1038/srep21241
- Ferretti, J., & Köhler, W. (2016). History of Streptococcal Research. In J. J. Ferretti (Eds.) *et. al*., *Streptococcus pyogenes*: Basic Biology to Clinical Manifestations. University of Oklahoma Health Sciences Center.
- Firon, A., Tazi, A., Da Cunha, V., Brinster, S., Sauvage, E., Dramsi, S., Golenbock, D. T., Glaser, P., Poyart, C., & Trieu-Cuot, P. (2013). The Abi-domain protein Abx1 interacts with the CovS histidine kinase to control virulence gene expression in group B *Streptococcus*. *PLoS Pathogens*, 9(2), e1003179. https://doi.org/10.1371/journal.ppat.1003179
- Fischer, P., Pawlowski, A., Cao, D., Bell, D., Kitson, G., Darsley, M., & Johansson-Lindbom, B. (2021). Safety and immunogenicity of a prototype recombinant alpha-like protein subunit vaccine (GBS-NN) against Group B *Streptococcus* in a randomised placebo-controlled double-blind phase 1 trial in healthy adult women. *Vaccine*, 39(32), 4489–4499. https://doi.org/10.1016/j.vaccine.2021.06.046
- Fisher S. H. (1999). Regulation of nitrogen metabolism in *Bacillus subtilis*: vive la différence! *Molecular Microbiology*, 32(2), 223–232. https://doi.org/10.1046/j.1365-2958.1999.01333.x
- Fouet A. (2010). AtxA, a *Bacillus anthracis* global virulence regulator. *Research in Microbiology*, 161(9), 735–742. https://doi.org/10.1016/j.resmic.2010.09.006
- Furfaro, L. L., Chang, B. J., & Payne, M. S. (2018). Perinatal *Streptococcus agalactiae* Epidemiology and Surveillance Targets. *Clinical Microbiology Reviews,* 31(4), e00049-18. https://doi.org/10.1128/CMR.00049-18
- Gangwal, A., Sangwan, N., Dhasmana, N., Kumar, N., Keshavam, C. C., Singh, L. K., Bothra, A., Goel, A. K., Pomerantsev, A. P., Leppla, S. H., & Singh, Y. (2022). Role of serine/threonine protein phosphatase PrpN in the life cycle of *Bacillus anthracis*. *PLoS Pathogens*, 18(8), e1010729. https://doi.org/10.1371/journal.ppat.1010729
- Geiger, T., & Wolz, C. (2014). Intersection of the stringent response and the CodY regulon in low GC Gram-positive bacteria. *International Journal of*

Medical Microbiology: IJMM, 304(2), 150–155. https://doi.org/10.1016/j.ijmm.2013.11.013

- Geng, J., Huang, S. C., Chen, Y. Y., Chiu, C. H., Hu, S., & Chen, Y. M. (2018). Impact of growth pH and glucose concentrations on the CodY regulatory network in *Streptococcus salivarius*. *BMC Genomics*, *19*(1), 386. https://doi.org/10.1186/s12864-018-4781-z
- Glaser, P., Rusniok, C., Buchrieser, C., Chevalier, F., Frangeul, L., Msadek, T., Zouine, M., Couvé, E., Lalioui, L., Poyart, C., Trieu-Cuot, P., & Kunst, F. (2002). Genome sequence of *Streptococcus agalactiae*, a pathogen causing invasive neonatal disease. *Molecular Microbiology*, *45*(6), 1499–1513. https://doi.org/10.1046/j.1365-2958.2002.03126.x
- Gonçalves, B. P., Procter, S. R., Paul, P., Chandna, J., Lewin, A., Seedat, F., Koukounari, A., Dangor, Z., Leahy, S., Santhanam, S., John, H. B., Bramugy, J., Bardají, A., Abubakar, A., Nasambu, C., Libster, R., Sánchez Yanotti, C., Horváth-Puhó, E., Sørensen, H. T., van de Beek, D., … CHAMPS team (2022). Group B *streptococcus* infection during pregnancy and infancy: estimates of regional and global burden. *The Lancet.* Global health, 10(6), e807–e819. https://doi.org/10.1016/S2214-109X(22)00093-6
- Graham, M. R., Smoot, L. M., Migliaccio, C. A., Virtaneva, K., Sturdevant, D. E., Porcella, S. F., Federle, M. J., Adams, G. J., Scott, J. R., & Musser, J. M. (2002). Virulence control in group A *Streptococcus* by a two-component gene regulatory system: global expression profiling and *in vivo* infection modeling. *Proceedings of the National Academy of Sciences of the United States of America*, 99(21), 13855–13860. https://doi.org/10.1073/pnas.202353699
- Grant, C. E., Bailey, T. L., & Noble, W. S. (2011). FIMO: scanning for occurrences of a given motif. *Bioinformatics (Oxford, England),* 27(7), 1017–1018. https://doi.org/10.1093/bioinformatics/btr064
- Graux, E., Hites, M., Martiny, D., Maillart, E., Delforge, M., Melin, P., & Dauby, N. (2021). Invasive group B *Streptococcus* among non-pregnant adults in Brussels-Capital Region, 2005-2019. *European Journal of Clinical Microbiology & Infectious Diseases: Official Publication of the European Society of Clinical Microbiology*, 40(3), 515–523. https://doi.org/10.1007/s10096-020-04041-0
- Gutekunst, H., Eikmanns, B. J., & Reinscheid, D. J. (2003). Analysis of RogB-controlled virulence mechanisms and gene repression in *Streptococcus agalactiae*. *Infection and Immunity*, 71(9), 5056–5064. https://doi.org/10.1128/IAI.71.9.5056-5064.2003.
- Gutekunst, H., Eikmanns, B. J., & Reinscheid, D. J. (2004). The novel fibrinogen-binding protein FbsB promotes *Streptococcus agalactiae* invasion into epithelial cells. *Infection and Immunity*, 72(6), 3495–3504. https://doi.org/10.1128/IAI.72.6.3495-3504.2004
- He, E. M., Chen, C. W., Guo, Y., Hsu, M. H., Zhang, L., Chen, H. L., Zhao, G. P., Chiu, C. H., & Zhou, Y. (2017). The genome of serotype VI *Streptococcus agalactiae* serotype VI and comparative analysis. *Gene*, 597, 59–65. https://doi.org/10.1016/j.gene.2016.10.030

- Hendriksen, W. T., Bootsma, H. J., Estevão, S., Hoogenboezem, T., de Jong, A., de Groot, R., Kuipers, O. P., & Hermans, P. W. (2008). CodY of *Streptococcus pneumoniae*: link between nutritional gene regulation and colonization. *Journal of Bacteriology*, 190(2), 590–601. https://doi.org/10.1128/JB.00917-07
- Heydorn, A., Nielsen, A. T., Hentzer, M., Sternberg, C., Givskov, M., Ersbøll, B. K., & Molin, S. (2000). Quantification of biofilm structures by the novel computer program COMSTAT. *Microbiology (Reading, England)*, *146*(Pt 10), 2395–2407. https://doi.org/10.1099/00221287-146-10-2395
- Ho, Y. R., Li, C. M., Yu, C. H., Lin, Y. J., Wu, C. M., Harn, I. C., Tang, M. J., Chen, Y. T., Shen, F. C., Lu, C. Y., Tsai, T. C., & Wu, J. J. (2013). The enhancement of biofilm formation in Group B streptococcal isolates at vaginal pH. *Medical Microbiology and Immunology*, 202(2), 105–115. https://doi.org/10.1007/s00430-012-0255-0
- Hooven, T. A., Catomeris, A. J., Akabas, L. H., Randis, T. M., Maskell, D. J., Peters, S. E., Ott, S., Santana-Cruz, I., Tallon, L. J., Tettelin, H., & Ratner, A. J. (2016). The essential genome of *Streptococcus agalactiae*. *BMC Genomics*, *17*, 406. https://doi.org/10.1186/s12864-016-2741-z
- Hull, J. R., Shannon, J. J., Tamura, G. S., & Castner, D. G. (2007). Atomic force microscopy and surface plasmon resonance investigation of fibronectin interactions with group B *streptococci*. *Biointerphases*, 2(2), 64–72. https://doi.org/10.1116/1.2738854
- Jarva, H., Hellwage, J., Jokiranta, T. S., Lehtinen, M. J., Zipfel, P. F., & Meri, S. (2004). The group B streptococcal beta and pneumococcal Hic proteins are structurally related immune evasion molecules that bind the complement inhibitor factor H in an analogous fashion. *Journal of Immunology* (Baltimore, Md.: 1950), 172(5), 3111–3118. https://doi.org/10.4049/jimmunol.172.5.3111
- Jiang, F., & Doudna, J. A. (2015). The structural biology of CRISPR-Cas systems. *Current Opinion in Structural Biology*, *30*, 100–111. https://doi.org/10.1016/j.sbi.2015.02.002
- Johri, A. K., Padilla, J., Malin, G., & Paoletti, L. C. (2003). Oxygen regulates invasiveness and virulence of group B *streptococcus*. *Infection and Immunity,* 71(12), 6707–6711. https://doi.org/10.1128/IAI.71.12.6707-6711.2003
- Jones, N., Bohnsack, J. F., Takahashi, S., Oliver, K. A., Chan, M. S., Kunst, F., Glaser, P., Rusniok, C., Crook, D. W., Harding, R. M., Bisharat, N., & Spratt, B. G. (2003). Multilocus sequence typing system for group B *streptococcus*. *Journal of Clinical Microbiology*, 41(6), 2530–2536. https://doi.org/10.1128/JCM.41.6.2530-2536.2003
- Jones, S., Newton, P., Payne, M., & Furfaro, L. (2022). Epidemiology, Antimicrobial Resistance, and Virulence Determinants of Group B *Streptococcus* in an Australian Setting. *Frontiers in Microbiology*, 13, 839079. https://doi.org/10.3389/fmicb.2022.839079.

- Kaiser, J. C., & Heinrichs, D. E. (2018). Branching Out: Alterations in Bacterial Physiology and Virulence Due to Branched-Chain Amino Acid Deprivation. *mBio*, 9(5), e01188-18. https://doi.org/10.1128/mBio.01188-18
- Kaiser, J. C., King, A. N., Grigg, J. C., Sheldon, J. R., Edgell, D. R., Murphy, M., Brinsmade, S. R., & Heinrichs, D. E. (2018). Repression of branched-chain amino acid synthesis in *Staphylococcus aureus* is mediated by isoleucine via CodY, and by a leucine-rich attenuator peptide. *PLoS Genetics*, 14(1), e1007159. https://doi.org/10.1371/journal.pgen.1007159
- Kaiser, J. C., Omer, S., Sheldon, J. R., Welch, I., & Heinrichs, D. E. (2015). Role of BrnQ1 and BrnQ2 in branched-chain amino acid transport and virulence in *Staphylococcus aureus*. *Infection and Immunity*, *83*(3), 1019–1029. https://doi.org/10.1128/IAI.02542-14
- Klinzing, D. C., Ishmael, N., Hotopp, J. C. D., Tettelin, H., Shields, K. R., Madoff, L. C., & Puopolo, K. M. (2013). The two-component response regulator LiaR regulates cell wall stress responses, pili expression and virulence in group B *Streptococcus*. *Microbiology* (Reading, England), 159(Pt 7), 1521–1534. https://doi.org/10.1099/mic.0.064444-0
- Konto-Ghiorghi, Y., Mairey, E., Mallet, A., Duménil, G., Caliot, E., Trieu-Cuot, P., & Dramsi, S. (2009). Dual role for pilus in adherence to epithelial cells and biofilm formation in *Streptococcus agalactiae*. *PLoS Pathogens*, 5(5), e1000422. https://doi.org/10.1371/journal.ppat.1000422
- Korir, M. L., Manning, S. D., & Davies, H. D. (2017). Intrinsic Maturational Neonatal Immune Deficiencies and Susceptibility to Group B *Streptococcus* Infection. *Clinical Microbiology Reviews*, 30(4), 973–989. https://doi.org/10.1128/CMR.00019-17
- Kreth, J., Chen, Z., Ferretti, J., & Malke, H. (2011). Counteractive balancing of transcriptome expression involving CodY and CovRS in *Streptococcus pyogenes*. *Journal of Bacteriology*, 193(16), 4153–4165. https://doi.org/10.1128/JB.00061-11
- Krishnan, V., Gaspar, A. H., Ye, N., Mandlik, A., Ton-That, H., & Narayana, S. V. (2007). An IgG-like domain in the minor pilin GBS52 of *Streptococcus agalactiae* mediates lung epithelial cell adhesion. *Structure (London, England: 1993),* 15(8), 893–903. https://doi.org/10.1016/j.str.2007.06.015
- Lamy, M. C., Zouine, M., Fert, J., Vergassola, M., Couve, E., Pellegrini, E., Glaser, P., Kunst, F., Msadek, T., Trieu-Cuot, P., & Poyart, C. (2004). CovS/CovR of group B *streptococcus*: a two-component global regulatory system involved in virulence. *Molecular Microbiology*, 54(5), 1250–1268. https://doi.org/10.1111/j.1365-2958.2004.04365.x
- Langmead B. (2010). Aligning short sequencing reads with Bowtie. *Current Protocols in Bioinformatics*, *Chapter 11*, Unit–11.7. https://doi.org/10.1002/0471250953.bi1107s32
- Lannes-Costa, P. S., Baraúna, R. A., Ramos, J. N., Veras, J. F. C., Conceição, M. V. R., Vieira, V. V., de Mattos-Guaraldi, A. L., Ramos, R. T. J., Doran, K. S., Silva, A., & Nagao, P. E. (2020). Comparative genomic analysis and identification of pathogenicity islands of hypervirulent ST-17 *Streptococcus* agalactiae Brazilian strain. *Infection, Genetics and Evolution: Journal of*

Molecular Epidemiology and Evolutionary Genetics in Infectious Diseases, 80, 104195. https://doi.org/10.1016/j.meegid.2020.104195

- Lencina, A. M., Franza, T., Sullivan, M. J., Ulett, G. C., Ipe, D. S., Gaudu, P., Gennis, R. B., & Schurig-Briccio, L. A. (2018). Type 2 NADH Dehydrogenase Is the Only Point of Entry for Electrons into the *Streptococcus agalactiae* Respiratory Chain and Is a Potential Drug Target. *mBio*, 9(4), e01034-18. https://doi.org/10.1128/mBio.01034-18
- Lentini, G., Famà, A., De Gaetano, G. V., Galbo, R., Coppolino, F., Venza, M., Teti, G., & Beninati, C. (2021). Role of Endosomal TLRs in *Staphylococcus aureus* Infection. *Journal of Immunology (Baltimore, Md.: 1950)*, *207*(5), 1448–1455. https://doi.org/10.4049/jimmunol.2100389
- Lentini, G., Midiri, A., Firon, A., Galbo, R., Mancuso, G., Biondo, C., Mazzon, E., Passantino, A., Romeo, L., Trieu-Cuot, P., Teti, G., & Beninati, C. (2018). The plasminogen binding protein PbsP is required for brain invasion by hypervirulent CC17 Group B streptococci. *Scientific Reports*, *8*(1), 14322. https://doi.org/10.1038/s41598-018-32774-8
- Levdikov, V. M., Blagova, E., Joseph, P., Sonenshein, A. L., & Wilkinson, A. J. (2006). The structure of CodY, a GTP- and isoleucine-responsive regulator of stationary phase and virulence in gram-positive bacteria. *The Journal of Biological Chemistry*, 281(16), 11366–11373. https://doi.org/10.1074/jbc.M513015200
- Levdikov, V. M., Blagova, E., Young, V. L., Belitsky, B. R., Lebedev, A., Sonenshein, A. L., & Wilkinson, A. J. (2017). Structure of the Branched-chain Amino Acid and GTP-sensing Global Regulator, CodY, from *Bacillus subtilis*. *The Journal of Biological Chemistry*, 292(7), 2714–2728. https://doi.org/10.1074/jbc.M116.754309
- Liao, Y., Smyth, G. K., & Shi, W. (2014). featureCounts: an efficient general purpose program for assigning sequence reads to genomic features. *Bioinformatics (Oxford, England)*, *30*(7), 923–930. https://doi.org/10.1093/bioinformatics/btt656
- Lin, W. J., Walthers, D., Connelly, J. E., Burnside, K., Jewell, K. A., Kenney, L. J., & Rajagopal, L. (2009). Threonine phosphorylation prevents promoter DNA binding of the Group B *Streptococcus* response regulator CovR. *Molecular Microbiology*, 71(6), 1477–1495. https://doi.org/10.1111/j.1365-2958.2009.06616.x
- Lobel, L., Sigal, N., Borovok, I., Belitsky, B. R., Sonenshein, A. L., & Herskovits, A. A. (2015). The metabolic regulator CodY links *Listeria monocytogenes* metabolism to virulence by directly activating the virulence regulatory gene *prfA*. *Molecular Microbiology*, 95(4), 624–644. https://doi.org/10.1111/mmi.12890
- Love, M. I., Huber, W., & Anders, S. (2014). Moderated estimation of fold change and dispersion for RNA-seq data with DESeq2. *Genome Biology*, *15*(12), 550. https://doi.org/10.1186/s13059-014-0550-8
- Lund, S. J., Patras, K. A., Kimmey, J. M., Yamamura, A., Butcher, L. D., Del Rosario, P., Hernandez, G. E., McCoy, A. M., Lakhdari, O., Nizet, V., &

Prince, L. S. (2020). Developmental Immaturity of Siglec Receptor Expression on Neonatal Alveolar Macrophages Predisposes to Severe Group B Streptococcal Infection. *iScience*, 23(6), 101207. https://doi.org/10.1016/j.isci.2020.101207

- Madoff, L. C., Paoletti, L. C., Tai, J. Y., & Kasper, D. L. (1994). Maternal immunization of mice with group B streptococcal type III polysaccharide-beta C protein conjugate elicits protective antibody to multiple serotypes. *The Journal of Clinical Investigation*, 94(1), 286–292. https://doi.org/10.1172/JCI117319
- Magalhães, V., Andrade, E. B., Alves, J., Ribeiro, A., Kim, K. S., Lima, M., Trieu-Cuot, P., & Ferreira, P. (2013). Group B *Streptococcus* hijacks the host plasminogen system to promote brain endothelial cell invasion. *PloS One*, 8(5), e63244. https://doi.org/10.1371/journal.pone.0063244
- Maisey, H. C., Doran, K. S., & Nizet, V. (2008). Recent advances in understanding the molecular basis of group B *Streptococcus* virulence. *Expert Reviews in Molecular Medicine*, 10, e27. https://doi.org/10.1017/S1462399408000811 (a)
- Maisey, H. C., Hensler, M., Nizet, V., & Doran, K. S. (2007). Group B streptococcal pilus proteins contribute to adherence to and invasion of brain microvascular endothelial cells. *Journal of Bacteriology*, 189(4), 1464–1467. https://doi.org/10.1128/JB.01153-06
- Maisey, H. C., Quach, D., Hensler, M. E., Liu, G. Y., Gallo, R. L., Nizet, V., & Doran, K. S. (2008). A group B streptococcal pilus protein promotes phagocyte resistance and systemic virulence. *FASEB Journal: Official Publication of the Federation of American Societies for Experimental Biology,* 22(6), 1715–1724. https://doi.org/10.1096/fj.07-093963 (b)
- Majerczyk, C. D., Dunman, P. M., Luong, T. T., Lee, C. Y., Sadykov, M. R., Somerville, G. A., Bodi, K., & Sonenshein, A. L. (2010). Direct targets of CodY in *Staphylococcus aureus*. *Journal of Bacteriology*, 192(11), 2861–2877. https://doi.org/10.1128/JB.00220-10
- Majerczyk, C. D., Sadykov, M. R., Luong, T. T., Lee, C., Somerville, G. A., & Sonenshein, A. L. (2008). *Staphylococcus aureus* CodY negatively regulates virulence gene expression. *Journal of Bacteriology*, 190(7), 2257–2265. https://doi.org/10.1128/JB.01545-07
- Manina, G., Dhar, N., & McKinney, J. D. (2015). Stress and host immunity amplify *Mycobacterium tuberculosis* phenotypic heterogeneity and induce nongrowing metabolically active forms. *Cell Host & Microbe*, *17*(1), 32–46. https://doi.org/10.1016/j.chom.2014.11.016
- Marques, M. B., Kasper, D. L., Pangburn, M. K., & Wessels, M. R. (1992). Prevention of C3 deposition by capsular polysaccharide is a virulence mechanism of type III group B *streptococci*. *Infection and Immunity*, 60(10), 3986–3993. https://doi.org/10.1128/iai.60.10.3986-3993.1992
- Mazzuoli, M. V., Daunesse, M., Varet, H., Rosinski-Chupin, I., Legendre, R., Sismeiro, O., Gominet, M., Kaminski, P. A., Glaser, P., Chica, C., Trieu-Cuot, P., & Firon, A. (2021). The CovR regulatory network drives the

evolution of Group B *Streptococcus* virulence. *PLoS Genetics*, 17(9), e1009761. https://doi.org/10.1371/journal.pgen.1009761

- McDowell, E. J., Callegari, E. A., Malke, H., & Chaussee, M. S. (2012). CodY-mediated regulation of *Streptococcus pyogenes* exoproteins. *BMC Microbiology*, 12, 114. https://doi.org/10.1186/1471-2180-12-114
- Mesavage, W. C., Suchy, S. F., Weiner, D. L., Nance, C. S., Flannery, D. B., & Wolf, B. (1985). Amino acids in amniotic fluid in the second trimester of gestation. *Pediatric Research*, *19*(10), 1021–1024. https://doi.org/10.1203/00006450-198510000-00014
- Milligan, T. W., Doran, T. I., Straus, D. C., & Mattingly, S. J. (1978). Growth and amino acid requirements of various strains of group B streptococci. *Journal of Clinical Microbiology*, *7*(1), 28–33. https://doi.org/10.1128/jcm.7.1.28-33.1978
- Mohammadi, N., Midiri, A., Mancuso, G., Patanè, F., Venza, M., Venza, I., Passantino, A., Galbo, R., Teti, G., Beninati, C., & Biondo, C. (2016). Neutrophils Directly Recognize Group B Streptococci and Contribute to Interleukin-1β Production during Infection. *PLoS One*, *11*(8), e0160249. https://doi.org/10.1371/journal.pone.0160249
- Montgomery, C. P., Boyle-Vavra, S., Roux, A., Ebine, K., Sonenshein, A. L., & Daum, R. S. (2012). CodY deletion enhances in vivo virulence of community-associated methicillin-resistant *Staphylococcus aureus* clone USA300. *Infection and Immunity*, 80(7), 2382–2389. https://doi.org/10.1128/IAI.06172-11
- Mu, R., Kim, B. J., Paco, C., Del Rosario, Y., Courtney, H. S., & Doran, K. S. (2014). Identification of a group B streptococcal fibronectin binding protein, SfbA, that contributes to invasion of brain endothelium and development of meningitis. *Infection and Immunity*, 82(6), 2276–2286. https://doi.org/10.1128/IAI.01559-13
- Nanduri, S. A., Petit, S., Smelser, C., Apostol, M., Alden, N. B., Harrison, L. H., Lynfield, R., Vagnone, P. S., Burzlaff, K., Spina, N. L., Dufort, E. M., Schaffner, W., Thomas, A. R., Farley, M. M., Jain, J. H., Pondo, T., McGee, L., Beall, B. W., & Schrag, S. J. (2019). Epidemiology of Invasive Early-Onset and Late-Onset Group B Streptococcal Disease in the United States, 2006 to 2015: Multistate Laboratory and Population-Based Surveillance. *JAMA Pediatrics*, 173(3), 224–233. https://doi.org/10.1001/jamapediatrics.2018.4826
- Nawrocki, K. L., Edwards, A. N., Daou, N., Bouillaut, L., & McBride, S. M. (2016). CodY-Dependent Regulation of Sporulation in *Clostridium difficile*. *Journal of Bacteriology*, 198(15), 2113–2130. https://doi.org/10.1128/JB.00220-16
- Oliveira, L., Simões, L. C., Costa, N. S., Zadoks, R. N., & Pinto, T. (2022). The landscape of antimicrobial resistance in the neonatal and multi-host pathogen group B *Streptococcus*: review from a One Health perspective. *Frontiers in Microbiology*, 13, 943413. https://doi.org/10.3389/fmicb.2022.943413

- Parker, R. E., Laut, C., Gaddy, J. A., Zadoks, R. N., Davies, H. D., & Manning, S. D. (2016). Association between genotypic diversity and biofilm production in group B *Streptococcus*. *BMC Microbiology*, *16*, 86. https://doi.org/10.1186/s12866-016-0704-9
- Pawlowski, A., Lannergård, J., Gonzalez-Miro, M., Cao, D., Larsson, S., Persson, J. J., Kitson, G., Darsley, M., Rom, A. L., Hedegaard, M., Fischer, P. B., & Johansson-Lindbom, B. (2022). A group B *Streptococcus* alpha-like protein subunit vaccine induces functionally active antibodies in humans targeting homotypic and heterotypic strains. *Cell Reports. Medicine*, 3(2), 100511. https://doi.org/10.1016/j.xcrm.2022.100511
- Pellegrini, A., Lentini, G., Famà, A., Bonacorsi, A., Scoffone, V. C., Buroni, S., Trespidi, G., Postiglione, U., Sassera, D., Manai, F., Pietrocola, G., Firon, A., Biondo, C., Teti, G., Beninati, C., & Barbieri, G. (2022). CodY Is a Global Transcriptional Regulator Required for Virulence in Group B *Streptococcus*. *Frontiers in Microbiology*, 13, 881549. https://doi.org/10.3389/fmicb.2022.881549
- Pendleton, A., Yeo, W. S., Alqahtani, S., DiMaggio, D. A., Jr, Stone, C. J., Li, Z., Singh, V. K., Montgomery, C. P., Bae, T., & Brinsmade, S. R. (2022). Regulation of the Sae Two-Component System by Branched-Chain Fatty Acids in *Staphylococcus aureus*. *mBio*, 13(5), e0147222. https://doi.org/10.1128/mbio.01472-22
- Petranovic, D., Guédon, E., Sperandio, B., Delorme, C., Ehrlich, D., & Renault, P. (2004). Intracellular effectors regulating the activity of the *Lactococcus lactis* CodY pleiotropic transcription regulator. *Molecular microbiology*, 53(2), 613–621. https://doi.org/10.1111/j.1365-2958.2004.04136.x
- Pezzicoli, A., Santi, I., Lauer, P., Rosini, R., Rinaudo, D., Grandi, G., Telford, J. L., & Soriani, M. (2008). Pilus backbone contributes to group B *Streptococcus* paracellular translocation through epithelial cells. *The Journal of Infectious Diseases*, 198(6), 890–898. https://doi.org/10.1086/591182
- Pietrocola, G., Arciola, C. R., Rindi, S., Montanaro, L., & Speziale, P. (2018). *Streptococcus agalactiae* Non-Pilus, Cell Wall-Anchored Proteins: Involvement in Colonization and Pathogenesis and Potential as Vaccine Candidates. *Frontiers in Immunology*, 9, 602. https://doi.org/10.3389/fimmu.2018.00602
- Pietrocola, G., Rindi, S., Rosini, R., Buccato, S., Speziale, P., & Margarit, I. (2016). The Group B *Streptococcus*-Secreted Protein CIP Interacts with C4, Preventing C3b Deposition via the Lectin and Classical Complement Pathways. *Journal of Immunology* (Baltimore, Md.: 1950), 196(1), 385–394. https://doi.org/10.4049/jimmunol.1501954
- Pietrocola, G., Schubert, A., Visai, L., Torti, M., Fitzgerald, J. R., Foster, T. J., Reinscheid, D. J., & Speziale, P. (2005). FbsA, a fibrinogen-binding protein from *Streptococcus agalactiae*, mediates platelet aggregation. *Blood*, 105(3), 1052–1059. https://doi.org/10.1182/blood-2004-06-2149
- Pinto, T. C., Costa, N. S., Corrêa, A. B., de Oliveira, I. C., de Mattos, M. C., Rosado, A. S., & Benchetrit, L. C. (2014). Conjugative transfer of resistance

determinants among human and bovine *Streptococcus agalactiae*. *Brazilian Journal of Microbiology: [publication of the Brazilian Society for Microbiology],* 45(3), 785–789. https://doi.org/10.1590/s1517-83822014000300004

- Pohl, K., Francois, P., Stenz, L., Schlink, F., Geiger, T., Herbert, S., Goerke, C., Schrenzel, J., & Wolz, C. (2009). CodY in *Staphylococcus aureus*: a regulatory link between metabolism and virulence gene expression. *Journal of Bacteriology*, 191(9), 2953–2963. https://doi.org/10.1128/JB.01492-08
- Poyart, C., & Trieu-Cuot, P. (1997). A broad-host-range mobilizable shuttle vector for the construction of transcriptional fusions to beta-galactosidase in gram-positive bacteria. *FEMS Microbiology Letters*, *156*(2), 193–198. https://doi.org/10.1111/j.1574-6968.1997.tb12726.x
- Poyart, C., Lamy, M. C., Boumaila, C., Fiedler, F., & Trieu-Cuot, P. (2001). Regulation of D-alanyl-lipoteichoic acid biosynthesis in *Streptococcus agalactiae* involves a novel two-component regulatory system. *Journal of Bacteriology,* 183(21), 6324–6334. https://doi.org/10.1128/JB.183.21.6324-6334.2001
- Prevention of Group B Streptococcal Early-Onset Disease in Newborns: ACOG Committee Opinion, Number 797. (2020). *Obstetrics and Gynecology,* 135(2), e51–e72. https://doi.org/10.1097/AOG.0000000000003668
- Quach, D., van Sorge, N. M., Kristian, S. A., Bryan, J. D., Shelver, D. W., & Doran, K. S. (2009). The CiaR response regulator in group B *Streptococcus* promotes intracellular survival and resistance to innate immune defenses. *Journal of Bacteriology*, 191(7), 2023–2032. https://doi.org/10.1128/JB.01216-08
- Rajagopal L. (2009). Understanding the regulation of Group B Streptococcal virulence factors. *Future Microbiology*, 4(2), 201–221. https://doi.org/10.2217/17460913.4.2.201
- Rajagopal, L., Vo, A., Silvestroni, A., & Rubens, C. E. (2006). Regulation of cytotoxin expression by converging eukaryotic-type and two-component signalling mechanisms in *Streptococcus agalactiae*. *Molecular Microbiology,* 62(4), 941–957. https://doi.org/10.1111/j.1365-2958.2006.05431.x
- Ren, W., Rajendran, R., Zhao, Y., Tan, B., Wu, G., Bazer, F. W., Zhu, G., Peng, Y., Huang, X., Deng, J., & Yin, Y. (2018). Amino Acids As Mediators of Metabolic Cross Talk between Host and Pathogen. *Frontiers in Immunology*, 9, 319. https://doi.org/10.3389/fimmu.2018.00319
- Richardson, A. R., Somerville, G. A., & Sonenshein, A. L. (2015). Regulating the Intersection of Metabolism and Pathogenesis in Gram-positive Bacteria. *Microbiology Spectrum*, 3(3), https://doi.org/10.1128/microbiolspec.MBP-0004-2014
- Rosini, R., Rinaudo, C. D., Soriani, M., Lauer, P., Mora, M., Maione, D., Taddei, A., Santi, I., Ghezzo, C., Brettoni, C., Buccato, S., Margarit, I., Grandi, G., & Telford, J. L. (2006). Identification of novel genomic islands coding for antigenic pilus-like structures in *Streptococcus agalactiae.*

Molecular Microbiology, 61(1), 126–141. https://doi.org/10.1111/j.1365-2958.2006.05225.x

- Roux, A. E., Robert, S., Bastat, M., Rosinski-Chupin, I., Rong, V., Holbert, S., Mereghetti, L., & Camiade, E. (2022). The Role of Regulator Catabolite Control Protein A (CcpA) in *Streptococcus agalactiae* Physiology and Stress Response. *Microbiology Spectrum*, e0208022. *Advance online publication*. https://doi.org/10.1128/spectrum.02080-22
- Rozhdestvenskaya, A. S., Totolian, A. A., & Dmitriev, A. V. (2010). Inactivation of DNA-binding response regulator Sak189 abrogates beta-antigen expression and affects virulence of *Streptococcus agalactiae*. *PloS One*, 5(4), e10212. https://doi.org/10.1371/journal.pone.0010212
- Samen, U. M., Eikmanns, B. J., & Reinscheid, D. J. (2006). The transcriptional regulator RovS controls the attachment of *Streptococcus agalactiae* to human epithelial cells and the expression of virulence genes. *Infection and Immunity*, 74(10), 5625–5635. https://doi.org/10.1128/IAI.00667-06
- Samen, U., Gottschalk, B., Eikmanns, B. J., & Reinscheid, D. J. (2004). Relevance of peptide uptake systems to the physiology and virulence of *Streptococcus agalactiae*. *Journal of Bacteriology*, *186*(5), 1398–1408. https://doi.org/10.1128/JB.186.5.1398-1408.2004
- Santi, I., Grifantini, R., Jiang, S. M., Brettoni, C., Grandi, G., Wessels, M. R., & Soriani, M. (2009). CsrRS regulates group B *Streptococcus* virulence gene expression in response to environmental pH: a new perspective on vaccine development. *Journal of Bacteriology*, 191(17), 5387–5397. https://doi.org/10.1128/JB.00370-09
- Santi, I., Scarselli, M., Mariani, M., Pezzicoli, A., Masignani, V., Taddei, A., Grandi, G., Telford, J. L., & Soriani, M. (2007). BibA: a novel immunogenic bacterial adhesin contributing to group B *Streptococcus* survival in human blood. *Molecular Microbiology*, 63(3), 754–767. https://doi.org/10.1111/j.1365-2958.2006.05555.x
- Schubert, A., Zakikhany, K., Pietrocola, G., Meinke, A., Speziale, P., Eikmanns, B. J., & Reinscheid, D. J. (2004). The fibrinogen receptor FbsA promotes adherence of *Streptococcus agalactiae* to human epithelial cells. *Infection and Immunity*, 72(11), 6197–6205. https://doi.org/10.1128/IAI.72.11.6197-6205.2004
- Seale, A. C., Baker, C. J., Berkley, J. A., Madhi, S. A., Ordi, J., Saha, S. K., Schrag, S. J., Sobanjo-Ter Meulen, A., & Vekemans, J. (2019). Vaccines for maternal immunization against Group B *Streptococcus* disease: WHO perspectives on case ascertainment and case definitions. *Vaccine*, 37(35), 4877–4885. https://doi.org/10.1016/j.vaccine.2019.07.012).
- Seo, H. S., Minasov, G., Seepersaud, R., Doran, K. S., Dubrovska, I., Shuvalova, L., Anderson, W. F., Iverson, T. M., & Sullam, P. M. (2013). Characterization of fibrinogen binding by glycoproteins Srr1 and Srr2 of *Streptococcus agalactiae*. *The Journal of Biological Chemistry*, 288(50), 35982–35996. https://doi.org/10.1074/jbc.M113.513358

- Seo, H. S., Mu, R., Kim, B. J., Doran, K. S., & Sullam, P. M. (2012). Binding of glycoprotein Srr1 of *Streptococcus agalactiae* to fibrinogen promotes attachment to brain endothelium and the development of meningitis. *PLoS Pathogens,* 8(10), e1002947. https://doi.org/10.1371/journal.ppat.1002947
- Shabayek, S., & Spellerberg, B. (2018). Group B Streptococcal Colonization, Molecular Characteristics, and Epidemiology. *Frontiers in Microbiology*, 9, 437. https://doi.org/10.3389/fmicb.2018.00437
- Sheppard, A. E., Vaughan, A., Jones, N., Turner, P., Turner, C., Efstratiou, A., Patel, D., Modernising Medical Microbiology Informatics Group, Walker, A. S., Berkley, J. A., Crook, D. W., & Seale, A. C. (2016). Capsular Typing Method for *Streptococcus agalactiae* Using Whole-Genome Sequence Data. *Journal of Clinical Microbiology*, 54(5), 1388–1390. https://doi.org/10.1128/JCM.03142-15
- Shivers, R. P., Dineen, S. S., & Sonenshein, A. L. (2006). Positive regulation of *Bacillus subtilis* ackA by CodY and CcpA: establishing a potential hierarchy in carbon flow. *Molecular Microbiology*, *62*(3), 811–822. https://doi.org/10.1111/j.1365-2958.2006.05410.x
- Sitkiewicz, I., Green, N. M., Guo, N., Bongiovanni, A. M., Witkin, S. S., & Musser, J. M. (2009). Transcriptome adaptation of group B *Streptococcus* to growth in human amniotic fluid. *PloS One*, *4*(7), e6114. https://doi.org/10.1371/journal.pone.0006114
- Six, A., Bellais, S., Bouaboud, A., Fouet, A., Gabriel, C., Tazi, A., Dramsi, S., Trieu-Cuot, P., & Poyart, C. (2015). Srr2, a multifaceted adhesin expressed by ST-17 hypervirulent Group B *Streptococcus* involved in binding to both fibrinogen and plasminogen. *Molecular Microbiology*, 97(6), 1209–1222. https://doi.org/10.1111/mmi.13097
- Slack, F. J., Serror, P., Joyce, E., & Sonenshein, A. L. (1995). A gene required for nutritional repression of the *Bacillus subtilis* dipeptide permease operon. *Molecular Microbiology*, 15(4), 689–702. https://doi.org/10.1111/j.1365-2958.1995.tb02378.x
- Sonenshein A. L. (2007). Control of key metabolic intersections in *Bacillus subtilis.* Nature reviews. *Microbiology*, 5(12), 917–927. https://doi.org/10.1038/nrmicro1772
- Spellerberg B. (2000). Pathogenesis of neonatal *Streptococcus agalactiae* infections. *Microbes and Infection*, 2(14), 1733–1742. https://doi.org/10.1016/s1286-4579(00)01328-9
- Spellerberg, B., Rozdzinski, E., Martin, S., Weber-Heynemann, J., & Lütticken, R. (2002). *rgf* encodes a novel two-component signal transduction system of *Streptococcus agalactiae*. *Infection and Immunity*, 70(5), 2434–2440. https://doi.org/10.1128/IAI.70.5.2434-2440.2002
- Tatusov, R. L., Galperin, M. Y., Natale, D. A., & Koonin, E. V. (2000). The COG database: a tool for genome-scale analysis of protein functions and evolution. *Nucleic Aids Research*, *28*(1), 33–36. https://doi.org/10.1093/nar/28.1.33
- Tazi, A., Disson, O., Bellais, S., Bouaboud, A., Dmytruk, N., Dramsi, S., Mistou, M. Y., Khun, H., Mechler, C., Tardieux, I., Trieu-Cuot, P., Lecuit,

M., & Poyart, C. (2010). The surface protein HvgA mediates group B *streptococcus* hypervirulence and meningeal tropism in neonates. *The Journal of Experimental Medicine*, 207(11), 2313–2322. https://doi.org/10.1084/jem.20092594

- Tenenbaum, T., Bloier, C., Adam, R., Reinscheid, D. J., & Schroten, H. (2005). Adherence to and invasion of human brain microvascular endothelial cells are promoted by fibrinogen-binding protein FbsA of *Streptococcus agalactiae*. *Infection and Immunity*, 73(7), 4404–4409. https://doi.org/10.1128/IAI.73.7.4404-4409.2005
- Tenenbaum, T., Spellerberg, B., Adam, R., Vogel, M., Kim, K. S., & Schroten, H. (2007). *Streptococcus agalactiae* invasion of human brain microvascular endothelial cells is promoted by the laminin-binding protein Lmb. *Microbes and Infection*, 9(6), 714–720. https://doi.org/10.1016/j.micinf.2007.02.015
- Tettelin, H., Masignani, V., Cieslewicz, M. J., Eisen, J. A., Peterson, S., Wessels, M. R., Paulsen, I. T., Nelson, K. E., Margarit, I., Read, T. D., Madoff, L. C., Wolf, A. M., Beanan, M. J., Brinkac, L. M., Daugherty, S. C., DeBoy, R. T., Durkin, A. S., Kolonay, J. F., Madupu, R., Lewis, M. R., … Fraser, C. M. (2002). Complete genome sequence and comparative genomic analysis of an emerging human pathogen, serotype V *Streptococcus agalactiae*. *Proceedings of the National Academy of Sciences of the United States of America*, 99(19), 12391–12396. https://doi.org/10.1073/pnas.182380799
- Thomas, L., & Cook, L. (2022). A Novel Conserved Protein in *Streptococcus agalactiae,* BvaP, Is Important for Vaginal Colonization and Biofilm Formation. *mSphere*, e0042122. *Advance online publication*. https://doi.org/10.1128/msphere.00421-22
- Thomas, L., & Cook, L. (2020). Two-Component Signal Transduction Systems in the Human Pathogen *Streptococcus agalactiae*. *Infection and Immunity*, 88(7), e00931-19. https://doi.org/10.1128/IAI.00931-19
- Tojo, S., Satomura, T., Morisaki, K., Deutscher, J., Hirooka, K., & Fujita, Y. (2005). Elaborate transcription regulation of the *Bacillus* subtilis *ilv-leu* operon involved in the biosynthesis of branched-chain amino acids through global regulators of CcpA, CodY and TnrA. *Molecular Microbiology*, *56*(6), 1560–1573. https://doi.org/10.1111/j.1365-2958.2005.04635.x
- Trespidi, G., Scoffone, V. C., Barbieri, G., Riccardi, G., De Rossi, E., & Buroni, S. (2020). Molecular Characterization of the *Burkholderia cenocepacia dcw* Operon and FtsZ Interactors as New Targets for Novel Antimicrobial Design. *Antibiotics (Basel, Switzerland)*, *9*(12), 841. https://doi.org/10.3390/antibiotics9120841
- Trollfors, B., Melin, F., Gudjonsdottir, M. J., Rupröder, R., Sandin, M., Dahl, M., Karlsson, J., & Backhaus, E. (2022). Group B *streptococcus* - a pathogen not restricted to neonates. *IJID Regions (Online),* 4, 171–175. https://doi.org/10.1016/j.ijregi.2022.08.002
- Vallejo, J. G., Baker, C. J., & Edwards, M. S. (1996). Interleukin-6 production by human neonatal monocytes stimulated by type III group B

streptococci. *The Journal of Infectious Diseases*, 174(2), 332–337. https://doi.org/10.1093/infdis/174.2.332

- van Schaik, W., Château, A., Dillies, M. A., Coppée, J. Y., Sonenshein, A. L., & Fouet, A. (2009). The global regulator CodY regulates toxin gene expression in *Bacillus anthracis* and is required for full virulence. *Infection and Immunity*, 77(10), 4437–4445. https://doi.org/10.1128/IAI.00716-09
- Verani, J. R., McGee, L., Schrag, S. J., & Division of Bacterial Diseases, National Center for Immunization and Respiratory Diseases, Centers for Disease Control and Prevention (CDC) (2010). Prevention of perinatal group B streptococcal disease--revised guidelines from CDC, 2010. MMWR. Recommendations and reports: Morbidity and mortality weekly report. *Recommendations and Reports*, 59(RR-10), 1–36.
- Wang, Z., Guo, C., Xu, Y., Liu, G., Lu, C., & Liu, Y. (2014). Two novel functions of hyaluronidase from *Streptococcus agalactiae* are enhanced intracellular survival and inhibition of proinflammatory cytokine expression. *Infection and Immunity*, 82(6), 2615–2625. https://doi.org/10.1128/IAI.00022-14
- Waters, N. R., Samuels, D. J., Behera, R. K., Livny, J., Rhee, K. Y., Sadykov, M. R., & Brinsmade, S. R. (2016). A spectrum of CodY activities drives metabolic reorganization and virulence gene expression in *Staphylococcus aureus*. *Molecular Microbiology*, 101(3), 495–514. https://doi.org/10.1111/mmi.13404
- Whidbey, C., Harrell, M. I., Burnside, K., Ngo, L., Becraft, A. K., Iyer, L. M., Aravind, L., Hitti, J., Adams Waldorf, K. M., & Rajagopal, L. (2013). A hemolytic pigment of Group B *Streptococcus* allows bacterial penetration of human placenta. *The Journal of Experimental Medicine*, 210(6), 1265–1281. https://doi.org/10.1084/jem.20122753
- Willett, N. P., & Morse, G. E. (1966). Long-chain fatty acid inhibition of growth of *Streptococcus agalactiae* in a chemically defined medium. *Journal of Bacteriology*, *91*(6), 2245–2250. https://doi.org/10.1128/jb.91.6.2245-2250.1966
- Wilson, M., Seymour, R., & Henderson, B. (1998). Bacterial perturbation of cytokine networks. *Infection and Immunity*, *66*(6), 2401–2409. https://doi.org/10.1128/IAI.66.6.2401-2409.1998
- Xia, F. D., Mallet, A., Caliot, E., Gao, C., Trieu-Cuot, P., & Dramsi, S. (2015). Capsular polysaccharide of Group B *Streptococcus* mediates biofilm formation in the presence of human plasma. *Microbes and Infection*, 17(1), 71–76. https://doi.org/10.1016/j.micinf.2014.10.007
- Yamamoto, Y., Pargade, V., Lamberet, G., Gaudu, P., Thomas, F., Texereau, J., Gruss, A., Trieu-Cuot, P., & Poyart, C. (2006). The Group B *Streptococcus* NADH oxidase Nox-2 is involved in fatty acid biosynthesis during aerobic growth and contributes to virulence. *Molecular Microbiology*, 62(3), 772–785. https://doi.org/10.1111/j.1365-2958.2006.05406.x
- Yang, Y., Luo, M., Zhou, H., Li, C., Luk, A., Zhao, G., Fung, K., & Ip, M. (2019). Role of Two-Component System Response Regulator *bceR* in the Antimicrobial Resistance, Virulence, Biofilm Formation, and Stress

Response of Group B *Streptococcus*. *Frontiers in Microbiology*, 10, 10. https://doi.org/10.3389/fmicb.2019.00010

- Young, J. W., Locke, J. C., Altinok, A., Rosenfeld, N., Bacarian, T., Swain, P. S., Mjolsness, E., & Elowitz, M. B. (2011). Measuring single-cell gene expression dynamics in bacteria using fluorescence time-lapse microscopy. *Nature Protocols*, *7*(1), 80–88. https://doi.org/10.1038/nprot.2011.432
- Zawaneh, S. M., Ayoub, E. M., Baer, H., Cruz, A. C., & Spellacy, W. N. (1979). Factors influencing adherence of group B *streptococci* to human vaginal epithelial cells. *Infection and Immunity*, 26(2), 441–447. https://doi.org/10.1128/iai.26.2.441-447.1979

Acknowledgements

Ringrazio innanzitutto la mia supervisor Giulia Barbieri, per i consigli indispensabili e le conoscenze trasmesse durante tutto il percorso di dottorato.

Ringrazio la mia famiglia ed il mio fidanzato per avermi sostenuto ed aiutato in ogni mia in-decisione.

Ringrazio infine tutti i colleghi di laboratorio, le colleghe di corso e gli amici preziosi per i ricordi, le risate nei giorni felici ed il supporto nei giorni difficili.

List of original manuscripts

Full papers

- **Pellegrini A**, Lentini G, Famà A, Bonacorsi A, Scoffone VC, Buroni S, ... & Barbieri G. (2022). CodY Is a Global Transcriptional Regulator Required for Virulence in Group B *Streptococcus*. *Frontiers in microbiology*, 1242. (IF: 6.064)
- Ursino E, Albertini AM, Fiorentino G, Gabrieli P, Scoffone VC, **Pellegrini A**, ... & Barbieri G. (2020). *Bacillus subtilis* as a host for mosquitocidal toxins production. *Microbial biotechnology*, *13*(6), 1972-1982. (IF: 5.813)
- Pietrocola G, **Pellegrini A**, Alfeo MJ, Marchese L, Foster TJ, & Speziale P. (2020). The iron-regulated surface determinant B (IsdB) protein from *Staphylococcus aureus* acts as a receptor for the host protein vitronectin. *Journal of Biological Chemistry*, *295*(29), 10008-10022. (IF: 5.157)

Abstracts

- **Pellegrini A.** CodY regulates virulence and metabolism in Group B *Streptococcus*. Cortona Procarioti 2022, Cortona, Italia, 23 - 25 june 2022 – ORAL PRESENTATION.

- **Pellegrini A**, Lentini G, Famà A, Bonacorsi A, Scoffone VC, Buroni S, Trespidi G, Postiglione U, Sassera D, Manai F, Pietrocola G, Firon G, Biondo C, Teti G, Beninati C, Barbieri G. The global transcriptional regulator CodY is essential for *in vivo* virulence of Group B *Streptococcus*. 22nd Lancefield International Symposium on Streptococci and Streptococcal Diseases - A Marcus Wallenberg Symposium, Stoccolma, Svezia, 7 - 10 June 2022 – POSTER.

- **Pellegrini A**, Lentini G, Famà A, Bonacorsi A, Scoffone VC, Buroni S, Trespidi G, Irudal S, Postiglione U, Sassera D, Manai F, Pietrocola G, Firon G, Biondo C, Teti G, Beninati C, Barbieri G. The CodY global regulator controls metabolism and virulence in Group B *Streptococcus.* ECCMID, Lisbona, Portogallo, 23-26 April 2022 – POSTER.

- **Pellegrini A**, Bonacorsi A, Scoffone VC, Lentini G, Buroni S, Manai F, Postiglione U, Sassera D, Beninati C, Biondo C, Barbieri G. CodY is a global regulator of gene expression and controls virulence in Group B *Streptococcus*. Virtual Congress AGI, 22-24 September 2021 – POSTER.

frontiers | Frontiers in Microbiology

ORIGINAL RESEARCH
published: 28 April 2022
doi: 10.3389/fmicb.2022.881549

CodY Is a Global Transcriptional Regulator Required for Virulence in Group B *Streptococcus*

*Angelica Pellegrini[1], Germana Lentini[2], Agata Famà[2], Andrea Bonacorsi[1], Viola Camilla Scoffone[1], Silvia Buroni[1], Gabriele Trespidi[1], Umberto Postiglione[1], Davide Sassera[1], Federico Manai[1], Giampiero Pietrocola[3], Arnaud Firon[4], Carmelo Biondo[2], Giuseppe Teti[5], Concetta Beninati[2] and Giulia Barbieri[1]**

[1] Department of Biology and Biotechnology "Lazzaro Spallanzani," University of Pavia, Pavia, Italy, [2] Department of Human Pathology and Medicine, University of Messina, Messina, Italy, [3] Department of Molecular Medicine, University of Pavia, Pavia, Italy, [4] Institut Pasteur, Université de Paris, CNRS UMR 6047, Unité Biologie des Bactéries Pathogènes à Gram-positif, Paris, France, [5] Charybdis Vaccines Srl, Messina, Italy

OPEN ACCESS

Edited by:
Daniela De Biase,
Sapienza University of Rome, Italy

Reviewed by:
Angela Tramonti,
Institute of Molecular Biology and Pathology, Italian National Research Council, Italy
Vincenzo Scarlato,
University of Bologna, Italy

***Correspondence:**
Giulia Barbieri
giulia.barbieri@unipv.it

Specialty section:
This article was submitted to Microbial Physiology and Metabolism, a section of the journal Frontiers in Microbiology

Received: 22 February 2022
Accepted: 21 March 2022
Published: 28 April 2022

Citation:
Pellegrini A, Lentini G, Famà A, Bonacorsi A, Scoffone VC, Buroni S, Trespidi G, Postiglione U, Sassera D, Manai F, Pietrocola G, Firon A, Biondo C, Teti G, Beninati C and Barbieri G (2022) CodY Is a Global Transcriptional Regulator Required for Virulence in Group B Streptococcus. Front. Microbiol. 13:881549. doi: 10.3389/fmicb.2022.881549

Group B *Streptococcus* (GBS) is a Gram-positive bacterium able to switch from a harmless commensal of healthy adults to a pathogen responsible for invasive infections in neonates. The signals and regulatory mechanisms governing this transition are still largely unknown. CodY is a highly conserved global transcriptional regulator that links nutrient availability to the regulation of major metabolic and virulence pathways in low-G+C Gram-positive bacteria. In this work, we investigated the role of CodY in BM110, a GBS strain representative of a hypervirulent lineage associated with the majority of neonatal meningitis. Deletion of *codY* resulted in a reduced ability of the mutant strain to cause infections in neonatal and adult animal models. The observed decreased *in vivo* lethality was associated with an impaired ability of the mutant to persist in the blood, spread to distant organs, and cross the blood-brain barrier. Notably, the *codY* null mutant showed reduced adhesion to monolayers of human epithelial cells *in vitro* and an increased ability to form biofilms, a phenotype associated with strains able to asymptomatically colonize the host. RNA-seq analysis showed that CodY controls about 13% of the genome of GBS, acting mainly as a repressor of genes involved in amino acid transport and metabolism and encoding surface anchored proteins, including the virulence factor Srr2. CodY activity was shown to be dependent on the availability of branched-chain amino acids, which are the universal cofactors of this regulator. These results highlight a key role for CodY in the control of GBS virulence.

Keywords: group B *Streptococcus*, *Streptococcus agalactiae*, CodY, Srr2, bacterial meningitis, RNA-Seq, global regulation of gene expression, pathogenesis

INTRODUCTION

Group B *Streptococcus* (GBS, *Streptococcus agalactiae*) is the leading cause of sepsis and meningitis in neonates (Thigpen et al., 2011; Okike et al., 2014). Maternal vaginal colonization during pregnancy represents the principal risk factor for GBS transmission to the newborn through *in utero* ascending infections or aspiration of contaminated amniotic or vaginal fluids during

delivery. Vertically acquired neonatal infections lead to early-onset (0–7 days of life) invasive disease manifesting as pneumonia that rapidly progresses to sepsis (Edmond et al., 2012; Patras and Nizet, 2018). GBS can also cause late-onset disease that manifests between 7 and 90 days of life with bacteremia and a high complication rate of meningitis (Tazi et al., 2019).

Group B *Streptococcus* is capable of causing these diverse clinical manifestations thanks to its capacity to invade different host niches and adapt to various environmental conditions. This versatility is made possible by the activity of several transcriptional regulators which, in response to environmental signals, control the expression of proteins involved in nutrient acquisition, adhesion, virulence, and immune evasion (Rajagopal, 2009; Thomas and Cook, 2020).

CodY is a global transcriptional regulator highly conserved in nearly all low-G+C Gram-positive bacteria, including the genera *Bacillus*, *Lactococcus*, *Streptococcus*, *Listeria*, *Staphylococcus*, *Clostridium*, and *Clostridioides* (Guédon et al., 2005; Lemos et al., 2008; Dineen et al., 2010; Kreth et al., 2011; Lobel et al., 2012; Belitsky and Sonenshein, 2013; Brinsmade et al., 2014; Feng et al., 2016; Waters et al., 2016; Geng et al., 2018). In these organisms, CodY directly and indirectly controls the expression of hundreds of metabolic genes in response to nutrient availability (Sonenshein, 2005). In pathogens, CodY regulates also critical virulence determinants and, therefore, links nutrient availability and metabolism to pathogenesis in a species-specific manner. The nutritional status of the cell is monitored by CodY by its interaction with two ligands: branched-chain amino acids (BCAAs) (Guedon et al., 2001; Shivers and Sonenshein, 2004; Brinsmade et al., 2010) and GTP (Ratnayake-Lecamwasam et al., 2001; Handke et al., 2008). However, while BCAAs are universal cofactors of CodY, GTP was not found to be involved in CodY activation in *Lactococcus* (Petranovic et al., 2004) and *Streptococcus* species (Hendriksen et al., 2008). Once activated by binding to its cofactors, CodY binds DNA at sites characterized by a 15-nt canonical consensus binding motif "AATTTTCWGAAAATT" (den Hengst et al., 2005; Belitsky and Sonenshein, 2013; Biswas et al., 2020). As the intracellular pools of BCAAs change, the hundreds of genes whose expression is controlled by CodY are expressed in a hierarchical manner, reflecting the choice of turning on specific metabolic pathways ahead of others (Brinsmade et al., 2014; Waters et al., 2016). In many cases, the hierarchy of gene expression stems in part from the interplay between CodY and other transcriptional regulators. That is, many direct targets of CodY regulation are also controlled by other factors and the expression of several transcriptional regulators is CodY-regulated. Consequently, regulatory circuits interlinking different pathways are created (Belitsky et al., 2015; Barbieri et al., 2016).

In this work, we aimed at providing the first global analysis of the CodY regulon in GBS and at investigating the role of this regulator in controlling and coordinating metabolism and virulence in this bacterium. To this purpose, a capsular serotype III strain belonging to the hypervirulent clonal complex 17 (CC17, as defined by Multi Locus Sequence Typing analysis) was employed. This lineage is responsible for the vast majority of cases of neonatal GBS –elicited meningitis worldwide (Manning et al., 2009; Joubrel et al., 2015; Seale et al., 2016).

MATERIALS AND METHODS

Bacterial Strains, Plasmids, and Growth Conditions

Bacterial strains and plasmids used in this work are listed in **Table 1** and **Supplementary Table 1**, respectively. Employed primers are listed in **Supplementary Table 2**. GBS was cultured in Todd Hewitt (TH, Difco Laboratories) supplemented with 5 g/liter of yeast extract (THY) or in chemically defined medium (CDM, **Supplementary Table 3**) (Willett and Morse, 1966) at 37°C, 5% CO_2, steady state. *E. coli* strains were cultured in Luria Bertani (LB) broth at 37°C. Antibiotics were used at the appropriate concentrations. For *E. coli*: kanamycin 50 μg/ml; erythromycin 150 μg/ml. For GBS: kanamycin 1 mg/ml; erythromycin 10 μg/ml.

Strains Construction

The pG1-Δ*codY* vector used to create the Δ*codY* derivative of BM110 (Δ*codY*) was constructed by Gibson assembly (NEBuilder HiFi DNA Assembly Cloning Kit, New England Biolabs) with PCR amplified genomic regions located upstream and downstream of *codY*, using pG1_codYUpF + BM_codYFusR and BM_codYFusF + pG1_BM_codYDwR primers, and an inverse PCR fragment obtained with the pG1R and pG1F oligonucleotides on the temperature-sensitive pG1 plasmid

TABLE 1 | Bacterial strains used in this work.

S. agalactiae

Strain	Relevant genotype	Plasmid	Source or Reference
BM110	Serotype III, ST-17, human hypervirulent clinical isolate		Tazi et al., 2010
Δ*codY*	BM110 carrying an in-frame *codY* deletion		This work
BM1102	BM110	pTCVΩP_{tet}	This work
BM1103	BM110	pTCVΩP_{tet}_*codY*	This work
BM1104	Δ*codY*	pTCVΩP_{tet}	This work
BM1105	Δ*codY*	pTCVΩP_{tet}_*codY*	This work
BM1106	BM110	pTCVlacZ_*livKp220*	This work
BM1107	Δ*codY*	pTCVlacZ_*livKp220*	This work
BM1114	BM110	pTCVlacZ_*livKp1-220*	This work
BM1115	Δ*codY*	pTCVlacZ_*livKp1-220*	This work

E. coli

Strain	Genotype	Source or reference
XL-1 Blue	*recA1 endA1 gyrA96 thi-1 hsdR17 supE44 relA1 lac [F i proAB lacI^q ZΔM15 Tn10 (Tet^r)]*	Agilent
BL21 DE3	*B F– ompT gal dcm lon hsdSB(rB–mB–) λ(DE3 [lacI lacUV5-T7p07 ind1 sam7 nin5]) [malB+]K-12(λS)*	

(Mistou et al., 2009). The three PCR fragments were fused by Gibson assembly and electroporated into *E. coli* XL1 blue. The obtained pG1-Δ*codY* plasmid was verified by sequencing and then electroporated in GBS. Transformants were selected at 30°C on TH plates supplemented with erythromycin. Plasmid integration and excision were performed as previously described (Biswas et al., 1993). The resulting in-frame deletion of *codY* on genomic DNA was verified by Sanger sequencing using external primers COH1_1525FUp and COH1_1527RDw.

To complement the *codY* deletion, the *codY* gene was amplified with oligonucleotides pTCV_codYF_Bam and pTCV_codYR_Pst, using BM110 chromosomal DNA as template. The obtained fragment was cloned between the *Bam*HI and *Pst*I sites of the pTCVΩP_{tet} vector (Buscetta et al., 2016). The resulting pTCVΩP_{tet}_*codY* plasmid was verified by sequencing and used to electroporate wild-type (WT) and Δ*codY* strains, thus obtaining BM1103 and BM1105, respectively (**Table 1**). Two control strains (BM1102 and BM1104) were prepared by electroporation of the empty pTCVΩP_{tet} plasmid into WT and Δ*codY* strains. Transformants were selected on TH agar plates supplemented with kanamycin.

Construction of *lacZ* Transcriptional Fusions and β-Galactosidase Assays

To prepare the pTCV-*lacZ*_*livK*p_{220} plasmid (**Supplementary Table 1**), a 269 bp fragment comprising the regulatory region and the first 27 nucleotides of the *livK* gene was amplified with primers livKp220F and livKp220R using the BM110 chromosomal DNA as template. The obtained amplicon was inserted by Gibson assembly between the *Eco*RI and *Bam*HI restriction sites of plasmid pTCV-*lacZ* (Poyart and Trieu-Cuot, 2006), upstream of the *lacZ* gene.

To create pTCVlacZ_*livKp1-220*, a 196 bp product containing the 5′ part of the *livK* regulatory region was amplified by using oligonucleotides livKp220F and mutagenic oligonucleotide livKp1R. A 125 bp fragment comprising the 3′ part of the regulatory region and the first 27 bp of the *livK* coding sequence was synthesized by using mutagenic oligonucleotide livKp1F and livKp220R as reverse primer. The two mutagenized, partially overlapping (52 bp overlap) PCR products and the *Eco*RI/*Bam*HI digested pTCV-*lacZ* plasmid were then fused by Gibson using the NEBuilder HiFi DNA Assembly Cloning Kit (New England Biolabs).

β-galactosidase specific activity was determined as previously described (Trespidi et al., 2020).

Time-Lapse Microscopy and Single-Cell Image Analysis

Agarose pads (Young et al., 2011) spotted with 5 μl of a 1:10 dilution of GBS cell cultures collected at mid-log phase of growth (OD600 0.5 in THY medium) were flipped and transferred to an imaging dish sealed with parafilm. Time-lapse imaging was performed using a Leica DMi8 widefield microscope, equipped with a 100× oil immersion objective (Leica HC PL Fluotar 100×/1.32 OIL PH3), a Leica DFC9000 sCMOS camera and driven by Leica LASX software. Experiments were performed using an environmental microscope incubator set at 37°C and bacteria were imaged in phase contrast, every 5-min and up to 6 h. Manual segmentation of individual cells and analysis of image stacks were performed using the ImageJ 1.52a software, as previously described (Manina et al., 2015). Data were analyzed using Prism 9.

RNA Preparation and Quantitative Real-Time-PCR

Group B *Streptococcus* total RNA was extracted from cells collected at mid-exponential phase of growth using the Quick-RNA Fungal/Bacterial Miniprep Kit (Zymo Research) as per the manufacturer's instructions. Traces of genomic DNA were removed from samples using the Turbo DNA-free DNase treatment and removal kit (Ambion). Reverse transcription and quantitative real-time PCR (qRT-PCR) experiments were performed in a single step using the iTaq Universal SYBR Green One-Step Kit (Bio-Rad). The reactions were performed in 20 μl volumes using 4 ng of DNAse I treated RNA and 400 nM primers targeting *livK*, *braB*, *brnQ*, and *gyrA* (used as reference gene).

RNA-Sequencing and Analysis

RNA-Seq was performed on four independent biological replicates for each strain. rRNA was depleted using the QIAseq FastSelect –5S/16S/23S Kit (QIAGEN). RNA was sequenced using Illumina sequencing technology (BMR-Genomics, Padua). For RNA-Seq data analysis, raw reads were quality checked using FASTQC[1] and processed by Trimmomatic (Bolger et al., 2014) to trim the adaptor sequences and remove low-quality reads. Clean reads were mapped onto the reference genome of *Streptococcus agalactiae* BM110 (Accession: NZ_LT714196.1) using Bowtie2 (Langmead, 2010). To quantify the known transcripts, the alignment results were input into featureCounts (Liao et al., 2014). Lastly, the R package DESeq2 (Love et al., 2014) was used to test for differential expression. We defined genes as differentially expressed using the following criteria: $|\text{Log2 Fold Change}| \geq 1$ and adjusted p-value FDR < 0.05. Prediction of orthologous groups was performed using COGnitor (Tatusov, 2000).

Mammalian Cell Culture and Epithelial Cell Adhesion Assays

A549 cells and HeLa cells were routinely grown in 75 cm^2 flasks in Dulbecco's modified Eagle's medium (DMEM) supplemented with 10% fetal bovine serum (FBS) at 37°C in 5% CO_2. Cells were seeded at 2×10^5 cell density per well in 24-well tissue culture plates and cultured in DMEM without antibiotics for 24 h. Bacteria grown to the mid-log phase were added to confluent monolayers at a multiplicity of infection of 10. After a 2-h incubation, monolayers were washed three times with PBS to remove the non-adherent bacteria, lysed, and serial dilutions of the cell lysates were plated to enumerate cell-associated bacteria. Percent of adhesion of each strain was calculated as follows (number of CFUs on plate)/(number of CFUs of initial

[1] https://qubeshub.org/resources/fastqc

inoculum) × 100. Percentage of adhesion was normalized to the WT strain, set at 100%.

Biofilm Formation Assay

For bacterial biofilm formation assays, a 1:20 dilution of an overnight culture grown in TH broth supplemented with 1% glucose and the appropriate antibiotic was used to inoculate (100 µl/well) a 96-well Tissue Culture Treated plate (16 technical replicates per strain). Non-adherent bacteria were removed by washing with PBS after 6 h of incubation at 37°C, 5% CO_2. Crystal violet staining was performed as previously described (Trespidi et al., 2021) after 19 h of incubation in TH + 1% glucose medium (37°C, 5% CO_2). Biofilm growth was evaluated by reading absorbance at 595 nm and normalizing the obtained value to the OD600 of the culture in the well.

For confocal microscopy analysis of biofilms, bacterial overnight cultures in TH broth supplemented with 1% glucose and the appropriate antibiotic were diluted in the same medium to an OD_{600} 0.05 (about 1 × 10^7 CFU/mL) before being added to a four-well Nunc Lab-Tek II Chambered Coverglass. Non-adherent cells were removed after 6 h. After overnight growth, biofilms were washed twice with PBS and stained with 5 µM Syto 9 (Invitrogen). Cells were imaged with a Leica TCS SP8 confocal microscope equipped with a Leica DMi8 inverted microscope, a tunable excitation laser source (White Light Laser, Leica Microsystems, Germany), and driven by Leica Application Suite X, ver. 3.5.6.21594, using a 63× oil immersion objective (Leica HC PL APO CS2 63X/1.40). Images were acquired using a 488 nm laser line as an excitation source, and the fluorescence emitted was collected in a 500–540 nm range for Syto 9 as previously described (Trespidi et al., 2020). Biofilm images were visualized and processed using ImageJ. Biofilm parameters were measured using the COMSTAT 2 software (Heydorn et al., 2000). All confocal

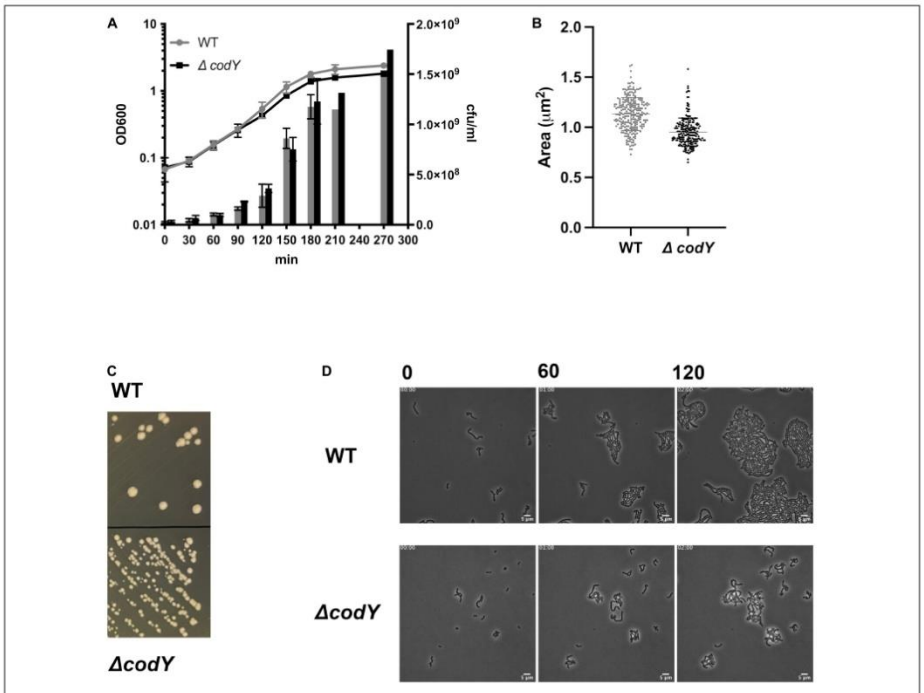

FIGURE 1 | Deletion of *codY* does not affect cell growth but is associated to a smaller cell size and colony morphology. **(A)** Growth of the BM110 strain (WT) and of the isogenic *codY* deletion mutant (Δ*codY*) in THY rich medium, evaluated as absorbance at OD_{600} (left axis) and cfu/ml (right axis). Data are the average ± SD of two independent experiments **(B)**. Single cell area measurements (µm²) of 50 cells of each strain. Reported data refer to two independent experiments. Statistically significant differences are indicated (Welch's *t*-test). **(C)** Colonies of the WT and Δ*codY* strains grown on THY agar plates. **(D)** Contrast-phase image stacks of BM110 and Δ*codY* cells during time-lapse microscopy. Scale bar is 5 µm.

scanning laser microscopy experiments were performed three times and standard deviations were measured.

Cloning, Overproduction, and Purification of CodY

The *codY* CDS was amplified with primers pET_GBS_codYF and pET_GBS_codYR. The obtained fragment was inserted by Gibson assembly between the *Eco*RI and *Bam*HI sites of plasmid pET28a. The CodY protein with an N-terminal 6X-His tag was produced in *E. coli* BL21 DE3 cells by IPTG (0.5 mM) induction at 28°C overnight. CodY protein was purified as previously described (Alfeo et al., 2021), and protein concentration was measured by Bradford protein assay (Bio-Rad).

Fragments Labeling and Electrophoretic Mobility Shift Assay

To be used as probes in gel-shift experiments, PCR products containing the regulatory region of the *livK* gene were amplified using the appropriate pTCV-*lacZ* derivative plasmid as template and the 5'FAM labeled, vector-specific primers Vlac1-FAM and Vlac2-FAM.

FAM-labeled fragments (50 nM) were incubated with increasing concentrations of CodY and electrophoretic mobility shift assays were performed as previously described (Barbieri et al., 2015). When indicated, BCAAs were added to the final concentration of 10 mM in the CodY-binding reaction mixture. Ten mM each isoleucine, leucine, and valine were also added to the 5% non-denaturing Tris-Glycine polyacrylamide gel and electrophoresis buffer.

Mouse Infection Models

In the neonatal model, 48-h-old mice of both sexes were inoculated subcutaneously with 8×10^4 CFU of the WT or the Δ*codY* strain, as previously described. Mice showing signs of irreversible disease, such as diffuse redness spreading from the infection site, were humanely euthanized. In the adult model of GBS sepsis, 8 week-old female mice were inoculated intraperitoneally with 5×10^8 CFU of the WT or the Δ*codY* strain, as previously described (Biondo et al., 2014). In the meningitis model, 8 week-old female mice were inoculated intravenously 1×10^9 CFU of WT or the Δ*codY* strain, as previously described (Lentini et al., 2018). Mice showing signs of irreversible disease, such as prolonged hunching, inactivity, or neurological symptoms were humanely euthanized. In further experiments, mice were euthanized at 16 h after challenge and bacterial burden was determined in organ homogenates, as previously described (Famà et al., 2020).

In vivo and *in vitro* Cytokine Induction

Female mice of 8 weeks of age were infected intraperitoneally with 1×10^9 CFU of the WT or the Δ*codY* strain. Mice were treated at 30 min post-challenge with penicillin (500 IU i.p.) to prevent bacterial overgrowth. Peritoneal lavage fluids were collected at the indicated times and analyzed for cytokine levels as previously described (Mohammadi et al., 2016). For *in vitro* cytokine induction, bone marrow-derived macrophages were obtained from 8-week-old female mice and cultured in the presence of M-CSF as previously described (Lentini et al., 2021). Macrophage cultures were then stimulated for 1 h with GBS grown to the late exponential phase at the indicated multiplicities of infection (MOI). Cultures were then treated with penicillin and gentamycin (100 IU and 50 μg/ml) to kill extracellular bacteria and supernatants were collected at 18 h after culture, as previously described (Lentini et al., 2021). Cytokine levels were measured in peritoneal lavage fluid samples or culture supernatants by ELISA, using Mouse TNF-alpha DuoSet ELISA DY410, Mouse IL-1 beta/IL-1F2 DuoSet ELISA DY401, Mouse CXCL2/MIP-2 DuoSet ELISA DY452, Mouse CXCL1/KC DuoSet ELISA DY453 (R&D Systems).

RESULTS

CodY Is Required for *in vivo* Virulence of Group B *Streptococcus*

A marker-free, in-frame deletion of the *codY* gene was created by allelic replacement in the CC17 wild-type strain BM110 (WT). The resulting Δ*codY* mutant showed no growth defects in rich THY liquid medium (**Figure 1A**). However, Δ*codY* cells showed a 10% reduced cell size and formed smaller colonies compared to the WT strain (**Figures 1B–D**), similarly to what was previously observed in *codY*-deleted mutants in other bacteria (Majerczyk et al., 2008; Geng et al., 2018).

To assess the *in vivo* impact of CodY on the ability of GBS to sustain infection, we determined the virulence properties of the Δ*codY* strain in several models of infection that closely mimic features of human infections (Magliani et al., 1998; Cusumano et al., 2004). In the first murine model of neonatal GBS sepsis, bacteria replicate at the inoculation site and spread systemically to the blood and distant organs. Newborn mice infected subcutaneously with the WT strain showed signs of irreversible infection within the first 24 h after challenge and were humanely euthanized. In contrast, nearly all neonates infected with the Δ*codY* strain survived and remained in good conditions until the end of the experiment (**Figure 2A**). In further studies, newborn mice were infected as above, and the organs were collected at 14 h after challenge. As shown in **Figures 2C,E,G**, considerable bacterial burden was detected in the blood, brain, and liver of all animals infected with WT GBS, while low bacterial numbers or no bacteria were present in the organs from mice infected with the *codY*-deleted strain. These data indicated that, in the absence of CodY, GBS is unable to replicate locally *in vivo* and to spread hematogenously to distant organs. Since GBS infections are being increasingly reported in adults, we sought to confirm the data obtained in newborn mice in an adult sepsis model. As shown in **Figure 2B** and **Supplementary Figures 1A–E**, all adult mice intraperitoneally inoculated with the *codY*-deleted strain survived while all mice infected with WT bacteria succumbed to overwhelming infection, confirming the results obtained in neonates. In view of the clinical importance of meningoencephalitis in the context of CC17 GBS infection, we also looked at the role of CodY in the ability of GBS to cross the blood-brain barrier using a meningoencephalitis

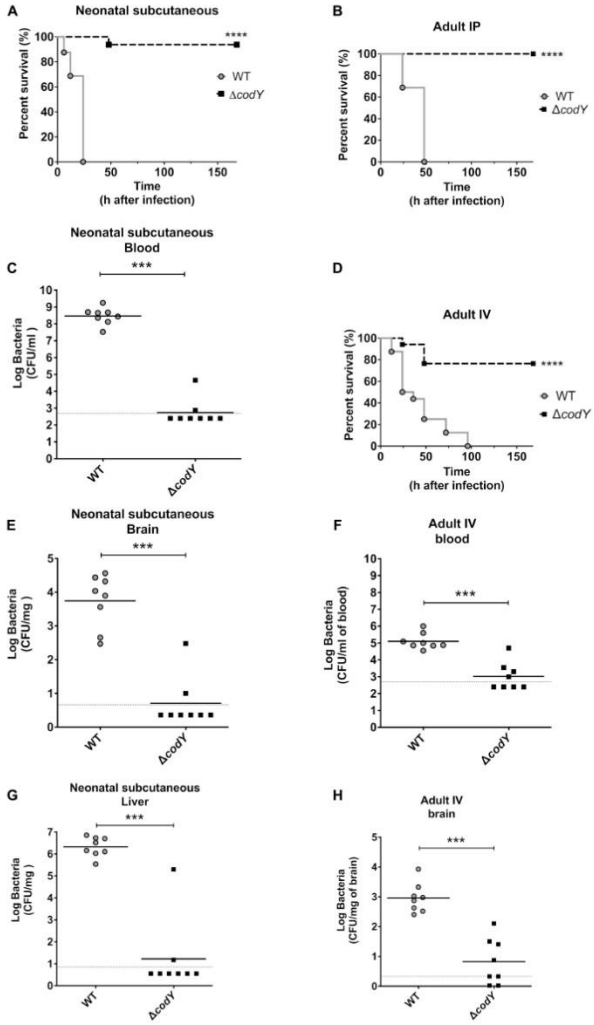

FIGURE 2 | *CodY* is necessary during neonatal and adult infections. **(A)** Lethality of newborn mice (8 per group) infected subcutaneously with 8×10^4 of the WT strain or the Δ*codY* mutant. **(C,E,G)** Bacterial burden in the indicated organs of newborn mice infected in the same experimental condition as in panel **(A)**; horizontal bars indicate mean log CFU values. **(B)** Lethality of adult mice (8 per group) infected intraperitoneally (IP) with 5×10^8 of the WT strain or Δ*codY* mutant. **(D)** Lethality of adult mice (8 per group) infected intravenously (IV) with 1×10^8 CFU. **(F,H)** Bacterial burden in the indicated organs of adult mice infected in the same experimental condition as in panel **(D)**; horizontal bars indicate mean log CFU values. ***$p < 0.001$; ****$p < 0.0001$ by the Kaplan Meier (panels **A,B,D**) or Mann Whitney test (panels **C, E–H**).

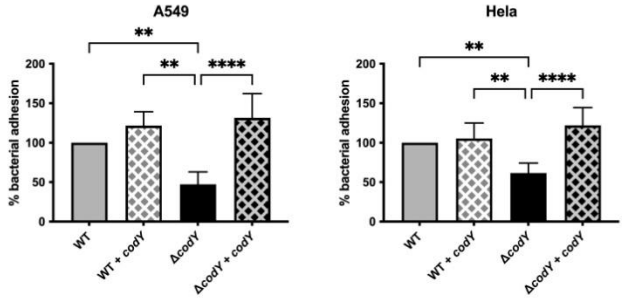

FIGURE 3 | CodY controls GBS adhesion to epithelial cells. Cell adhesion was quantified using HeLa and A549 immortalized cell lines. The WT and the Δ*codY* mutant contain the empty vector pTCVΩP_{tet} or the complementing vector pTCVΩP_{tet}_*codY* (+ *codY*). The percent of adhesion of each strain was calculated relative to the initial inoculum and was normalized to the adhesion of the WT strain, set as 100%. Represented data are the average ± SD of six independent experiments, each performed in duplicate. Statistically significant differences are indicated (One-way ANOVA). $^{**}p < 0.01$, $^{****}p < 0.0001$.

model in which bacteria are inoculated intravenously. Under these conditions, the Δ*codY* mutant displayed a considerably decreased ability to persist in the blood and to cause lethal encephalitis compared to WT bacteria (**Figures 2D,F,H**).

Deletion of CodY Does Not Impact the Host Cytokine Response to Group B *Streptococcus* Infection

To investigate whether the reduced virulence of GBS in the absence of CodY could be related to altered induction of pro-inflammatory cytokines, we used a sepsis model in which mice are infected intraperitoneally and cytokine levels are measured in peritoneal lavage fluid samples at different times after challenge. To avoid bacterial overgrowth, penicillin was administered at 30 min post-challenge. Under these conditions, TNF-α, IL-1β, Cxcl1, and Cxcl2 levels rapidly increased, to reach peak levels at 3 h after challenge with a WT strain (**Supplementary Figures 2A–D**). However, similar cytokine levels were detected in mice infected with the WT and Δ*codY* strains. Similarly, no differences were detected in TNF-α or IL-1β induction in peritoneal macrophages stimulated with the two strains (**Supplementary Figures 2E,F**).

CodY Contributes to Group B *Streptococcus* Adhesion to Epithelial Cells

Adhesion to host cells and tissue colonization are necessary for the establishment of a successful infection. Deletion of *codY* resulted in a 50% decrease in adherence to human epithelial cervix adenocarcinoma (HeLa) and human epithelial lung carcinoma (A549) cell lines compared to the WT strain (**Figure 3**). Complementation of *codY* deletion by plasmid-mediated expression of *codY* under the control of the constitutive Ptet promoter restored adhesion to levels similar to the WT strain. Plasmid-mediated CodY expression in the WT strain did not affect the adhesion ability of the parental strain.

CodY Controls the Ability of BM110 to Form Biofilms

The role of CodY in the ability of GBS to form biofilms was evaluated by crystal violet staining (**Figure 4A**) and confocal laser scanning microscopy (**Figure 4B**). While the WT strain formed a weak biofilm, the *codY*-deleted mutant formed a thicker, more compact biofilm able to completely cover the surface of the well and of the chambered coverglass (**Figures 4B–D**). The biofilm-forming ability was significantly reduced after complementation of the *codY* deletion. Eradication experiments revealed that biofilms formed by the Δ*codY* mutant were strongly reduced by treatment with proteinase K, while DNAse I was less effective against the biofilm biomass (**Figure 4A**). These results suggest that extracellular proteins are a major constituent of the Δ*codY* biofilm.

CodY Is a Global Regulator of Gene Expression in Group B *Streptococcus*

To determine the transcriptional changes associated with *codY* deletion, an RNA-Seq experiment was performed on WT and Δ*codY* bacteria during exponential growth in rich THY medium, i.e., under conditions of maximal CodY activity. A total of 277 genes (out of 2,128 analyzed genes) were differentially expressed at least twofold (adjusted p-value < 0.05) in the Δ*codY* strain, demonstrating a global regulatory role for CodY (**Supplementary Datasets 1A–C**). Among these, 256 genes were up-regulated (**Supplementary Dataset 1B**) and 21 genes were down-regulated (**Supplementary Dataset 1C**) in the mutant, supporting a role for CodY mainly as a repressor of gene expression (**Figure 5A**). Overall, fold changes associated with negative regulation were higher than those associated

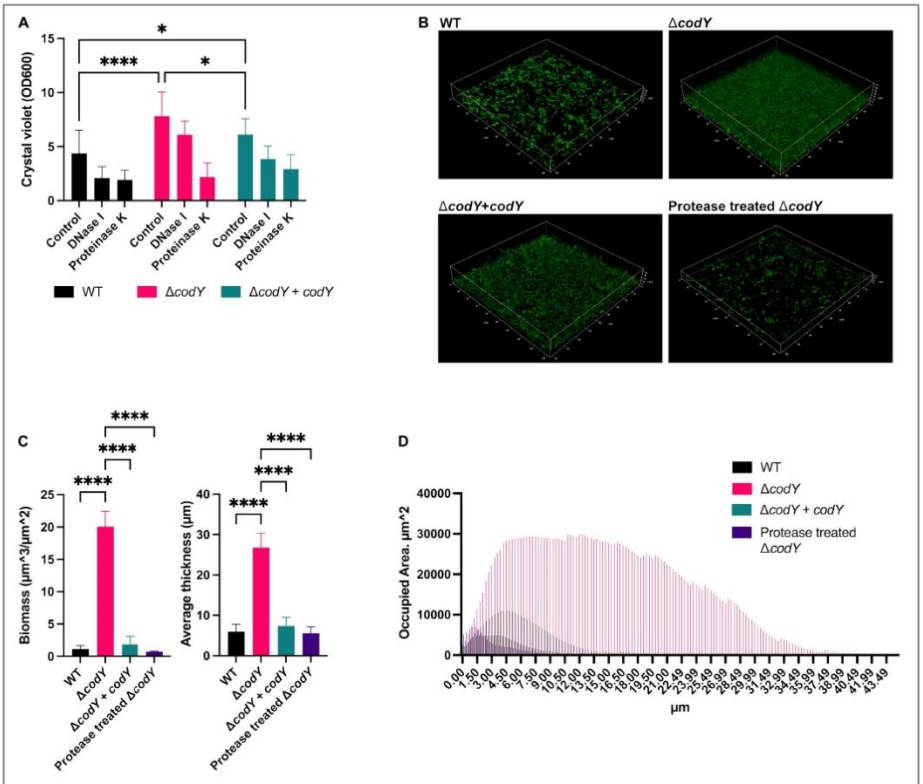

FIGURE 4 | CodY inhibits biofilm formation. **(A)** Biofilm biomass was measured by crystal violet staining after static culture for 19 h. The WT and the Δ*codY* strain contain the empty vector pTCVΩP_{tet} or the complementing vector pTCVΩP_{tet}_*codY* (+ *codY*). The role of eDNA and extracellular proteins as biofilm structural components was assessed by individual treatments with DNase I and proteinase K, respectively. Represented data are the average ± SD of two independent experiments, each performed in 8 replicates. Statistically significant differences are reported (two-way ANOVA). **(B)** Confocal laser scanning microscopic images of biofilms formed by WT, Δ*codY* and Δ*codY* + *codY* GBS strains grown for 19 h in Nunc™ Lab-Tek™ II Chambered Coverglass. The effect of treatment with proteinase K on the Δ*codY* biofilm is reported. **(C,D)** Analysis of biofilm properties by COMSTAT 2. Measures of total biomass, average thickness **(C)** and % of the area occupied by biofilm distribution **(D)**. Data are the average ± SD of the results from three independent replicates. : $*p < 0.05$, $****p < 0.0001$ (one-way ANOVA test).

with positive regulation. Notably, 55% (140/256) of the over-expressed genes were located in four prophages. The 98 genes whose expression was affected by *codY* deletion at least fourfold (94 up-regulated and 4 down-regulated genes) (**Supplementary Datasets 1D,E**) could be classified into seventeen categories by the Cluster of Orthologous Genes (COGs) analysis (**Supplementary Dataset 2** and **Figure 5B**). Among these, the most represented groups included genes involved in "amino acid transport and metabolism," "cell wall/membrane/envelope biogenesis," and "mobilome: prophages, transposons."

Specifically, CodY-repressed genes (**Supplementary Dataset 1D** and **Figure 5A**) included those encoding BCAAs transporters (*braB*, *brnQ*, all the genes belonging to the *livK-G* operon), the (oligo)peptide permease OppA1-F, adhesins, and serine peptidases anchored to the cell wall through the LPxTG motif, as well as proteins involved in DNA replication, recombination, and repair. Interestingly, the genes of the *cas* operon, involved in adaptive immunity, were among the ones more intensely up-regulated in the Δ*codY* mutant. Notably, the operon encoding for the CC17-specific virulence factor Srr2 was

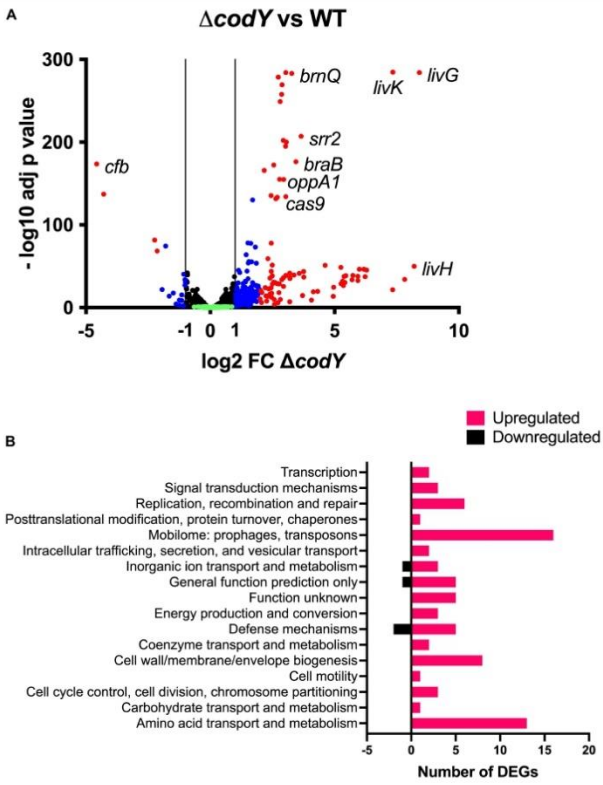

FIGURE 5 | (A) Volcano plot of the Δ*codY* transcriptome at mid-exponential phase in THY. Each dot represents a gene with its RNA-seq fold change and adjusted *p*-value calculated from four independent replicates. Genes showing a significant differential expression in the Δ*codY* strain (adjusted *p*-value < 0.05) are represented in blue (−2 ≤ log2FC ≤ −1 or 1 ≤ log2FC ≤ 2) and red (log2FC < −2 or log2FC > 2) according to their fold change relative to the WT strain. Black dots represent genes whose expression is not affected by *codY* deletion (−1 < log2FC < 1; adjusted *p*-value < 0.05). Green dots correspond to non-significant (adjusted *p*-value > 0.05) differentially transcribed genes. **(B)** COGs associated to downregulated and upregulated genes.

over-expressed in the absence of CodY. On the contrary, the gene encoding the CAMP factor pore-forming toxin Cfb was under positive regulation by CodY (**Supplementary Dataset 1E** and **Figure 5A**).

Using the FIMO Motif Search Tool (Grant et al., 2011), the genome of BM110 was scanned to search for sequences matching the conserved AATTTTCWGAAATT CodY binding motif. One hundred and one matches were retrieved from the genomic regions located upstream of the coding sequences of the genes, using a *p*-value lower than 0.0001. At least one of these sites was located in the proximity of the coding sequence of eighteen genes differentially expressed in the Δ*codY* strain (**Supplementary Datasets 1A–D** and **Supplementary Table 4**), predicting that these genes might be targets of direct CodY-mediated regulation.

Group B *Streptococcus* CodY Controls Gene Expression in Response to Branched-Chain Amino Acid Availability

As BCAAs (isoleucine, leucine, and valine, ILV) are universal positive cofactors of CodY (Richardson et al., 2015), the expression of CodY-dependent genes is expected to change in response to the availability of these amino acids. To test this hypothesis, the expression of CodY-regulated genes was analyzed

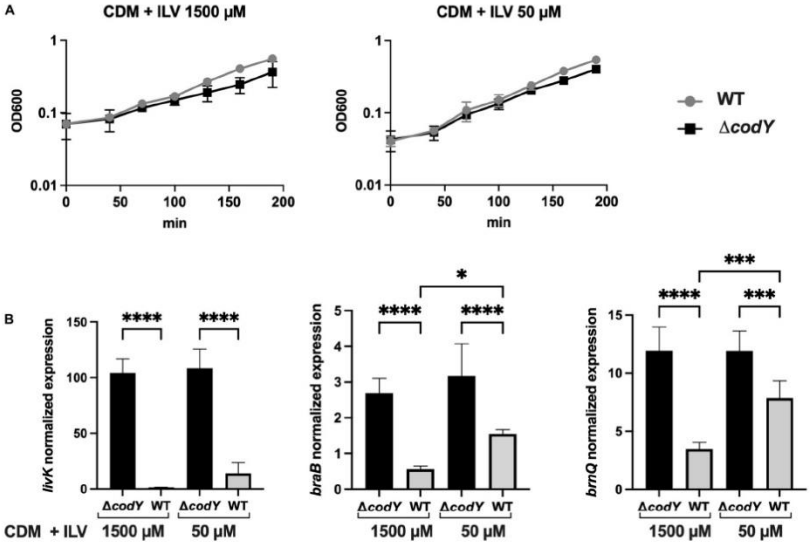

FIGURE 6 | CodY activity is dependent on branched-chain amino acids availability. **(A)** Growth of the WT (gray) and Δ*codY* mutant (black) in CDM supplemented with high (1500 μM) and low (50 μM) ILV concentrations. Reported data are the average ± SD of two independent experiments. **(B)** Expression analysis by qRT-PCR of the genes *livK*, *braB*, and *brnQ* in the WT and Δ*codY* mutant grown under high and low ILV concentrations. Gene expression is normalized to the expression of the housekeeping *gyrA* gene. Asterisks denote statistically significant differences as assessed by One-way ANOVA analysis $^{*}p < 0.05$, $^{***}p < 0.001$, $^{****}p < 0.0001$.

by qRT-PCR in WT and Δ*codY* cells grown to mid-log phase in CDM (Willett and Morse, 1966) containing a mix of all amino acids and supplemented with high (1,500 μM) or low (50 μM) concentrations of ILV. As GBS is unable to synthesize the precursors of most amino acids, including the BCAA (Glaser et al., 2002), ILV cannot be omitted from the growth medium. Under both conditions tested, the two strains showed similar growth kinetics, displaying approximately a two-fold increase in their doubling time compared to growth in rich, THY medium (**Figure 6A**). Three genes encoding BCAAs transporters and identified by RNA-Seq analysis (**Supplementary Dataset 1D** and **Figure 5A**) and qRT-PCR (**Supplementary Figure 3**) as subjected to different levels of CodY-mediated repression during growth in rich THY medium were included in the analysis. In the WT strain, transcription of all three genes increased when BCAA were less abundant in the defined medium, in accord with expected decrease in CodY activity. All three target genes were further and significantly over-expressed in the Δ*codY* mutant compared to the WT strain under both conditions tested, however, the extent of this overexpression was higher in *livK* (82-fold and 11-fold increase in CDM + 1500 μM and in CDM + 50 μM ILV, respectively) and lower in *braB* (3.4-fold and 2.3-fold increase in CDM + 1500 μM and in CDM + 50 μM ILV, respectively) and *brnQ* (4.8-fold and 2.8-fold increase in CDM + 1500 μM and in CDM + 50 μM ILV, respectively) (**Figure 6B** and **Supplementary Table 5**). The high level of gene expression in the Δ*codY* mutant was not affected by ILV levels. The obtained results in the WT strain suggest that, as the levels of BCAAs decrease, the expression of CodY-repressed genes increases in a gene-specific manner (**Figure 6B**).

Direct Transcriptional Repression of the *livK-G* Operon by CodY

The mechanism of CodY-mediated regulation of the *livK-G* operon, encoding an ABC-type BCAAs transporter, was investigated. Two putative CodY-binding motifs, with three and two mismatches to the consensus sequence, were identified by FIMO analysis at positions from −64 to −50 and from −31 to −17 respectively, with respect to the transcription start site (Mazzuoli et al., 2021) of the *livK* gene, the first gene of the operon (**Figure 7A**).

An electrophoretic-mobility shift assay (EMSA) was performed using purified CodY and a 6-carboxyfluorescein (FAM) labeled fragment encompassing the *livK* regulatory region from position −168 to +52 with respect to the transcription start site of the gene (**Figure 7A**). In the presence of 10 mM ILV, CodY bound the *livK* fragment with an apparent equilibrium

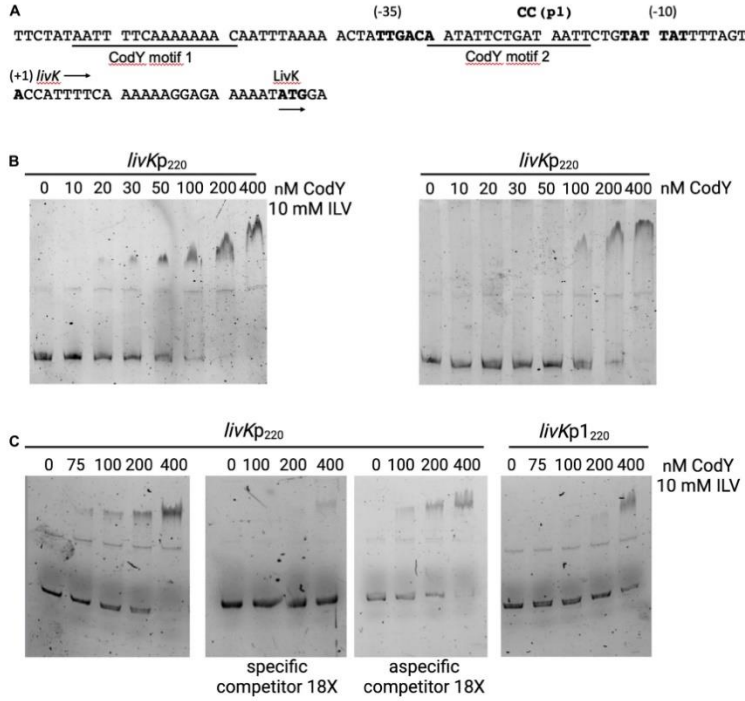

FIGURE 7 | CodY binds to the *livK* promoter. **(A)** Sequence (5' to 3') of the *livK* regulatory region. Coordinates are reported with respect to the transcription start point (Mazzuoli et al., 2021). The transcription start site, −10 and −35 promoter regions, and the starting codon of the *livK* CDS are in boldface. The directions of transcription and translation are indicated by the horizontal arrows. The sequences of the two CodY-binding motifs are underlined. The mutated nucleotides (p1) are shown above the sequence. **(B)** Electrophoretic mobility shift assays (EMSA) for binding of CodY to the *livK* regulatory region. CodY and the WT $livKp_{220}$ fragment were incubated in the presence or absence of 10 mM each isoleucine, leucine, and valine (ILV). When ILV were included in the reaction mixture, the non-denaturing polyacrylamide gel and the electrophoresis buffer were supplemented with 10 mM ILV. **(C)** EMSA performed with the WT $livKp_{220}$ and mutated $livKp1_{220}$ fragments. Specificity of binding was evaluated by performing the experiment with the WT fragment in the absence or presence of a specific (unlabeled $livKp_{220}$ fragment) or non-specific competitor. DNA-Protein mixtures were separated on 5% non-denaturing gel in presence of 10 mM ILV.

dissociation constant (K_D) of ≈50 nM (here, K_D reflects the concentration of CodY required to shift 50% of DNA fragments under conditions of vast protein excess over DNA) (**Figure 7B**). When ILV were omitted from the binding mixture, affinity of CodY for the *livK* regulatory region decreased (KD ≈150 nM), suggesting that BCAAs enhance CodY activity. Specificity of CodY binding was assessed by competitive and non-competitive binding assays in the presence of ILV and 18-fold excess of unlabeled specific or non-specific competitor DNA, respectively (**Figure 7C**).

A *lacZ* transcriptional fusion ($livKp_{220}$-*lacZ*) including the region spanning from position −168 to +52 with respect to the *livK* transcription start site was constructed using the pTCV-*lacZ* plasmid (Poyart and Trieu-Cuot, 2006). Under conditions of maximal CodY activity, during the exponential phase of growth in THY medium, expression of the $livKp_{220}$-*lacZ* fusion was about 400-fold higher in the *codY*-null mutant strain, BM1107, than in the WT strain, BM1106 (**Table 2**). A two-nucleotide substitution mutation was introduced at positions −22 and −23 with respect to the *livK* transcription start site, within the putative CodY-binding site located immediately upstream of the *livK* coding region ($livKp1_{220}$-*lacZ*). The p1 mutation, aimed at decreasing the similarity of the motif to the CodY-binding consensus sequence, strongly reduced the affinity of CodY for the

livK regulatory region (**Figure 7C**) and abolished CodY's ability to repress the *livK* promoter (**Table 2**).

DISCUSSION

In this study, we showed that the global transcriptional regulator CodY is essential for GBS virulence in several animal models of infection.

In low-G+C Gram-positive pathogens, this conserved transcriptional regulator coordinates metabolism and virulence in response to nutrient availability (Brinsmade, 2017). While CodY controls global metabolism in a generally conserved manner, genes involved in virulence are subjected to species-specific modes of regulation, depending on the occupied niche during infection and on the type of interaction that the bacterium establishes with the host. In *S. aureus* and *C. difficile* CodY strongly represses virulence genes, so that their expression is activated only when BCAA levels are low (Dineen et al., 2007, 2010; Majerczyk et al., 2008, 2010; Waters et al., 2016). On the contrary, in *Bacillus anthracis* and *Listeria monocytogenes* virulence is positively controlled by CodY (van Schaik et al., 2009; Château et al., 2011; Lobel et al., 2012, 2015). While understanding the function of CodY in *S. pneumoniae* is complicated by the *codY* essentiality in this important human pathogen (Caymaris et al., 2010), a role for this regulator in the control of virulence was demonstrated in other Streptococcal species (Malke et al., 2006; Lemos et al., 2008; Kreth et al., 2011; Feng et al., 2016; Geng et al., 2018).

Here, we confirmed that *codY* is not essential for the growth of GBS in complex or chemically defined liquid medium (Hooven et al., 2016) but is required *in vivo*. The reduced ability of the Δ*codY* mutant to cause infection is associated with a lower ability to disseminate, colonize host tissues, persist in blood and cause meningitis. This reduced virulence is not associated with an altered cytokine response in the host but is related to pleiotropic effects of the *codY* deletion, such as the decreased ability of the mutant strain to bind to human epithelial cells *in vitro* and the increased ability to form biofilm. Of note, while strains of the CC17, responsible for neonatal invasive infections, are generally weak biofilms formers, the ability to form strong biofilms is a common phenotype of strains able to asymptomatically colonize the host (Parker et al., 2016). As proteins appear to play a major role in promoting Δ*codY* biofilm structural stability, it is possible to speculate that surface proteins involved in bacterial adherence and encoded by genes that are repressed by CodY (e.g., Srr2, FbsB, and ScpB3) might be required for biofilm formation in GBS (Park et al., 2012).

The transcriptomic analysis in GBS strengthens the conserved role of CodY as a global regulator of metabolism, with genes encoding functions involved in the uptake of amino acids and oligopeptides subjected to the highest level of regulation. As genes required for the biosynthesis of precursors of most amino acids, including BCAAs, are missing in the genome of GBS, this bacterium relies on transporters and peptidases for amino acids metabolism (Milligan et al., 1978; Glaser et al., 2002). The capacity to take up exogenous oligopeptides is particularly important to support growth in amniotic fluid, which contains only low amounts of free amino acids (Mesavage et al., 1985; Samen et al., 2004). Notably, the majority of the genes involved in peptide and amino acid transport and metabolism that are upregulated during GBS growth in amniotic fluid (*oppA1-F* and *livK* operons, *braB*, *brnQ*, BQ8897_RS10635) are members of the CodY regulon identified in this work. As the *codY* gene itself is downregulated 11-fold during growth in amniotic fluid compared to a rich laboratory medium (Sitkiewicz et al., 2009), it might be hypothesized that the reduced levels of this repressor could be at the origin of the overexpression of peptides and amino acids transport systems in amniotic fluid.

We confirmed that the CodY response in GBS is dependent on the concentration of extracellular BCAAs which, besides being abundant amino acids in proteins, are precursors of branched-chain fatty acids, the predominant membrane fatty acids in Gram-positive bacteria (Richardson et al., 2015). CodY-mediated regulation of three genes involved in amino acid uptake (*livK*, *braB*, *brnQ*) is dependent on the level of BCAAs available in the growth medium. Therefore, as the abundance of its cofactors decreases, CodY-mediated repression of genes required for amino acid uptake is relieved. Among the analyzed genes, very low levels of *livK* expression were observed in a WT strain even under conditions of low BCAA-abundance. This result suggests that very few active molecules of CodY are sufficient to efficiently bind the regulatory region of the *livK* operon and repress its expression.

The CodY regulatory network links the metabolic status of several bacteria with the regulation of their virulence (Lobel et al., 2012; Waters et al., 2016). In GBS, CodY directly and indirectly regulates numerous genes involved in carbon and energy metabolism, cell wall and membrane biogenesis and virulence. The latter category includes surface-anchored proteins such as the Srr2 adhesin. This CC17-specific adhesin is a major virulence factor that supports the ability of GBS to cross the developing neonatal gastrointestinal epithelium and to adhere to and invade cerebral endothelial cells, thus leading to invasive infections and meningitis in neonates (Seifert et al., 2006; Six et al., 2015; Hays et al., 2019; Gori et al., 2020;

TABLE 2 | Expression of *livK-lacZ* fusions[a].

Strain	Relevant genotype[b]	Fusion genotype	β-galactosidase activity[c]		
			Miller Units[a]	%[b]	Repression[c] ratio
BM1106	wild-type	*livKp*$_{220}$-*lacZ*	0.47 ± 0.07	0.3	393.62
BM1107	Δ*codY*		185 ± 19.02	100.0	
BM1114	wild-type	*livKp1*$_{220}$-*lacZ*	157.6 ± 0.35	97.3	1.03
BM1115	Δ*codY*		161.9 ± 6.86	100.0	

[a] *β-galactosidase activity is reported in Miller Units. Data are the average ± SD of two independent experiments, each performed in duplicate.*
[b] *β-galactosidase activity of each fusion in the codY-deleted strain was normalized to 100%.*
[c] *The repression ratio is the ratio of expression values for the corresponding fusions in the codY null mutant in and wild-type strain.*

Deshayes de Cambronne et al., 2021). Importantly, the transcription of the *srr2* operon and of other genes included in the CodY regulon are directly repressed by the master regulator of virulence CovR (Mazzuoli et al., 2021). In the related pathogen *S. pyogenes*, CodY represses *covR* expression allowing to counterbalance CovRS activity according to the nutritional status of the cell (Kreth et al., 2011). Noteworthy, in GBS, CovR and CodY do not control each other's transcription (Mazzuoli et al., 2021), suggesting the existence of a different wiring between these two major regulatory pathways. A detailed investigation of the interplay between CodY and CovR regulations is necessary to define the mechanism(s) allowing a concerted regulation of virulence and metabolism in GBS.

Understanding how CodY activity is coordinated with the network of regulators controlling GBS adaptation and virulence will allow deciphering the signals and conditions governing host-pathogen interaction during colonization and infection.

DATA AVAILABILITY STATEMENT

The data presented in the study are deposited in the NCBI BioProject database (https://www.ncbi.nlm.nih.gov/bioproject/), BioProject accession number PRJNA808867.

ETHICS STATEMENT

The animal study was reviewed and approved by the Animal Welfare Committee of the University of Messina and the Ministero della Salute of Italy (Permit number 786/2018-PR prot. 5E567.10).

AUTHOR CONTRIBUTIONS

GB, GP, CBe, GTe, AFi, and CBi conceived the work and designed the experiments. AP, AB, VS, GTr, FM, and SB conducted the experiments. UP and DS performed the bioinformatic analyses. GL and AFa performed *in vivo* experiments. GB and AP wrote the manuscript. All authors contributed to the article and approved the submitted version.

FUNDING

This research was funded by Cariplo Foundation grant 2017-0785 to GB and by the Italian Ministry of Education, University and Research (MIUR) (Dipartimenti di Eccellenza, Program 2018–2022) to Department of Biology and Biotechnology, "L. Spallanzani," University of Pavia.

ACKNOWLEDGMENTS

We thank the PASS-BioMed Facility (Centro Grandi Strumenti) of the University of Pavia for the provision of confocal microscope infrastructure and the associated technical support provided by Amanda Oldani and Patrizia Vaghi. We thank Abraham L. Sonenshein and Boris R. Belitsky for helpful reading of the manuscript.

SUPPLEMENTARY MATERIAL

The Supplementary Material for this article can be found online at: https://www.frontiersin.org/articles/10.3389/fmicb.2022.881549/full#supplementary-material

REFERENCES

Alfeo, M. J., Pagotto, A., Barbieri, G., Foster, T. J., Vanhoorelbeke, K., De Filippis, V., et al. (2021). *Staphylococcus aureus* iron-regulated surface determinant B (IsdB) protein interacts with von Willebrand factor and promotes adherence to endothelial cells. *Sci. Rep.* 11:22799. doi: 10.1038/s41598-021-02065-w

Barbieri, G., Albertini, A. M., Ferrari, E., Sonenshein, A. L., and Belitsky, B. R. (2016). Interplay of CodY and ScoC in the regulation of major extracellular protease genes of *Bacillus subtilis*. *J. Bacteriol.* 198, 907–920. doi: 10.1128/JB.00894-15

Barbieri, G., Voigt, B., Albrecht, D., Hecker, M., Albertini, A. M., Sonenshein, A. L., et al. (2015). CodY regulates expression of the *Bacillus subtilis* extracellular proteases Vpr and Mpr. *J. Bacteriol.* 197, 1423–1432. doi: 10.1128/JB.02588-14

Belitsky, B. R., Barbieri, G., Albertini, A. M., Ferrari, E., Strauch, M. A., and Sonenshein, A. L. (2015). Interactive regulation by the *Bacillus subtilis* global regulators CodY and ScoC. *Mol. Microbiol.* 97, 698–716. doi: 10.1111/mmi.13056

Belitsky, B. R., and Sonenshein, A. L. (2013). Genome-wide identification of *Bacillus subtilis* CodY-binding sites at single-nucleotide resolution. *Proc. Natl. Acad. Sci. U.S.A.* 110, 7026–7031. doi: 10.1073/pnas.1300428110

Biondo, C., Mancuso, G., Midiri, A., Signorino, G., Domina, M., Lanza Cariccio, V., et al. (2014). Essential role of interleukin-1 signaling in host defenses against group B *Streptococcus*. *mBio*. 5:e1428-14. doi: 10.1128/mBio.01428-14

Biswas, I., Gruss, A., Ehrlich, S. D., and Maguin, E. (1993). High-efficiency gene inactivation and replacement system for gram-positive bacteria. *J. Bacteriol.* 175, 3628–3635. doi: 10.1128/jb.175.11.3628-3635.1993

Biswas, R., Sonenshein, A. L., and Belitsky, B. R. (2020). Genome-wide identification of *Listeria monocytogenes* CodY-binding sites. *Mol. Microbiol.* 113, 841–858. doi: 10.1111/mmi.14449

Bolger, A. M., Lohse, M., and Usadel, B. (2014). Trimmomatic: a flexible trimmer for Illumina sequence data. *Bioinformatics* 30, 2114–2120. doi: 10.1093/bioinformatics/btu170

Brinsmade, S. R. (2017). CodY, a master integrator of metabolism and virulence in Gram-positive bacteria. *Curr. Genet.* 63, 417–425. doi: 10.1007/s00294-016-0656-5

Brinsmade, S. R., Alexander, E. L., Livny, J., Stettner, A. I., Segre, D., Rhee, K. Y., et al. (2014). Hierarchical expression of genes controlled by the *Bacillus subtilis* global regulatory protein CodY. *Proc. Natl. Acad. Sci. U.S.A.* 111, 8227–8232. doi: 10.1073/pnas.1321308111

Brinsmade, S. R., Kleijn, R. J., Sauer, U., and Sonenshein, A. L. (2010). Regulation of CodY activity through modulation of intracellular branched-chain amino acid pools. *J. Bacteriol.* 192, 6357–6368. doi: 10.1128/JB.00937-10

Buscetta, M., Firon, A., Pietrocola, G., Biondo, C., Mancuso, G., Midiri, A., et al. (2016). PbsP, a cell wall-anchored protein that binds plasminogen to promote hematogenous dissemination of group B *Streptococcus*. *Mol. Microbiol.* 101, 27–41. doi: 10.1111/mmi.13357

Caymaris, S., Bootsma, H. J., Martin, B., Hermans, P. W. M., Prudhomme, M., and Claverys, J.-P. (2010). The global nutritional regulator CodY is an essential

protein in the human pathogen *Streptococcus pneumoniae*. *Mol. Microbiol.* 78, 344–360. doi: 10.1111/j.1365-2958.2010.07339.x

Château, A., Schaik, W., Six, A., Aucher, W., and Fouet, A. (2011). CodY regulation is required for full virulence and heme iron acquisition in *Bacillus anthracis*. *FASEB J.* 25, 4445–4456. doi: 10.1096/fj.11-188912

Cusumano, V., Midiri, A., Cusumano, V. V., Bellantoni, A., De Sossi, G., Teti, G., et al. (2004). Interleukin-18 is an essential element in host resistance to experimental group B streptococcal disease in neonates. *Infect. Immun.* 72, 295–300. doi: 10.1128/IAI.72.1.295-300.2004

den Hengst, C. D., van Hijum, S. A., Geurts, J. M., Nauta, A., Kok, J., and Kuipers, O. P. (2005). The *Lactococcus lactis* CodY regulon. *J. Biol. Chem.* 280, 34332–34342. doi: 10.1074/jbc.M502349200

Deshayes de Cambronne, R., Fouet, A., Picart, A., Bourrel, A.-S., Anjou, C., Bouvier, G., et al. (2021). CC17 group B *Streptococcus* exploits integrins for neonatal meningitis development. *J. Clin. Invest.* 131:e136737. doi: 10.1172/JCI136737

Dineen, S. S., McBride, S. M., and Sonenshein, A. L. (2010). Integration of metabolism and virulence by *Clostridium difficile* CodY. *J. Bacteriol.* 192, 5350–5362. doi: 10.1128/JB.00341-10

Dineen, S. S., Villapakkam, A. C., Nordman, J. T., and Sonenshein, A. L. (2007). Repression of *Clostridium difficile* toxin gene expression by CodY. *Mol. Microbiol.* 66, 206–219. doi: 10.1111/j.1365-2958.2007.05906.x

Edmond, K. M., Kortsalioudaki, C., Scott, S., Schrag, S. J., Zaidi, A. K., Cousens, S., et al. (2012). Group B streptococcal disease in infants aged younger than 3 months: systematic review and meta-analysis. *Lancet* 379, 547–556. doi: 10.1016/S0140-6736(11)61651-6

Famà, A., Midiri, A., Mancuso, G., Biondo, C., Lentini, G., Galbo, R., et al. (2020). Nucleic acid-sensing toll-like receptors play a dominant role in innate immune recognition of Pneumococci. *mBio* 11:e00415-20. doi: 10.1128/mBio.00415-20

Feng, L., Zhu, J., Chang, H., Gao, X., Gao, C., Wei, X., et al. (2016). The CodY regulator is essential for virulence in *Streptococcus suis* serotype 2. *Sci. Rep.* 6:21241. doi: 10.1038/srep21241

Geng, J., Huang, S.-C., Chen, Y.-Y., Chiu, C.-H., Hu, S., and Chen, Y.-Y. M. (2018). Impact of growth pH and glucose concentrations on the CodY regulatory network in *Streptococcus salivarius*. *BMC Genomics* 19:386. doi: 10.1186/s12864-018-4781-z

Glaser, P., Rusniok, C., Buchrieser, C., Chevalier, F., Frangeul, L., Msadek, T., et al. (2002). Genome sequence of *Streptococcus agalactiae*, a pathogen causing invasive neonatal disease. *Mol. Microbiol.* 45, 1499–1513. doi: 10.1046/j.1365-2958.2002.03126.x

Gori, A., Harrison, O. B., Mlia, E., Nishihara, Y., Chan, J. M., Msefula, J., et al. (2020). Pan-GWAS of *Streptococcus agalactiae* highlights lineage-specific genes associated with virulence and niche adaptation. *mBio* 11:e00728-20. doi: 10.1128/mBio.00728-20

Grant, C. E., Bailey, T. L., and Noble, W. S. (2011). FIMO: scanning for occurrences of a given motif. *Bioinformatics* 27, 1017–1018. doi: 10.1093/bioinformatics/btr064

Guedon, E., Serror, P., Ehrlich, S. D., Renault, P., and Delorme, C. (2001). Pleiotropic transcriptional repressor CodY senses the intracellular pool of branched-chain amino acids in *Lactococcus lactis*. *Mol. Microbiol.* 40, 1227–1239. doi: 10.1046/j.1365-2958.2001.02470.x

Guédon, E., Sperandio, B., Pons, N., Ehrlich, S. D., and Renault, P. (2005). Overall control of nitrogen metabolism in *Lactococcus lactis* by CodY, and possible models for CodY regulation in Firmicutes. *Microbiology* 151, 3895–3909. doi: 10.1099/mic.0.28186-0

Handke, L. D., Shivers, R. P., and Sonenshein, A. L. (2008). Interaction of *Bacillus subtilis* CodY with GTP. *J. Bacteriol.* 190, 798–806. doi: 10.1128/JB.01115-07

Hays, C., Touak, G., Bouaboud, A., Fouet, A., Guignot, J., Poyart, C., et al. (2019). Perinatal hormones favor CC17 group B *Streptococcus* intestinal translocation through M cells and hypervirulence in neonates. *eLife* 8:e48772. doi: 10.7554/eLife.48772

Hendriksen, W. T., Bootsma, H. J., Estevão, S., Hoogenboezem, T., de Jong, A., de Groot, R., et al. (2008). CodY of *Streptococcus pneumoniae* : link between nutritional gene regulation and colonization. *J. Bacteriol.* 190, 590–601. doi: 10.1128/JB.00917-07

Heydorn, A., Nielsen, A. T., Hentzer, M., Sternberg, C., Givskov, M., Ersbøll, B. K., et al. (2000). Quantification of biofilm structures by the novel computer program comstat. *Microbiology* 146, 2395–2407. doi: 10.1099/00221287-146-10-2395

Hooven, T. A., Catomeris, A. J., Akabas, L. H., Randis, T. M., Maskell, D. J., Peters, S. E., et al. (2016). The essential genome of *Streptococcus agalactiae*. *BMC Genomics* 17:406. doi: 10.1186/s12864-016-2741-z

Joubrel, C., Tazi, A., Six, A., Dmytruk, N., Touak, G., Bidet, P., et al. (2015). Group B *Streptococcus* neonatal invasive infections, France 2007–2012. *Clin. Microbiol. Infect.* 21, 910–916. doi: 10.1016/j.cmi.2015.05.039

Kreth, J., Chen, Z., Ferretti, J., and Malke, H. (2011). Counteractive balancing of transcriptome expression involving CodY and CovRS in *Streptococcus pyogenes*. *J. Bacteriol.* 193, 4153–4165. doi: 10.1128/JB.00061-11

Langmead, B. (2010). Aligning short sequencing reads with Bowtie. *Curr. Protoc. Bioinform.* 11:11.7. doi: 10.1002/0471250953.bi1107s32

Lemos, J. A., Nascimento, M. M., Lin, V. K., Abranches, J., and Burne, R. A. (2008). Global regulation by (p)ppGpp and CodY in *Streptococcus mutans*. *J. Bacteriol.* 190, 5291–5299. doi: 10.1128/JB.00288-08

Lentini, G., Famà, A., De Gaetano, G. V., Galbo, R., Coppolino, F., Venza, M., et al. (2021). Role of endosomal TLRs in *Staphylococcus aureus* infection. *J. Immunol.* 207, 1448–1455. doi: 10.4049/jimmunol.2100389

Lentini, G., Midiri, A., Firon, A., Galbo, R., Mancuso, G., Biondo, C., et al. (2018). The plasminogen binding protein PbsP is required for brain invasion by hypervirulent CC17 Group B streptococci. *Sci. Rep.* 8:14322. doi: 10.1038/s41598-018-32774-8

Liao, Y., Smyth, G. K., and Shi, W. (2014). FeatureCounts: an efficient general purpose program for assigning sequence reads to genomic features. *Bioinformatics* 30, 923–930. doi: 10.1093/bioinformatics/btt656

Lobel, L., Sigal, N., Borovok, I., Belitsky, B. R., Sonenshein, A. L., and Herskovits, A. A. (2015). The metabolic regulator CodY links *Listeria monocytogenes* metabolism to virulence by directly activating the virulence regulatory gene *prfA*. *Mol. Microbiol.* 95, 624–644. doi: 10.1111/mmi.12890

Lobel, L., Sigal, N., Borovok, I., Ruppin, E., and Herskovits, A. A. (2012). Integrative genomic analysis identifies isoleucine and CodY as regulators of *Listeria monocytogenes* virulence. *PLoS Genet.* 8:e1002887. doi: 10.1371/journal.pgen.1002887

Love, M. I., Huber, W., and Anders, S. (2014). Moderated estimation of fold change and dispersion for RNA-seq data with DESeq2. *Genome Biol.* 15:550. doi: 10.1186/s13059-014-0550-8

Magliani, W., Polonelli, L., Conti, S., Salati, A., Rocca, P. F., Cusumano, V., et al. (1998). Neonatal mouse immunity against group B streptococcal infection by maternal vaccination with recombinant anti-idiotypes. *Nat. Med.* 4, 705–709. doi: 10.1038/nm0698-705

Majerczyk, C. D., Dunman, P. M., Luong, T. T., Lee, C. Y., Sadykov, M. R., Somerville, G. A., et al. (2010). Direct Targets of CodY in *Staphylococcus aureus*. *J. Bacteriol.* 192, 2861–2877. doi: 10.1128/JB.00220-10

Majerczyk, C. D., Sadykov, M. R., Luong, T. T., Lee, C., Somerville, G. A., and Sonenshein, A. L. (2008). *Staphylococcus aureus* CodY negatively regulates virulence gene expression. *J. Bacteriol.* 190, 2257–2265. doi: 10.1128/JB.01545-07

Malke, H., Steiner, K., McShan, W. M., and Ferretti, J. J. (2006). Linking the nutritional status of *Streptococcus pyogenes* to alteration of transcriptional gene expression: the action of CodY and RelA. *Int. J. Med. Microbiol.* 296, 259–275. doi: 10.1016/j.ijmm.2005.11.008

Manina, G., Dhar, N., and McKinney, J. D. (2015). Stress and host immunity amplify *Mycobacterium tuberculosis* phenotypic heterogeneity and induce nongrowing metabolically active forms. *Cell Host Microbe* 17, 32–46. doi: 10.1016/j.chom.2014.11.016

Manning, S. D., Springman, A. C., Lehotzky, E., Lewis, M. A., Whittam, T. S., and Davies, H. D. (2009). Multilocus sequence types associated with neonatal group B streptococcal sepsis and meningitis in Canada. *J. Clin. Microbiol.* 47, 1143–1148. doi: 10.1128/JCM.01424-08

Mazzuoli, M.-V., Daunesse, M., Varet, H., Rosinski-Chupin, I., Legendre, R., Sismeiro, O., et al. (2021). The CovR regulatory network drives the evolution of Group B *Streptococcus* virulence. *PLoS Genet.* 17:e1009761. doi: 10.1371/journal.pgen.1009761

Mesavage, W. C., Suchy, S. F., Weiner, D. L., Nance, C. S., Flannery, D. B., and Wolf, B. (1985). Amino acids in amniotic fluid in the second trimester of gestation. *Pediatr. Res.* 19, 1021–1024. doi: 10.1203/00006450-198510000-00014

Milligan, T. W., Doran, T. I., Straus, D. C., and Mattingly, S. J. (1978). Growth and amino acid requirements of various strains of group B Streptococci. *J. Clin. Microbiol.* 7, 28–33. doi: 10.1128/jcm.7.1.28-33.1978

Mistou, M.-Y., Dramsi, S., Brega, S., Poyart, C., and Trieu-Cuot, P. (2009). Molecular dissection of the *secA2* locus of group B *Streptococcus* reveals that glycosylation of the Srr1 LPXTG protein is required for full virulence. *J. Bacteriol.* 191, 4195–4206. doi: 10.1128/JB.01673-08

Mohammadi, N., Midiri, A., Mancuso, G., Patanè, F., Venza, M., Venza, I., et al. (2016). Neutrophils directly recognize group B Streptococci and contribute to interleukin-1β production during infection. *PLoS One* 11:e0160249. doi: 10.1371/journal.pone.0160249

Okike, I. O., Johnson, A. P., Henderson, K. L., Blackburn, R. M., Muller-Pebody, B., Ladhani, S. N., et al. (2014). Incidence, etiology, and outcome of bacterial meningitis in infants aged <90 days in the United Kingdom and Republic of Ireland: prospective, enhanced, national population-based surveillance. *Clin. Infect. Dis.* 59, e150–e157. doi: 10.1093/cid/ciu514

Park, S. E., Jiang, S., and Wessels, M. R. (2012). CsrRS and environmental pH regulate group B *Streptococcus* adherence to human epithelial cells and extracellular matrix. *Infect. Immun.* 80, 3975–3984. doi: 10.1128/IAI.00699-12

Parker, R. E., Laut, C., Gaddy, J. A., Zadoks, R. N., Davies, H. D., and Manning, S. D. (2016). Association between genotypic diversity and biofilm production in group B *Streptococcus*. *BMC Microbiol.* 16:86. doi: 10.1186/s12866-016-0704-9

Patras, K. A., and Nizet, V. (2018). Group B Streptococcal maternal colonization and neonatal disease: molecular mechanisms and preventative approaches. *Front. Pediatr.* 6:27. doi: 10.3389/fped.2018.00027

Petranovic, D., Guédon, E., Sperandio, B., Delorme, C., Ehrlich, D., and Renault, P. (2004). Intracellular effectors regulating the activity of the *Lactococcus lactis* CodY pleiotropic transcription regulator. *Mol. Microbiol.* 53, 613–621. doi: 10.1111/j.1365-2958.2004.04136.x

Poyart, C., and Trieu-Cuot, P. (2006). A broad-host-range mobilizable shuttle vector for the construction of transcriptional fusions to β-galactosidase in Gram-positive bacteria. *FEMS Microbiol. Lett.* 156, 193–198. doi: 10.1111/j.1574-6968.1997.tb12726.x

Rajagopal, L. (2009). Understanding the regulation of Group B Streptococcal virulence factors. *Future Microbiol.* 4, 201–221. doi: 10.2217/17460913.4.2.201

Ratnayake-Lecamwasam, M., Serror, P., Wong, K.-W., and Sonenshein, A. L. (2001). *Bacillus subtilis* CodY represses early-stationary-phase genes by sensing GTP levels. *Genes Dev.* 15, 1093–1103. doi: 10.1101/gad.874201

Richardson, A. R., Somerville, G. A., and Sonenshein, A. L. (2015). Regulating the intersection of metabolism and pathogenesis in Gram-positive bacteria. *Microbiol. Spectr.* 3:MBP-0004-2014. doi: 10.1128/microbiolspec.MBP-0004-2014

Samen, U., Gottschalk, B., Eikmanns, B. J., and Reinscheid, D. J. (2004). Relevance of peptide uptake systems to the physiology and virulence of *Streptococcus agalactiae*. *J. Bacteriol.* 186, 1398–1408. doi: 10.1128/JB.186.5.1398-1408.2004

Seale, A. C., Koech, A. C., Sheppard, A. E., Barsosio, H. C., Langat, J., Anyango, E., et al. (2016). Maternal colonization with *Streptococcus agalactiae* and associated stillbirth and neonatal disease in coastal Kenya. *Nat. Microbiol.* 1:16067. doi: 10.1038/nmicrobiol.2016.67

Seifert, K. N., Adderson, E. E., Whiting, A. A., Bohnsack, J. F., Crowley, P. J., and Brady, L. J. (2006). A unique serine-rich repeat protein (Srr-2) and novel surface antigen (ε) associated with a virulent lineage of serotype III *Streptococcus agalactiae*. *Microbiology* 152, 1029–1040. doi: 10.1099/mic.0.28516-0

Shivers, R. P., and Sonenshein, A. L. (2004). Activation of the *Bacillus subtilis* global regulator CodY by direct interaction with branched-chain amino acids. *Mol. Microbiol.* 53, 599–611. doi: 10.1111/j.1365-2958.2004.04135.x

Sitkiewicz, I., Green, N. M., Guo, N., Bongiovanni, A. M., Witkin, S. S., and Musser, J. M. (2009). Transcriptome adaptation of Group B *Streptococcus* to growth in human amniotic fluid. *PLoS One* 4:e6114. doi: 10.1371/journal.pone.0006114

Six, A., Bellais, S., Bouaboud, A., Fouet, A., Gabriel, C., Tazi, A., et al. (2015). Srr2, a multifaceted adhesin expressed by ST-17 hypervirulent Group B *Streptococcus* involved in binding to both fibrinogen and plasminogen. *Mol. Microbiol.* 97, 1209–1222. doi: 10.1111/mmi.13097

Sonenshein, A. L. (2005). CodY, a global regulator of stationary phase and virulence in Gram-positive bacteria. *Curr. Opin. Microbiol.* 8, 203–207. doi: 10.1016/j.mib.2005.01.001

Tatusov, R. L. (2000). The COG database: a tool for genome-scale analysis of protein functions and evolution. *Nucleic Acids Res.* 28, 33–36. doi: 10.1093/nar/28.1.33

Tazi, A., Disson, O., Bellais, S., Bouaboud, A., Dmytruk, N., Dramsi, S., et al. (2010). The surface protein HvgA mediates group B *Streptococcus* hypervirulence and meningeal tropism in neonates. *J. Exp. Med.* 207, 2313–2322. doi: 10.1084/jem.20092594

Tazi, A., Plainvert, C., Anselem, O., Ballon, M., Marcou, V., Seco, A., et al. (2019). Risk factors for infant colonization by hypervirulent CC17 Group B *Streptococcus*: toward the understanding of late-onset disease. *Clin. Infect. Dis.* 69, 1740–1748. doi: 10.1093/cid/ciz033

Thigpen, M. C., Whitney, C. G., Messonnier, N. E., Zell, E. R., Lynfield, R., Hadler, J. L., et al. (2011). Bacterial meningitis in the United States, 1998–2007. *N. Engl. J. Med.* 364, 2016–2025. doi: 10.1056/NEJMoa1005384

Thomas, L., and Cook, L. (2020). Two-component signal transduction systems in the human pathogen *Streptococcus agalactiae*. *Infect. Immun.* 88:e931-9. doi: 10.1128/IAI.00931-19

Trespidi, G., Scoffone, V. C., Barbieri, G., Marchesini, F., Abualsha'ar, A., Coenye, T., et al. (2021). Antistaphylococcal activity of the FtsZ Inhibitor C109. *Pathogens* 10:886. doi: 10.3390/pathogens10070886

Trespidi, G., Scoffone, V. C., Barbieri, G., Riccardi, G., De Rossi, E., and Buroni, S. (2020). Molecular characterization of the *Burkholderia cenocepacia dcw* operon and FtsZ interactors as new targets for novel antimicrobial design. *Antibiotics* 9:841. doi: 10.3390/antibiotics9120841

van Schaik, W., Château, A., Dillies, M.-A., Coppée, J.-Y., Sonenshein, A. L., and Fouet, A. (2009). The global regulator CodY regulates toxin gene expression in *Bacillus anthracis* and Is required for full virulence. *Infect. Immun.* 77, 4437–4445. doi: 10.1128/IAI.00716-09

Waters, N. R., Samuels, D. J., Behera, R. K., Livny, J., Rhee, K. Y., Sadykov, M. R., et al. (2016). A spectrum of CodY activities drives metabolic reorganization and virulence gene expression in *Staphylococcus aureus*. *Mol. Microbiol.* 101, 495–514. doi: 10.1111/mmi.13404

Willett, N. P., and Morse, G. E. (1966). Long-chain fatty acid inhibition of growth of *Streptococcus agalactiae* in a chemically defined medium. *J. Bacteriol.* 91, 2245–2250. doi: 10.1128/jb.91.6.2245-2250.1966

Young, J. W., Locke, J. C. W., Altinok, A., Rosenfeld, N., Bacarian, T., Swain, P. S., et al. (2011). Measuring single-cell gene expression dynamics in bacteria using fluorescence time-lapse microscopy. *Nat. Protoc.* 7, 80–88. doi: 10.1038/nprot.2011.432

Conflict of Interest: The authors declare that the research was conducted in the absence of any commercial or financial relationships that could be construed as a potential conflict of interest.

Publisher's Note: All claims expressed in this article are solely those of the authors and do not necessarily represent those of their affiliated organizations, or those of the publisher, the editors and the reviewers. Any product that may be evaluated in this article, or claim that may be made by its manufacturer, is not guaranteed or endorsed by the publisher.

microbial biotechnology

Open Access

Bacillus subtilis as a host for mosquitocidal toxins production

Emanuela Ursino, Alessandra M. Albertini, Giulia Fiorentino, Paolo Gabrieli[†] Viola Camilla Scoffone, Angelica Pellegrini, Giuliano Gasperi, Alessandro Di Cosimo and Giulia Barbieri[*]
Department of Biology and Biotechnology, Università degli Studi di Pavia, Pavia, Italy.

Summary

Aedes albopictus **transmits several arboviral infections. In the absence of vaccines, control of mosquito populations is the only strategy to prevent vector-borne diseases. As part of the search for novel, biological and environmentally friendly strategies for vector control, the isolation of new bacterial species with mosquitocidal activity represents a promising approach. However, new bacterial isolates may be difficult to grow and genetically manipulate. To overcome these limits, here we set up a system allowing the expression of mosquitocidal bacterial toxins in the well-known genetic background of** ***Bacillus subtilis*****. As a proof of this concept, the ability of** ***B. subtilis*** **to express individual or combinations of toxins of** ***Bacillus thuringiensis israelensis*** **(Bti) was studied. Different expression systems in which toxin gene expression was driven by IPTG-inducible, auto-inducible or toxin gene-specific promoters were developed. The larvicidal activity of the resulting** ***B. subtilis*** **strains against second-instar** ***Ae. albopictus*** **larvae allowed studying the activity of individual toxins or the synergistic interaction among Cry and Cyt toxins. The expression systems here presented lay the foundation for a better improved system to be used in the future to characterize the larvicidal activity of toxin genes from new environmental isolates.**

Received 31 March, 2020; accepted 23 July, 2020.
*For correspondence. E-mail giulia.barbieri@unipv.it; Tel: +39 0382 985571; Fax: ++39382528496.
[†]Present address: Department of Biosciences, Università degli Studi di Milano, Milano, Italy.
Microbial Biotechnology (2020) **13**(6), 1972–1982
doi:10.1111/1751-7915.13648
Funding information
Fondazione Bussolera-Branca. Italian Ministry of Education, University and Research (MIUR): Dipartimenti di Eccellenza Program (2018–2022) - Department of Biology and Biotechnology "L. Spallanzani", University of Pavia.

Introduction

Mosquito-borne viruses and pathogens are responsible for the deadliest diseases, causing more than 700 000 deaths each year (Gates, 2017). Given that no vaccines or drugs are available to prevent or cure the majority of them, the most effective control strategy is targeting the mosquito vectors through the use of insecticides. However, the spread of populations resistant to their action is hampering their efficacy (Moyes *et al.*, 2017) and the environmental pollution associated with their extensive use is raising concerns (Benelli and Beier, 2017). Therefore, the development of new, possibly environmentally friendly tools is urgently needed. In this context, the biological control of mosquitoes using bacterial toxins, such as those produced by *Bacillus thuringiensis israelensis*, is increasingly attracting attention as a possible alternative control strategy in many field settings and the expansion of the toolbox of available toxins active against mosquitoes is desirable (Contreras *et al.*, 2019). The isolation of new bacterial species with mosquitocidal activity is an active research topic (Ramirez *et al.*, 2014). In order to identify and characterize new toxins from newly isolated mosquitocidal bacteria, it would be useful to create systems allowing the expression of the genes encoding putative new toxins in a well-known genetic background. This strategy would allow investigating the structural and functional properties of the protein of interest using well-studied organisms that are known to be safe for human health, overcoming the limitations of working with environmental isolates that could be difficult to genetically manipulate and possibly toxic for human beings.

On these premises, the specific aim of this work is the set-up in *Bacillus subtilis* of expression systems that can be used to produce and characterize mosquitocidal toxins of new environmental isolates. As a proof of concept, we created *Bacillus subtilis* strains expressing one or more toxin genes of *Bacillus thuringiensis israelensis* (Bti) and tested their toxicity towards larvae of the Asian tiger mosquito, *Aedes albopictus*.

According to the Global Invasive Species Database (2019), *Ae. albopictus* is one of the world's worst invasive species and is a competent vector of many arboviruses, including West Nile, Yellow fever, Dengue, Zika and Chikungunya (Benedict *et al.*, 2007). It is native to Southeast Asia but human activities, especially the international trade in flowers/plants or used car tires,

favoured by global warming, allowed it to spread to all continents, except Antarctica (Kraemer *et al.*, 2015).

Bacillus subtilis is a well-known and easy-to-handle Gram-positive soil bacterium that is considered as a GRAS organism (Generally Recognized As Safe). Its ability to produce and secrete high concentrations of proteins into the medium (Harwood, 1992) renders it an efficient expression host for the production of proteins of industrial interest (Schallmey *et al.*, 2004; Westers *et al.*, 2004). Two major extracellular proteases (AprE – also called subtilisin – and NprE) are expressed at the beginning of the stationary phase. Because of their commercial interest, they have been extensively studied, leading to a good knowledge of their synthesis and regulation systems. In particular, the expression of *aprE* is controlled by many different transcription factors that can bind different sites in the *aprE* regulatory region, enhancing or lowering its expression (Ogura *et al.*, 2004). A major positive regulator of *aprE* expression is DegU. This protein is part of the DegS-DegU two-component system. In its phosphorylated form, DegU acts as an activator of *aprE* (Kunst *et al.*, 1974). A particular mutation of the *degU* gene, *degU32(hy)*, mimics the phosphorylated, active form of the transcriptional activator DegU (DegU-P), enhancing the transcription of *aprE* (Mader *et al.*, 2002). In this work, the knowledge of the mechanisms controlling gene expression in *B. subtilis* was exploited to express Bti toxins.

The larvicidal activity of Bti is a long and well-known biological phenomenon and it is due to the presence of pBtoxis, a 128 kb plasmid, which encodes four major protoxins (Cry4Aa, Cry4Ba, Cry11Aa and Cyt1Aa) and two minor toxins (Cry10Aa and Cyt2Ba) that are expressed as parasporal crystalline bodies at the onset of sporulation (Ben-Dov *et al.*, 1999; Berry *et al.*, 2002). This plasmid also contains additional genes that encode for proteins that help the folding and activity of the toxins Cry11Aa and Cyt1Aa. Among the Dipteran-specific toxins synthesized by Bti in late stationary phase during sporulation, the Cry11Aa δ-endotoxin targets very efficiently *Ae. albopictus* larvae (Otieno-Ayayo *et al.*, 2008; Ben-Dov, 2014). The gene encoding the Cry11Aa toxin is included in the *p19-cry11Aa-p20* tri-cistronic operon (Berry *et al.*, 2002). While the function of P19 is not known, the P20 protein was previously reported to stabilize both Cyt1Aa and Cry11Aa by protecting the nascent polypeptides from proteolysis (Adams *et al.*, 1989; Visick and Whiteley, 1991; Xu *et al.*, 2001; Sazhenskiy *et al.*, 2010) and to enhance the expression of Cry11Aa not only in *B. thuringiensis* (Wu and Federici, 1995) but even in recombinant *E. coli* (Xu *et al.*, 2001).

The deep knowledge of the *B. subtilis* genetics and of the *B. thuringensis israeliensis* toxins allowed us to investigate the feasibility of using *B. subtilis* as host to produce known and yet unknown larvicidal toxins in a safe organism.

Results

Expression of Cry11Aa by an IPTG-inducible system

To evaluate the ability of *B. subtilis* as an expression system for Bti δ-endotoxins, the *cry11Aa* gene, with and without its downstream gene *p20*, was amplified from a wild-type strain of *Bacillus thuringiensis israelensis* (4Q1) and cloned into the *amyE* chromosomal integrative plasmid pDR111 (Ben-Yehuda *et al.*, 2003), downstream of the *Phyperspank* IPTG-inducible promoter. The obtained constructs were inserted by double cross-over in the *amyE* gene of *Bacillus subtilis* strain PB1831. The resulting strains PB7223 (*amyE*::*Phyperspank-cry11Aa*) and PB7226 (*amyE*::*Phyperspank-cry11Aa-p20*; Fig. S1A) displayed no growth defects compared to the control strain PB7222 (*amyE*::*spc*) when grown in 2xSG sporulation medium (Fig. S1B).

As revealed by SDS-PAGE analysis on cells collected at 20 h after IPTG induction, Cry11Aa was successfully expressed by both strains but, unexpectedly, the amount of Cry11Aa produced by *B. subtilis* cells expressing both *cry11Aa* and *p20* resulted to be about 15-fold lower than that displayed by cells expressing only *cry11Aa* (Fig. S1C). Notably, P20 expression could not be detected by SDS-PAGE analysis even in the control sample Bti 4Q1.

Accordingly, strain PB7223, expressing only Cry11Aa, displayed a higher larvicidal activity against *Aedes albopictus* as compared to PB7226, expressing both proteins (48-h, $P = 0.033$; 72-h, $P = 0.016$; Fig. 1A). The larvicidal activity induced by both strains increased over time, up to 72 h of exposure to the toxins. At 96 h after the beginning of the assay, no significant increase in mortality was detected compared to the 72-h time point (data not shown).

Previous studies reported that the P20 helper protein is required for efficient expression of Cyt1Aa and other Cry toxins (Wu and Federici, 1993; Sazhenskiy *et al.*, 2010). As in this work we are interested in expressing different combinations of genes and in studying the interaction among different toxins of Bti, the *p20* gene was maintained in the construct.

Expression of Cry11Aa and the helper protein P20 in an auto-inducible system

In order to create an auto-inducible expression system, the region upstream of the *B. subtilis aprE* gene, extending from positions −614 to −1 with respect to the beginning of the *aprE* coding sequence and comprising the entire transcriptional control region (TCR) and the 5'UTR of the gene (Ferrari *et al.*, 1993; Ogura *et al.*, 2004), was

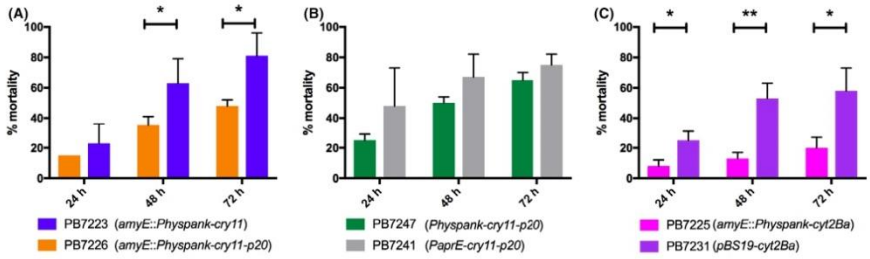

Fig. 1. Percentage of *Aedes albopictus* larval mortality at different time points after treatment with 2 g l^{-1} (wet weight) of cells, spore–parasporal bodies mixture (collected at T20) of strains A. PB7223, PB7226, B. PB7241, PB7247, C. PB7225, PB7231. $^{*}P < 0.05$; $^{**}P < 0.01$. Results are means ± SD of at least three independent experiments, each performed in duplicate.

fused to the Bti *cry11Aa-p20* genes. The obtained construct was cloned into the *B. subtilis* integrative plasmid pJM113 (Perego, 1993). The resulting pBG105 vector and the control vector pBG109, bearing only the TCR and 5'UTR of *aprE*, were integrated by single cross-over at the *PaprE* region of the *B. subtilis* wild-type strain PB168. The resulting strains did not show detectable levels of Cry11Aa by SDS-PAGE and did not have any larvicidal activity towards *Ae. albopictus* larvae (data not shown). In order to upregulate *PaprE* activity and to increase Cry11Aa protein yield, pBG105 and pBG109 were used to transform PB7007, a strain carrying the *degU32(hy)* allele and the inactivation (deletion of part of the cds) of the two major exoprotease genes *aprE* and *nprE*, to allow a more stable production of heterologous proteins. The resulting strains PB7241 (Δ*aprE*::*PaprE-cry11Aa-p20*) and PB7242 (Δ*aprE*::*PaprE*; Fig. S2A) displayed similar growth patterns in 2xSG sporulation medium (Fig. S2B). SDS-PAGE analysis of the cells, spore and parasporal body mixtures collected at 4, 15, 20, 24, 48 and 72 h after the beginning of the stationary phase showed that the expression of the heterologous toxin gene starts at the onset of sporulation, concomitantly with the activation of the *aprE* promoter. The production of Cry11Aa is still absent 4 h after the beginning of the stationary phase, while it accumulates up to 72 h (Fig. S2C). Treatment with 2 g l^{-1} of spore–parasporal bodies mixtures of the auto-inducible strain PB7241 collected 20 h after the beginning of stationary phase (T20) induced almost 80% mortality in *Ae. albopictus* larvae after 72h of treatment (Fig. 1B).

To compare the expression and the toxicity of the above-mentioned *Phyperspank-cry11Aa-p20* and *PaprE-cry11Aa-p20* constructs in the same genetic background, the *Phyperspank-cry11Aa-p20* construct was integrated at the *amyE* locus of the *degU32(hy) Bacillus subtilis* strain PB7007. The resulting strain (PB7247) did not show any growth defect but expressed Cry11Aa at a lower level compared to PB7241 (Fig. S3A and B). Accordingly, when assayed for toxicity, at all sampling times studied, PB7247 spores–parasporal bodies conferred a lower larval mortality (not statistically significant, $P = 0.32$) compared to that of the strain carrying the *PaprE*-dependent auto-inducible construct (PB7241; Fig. 1B). Interestingly, expression of the *Phyperspank-cry11Aa-p20* construct in a *degUhy* background (PB7247) confers a higher toxicity against *Ae. albopictus* larvae compared to PB7226 strain (72-h time point, $P = 0.0003$; Fig. 1A and B).

Cyt1Aa is toxic against B. subtilis

Previous studies proposed a synergist effect of Cyt1Aa on Cry11Aa (Perez *et al*., 2005; Perez *et al*., 2007). We therefore analysed the toxicity of *B. subtilis* strains expressing Cyt1Aa. First, the pBtoxis region encompassing the *cyt1Aa* and *p21* genes was cloned into pDR111, under the control of the *Phyperspank* promoter. The gene *p21* is oriented in the opposite direction with respect to *cyt1Aa* and cannot be expressed by our construct. However, this sequence was included in the cloned region as it comprises the *cyt1Aa* terminator hairpin which plays a role in *cyt1Aa* mRNA stability (Sakano *et al*., 2017). The resulting *Phyperspank-cyt1Aa-p21* construct was integrated in the *amyE* gene of PB1831. Surprisingly, Cyt1Aa could not be detected by SDS-PAGE analysis of PB7232 cells–spores mixture collected at 72h after induction, suggesting that single copy integration of *cyt1Aa* in the *B. subtilis* chromosome under the control of the IPTG-inducible promoter is not sufficient for efficient Cyt1Aa expression (Fig. S4). The *cyt1Aa-p21* gene cluster was then cloned under the control of the *cyt1Aa* promoter region into the *B. subtilis* multicopy replicative plasmid pBS19. The PB1831

derivative strain carrying the pBS19-*Pcyt1Aa-p21* plasmid (PB7230) produced Cyt1Aa protein (Fig. S4) and caused 85% mortality against *Aedes albopictus* larvae after 24 h from the beginning of the assay (data not shown). Unfortunately, Cyt1Aa overexpression in our *B. subtilis* strain is toxic, inhibiting growth, cell division and sporulation hence leading to the death of the host cells (Table S3; Fig. S5). For this reason, we decided to focus our attention on another cytolytic protein: the minor toxin Cyt2Ba.

Coexpression of Cry11Aa and Cyt2Ba toxins

In order to study the interaction between Cyt2Ba and Cry11Aa toxins, the gene encoding the cytolytic protein Cyt2Ba was cloned downstream of the *Phyperspank* promoter in plasmid pDR111 and the resulting construct was integrated by double cross-over in the *amyE* gene of *B. subtilis* PB1831 (strain PB7225). The *cyt2Ba* gene was also cloned in the pBS19 multicopy replicative plasmid under the control of its own promoter (strain PB7231). The two resulting recombinant strains did not show any growth defect compared to their respective control strains PB7222 (*amyE::spc*) and PB7229 (pBS19) respectively (Fig. S6A). SDS-PAGE analysis of the pellets collected 24 h after the beginning of the stationary phase showed a lower level of Cyt2Ba expression in strain PB7225 compared to PB7231 (Fig. S6B). Accordingly, when assayed for toxicity, PB7231 displayed a significantly higher larvicidal activity against *Aedes albopictus* compared to PB7225 (24-h, $P = 0.029$; 48-h, $P = 0.008$; 72-h, $P = 0.030$; Fig. 1C).

To evaluate whether coexpression of Cry11Aa and Cyt2Ba resulted in a synergistic or additive effect in terms of larvicidal activity, two additional strains were prepared. Strain PB7240 was obtained by transformation of the PB1831 derivative carrying the *amyE::Phyperspank-cry11p20* construct (PB7226) with plasmid pBS19-*Pcyt2Ba*. Strain PB7265 was prepared by integrating the *Phyperspank-cyt2Ba* construct in the *amyE* gene of the *degU32(hy)* strain PB7241, carrying the *PaprE-cry11Aa-p20* construct integrated by single cross-over in the *aprE* locus. Coexpression of the two toxins did not affect the growth characteristics of the two strains compared to the corresponding parental strains (Fig. S7).

Strains PB7240 and PB7265 were both able to produce the two Bti toxins but differed in the relative abundance of the two proteins (Fig. 2). In particular, as revealed by quantification of band intensity, coexpression of Cry11Aa and Cyt2Ba in PB7240 resulted in an increase in Cyt2Ba levels and in a decrease in Cry11Aa abundance compared to strains PB7231 and PB7233, expressing the two toxins individually. On the contrary, Cry11Aa and Cyt2Ba protein levels in PB7265 were similar to those observed when the two toxins were expressed individually. While the two strains coexpressing both toxins showed similar levels of Cry11Aa, PB7240 displayed a higher abundance of the cytolytic protein. When assayed for their toxicity against second-instar larvae of *Ae. albopictus,* PB7240 and PB7265 revealed differences in their larvicidal activities (Fig. 3). Pellets collected 48 h after the beginning of the stationary phase and containing a mix of spore–cells and parasporal bodies were resuspended in dH_2O and used at decreasing concentrations (expressed as biomass wet weight l^{-1}) in larvicidal assays. As assessed at 48 h after the beginning of the assay, after induction, strain PB7265 was more toxic than PB7240, with a statistically significant difference displayed at the assayed concentrations of 100 and 10 mg l^{-1} ($P = 0.013$ and 0.025 respectively). Notably, PB7265 was the most toxic engineered *B. subtilis* strain built in this work.

The larvicidal activity of the strains coexpressing Cry11Aa and Cyt2Ba was compared to the one of their corresponding parental strains expressing each toxin individually. As reported in Fig. 3A, when tested at the final concentration of 500 mg l^{-1} or lower, strain PB7240, expressing both toxins, induced a percentage of larval mortality (84% at 500 mg l^{-1}; 50% at 100 mg l^{-1}; 5% at 10 mg l^{-1}) that is higher than the sum of the mortality induced by the strains expressing Cyt2Ba (PB7231) or Cry11Aa (PB7233) alone (0.07% and 0.03% at 500 mg l^{-1}, respectively; no mortality induced by any of the two strains at lower concentrations; Fig. 3A). On the contrary, in the *degU32(hy)* strain PB7265, the concomitant expression of Cyt2Ba (IPTG-induced from a single copy gene) and Cry11Aa (*PaprE-cry11Aa-p20*) resulted in a larvicidal activity similar to the sum of the activities of the two toxins expressed individually. This additive effect of the two toxins on larval mortality could be easily appreciated at the assayed concentration of 100 mg l^{-1} (Fig. 3B). At the two highest concentrations (1 g l^{-1} and 500 mg l^{-1}) used in the assay, larval mortality reached almost 100% in all tested conditions, masking any significant difference in larvicidal activity between conditions in which the two toxins were expressed individually or in combination.

Worthy of note, strain PB7266, expressing *cyt2Ba* under the control of the P*hyperspank* promoter in a *degUhy* background, shows a significantly higher larvicidal activity when compared to PB7231 ($P = 0.0097$, 1 g l^{-1}, 48-h from the beginning of the assay): while the toxicity of PB7266 is detectable even at lower concentrations (up to 10 mg l^{-1}), the larvicidal activity of PB7231 can be observed only at the concentration of 1 g l^{-1} (Fig. 3A and B).

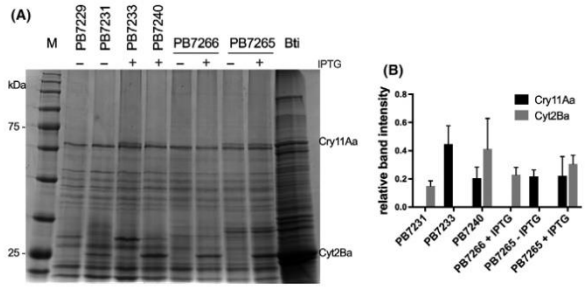

Fig. 2. A. 10% SDS-PAGE analysis of spore–parasporal body mixtures of strains PB7229 (pBS19), PB7231 (pBS19-*Pcyt2Ba*), PB7233 (*amyE::Phyperspank-cry11p20*, pBS19 – induced with IPTG 1 mM at T0), PB7240 (*amyE::Phyperspank-cry11p20*, pBS19-P*cyt2Ba* – induced with IPTG 1 mM at T0), PB7266 (*amyE::Phyperspank-cyt2Ba)* not induced and induced at T0, PB7265 (*amyE::Phyperspank-cyt2Ba*, *ΔaprE::PaprE-cry11Aa-p20*) not induced and induced at T0. All strains were grown simultaneously in 2xSG, and the cultures containing cells, spores and parasporal body mixtures were collected 48 h after the beginning of the stationary phase (T48). Bti 4Q1 spore–parasporal bodies collected at T48 were used as positive control. M: (A), Protein Marker VI (10–245) prestained (PanReac). B. Graphical representation of relative Cry11Aa and Cyt2Ba band intensities. Each value represents the average ± SD of three independent replicas. The intensities of the bands corresponding to Cry11Aa and Cyt2Ba were normalized relative to the intensities of the 70 and 22 kDa bands of the protein marker respectively. Each value represents the average ± SD of the three independent replicas.

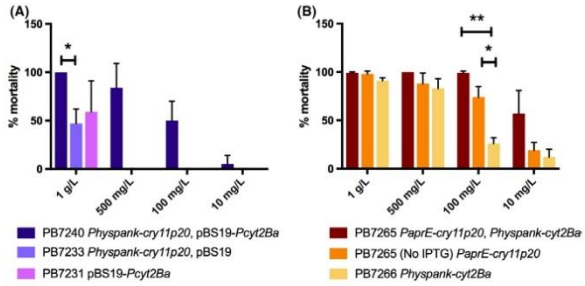

Fig. 3. Percentage of *Aedes albopictus* larval mortality at 48 h after the beginning of the assay. The effect of treatment with decreasing concentrations of cells–spores–parasporal bodies mixtures (biomass wet weight l^{-1}) collected 48 h after the beginning of the stationary phase was assessed.
A. Strains PB7233, PB7231 and PB7240. Statistically significant differences were observed between PB7240 and strains PB7233 (1 g l^{-1}, $P = 0.014$; 500 mg l^{-1}, $P = 0.014$; 100 mg l^{-1}, $P = 0.024$) and PB7231 (500 mg l^{-1}, $P = 0.017$, 100 mg l^{-1}, $P = 0.036$).
B. Strains PB7265 (not induced and induced with 1 mM IPTG) and PB7266 induced (*amyE::Physpanc-cyt2Ba*). $^{**}P = 0.0002$; $^{*}P = 0.016$.
Results are means ± SD of at least three independent experiments, each performed in duplicate.

Discussion

In this work, *B. subtilis* was used as a host for the expression of heterologous mosquitocidal toxins. By using diverse expression systems, we created different engineered strains expressing Bti δ-endotoxins and showing different degrees of larvicidal activity. The toxic activity of three Bti toxins, Cry11Aa, Cyt1Aa and Cyt2Ba, was studied individually or in combination, in different genetic backgrounds and under the control of different promoters.

The ability of recombinant *B. subtilis* to synthesize active δ-endotoxins of the phylogenetically related bacterium *B. thuringiensis israelensis* was previously demonstrated using *Ae. albopictus* cells (Ward *et al.*, 1986; Calogero *et al.*, 1989). In this work, for the first time, *Ae. albopictus* larvae were used to test the larvicidal activity of recombinant *B. subtilis* strains expressing Bti δ-endotoxins.

The ability of *B. subtilis* to express active Bti Cry11Aa endotoxin, with and without the helper protein P20, was

evaluated by using an IPTG-inducible system. Previous studies showed that coexpression of Cry11Aa and P20 in recombinant *B. thuringiensis* (Wu and Federici, 1995) and in Gram-negative bacteria (Xu *et al.*, 2001) resulted in a greater amount of Cry11Aa protein levels and in a higher toxicity against third-instar *Ae. aegypti* larvae with respect to expression of Cry11Aa protein alone. These previous works were performed by either cloning the two adjacent genes in multicopy plasmids, downstream of their own promoter (Wu and Federici, 1995) or by using the inducible T5 promoter (Xu *et al.*, 2001). In this work, the *amyE* integrated *Phyperspank-cry11Aa* construct displayed a higher efficiency in Cry11Aa expression compared to *Phyperspank-cry11Aa-p20* (Fig. S1). A direct correlation between Cry11Aa expression level and the larvicidal activity of the engineered strain was observed (Fig. 1A). The collected results therefore suggest that in *B. subtilis* Cry11Aa can be efficiently expressed even in the absence of P20 and that its expression is sufficient to confer larvicidal activity. We cannot exclude that the unexpected lower expression of Cry11Aa in PB7226 is due to a lower stability of the longer *Phyperspank-cry11Aa-p20* transcript compared to *Phyperspank-cry11Aa*. The lack of a band corresponding to P20 as verified by SDS-PAGE is consistent with results reported in previous studies (e.g. Wu and Federici, 1995; Tang *et al.*, 2006; Valtierra-de-Luis *et al.*, 2020). The role of P20 in affecting Cry11Aa levels and stability in *B. subtilis* should be further investigated by using combinations of construct expressing *cry11Aa* and *p20* individually.

As the 20-kDa helper protein was previously reported to be required for efficient expression of Cyt1Aa (Wu and Federici, 1993; Sazhenskiy *et al.*, 2010) and other Cry toxins (Shao *et al.*, 2001; Diaz-Mendoza *et al.*, 2012; Elleuch *et al.*, 2015), the *cry11Aa-p20* construct was retained for further experiments.

Inducible systems require constant cell-culture monitoring and their use increases the cost of the commercial product. The generation of a more physiological, auto-inducible expression system could therefore be useful to overcome the limits associated with IPTG induction. To this purpose, *cry11Aa* and *p20* were cloned under the control of the endogenous *aprE* promoter in *B. subtilis*. In the wild-type strain, the transcription from the *PaprE* was not strong enough to drive *cry11Aa* expression. Therefore, a *degU32(hy)* mutant strain of *B. subtilis* was used as a host, allowing hyper-transcription from *PaprE* (Kunst *et al.*, 1974; Henner *et al.*, 1988; Ogura *et al.*, 2004). The auto-inducible system drove the expression of the heterologous protein during the stationary phase and concurrently to the onset of sporulation, concomitantly with the activation of *PaprE* (Fig. S2). By affecting only one of the regulators (DegU) controlling the expression of *aprE*, a good level of synthesis of the heterologous protein was achieved, leading also to a good level of toxicity. Worthy of note, the intrinsic instability of integrations by single cross-over leads to the presence of a variable number of the *PaprE-cry11Aa-p20* construct on the chromosome: low concentrations of antibiotic in the medium should ensure an average of 1–2 copies per cell.

Cyt1Aa toxin is a cytolytic protein able to synergize with other Cry toxins such as Cry4A, Cry4Ba and Cry11Aa (Wu and Chang, 1985; Crickmore *et al.*, 1995; Poncet *et al.*, 1995). It was demonstrated that Cyt1Aa functions as a Cry11Aa membrane receptor (Perez *et al.*, 2005). The interaction between the two proteins supports toxicity both by pore formation and by oligomerization of Cry11Aa toxin (Soberon *et al.*, 2013). Cyt1Aa expression in *B. subtilis* was previously reported to cause mortality against third-instar *Ae. aegypti* larvae (Ward *et al.*, 1986). However, in this work, when the same *cyt1Aa-p21* region was cloned downstream of the IPTG-inducible *Phyperspank* promoter and integrated in the *B. subtilis* chromosome, no detectable levels of Cyt1Aa could be observed. On the contrary, the cytolytic protein was highly produced by cloning the same construct downstream of its own promoter, in a multicopy plasmid (pBS19-*cyt1Aa-p21*; Fig. S4). The high relative abundance of Cyt1Aa in the Bti parasporal body can be attributed to different factors, including the level of *cyt1Aa* gene expression, as well as its transcript and protein stability. While both the *Phyperspank-cyt1Aa-p21* and the pBS19- *cyt1Aa-p21* constructs include the 3'-UTR stem-loop structure involved in *cyt1Aa* transcription termination and mRNA stability (Sakano *et al.*, 2017), they differ in their copy number and in the promoter used to drive gene expression. Both these elements were previously reported to affect Cyt1Aa levels. In Bti, the expression of *cyt1Aa* is controlled by three functional non-overlapping promoters (BtI, BtII and BtIII) that are activated during sporulation by σ^E (BtI and BtIII) and σ^K (BtII) transcription factors (Sakano *et al.*, 2017). While the combination of BtI, BtII and BtIII leads to the highest level of *cyt1Aa* expression, transcript levels can be modulated by using independent or different combinations of Bt promoters. In this work, the 1224 bp region cloned in pBS19 and comprising the *cyt1Aa* gene and the region upstream of its cds include all three Bt promoters for full *cyt1Aa* expression. An additional factor influencing Cyt1Aa protein production is plasmid copy number. At least four copies of a plasmid carrying the *cyt1Aa* gene downstream of the BtIII promoter must be present in Bti to obtain detectable Cyt1Aa levels (Park *et al.*, 2016). Interestingly, no synthesis of Cyt1Aa was detected in Bti recombinant strains transformed with a low copy number (2–3) plasmid carrying a pBtoxis minireplicon comprising the *cyt1Aa* gene and its three Bt promoters (Tang *et al.*,

2006). We therefore hypothesize that the presence of a single copy of *cyt1Aa* might be the reason of the lack of efficient Cyt1Aa protein production in PB7232. In this strain, the *Phyperspank* promoter is unable to drive sufficient expression of the cytotoxic gene. On the contrary, the pBS19-*cyt1Aa-p21* construct, including all three Bt promoters and present in multiple copies per cell, allowed achieving a high level of Cyt1Aa expression. Notably, high Cyt1A expression resulted to be cytotoxic against *B. subtilis* itself (Table S3, Fig. S5). As overexpression of Cyt1Aa toxin in Bti was previously reported to result in significantly fewer spores per unit medium and in the formation of imperfect crystals (Park *et al.*, 2016), it can be hypothesized that, even in *B. thuringiensis israelensis*, Cyt1Aa expression needs to be tightly regulated to prevent off-target toxicity.

Despite different studies described the role of Cyt1Aa in enhancing the toxicity of Bti and in delaying the insurgence of resistance, the interactions of Cyt2Ba with other components of the Bti crystals are still poorly investigated. Synergy between Cyt2Ba and Cry4Aa proteins was previously reported against larvae of *Ae. aegypti* (Manasherob *et al.*, 2006). Moreover, very recently, the co-administration of two recombinant Bt strains, each expressing Cry10 or Cyt2Ba, respectively, revealed a synergistic interaction between the two toxins when simultaneously ingested by *A. aegypti* larvae (Valtierra-de-Luis *et al.*, 2020). Here, the possible interaction between Cry11Aa and Cyt2Ba was investigated.

We constructed mosquitocidal *B. subtilis* strains in which *cyt2Ba* was cloned either in single copy, downstream of the *amyE* integrated *Phyperspank* promoter, or in the multicopy vector pBS19, under the control of its own promoter. The cytolytic toxin was expressed efficiently in both constructs, conferred larvicidal activity and its expression was not lethal for the host. We therefore decided to study the possible synergism between Cyt2Ba and Cry11Aa. To this purpose, strains PB7240 (*Phyperspank-cry11Aa-p20* pBS19-*Pcyt2Ba*) and PB7265 (*PaprE-cry11Aa-p20, amyE::Phyperspank-cyt2Ba*) were prepared.

In strain PB7240, the coexpression of the two toxin genes resulted in a twofold increase in Cyt2Ba levels and in a concomitant twofold decrease in Cry11Aa abundance with respect to the corresponding parental strains (PB7231 and PB7233) expressing each toxin individually. As the protein P20 was previously reported to be involved in the stabilization of Cyt1Aa (Visick and Whiteley, 1991; Wu and Federici, 1993), we may hypothesize that it may also contribute to a higher stability of Cyt2Ba. Similarly to what described in *E. coli* for Cyt1Aa, P20 may prevent Cyt2Ba proteolytic degradation, leading to higher levels of the cytolytic protein in strain PB7240 compared to PB7231. The increase in Cyt2Ba levels in PB7240 was concomitant to a decrease in Cry11Aa yields with respect to PB7233, possibly due to energy expenditure dedicated the synthesis of the cytolytic protein. Strain PB7240 displayed a larvicidal activity higher than the sum of larval mortality induced by the corresponding strains expressing each toxin individually (Fig. 3A). This increase in larvicidal activity cannot be ascribed only to the twofold increase in Cyt2Ba levels, since at concentrations at which no larvicidal activity can be observed for strain PB7231 (e.g. at 100 mg l^{-1}), PB7240 can still induce a larval mortality similar to the one induced by PB7231 when used at a 10-fold higher concentration. These observations suggest a synergism between Cry11Aa and Cyt2Ba in this genetic background.

On the contrary, an additive effect between the two toxins was observed when using a *degU32(hy)* and protease-deficient (Δ*aprE* and Δ*nprE*) *B. subtilis* strain. In this genetic background, the IPTG-dependent expression of *cyt2BA* in PB7266 allowed obtaining levels of cytolytic protein similar to those displayed by PB7231. However, in contrast to what observed in PB7240, no increase in Cyt2Ba levels was observed in PB7265 when both toxins were produced: after IPTG induction, PB7265 displayed levels of Cyt2Ba similar to those observed in strain PB7266 (+ IPTG). As detected in the parental strain PB7241 (Fig. S2), being the P*aprE* promoter activated at the beginning of sporulation, its use for driving gene expression leads to the accumulation of the produced proteins during late stationary phase. On the contrary, in PB7233, expression of the *Phyperspank-cry11Aa-p20* construct is induced earlier, i.e. at the moment of transition from exponential to stationary phase. The delayed expression of *cry11Aa* in PB7265 compared to PB7233 results in a lower level of Cry11Aa toxin observed 48 h after the beginning of the stationary phase. For the same reason, the amount of P20 produced by PB7265 could be insufficient to exert any effect on the stability of Cy2Ba, whose levels remain similar in PB7266 and PB7265. Notably, in the absence of an increase in Cyt2Ba, the ability of PB7265 to produce Cry11Aa is not affected by the IPTG-dependent induction of P*hyperspank-cyt2Ba*.

It is noteworthy that, despite expressing similar or even lower levels of Cry11Aa and Cyt2Ba, PB7266 and PB7265 displayed a significantly higher larvicidal activity compared to PB7231, PB7233 and PB7240. We may speculate that the lack of the two major *B. subtilis* exoproteases may allow a higher stability of the produced proteins, resulting in a higher toxicity of the strains expressing the two toxins, individually or in combination.

The results here obtained demonstrate that *B. subtilis* can be efficiently used as a host system to study the activity of individual or combinations of toxins identified

in mosquitocidal bacterial strains. The deep knowledge of its genetics, together with the availability of well-established tools for its manipulation, allows the modulation and optimization of heterologous toxin production. The expression systems here presented lay the foundation for the construction of a better improved system that might be used to characterize, modulate and evaluate the level of expression and the larvicidal activity of individual toxin genes from new environmental isolates.

Experimental procedures

Bacterial strains, plasmids, primers and growth conditions

The *Bacillus thuringiensis israelensis* strain 4Q1 (Bacillus Genetic Stock Center, original code HD567 (Goldberg and Margalit, 1977)) was used as source of template DNA for cloning and as positive control in δ-endotoxins expression analysis and in larvicidal assays. The *B. subtilis* bacterial strains constructed and used in this work are listed in Table 1 and prepared as described in Supplementary Information. *Escherichia coli* DH5α was used for construction and maintenance of plasmids (Table S2). The primers and plasmids used in this work are listed in Tables S1 and S2 respectively. Growth media employed in this work include Luria-Bertani medium (LB), LM, MD and MDCH (Kunst and Rapoport, 1995) and 2xSG sporulation medium: 16 g l^{-1} of Nutrient Broth (Difco), 2 g l^{-1} KCl, 0.5 g l^{-1} $MgSO_4$*$7H_2O$, 1 mM Ca $(NO_3)_2$, 0.1 mM $MnCl_2$*$4H_2O$, 1 M $FeSO_4$ and 0.1% glucose (Leighton and Doi, 1971). Antibiotics were used at the following concentrations: ampicillin, Amp (for *E. coli*) 100 μg ml^{-1}; chloramphenicol, Caf 5 μg ml^{-1}; spectinomycin, Spc 100 μg ml^{-1}; kanamycin, kana 20 μg ml^{-1}, erythromycin, Ery 0.5 μg ml^{-1}; and lincomycin, Linc 12.5 μg ml^{-1}.

Table 1. *Bacillus subtilis* strains used in this study.

Strain name	Genotype	Source or origin
PB168	*trpC2*	BGSC[a] strain 1A1
PB1831	*trpC2, phe-1*	BGSC[a] strain 1A96 (JH642, J. Hoch)
PB7007	*ΔaprE, ΔnprE, thr-, amyE::[comK (ery)], degU32H*	University of Pavia Collection
PB7222	*trpC2, phe-1, amyE::spc*	PB1831 × pDR111
PB7223	*trpC2, phe-1, amyE::Physpank-cry11Aa*	PB1831 × pDR111-*cry11Aa*
PB7225	*trpC2, phe-1, amyE::Physpank-cyt2Ba*	PB1831 × pDR111-*cyt2Ba*
PB7226	*trpC2, phe-1, amyE::Physpank-cry11Aa-p20*	PB1831 × pDR111-*cry11Aa-p20*
PB7229	*trpC2, phe-1, pBS19*	PB1831 × pBS19
PB7230	*trpC2, phe-1, pBS19-Pcyt1Aa-p21*	PB1831 × pBS19-*Pcyt1Aa-p21*
PB7231	*trpC2, phe-1, pBS19-Pcyt2Ba*	PB1831 × pBS19-*Pcyt2Ba*
PB7232	*trpC2, phe-1, amyE::Physpank-cyt1Aa-p21*	PB1831 × pDR111-*cyt1Aa-p21*
PB7233	*trpC2, phe-1, amyE::Physpank-cry11Aa-p20, pBS19*	PB7226 × pBS19
PB7240	*trpC2, phe-1, amyE::Physpank-cry11Aa-p20, pBS19-Pcyt2Ba*	PB7226 × pBS19-*Pcyt2Ba*
PB7241	*ΔnprE, thr-, amyE::[comK (ery)], degU32H ΔaprE::PaprEcry11Aap20*	PB7007 × pBG105
PB7242	*ΔnprE, thr-, amyE::[comK (ery)], degU32H ΔaprE::PaprE*	PB7007 × pBG109
PB7246	*ΔaprE, ΔnprE, thr-, amyE::spc, degU32H*	PB7007x PB7222
PB7247	*ΔaprE, ΔnprE, thr-, amyE::Physpank-cry11Aa-p20, degU32H*	PB7007 × PB7226
PB7265	*ΔnprE, thr-, amyE::Physpank-cyt2Ba, degU32H ΔaprE::PaprEcry11Aap20*	PB7241 × PB7225
PB7266	*ΔnprE, thr-, amyE::Physpank-cyt2Ba, degU32H ΔaprE::PaprE*	PB7242 × PB7225

a. BGSC: *Bacillus* Genetic Stock Center culture collection catalogue number.

Preparation of spores, parasporal bodies and cells mixtures

Engineered *B. subtilis* strains were cultured in 10 ml LB overnight. The following day, the o/n preculture was diluted to OD_{600} = 0.05 in 20 ml of 2xSG sporulation medium and incubated with shaking to OD_{600} = 1. Then, the culture was re-diluted to OD_{600} = 0.1 in 60 ml of fresh 2xSG and grown at 37 °C, 250 rpm. Heterologous gene expression driven by the P*hyperspank* promoter was induced with 1 mM IPTG at the beginning of the stationary phase (T0). At the time of collection, 20 ml of culture containing whole spores, cells and parasporal bodies were harvested and then pelleted by centrifugation (10 000 rpm × 15' 4 °C). The pellets were then suspended in Tris-HCl 10 mM (pH = 7) and aliquots of 1 ml were prepared. After a new centrifugation at 12 000 *g* × 10' at 4 °C, the pellets were stored at –20 °C or immediately used for protein analysis by SDS-PAGE 10%, sporulation and larvicidal assay.

Protein detection and quantification

Pellets of spores–crystal mixtures were resuspended in dH_2O to a final concentration of 200 mg ml^{-1} wet weight/volume. Samples (15 μl) were heated in a thermocycler at 95 °C for 5 min in loading buffer (0.05 M Tris pH 6.8, 10% glycerol, 2% SDS, 5% β-mercaptoethanol and 0.05% bromophenol blue) and subjected to electrophoresis in 10% SDS-PAGE. Gels were stained with Coomassie Brilliant Blue. Images were acquired using a Bio-Rad ChemiDoc MP Imaging System. Quantification of bands intensities was performed using ImageJ Software (Schneider *et al.*, 2012).

Larvicidal assay

The larvicidal activity of the engineered *Bacillus subtilis* strains was analysed by mortality assays. Twenty-five second-instar larvae of *Aedes albopictus* Rimini strain reared at 28 °C, in a 12 h-light/12 h-dark photoperiod, with 70% of humidity, were placed in 100 ml of deionized water and were fed with mixtures of engineered *B. subtilis* spores, parasporal bodies and cells. Mixtures were added at different concentrations, expressed as biomass wet weight/litre. Mortality was recorded after 24, 48 and 72 h from the beginning of the assay. No nutritional supplement was added. The experiments were carried out at room temperature, and each test was conducted with three independent culture replicates. 4Q1 Bti spores, parasporal bodies and cells collected after 72 h of growth in 2xSG were used as positive controls. Not-induced cultures and cells transformed with empty vectors were used as negative controls.

Sporulation assay

To calculate the number of heat-resistant spores, appropriate dilutions of the resuspended pellets were plated on LB plates supplemented with antibiotic (when needed) before and after treatment at 80 °C for 10 min. The percentage of sporulation was calculated according to the following formula:

$$\frac{\text{No of CFUs/ml grown after heat} - \text{treatment}}{\text{No of CFUs/ml grown before heat} - \text{treatment}} \times 100$$

Statistical analysis

Statistical analysis was performed on ≥ 3 independent experiments using GraphPad Prism version 8 software. Statistical significance was determined using the Holm–Sidak method, with alpha = 0.05.

Acknowledgements

We acknowledge Dr. Eugenio Ferrari for helpful suggestions and discussion and Mrs. Elisabetta Andreoli for expert technical assistance. For acquisition of Transmission Electron Microscopy images, we thank Prof. Luciano Sacchi, Mrs. Emanuela Clementi and Prof. Davide Sassera.

Conflict of interest

None declared.

References

Adams, L.F., Visick, J.E., and Whiteley, H.R. (1989) A 20-kilodalton protein is required for efficient production of the *Bacillus-thuringiensis* subsp *israelensis* 27-kilodalton crystal protein in *Escherichia coli*. *J Bacteriol* **171:** 521–530.

Ben-Dov, E. (2014) *Bacillus thuringiensis* subsp. *israelensis* and its dipteran-specific toxins. *Toxins* **6:** 1222–1243.

Ben-Dov, E., Nissan, G., Pelleg, N., Manasherob, R., Boussiba, S., and Zaritsky, A. (1999) Refined, circular restriction map of the *Bacillus thuringiensis* subsp *israelensis* plasmid carrying the mosquito larvicidal genes. *Plasmid* **42:** 186–191.

Benedict, M.Q., Levine, R.S., Hawley, W.A., and Lounibos, L.P. (2007) Spread of the tiger: Global risk of invasion by the mosquito *Aedes albopictus*. *Vector Borne Zoonotic Dis* **7:** 76–85.

Benelli, G., and Beier, J.C. (2017) Current vector control challenges in the fight against malaria. *Acta Trop* **174:** 91–96.

Ben-Yehuda, S., Rudner, D.Z., and Losick, R. (2003) RacA, a bacterial protein that anchors chromosomes to the cell poles. *Science* **299:** 532–536.

Berry, C., O'Neil, S., Ben-Dov, E., Jones, A.F., Murphy, L., Quail, M.A., *et al.* (2002) Complete sequence and organization of pBtoxis, the toxin-coding plasmid of *Bacillus thuringiensis* subsp *israelensis*. *Appl Environ Microbiol* **68:** 5082–5095.

Calogero, S., Albertini, A.M., Fogher, C., Marzari, R., and Galizzi, A. (1989) Expression of a cloned *Bacillus thuringiensis* delta-endotoxin gene in *Bacillus subtilis*. *Appl Environ Microbiol* **55:** 446–453.

Contreras, E., Masuyer, G., Qureshi, N., Chawla, S., Dhillon, H.S., Lee, H.L., *et al.* (2019) A neurotoxin that specifically targets *Anopheles mosquitoes*. *Nat Commun* **10:** 2869.

Crickmore, N., Bone, E.J., Williams, J.A., and Ellar, D.J. (1995) Contribution of the individual components of the delta-endotoxin crystal to the mosquitocidal activity of *Bacillus thuringiensis* subsp *israelensis*. *Fems Microbiol Lett* **131:** 249–254.

Diaz-Mendoza, M., Bideshi, D.K., Ortego, F., Farinós, G.P., and Federici, B.A. (2012) The 20-kDa chaperone-like protein of *Bacillus thuringiensis* ssp. *israelensis* enhances yield, crystal size and solubility of Cry3A. *Lett Appl Microbiol* **54:** 88–95.

Elleuch, J., Zghal, R.Z., Ben Fguira, I., Lacroix, M.N., Suissi, J., Chandre, F., *et al.* (2015) Effects of the P20 protein from *Bacillus thuringiensis israelensis* on insecticidal crystal protein Cry4Ba. *Int J Biol Macromol* **79:** 174–179.

Ferrari, E., Jamagin, A.S., and Schmidt, B.F. (1993) Commercial production of extracellular enzymes. In *Bacillus subtilis and Other Gram-Positive Bacteria.* Sonenshein, A.L., Hoch, J.A., and Losick, R. (eds). Washington, DC: American Society of Microbiology, pp. 917–937.

Gates, B. (2017) The deadliest animal in the world. *Gatesnotes* [WWW document]. URL https://www.gatesnotes.com/Health/Most-Lethal-Animal-Mosquito-Week.

Global Invasive Species Database (2019) *Species profile: Aedes albopictus* [WWW document]. URL http://www.iucngisd.org/gisd/species.php?sc=109.

Goldberg, L.J., and Margalit, J. (1977) A bacterial spore demonstrating rapid larvicidal activity against *Anopheles sergentii, Uranotaenia unguiculata, Culex univitattus, Aedes aegypti* and *Culex pipiens*. *Mosq News* **37:** 355–358.

Harwood, C.R. (1992) *Bacillus subtilis* and its relatives - molecular biological and industrial workhorses. *Trends Biotechnol* **10:** 247–256.

Henner, D.J., Ferrari, E., Perego, M., and Hoch, J.A. (1988) Location of the targets of the *hpr-97*, *sacU32(Hy)*, and *sacQ36(Hy)* mutations in upstream regions of the subtilisin promoter. *J Bacteriol* **170:** 296–300.

Kraemer, M.U., Sinka, M.E., Duda, K.A., Mylne, A.Q., Shearer, F.M., Barker, C.M., *et al.* (2015) The global distribution of the arbovirus vectors *Aedes aegypti* and *Ae. albopictus*. *eLife* **4:** e08347. https://doi.org/10.7554/eLife.08347.

Kunst, F., and Rapoport, G. (1995) Salt stress is an environmental signal affecting degradative enzyme-synthesis in *Bacillus subtilis*. *J Bacteriol* **177:** 2403–2407.

Kunst, F., Pascal, M., Lepesant-Kejzlarova, J., Lepesant, J.A., Billault, A., and Dedonder, R. (1974) Pleiotropic mutations affecting sporulation conditions and the syntheses of extracellular enzymes in *Bacillus subtilis* 168. *Biochimie* **56:** 1481–1489.

Leighton, T.J., and Doi, R.H. (1971) The stability of messenger ribonucleic acid during sporulation in *Bacillus subtilis*. *J Biol Chem* **246:** 3189–3195.

Mader, U., Antelmann, H., Buder, T., Dahl, M.K., Hecker, M., and Homuth, G. (2002) *Bacillus subtilis* functional genomics: genome-wide analysis of the DegS-DegU regulon by transcriptomics and proteomics. *Mol Genet Genomics* **268:** 455–467.

Manasherob, R., Itsko, M., Sela-Baranes, N., Ben-Dov, E., Berry, C., Cohen, S., and Zaritsky, A. (2006) Cyt1Ca from *Bacillus thuringiensis subsp. israelensis*: production in *Escherichia coli* and comparison of its biological activities with those of other Cyt-like proteins. *Microbiology* **152:** 2651–2659.

Moyes, C.L., Vontas, J., Martins, A.J., Ng, L.C., Koou, S.Y., Dusfour, I., *et al.* (2017) Contemporary status of insecticide resistance in the major *Aedes* vectors of arboviruses infecting humans. *PLoS Negl Trop Dis* **11:** e0005625.

Ogura, M., Matsuzawa, A., Yoshikawa, H., and Tanaka, T. (2004) *Bacillus subtilis* SalA (YbaL) negatively regulates expression of *scoC*, which encodes the repressor for the alkaline Exoprotease gene, *aprE*. *J Bacteriol* **186:** 3056–3064.

Otieno-Ayayo, Z.N., Zaritsky, A., Wirth, M.C., Manasherob, R., Khasdan, V., Cahan, R., and Ben-Dov, E. (2008) Variations in the mosquito larvicidal activities of toxins from *Bacillus thuringiensis* ssp *israelensis*. *Environ Microbiol* **10:** 2191–2199.

Park, H.-W., Hice, R.H., and Federici, B.A. (2016) Effect of Promoters and Plasmid Copy Number on Cyt1A Synthesis and Crystal Assembly in *Bacillus thuringiensis*. *Curr Microbiol* **72:** 33–40.

Perego, M. (1993) Integrational vectors for genetic manipulation in *Bacillus subtilis*. In *Bacillus subtilis and Other Gram-Positive Bacteria*. Sonenshein, A.L., Hoch, J.A., and Losick, R. (eds). Washington, DC: American Society of Microbiology, pp. 615–624.

Perez, C., Fernandez, L.E., Sun, J.G., Folch, J.L., Gill, S.S., Soberon, M., and Bravo, A. (2005) *Bacillus thuringiensis* subsp *israelensis* Cyt1Aa synergizes Cry11Aa toxin by functioning as a membrane-bound receptor. *Proc Natl Acad Sci USA* **102:** 18303–18308.

Perez, C., Munoz-Garay, C., Portugal, L.C., Sanchez, J., Gill, S.S., Soberon, M., and Bravo, A. (2007) *Bacillus thuringiensis* ssp *israelensis* Cyt1Aa enhances activity of Cry11Aa toxin by facilitating the formation of a pre-pore oligomeric structure. *Cell Microbiol* **9:** 2931–2937.

Poncet, S., Delecluse, A., Klier, A., and Rapoport, G. (1995) Evaluation of synergistic interactions among the CryIVA, CryIVB, and CryVD toxic components of *Bacillus thuringiensis* subsp *israelensis* crystals. *J Invertebr Pathol* **66:** 131–135.

Ramirez, J.L., Short, S.M., Bahia, A.C., Saraiva, R.G., Dong, Y., Kang, S., *et al.* (2014) Chromobacterium Csp_P reduces malaria and dengue infection in vector mosquitoes and has entomopathogenic and *in vitro* anti-pathogen activities. *PLoS Pathog* **10:** e1004398.

Sakano, Y., Park, H.W., Bideshi, D.K., Ge, B., and Federici, B.A. (2017) Contributions of 5'-UTR and 3'-UTR cis elements to Cyt1Aa synthesis in *Bacillus thuringiensis subsp. israelensis*. *J Invertebr Pathol.* **149:** 66–75.

Sazhenskiy, V., Zaritsky, A., and Itsko, M. (2010) Expression in *Escherichia coli* of the Native *cyt1Aa* from *Bacillus thuringiensis* subsp *israelensis*. *Appl Environ Microbiol* **76:** 3409–3411.

Schallmey, M., Singh, A., and Ward, O.P. (2004) Developments in the use of *Bacillus* species for industrial production. *Can J Microbiol* **50:** 1–17.

Schneider, C.A., Rasband, W.S., and Eliceiri, K.W. (2012) NIH Image to ImageJ: 25 years of image analysis. *Nat Methods* **9:** 671–675.

Shao, Z., Liu, Z., and Yu, Z. (2001) Effects of the 20-kilodalton helper protein on Cry1Ac production and spore formation in *Bacillus thuringiensis*. *Appl Environ Microbiol* **67:** 5362–5369.

Soberon, M., Lopez-Diaz, J.A., and Bravo, A. (2013) Cyt toxins produced by *Bacillus thuringiensis*: A protein fold conserved in several pathogenic microorganisms. *Peptides* **41:** 87–93.

Tang, M., Bideshi, D.K., Park, H.W., and Federici, B.A. (2006) Minireplicon from pBtoxis of *Bacillus thuringiensis subsp. israelensis*. *Appl Environ Microbiol* **72:** 6948–6954.

Valtierra-de-Luis, D., Villanueva, M., Lai, L., Williams, T., and Caballero, P. (2020) Potential of Cry10Aa and Cyt2Ba, two minority δ-endotoxins produced by *Bacillus thuringiensis ser. israelensis*, for the control of *Aedes aegypti* larvae. *Toxins* **12:** E355.

Visick, J.E., and Whiteley, H.R. (1991) Effect of a 20-kilodalton protein from *Bacillus thuringiensis* subsp *israelensis* on production of the CytA protein by *Escherichia coli*. *J Bacteriol* **173:** 1748–1756.

Ward, E.S., Ridley, A.R., Ellar, D.J., and Todd, J.A. (1986) *Bacillus thuringiensis* var *israelensis* delta-endotoxin - Cloning and expression of the toxin in sporogenic and asporogenic strains of *Bacillus subtilis*. *J Mol Biol* **191:** 13–22.

Westers, L., Westers, H., and Quax, W.J. (2004) *Bacillus subtilis* as cell factory for pharmaceutical proteins: a biotechnological approach to optimize the host organism. *Biochim Biophys Acta* **1694:** 299–310.

Wu, D., and Chang, F.N. (1985) Synergism in mosquitocidal activity of 26-kDa and 65 kDa proteins from *Bacillus*

thuringiensis subsp *israelensis* crystal. *FEBS Lett* **190:** 232–236.

Wu, D., and Federici, B.A. (1993) A 20-kilodalton protein preserves cell viability and promotes CytA crystal-formation during sporulation in *Bacillus thuringiensis*. *J Bacteriol* **175:** 5276–5280.

Wu, D., and Federici, B.A. (1995) Improved production of the insecticidal CryIVD protein in *Bacillus thuringiensis* using *cryIa(c)* promoters to express the gene for an associated 20-kDa protein. *Appl Microbiol Biotechnol* **42:** 697–702.

Xu, Y., Nagai, M., Bagdasarian, M., Smith, T.W., and Walker, E.D. (2001) Expression of the *p20* gene from *Bacillus thuringiensis* H-14 increases Cry11A toxin production and enhances mosquito-larvicidal activity in recombinant gram-negative bacteria. *Appl Environ Microbiol* **67:** 3010–3015.

Supporting information

Additional supporting information may be found online in the Supporting Information section at the end of the article.

Fig. S1 Expression of the *cry11Aa* Bti toxin gene in *B. subtilis* under the control of the *Phyperspank* promoter. A. Schematic representation of the *Phyperspank-cry11Aa* and *Phyperspank-cry11Aa-p20* constructs integrated by double cross-over in the *amyE* gene of *B. subtilis* PB1831. B. Growth of strains PB7222 (*amyE::spc*), PB7223 (*amyE::Phyperspank-cry11Aa*) and PB7226 (*amyE::Phyperspank-cry11Aa-p20*) in 2xSG sporulation medium. Heterologous protein expression was induced with 1 mM IPTG at T0, defined as the time point of transition from exponential to stationary phase of growth. C. SDS-PAGE 10% of cells-spores-parasporal bodies mixtures (15 µl of 200 mg/ml [wet weight/vol] suspension/well) of strains PB7222, PB7223 and PB7226 collected 20 hours after the beginning of the stationary phase (T20). Bti: 4Q1 *B. thuringiensis israelensis* spore-parasporal bodies mixtures collected at T72 as positive control. M: PageRuler Unstained Protein Ladder. Strain PB7226 displays a 15-fold lower Cry11Aa protein level relative to PB7223, as quantified by band intensity using ImageJ software. Band intensity was normalized with respect to the 70 kDa band of the protein marker.

Fig. S2 Expression of the *cry11Aa* toxin gene in *B. subtilis* under the control of the *PaprE* promoter. A.Schematic representation of the *PaprE-cry11Aa-p20* construct integrated by single cross-over in the regulatory region of the *aprE* gene in *B. subtilis* PB1831. B. Growth of PB7241 (*PaprE-cry11Aa-p20*) and PB7242 (*PaprE*) in 2xSG medium. Data are the average ± SD of two independent experiments. C. SDS-PAGE 10% of PB7241 cells-spore-parasporal bodies collected at different time points (4, 15, 20 24, 48, 72 hours) after the beginning of the stationary phase (a time point indicated as T0). Bti: Spore-parasporal bodies of *B. thuringiensis* israelensis 4Q1 collected at T72. Fifteen µl of cells-spores-parasporal bodies suspensions at the concentration of 200 mg/ml [wet weight/vol] were loaded in each well. M: PageRuler Unstained Protein Ladder.

Fig. S3 A. Growth of the *degU32(hy)* strains PB7241 (*PaprE-cry11Aa-p20*) and PB7247 (*amyE::Phyperspank-cry11Aa-p20*) in 2xSG medium. Data are the average ±SD of two independent experiments. B. SDS-PAGE 10% of cells-spores-parasporal bodies of strains PB7241, PB7247 and of the respective control strains PB7242 (*aprE::PaprE-kanR, degU32(hy)*) and PB7246 (*amyE::spc, degU32(hy)*) collected after 48 hours from the beginning of the stationary phase. The strains PB7246 and PB7247 were IPTG induced at T0. Intensity of the Cry11Aa band of the two strains was quantified using ImageJ software and normalized relative to the intensity of the 63 kDa band of the protein marker. Bti: 4Q1 spore-parasporal bodies collected at T48. M: Protein Marker VI (20-345) prestained (PanReac).

Fig. S4 SDS-PAGE 10% of the spore-parasporal body mixtures of the strains PB7222 (*amyE::spc*), PB7232 (*amyE::Phyperspank-cyt1Aa-p21*), PB7230 (pBS19-*Pcyt1Aa-p21*) and PB7229 (pBS19) collected after 20 hours from the beginning of the stationary phase. PB7222 and PB7232 strains were IPTG induced at T0. Bti 4Q1 spore-parasporal bodies collected at T72 was used as positive control; M: PageRuler Unstained Protein Ladder.

Fig. S5 TEM (7000x) of PB7230 (pBS19-*Pcyt1Aa-p21*) strain collected at 72 hours from the beginning of the stationary phase. Expression of Cyt1Aa causes death of *B. subtilis* cells.

Fig. S6 A. Growth of *B. subtilis* recombinant strains expressing Cyt2Ba. Strains PB7222 (*amyE::spc*), PB7225 (*amyE::Phyperspank-cyt2Ba*), PB7229 (pBS19) and PB7231 (pBS19-*Pcyt2Ba*) were grown in 2xSG medium. Data are the average ± SD of two independent experiments. B. SDS-PAGE 10% of the cells-spores-parasporal body mixtures of the strains PB7222 (*amyE::spc*), PB7225 (*amyE::Phyperspank-cyt2Ba*), PB7229 (pBS19) and PB7231 (pBS19-*Pcyt2Ba*). PB7222 and PB7225 were IPTG induced at T0. All the strains were collected 24 hours after the beginning of the stationary phase. Bti: 4Q1 spore-parasporal bodies collected at T72. M: PageRuler Unstained Protein Ladder. Intensity of the Cyt2Ba band of strains PB7231 and PB7225 was quantified using ImageJ software and normalized relative to the intensity of the 25 kDa band of the protein marker.

Fig. S7 Growth of *B. subtilis* recombinant strains expressing Cyt2Ba (PB7231, PB7266 + IPTG), Cry11Aa (PB7233, PB7265) or both toxins (PB7240 and PB7265 + IPTG) compared to control strains PB7229 and PB7266. All strains were grown in 2xSG medium. Data from a single representative experiments are reported.

Table S1. Primers used for cloning. Restriction sites are shown in capital letters.

Table S2. Plasmids used in this work.

Table S3. Titer of cells and spores (cfu ml^{-1}) in spore-parasporal bodies mixtures resuspended at the concentration of 100 mg l^{-1}. Results refer to the following strains: PB7229 (negative control, pBS19) and PB7230 (pBS19-*Pcyt1Aa-p21*), collected at 24, 48, 72 h after the beginning of the stationary phase (T24, T48, T72). Results are means of three replicas ± SD.

Supplementary Information. Genetic techniques employed in the study and detailed description of the preparation of the *B. subtilis* strains expressing δ-endotoxins.

JBC ARTICLE

The iron-regulated surface determinant B (IsdB) protein from *Staphylococcus aureus* acts as a receptor for the host protein vitronectin

Received for publication, March 18, 2020, and in revised form, June 1, 2020 Published, Papers in Press, June 4, 2020, DOI 10.1074/jbc.RA120.013510

Giampiero Pietrocola[1,*], Angelica Pellegrini[1], Mariangela J. Alfeo[1], Loredana Marchese[1], Timothy J. Foster[2], and Pietro Speziale[1,*]

From the [1]Department of Molecular Medicine, Unit of Biochemistry, University of Pavia, Pavia, Italy, [2]Department of Microbiology, Trinity College Dublin, Dublin, Ireland

Edited by Chris Whitfield

Staphylococcus aureus **is an important bacterial pathogen that can cause a wide spectrum of diseases in humans and other animals. *S. aureus* expresses a variety of virulence factors that promote infection with this pathogen. These include cell-surface proteins that mediate adherence of the bacterial cells to host extracellular matrix components, such as fibronectin and fibrinogen. Here, using immunoblotting, ELISA, and surface plasmon resonance analysis, we report that the iron-regulated surface determinant B (IsdB) protein, besides being involved in heme transport, plays a novel role as a receptor for the plasma and extracellular matrix protein vitronectin (Vn). Vn-binding activity was expressed by staphylococcal strains grown under iron starvation conditions when Isd proteins are expressed. Recombinant IsdB bound Vn dose dependently and specifically. Both near-iron transporter motifs $NEAT_1$ and $NEAT_2$ of IsdB individually bound Vn in a saturable manner, with K_D values in the range of 16–18 nM. Binding of Vn to IsdB was specifically blocked by heparin and reduced at high ionic strength. Furthermore, IsdB-expressing bacterial cells bound significantly higher amounts of Vn from human plasma than did an *isdB* mutant. Adherence to and invasion of epithelial and endothelial cells by IsdB-expressing *S. aureus* cells was promoted by Vn, and an $\alpha_v\beta_3$ integrin-blocking mAb or cilengitide inhibited adherence and invasion by staphylococci, suggesting that Vn acts as a bridge between IsdB and host $\alpha_v\beta_3$ integrin.**

Staphylococcus aureus causes a wide range of opportunistic infections that range from superficial skin infections to life-threatening diseases, including endocarditis, pneumonia, and septicemia (1). Adherence of bacteria to host matrix components is the initial critical event in the pathogenesis of most infections. The extracellular matrix (ECM) essentially consists of macromolecules, such as collagens, proteoglycans, and glycoproteins, that serve as a substrate for the adhesion and migration of tissue cells. These processes involve integrins, a family of heterodimeric cell surface receptors that recognize specific ECM proteins (2, 3).

Bacteria, including *S. aureus*, also utilize the ECM as substrata for their adhesion through a family of cell wall-anchored (CWA) adhesins called MSCRAMMs (microbial surface component recognizing adhesive matrix molecules) that specifically recognize host matrix components (4, 5).

Vitronectin (Vn) is a glycoprotein that is synthesized in the liver and secreted into plasma (6) and is also an important component of the ECM (7). Vn is found at a high concentration in plasma (200–700 μg/ml) (8, 9) and is also present in different human tissues (10). The N-terminal portion of mature Vn (43 aa residues) consists of a somatomedin B (SMB) domain followed by the classical integrin-binding motif, Arg-Gly-Asp (RGD). Members of the integrin family that engage in Vn binding include integrin $\alpha3\beta1$, $\alpha_v\beta_3$, $\alpha_v\beta_5$, and $\alpha_5\beta_1$ (11). The next domain comprises four hemopexin-like domains with putative heme-binding motifs. In addition, Vn has three heparin-binding domains (HBD) spanning residues Vn82–137 (HBD-1), Vn175–219 (HBD-2), and Vn348–361 (HBD-3) (12–14) (Fig. S1*A*). Vn is present in the organism in different conformational states: as the native, folded monomer (65–75 kDa, the 65-kDa form being derived from the proteolytic cleavage in the C-terminal region of the protein) in plasma/serum and as a multimeric unfolded form in the ECM (6, 15, 16). Conformational change from the monomeric to the activated, multimeric state is promoted by exposure of Vn to agents, such as urea, or binding to physiological ligands, such as the thrombin-antithrombin complex and the membrane attack complex. Vn conformational activation reveals a number of cryptic sites, including the full exposure of the heparin-binding site at the C-terminal domain of the protein (17, 18) and cell-binding motif (RGD) (19, 20). Vn binds the terminal complement C5b-7 complex. It occupies the metastable membrane binding site and thereby inhibits membrane insertion of the complex (21). It also binds C9 and directly inhibits C9 polymerization (21, 22).

Several bacterial species interact with host cell-bound multimeric Vn, facilitating adherence to epithelial cells and artificial surfaces (23). Simultaneous interaction of Vn with an integrin and bacterial surface proteins results in the formation of a bridge between bacteria and host cells. This leads to internalization of bacteria, as exemplified by *Streptococcus pneumoniae* (24) or *Pseudomonas aeruginosa* (25), resulting in downstream signaling events (24).

Staphylococci contain several Vn-binding proteins, including the autolysins AtlE and Aae from *S. epidermidis* and the homologous proteins AtlA and Aaa from *S. aureus* (26, 27). Also,

This article contains supporting information.

* For correspondence: Giampiero Pietrocola, giampiero.pietrocola@unipv.it; Pietro Speziale, pspeziale@unipv.it.

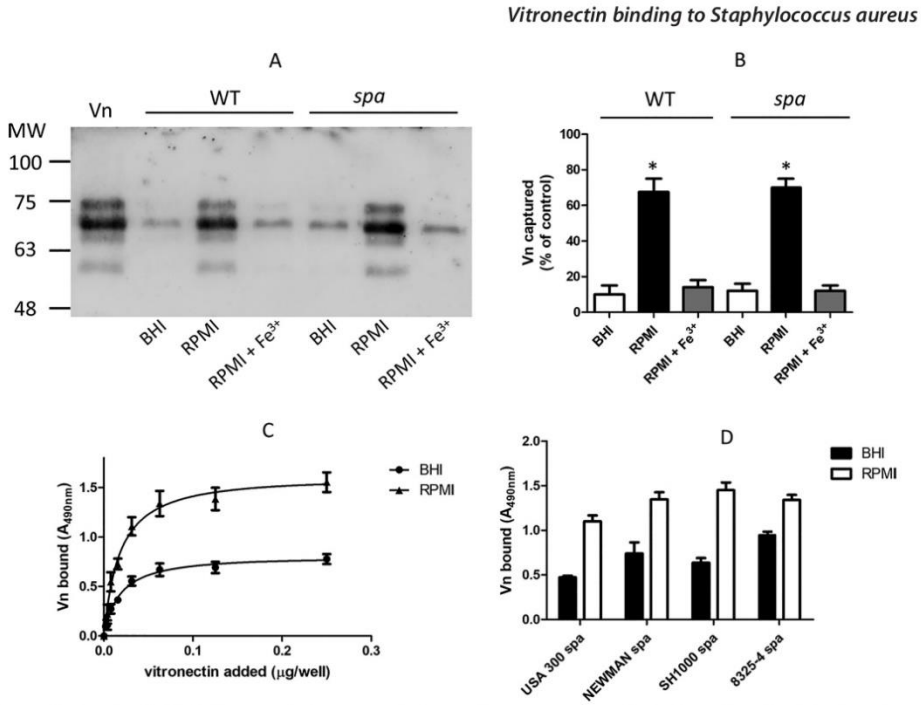

Figure 1. Binding of purified Vn by *S. aureus* cells. *A*, *S. aureus* strain SH1000 and its *spa* mutant grown either in BHI or RPMI medium in the absence/presence of 1 mM $FeCl_3$ were incubated with purified Vn. Bacterium-bound proteins were released by extraction buffer and separated by SDS-PAGE under reducing conditions and analyzed by far Western blotting. The membrane was probed with sheep anti-human Vn, followed by HRP-conjugated rabbit anti-sheep IgG. Molecular masses of standard proteins are indicated on the left. *B*, densitometric analysis of Vn bound to *S. aureus* SH1000 and the *spa* mutant as reported in *panel A*. The band intensity was quantified relative to a sample of purified human Vn (8 μg). The reported data are the mean values ± S.D. from three independent experiments. *C*, binding of increasing concentrations of Vn to immobilized *S. aureus* SH1000 *spa* cells grown in RPMI or BHI medium is shown. Bound Vn was detected as described above. The data points are the means ± S.D. from three independent experiments, each performed in triplicate. A statistically significant difference is indicated (Student's *t* test; *, $p < 0.05$). *D*, binding of Vn to strains of *S. aureus spa*. Microtiter wells coated with *S. aureus spa* strains grown in RPMI or BHI were incubated with Vn. Bound Vn was detected by addition of sheep anti-Vn polyclonal IgG and rabbit HRP-conjugated anti-sheep IgG.

the multifunctional autolysin AtlL from *Staphylococcus lugdunensis* interacts with Vn (28).

Atl autolysins have a similar modular organization (signal peptide, propeptide, amidase activity, three major repeats, R1 to R3, and glucosaminidase activity), share a high degree of sequence similarity, and are functionally interchangeable (29). R1-R2 repeats are critical for autolysin binding to Vn (30). Moreover, the major autolysin, Atl, mediates *S. aureus* internalization via direct interaction with host heat shock protein Hsc70 (31).

Studies on *S. aureus* adhesion to and invasion of host cells have been performed with bacteria grown in rich medium containing iron (4). In contrast, *in vivo S. aureus* has restricted access to iron, and the lack of available iron leads to the upregulation of a number of genes, among which are those that encode surface determinant (Isd) proteins (32). The Isd system contains nine proteins whose expression is coordinately upregulated under iron-depleted conditions (33–36). The primary role of Isd proteins is to capture heme from hemoglobin (Hb) and transport it into the cell (32). These include IsdA, IsdB, IsdC, and IsdH, which are anchored to cell wall peptidoglycan by sortases and are exposed on the cell surface (37, 38). Each protein contains a structurally conserved near iron transporter (NEAT) motif(s) that binds Hb and heme. IsdA and IsdC contain one NEAT domain each, whereas IsdB and IsdH contain two and three NEAT domains, respectively. The NEAT domains adopt a beta sandwich fold that consists of two five-stranded antiparallel beta sheets (39).

Fig. S1*B* shows the organization and primary sequence comparisons between the seven known NEAT domains in *S. aureus*.

Sequence homologs of this class of proteins are found in a number of important human pathogens, such as *S. lugdunensis*, (40–42), *Listeria monocytogenes* (43), *Bacillus anthracis* (44), and *Streptococcus pyogenes* (45).

IsdA, IsdB, and IsdH of *S. aureus* are known to have other biological functions. IsdA interacts with an array of host proteins (36) and confers resistance to the innate defenses of the human

skin (46). IsdH plays a role in the evasion of phagocytosis as a result of accelerated degradation of C3b (47). IsdB binds to platelets via direct interaction with the platelet integrin GPIIb/IIIa and also promotes *S. aureus* adherence to and internalization by nonphagocytic human cells (48). The objective of the current study was to investigate in more detail the binding of Vn to *S. aureus* cells. We show that cells expressing IsdB specifically bind to Vn and analyze the nature and the biological consequences of this interaction.

Results

Vn binding by S. aureus is promoted by growth under iron-restricted conditions

In preliminary experiments, we tested the capture of Vn by *S. aureus* strain SH1000 grown to stationary phase in rich brain heart infusion (BHI) or iron-restricted Roswell Park Memorial Institute 1640 (RPMI) medium with or without $FeCl_3$. Bacteria grown in RPMI showed a higher ability to capture Vn than those grown in iron-rich medium or in RPMI supplemented with $FeCl_3$, suggesting that binding of strain SH1000 depends on proteins induced by iron starvation. Interestingly, a protein A-deficient (*spa*) mutant showed a Vn-binding profile overlapping that of the WT strain, suggesting that Vn binding to the bacterial surface is not related to protein A expression (Fig. 1, *A* and *B*).

To further analyze the interaction of Vn with *S. aureus*, SH1000 *spa* organisms grown in BHI and RPMI medium were immobilized onto microtiter wells and allowed to interact with increasing amounts of soluble Vn (Fig. 1*C*). Under both conditions, Vn bound to bacteria in a dose-dependent and saturable fashion. RPMI-grown bacteria captured significantly larger amounts of Vn, suggesting that *S. aureus* cells express a larger number of receptors on their surface or that novel receptors were induced when grown in iron starvation. To compare the Vn binding potential of different *S. aureus* strains, *spa* mutants of the *S. aureus* laboratory strains Newman, SH1000, and 8325-4 and the clinical strain USA300 grown in BHI or RPMI medium to the stationary phase were immobilized in microtiter wells and tested for binding to soluble Vn. All the strains grown in RPMI medium showed a higher ability to bind Vn when grown under iron starvation conditions than in iron-rich medium (Fig. 1*D*).

Identification of a Vn-binding protein

To identify the surface component(s) involved in Vn binding, SH1000 *spa* cells grown in BHI or RPMI medium were digested with lysostaphin and the released material subjected to SDS-PAGE under reducing conditions and far Western blotting. The nitrocellulose membrane was incubated with Vn, and the bound ligand was detected with anti-Vn IgG. A strong signal corresponding to a molecule of 75 kDa was noted in protein from cells grown in RPMI medium, whereas no significant signal was detected in material released from cells grown in BHI medium (Fig. 2, *lanes 1 and 2*).

To further investigate this issue, proteins were separated by SDS-PAGE under reducing conditions and visualized by staining with Coomassie brilliant blue (Fig. 2, *lane 3*). A candidate protein of 75 kDa was excised from the stained gel, digested with trypsin, and analyzed by MS. The database search unequivocally identified IsdB as the potential Vn-binding protein of *S. aureus* SH1000 (Fig. S2*A*).

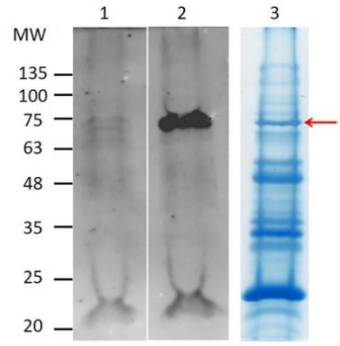

1: *S. aureus* SH1000 *spa* grown in BHI
2: *S. aureus* SH1000 *spa* grown in RPMI
3: S. aureus SH1000 spa grown in RPMI

Figure 2. Far Western blotting of lysostaphin-released material from cells of SH1000 *spa*. Cells of SH1000 *spa* grown in BHI (*lane 1*) and RPMI (*lane 2*) were digested with lysostaphin and the released material subjected to far Western blotting. The nitrocellulose membrane was probed with Vn, followed by sheep anti-Vn and HRP-conjugated rabbit anti-sheep IgG. Molecular mass standards are indicated on the *left*. The lysostaphin-released material from cells of SH1000 *spa* grown in RPMI was also subjected to SDS-PAGE and stained with Coomassie blue (*lane 3*). The band corresponding to the 75-kDa bacterial component is marked by an *arrow*.

isdB gene expression is growth-phase dependent

Since *S. aureus* SH1000 *spa* cells grown to stationary phase in BHI medium bound Vn significantly less than when grown in RPMI medium (Fig. 1), we analyzed the expression of the *isdB* gene in cells grown both in BHI or RPMI medium to mid-exponential and stationary phases of growth by quantitative RT-PCR (qRT-PCR). Expression of *isdB* in cells grown to stationary phase in RPMI medium was about 5-fold higher than that in cells grown in BHI medium or cells grown to mid-exponential phase in either medium (Fig. S2*B*).

This finding was validated by comparing the expression levels of the IsdB protein by bacteria grown to mid-exponential and stationary phases in BHI and RPMI media by Western immunoblotting. While IsdB was virtually undetectable in material released from bacteria grown to both the mid-exponential and stationary phases in BHI medium, the protein was abundant in material released from bacteria grown to the stationary phase in RPMI medium (Fig. S2*C*).

Ectopic expression of IsdB by L. lactis and binding to Vn

To study IsdB in isolation from other *S. aureus* CWA proteins, a strain of *L. lactis* expressing IsdB from a gene cloned into the plasmid vector pNZ8037 was used. To validate the expression of IsdB from the bacterium, *L. lactis* pNZ8037::*isdB*

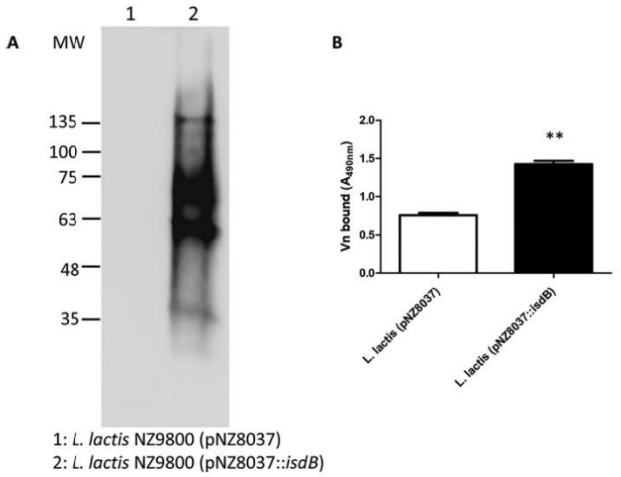

Figure 3. Interaction of *L. lactis*-expressing IsdB with Vn. *A*, cell wall proteins were released by mutanolysin/lysozyme treatment from *L. lactis* expressing IsdB (pNZ8037::*isdB*) and control cells carrying the empty vector. The protein components in the mixture were separated by SDS-PAGE and subjected to far Western blotting. The membrane was probed with Vn, followed by sheep anti-Vn and HRP-conjugated rabbit anti-sheep IgG. The figure is representative of three independent experiments. Molecular mass standards are indicated on the *left*. *B*, interaction of Vn with *L. lactis*-expressing IsdB and cells carrying the empty vector assessed by ELISA. Bacteria were immobilized in microtiter plates and incubated with Vn, followed by addition to the wells of sheep anti-Vn polyclonal IgG and HRP-conjugated rabbit anti-sheep antibody. The data points are the means ± S.D. from three independent experiments, each performed in triplicate. Statistically significant differences are indicated (Student's *t* test; **, $p < 0.01$).

and the isogenic strain carrying the empty vector were treated with mutanolysin and lysozyme, and the released material subjected to far Western blotting. A Vn binding protein of 75 kDa was detected (along with an approximately 60-kDa protein, which may be a breakdown product), whereas the material released from *L. lactis* (pNZ8037) lacked reactivity (Fig. 3*A*). Moreover, the lactococci were immobilized onto microtiter wells, and binding of soluble Vn was examined by ELISA. Significantly higher binding of Vn to *L. lactis* (pNZ8037::*isdB*) was observed compared to that of *L. lactis* harboring the empty vector (Fig. 3*B*).

Specificity of Vn binding to IsdB

To investigate the specificity of Vn binding to IsdB, recombinant IsdB $NEAT_1$-$NEAT_2$ protein was immobilized onto microtiter wells and tested for binding to extracellular matrix proteins, including fibrinogen, fibronectin, collagen, and Vn. Only Vn bound to the surface-coated IsdB, whereas no binding of the other proteins was observed (Fig. 4*A*).

Localization of the binding sites within IsdB

To localize the Vn-binding region within the IsdB protein, the $NEAT_1$ and $NEAT_2$ domains were expressed in *E. coli* and employed in binding studies. First, the binding of soluble Vn to immobilized recombinant $NEAT_1$ and $NEAT_2$ was determined by ELISA. Vn bound dose dependently and saturably to both $NEAT_1$ and $NEAT_2$ fragments and with a binding profile

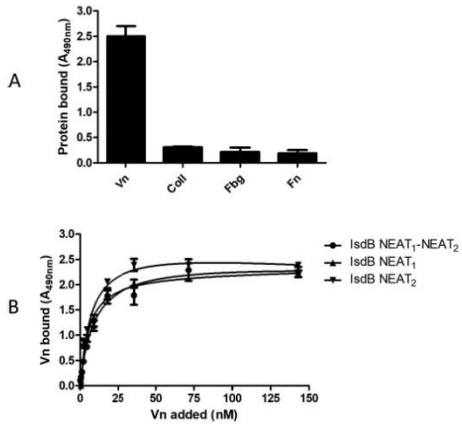

Figure 4. Characterization of Vn-binding activity of IsdB. *A*, specificity of recombinant IsdB interaction with extracellular matrix proteins. Microtiter wells were coated with IsdB NEAT1-NEAT2 and then incubated with the indicated extracellular matrix proteins Vn, collagen type I, fibrinogen, and fibronectin. Each bound protein was detected by the addition of ligand-specific polyclonal antibody and HRP-conjugated secondary IgG. The data points are the means ± S.D. from three independent experiments, each performed in triplicate. *B*, Vn binding to IsdB $NEAT_1$-$NEAT_2$ and its derivatives, $NEAT_1$ and $NEAT_2$. Recombinant IsdB $NEAT_1$-$NEAT_2$ and its derivatives, $NEAT_1$ and $NEAT_2$, were immobilized onto microtiter wells and incubated with increasing amounts of Vn. Bound Vn was detected by the addition of sheep anti-Vn polyclonal IgG and HRP-conjugated rabbit anti-sheep. The data points are the means ± S.D. from three independent experiments, each performed in triplicate.

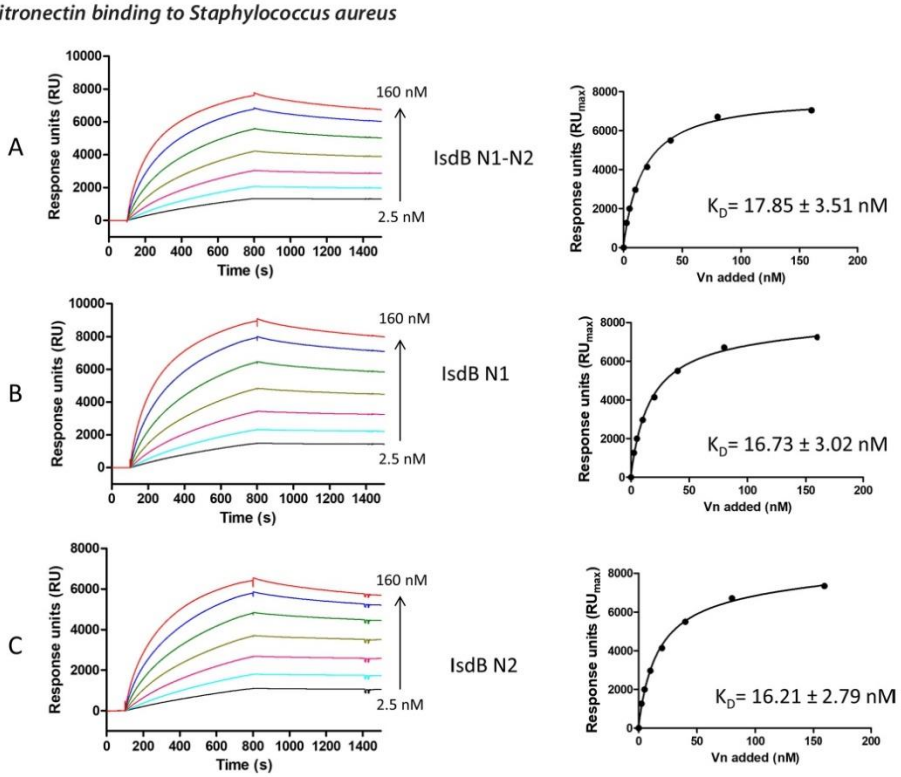

Figure 5. Analysis of the interaction between IsdB $NEAT_1$-$NEAT_2$ and its derivatives, $NEAT_1$ and $NEAT_2$, with Vn by SPR. Twofold linear dilution series (2.5–160 nM) of Vn were injected over the IsdB $NEAT_1$-$NEAT_2$ or its derivatives, $NEAT_1$ and $NEAT_2$, immobilized on the surface of a CM5 sensor chip. The sensorgrams obtained were normalized *versus* the response obtained when Vn was flowed over uncoated chips. The affinity was calculated from curve fitting to a plot of the response unit values at the steady state (RU_{max}) against increasing concentrations of Vn (*left*). Shown is one representative of three experiments.

resembling that exhibited by intact full-length IsdB $NEAT_1$-$NEAT_2$ (Fig. 4*B*).

IsdB $NEAT_1$-$NEAT_2$ and single $NEAT_1$ and $NEAT_2$ domains bind to Vn with high affinity

Surface plasmon resonance (SPR) experiments were performed to compare the binding of Vn to those of immobilized IsdB $NEAT_1$-$NEAT_2$ and single $NEAT_1$ and $NEAT_2$ fragments. Vn displayed a high binding activity, as indicated by the high response values and the slow dissociation of the IsdB-Vn complexes upon removal of the ligand. The best fit of the data points was obtained with the Langmuir isotherm equation describing a one-site binding model. From this analysis, we obtained dissociation constant (K_D) values of 17.85 ± 3.51 nM, 16.73 ± 3.02 nM, and 16.21 ± 2.79 nM for IsdB $NEAT_1$-$NEAT_2$/Vn, $NEAT_1$/Vn, and $NEAT_2$/Vn, respectively (Fig. 5). All these findings show that full-length IsdB contains two separate binding sites that interact with nearly identical high affinities for Vn.

Binding of Vn to IsdB is blocked by heparin and dependent on ionic strength

To investigate whether IsdB competes with glycosaminoglycans for binding to Vn, the effect of heparin, heparan sulfate, and chondroitin sulfate on Vn binding to immobilized IsdB $NEAT_1$-$NEAT_2$ was studied. In contrast to heparan sulfate and chondroitin sulfate, heparin dose dependently inhibited the IsdB-Vn interaction, suggesting that IsdB interacts with the heparin-binding domain(s) of the protein (Fig. S3*A*). To determine if ionic forces play a role in the interaction of IsdB with Vn, the effect of sodium chloride on Vn binding to IsdB was assessed. Addition of NaCl significantly reduced binding of Vn to immobilized IsdB, and at a concentration of 500 mM, NaCl reduced Vn binding to IsdB by almost 80% (Fig. S3*B*).

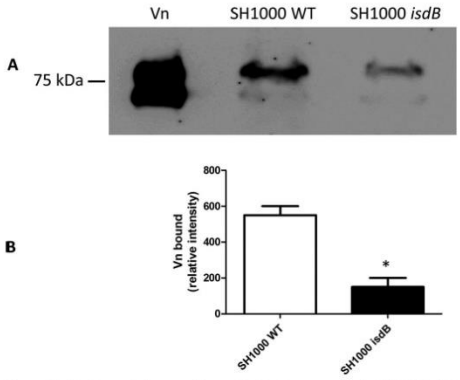

Figure 6. Capture of plasma vitronectin by *S. aureus* strain SH1000. *A*, *S. aureus* SH1000 and its isogenic *isdB* mutant were mixed with 1 ml of human plasma for 60 min. Proteins bound to the cell surface were released by extraction buffer, separated by SDS-PAGE under nonreducing conditions, and analyzed by Western blotting. The membrane was probed with sheep anti-Vn polyclonal IgG and HRP-conjugated rabbit anti-sheep and developed with the ECL Western blotting detection kit. The pure human Vn sample is shown on the *left*. *B*, densitometric analysis of Vn bound to and released from *S. aureus* SH1000 and its isogenic *isdB* mutant. The reported data are the mean values ± S.D. from three independent experiments. Statistically significant differences are indicated (Student's *t* test; *, $p < 0.05$).

S. aureus IsdB captures Vn from plasma

To investigate if *S. aureus* cells expressing IsdB can recruit Vn from plasma, bacteria were incubated with human plasma and the amount of Vn captured was quantified by Western blotting and densitometry. *S. aureus* expressing IsdB captured approximately 4-fold more Vn than the *isdB* mutant. Thus, it can be concluded that IsdB expression is important for *S. aureus* to capture Vn from human plasma. However, it must be pointed out that a substantial amount of Vn bound to the *isdB* mutant, indicating that other Vn receptors are operational on the surface of *S. aureus* cells (Fig. 6).

Vn mediates adherence to and invasion of HeLa and HUVEC monolayers

To investigate the role of the Vn-binding activity of IsdB in promoting adherence of *S. aureus* SH1000 to host cells, bacteria were grown to the stationary phase in BHI or RPMI medium and then tested for attachment to HeLa and human umbilical vein endothelial cell (HUVEC) monolayers (Fig. 7, *A* and *C*) in the absence of Vn. No adherence of the strain grown under either condition was observed. Conversely, the addition of exogenous human Vn to the cell monolayers promoted a high level of adhesion of the RPMI-grown but not the BHI-grown bacteria. Almost complete inhibition of adhesion was observed when the assays were performed in the presence of an integrin $\alpha_v\beta_3$ -binding mAb or the specific $\alpha_v\beta_3$ inhibitor cilengitide, suggesting the involvement of integrin $\alpha_v\beta_3$. To examine whether IsdB/Vn is also involved in the staphylococcal invasion of HeLa cells or HUVECs (Fig. 7, *B* and *D*), BHI- and RPMI-grown bacteria were incubated with cell monolayers in the presence or absence of Vn and then tested for internalization. We found a moderate level of invasion only by RPMI-grown bacteria in the presence of Vn, while no internalization was observed with BHI-grown bacteria even in the presence of Vn. In confirmation of this, neither adhesion nor invasion was observed with the *isdB* mutant (Fig. 7). Together, these data suggest that for promoting efficient adhesion and gaining entry of bacteria into HeLa cells or HUVECs, *S. aureus* can use Vn as a molecular bridge between surface-expressed IsdB and the $\alpha_v\beta_3$ integrin.

Staphylococcal adhesion to HeLa and HUVEC cell lines was similar, while bacterial invasion of HUVECs was 50-fold more effective than that of the HeLa cell line. Variation in expression levels of the $\alpha_v\beta_3$ integrin on the two cell types may contribute to the difference in pathogen invasiveness.

Notably, a persistent, low level of bacterial invasion was observed when bacteria grown in RPMI were incubated with HeLa and HUVECs in the absence of Vn, suggesting that other internalization mechanisms are operational.

Discussion

In our search for *S. aureus* MSCRAMMs with Vn-binding activity, here we show that *S. aureus* IsdB interacts with Vn. As previously demonstrated, IsdB is strongly upregulated under conditions of iron restriction and, in accordance with this property, Vn binding was strictly related to the expression of IsdB by bacterial strains. Bacteria bind Vn when grown under iron starvation conditions and not in an iron-rich medium. Moreover, binding of Vn by bacteria was mostly expressed by cells in the stationary phase of growth.

To characterize this binding to IsdB, we purified and used multimeric Vn, the conformational form of the protein found in the ECM. Notably, we found that bacteria expressing IsdB also captured Vn from plasma, where the monomeric form of the protein prevails. Thus, it seems that IsdB binds to both conformational states of Vn. This is reminiscent of the situation observed with *Moraxella catarrhalis* and *Haemophilus influenzae*, which interact with both isoforms of Vn (23).

The interaction of IsdB with Vn was confirmed using several approaches, including far Western blotting, ELISA, and SPR. Binding of IsdB to Vn was specific and saturable and exhibited a K_D in the nanomolar range, which is comparable to that recorded for high-affinity CWA protein–host protein interactions (49–52).

To narrow down the Vn binding site(s) of IsdB, the $NEAT_1$ and $NEAT_2$ domains were recombinantly produced and tested for their ability to bind the ligand. The individual modules interacted with an affinity for Vn comparable to that of the full-length IsdB, suggesting that each module represents the minimal motif required for efficient interaction of IsdB with Vn and that IsdB potentially can bind two Vn molecules. The finding that both domains interact with Vn is particularly intriguing, in view of the fact that the two NEAT domains of IsdB have very low sequence identity (about 12%) and that they are functionally different. In fact, the $NEAT_1$ domain is involved in Hb binding while $NEAT_2$ plays a role in heme extraction from α and β chains of Hb (53). In view of the discovery that even NEAT motifs with low sequence identity show Vn-binding

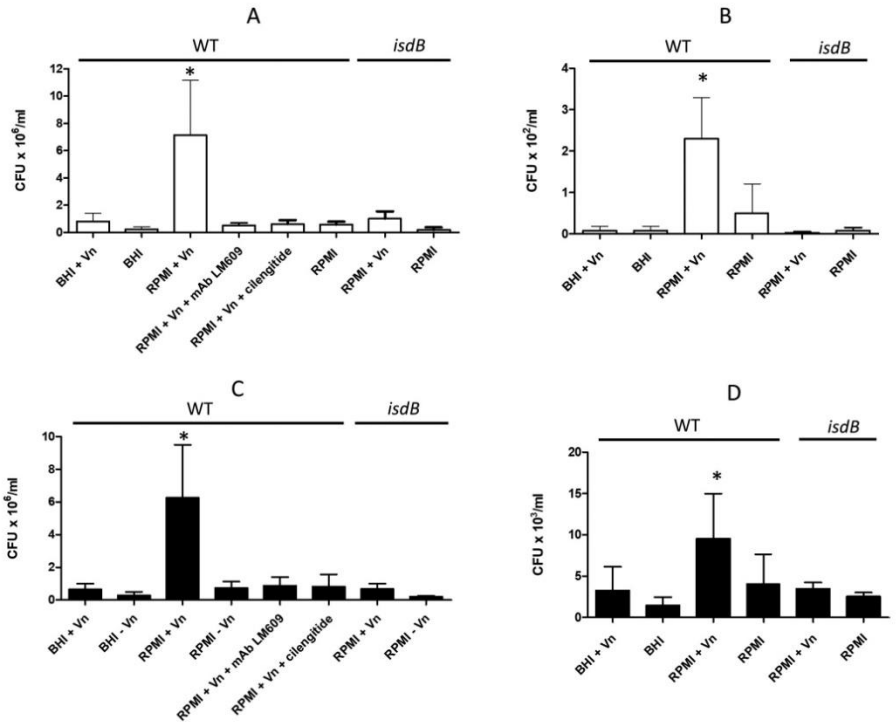

Figure 7. Adhesion and internalization of *S. aureus* cells. Bacterial strains were grown overnight in BHI or RPMI medium, added to HeLa (*A* and *B*) or HUVEC (*C* and *D*) cell monolayers, and tested for adhesion (*A* and *C*) or internalization (*B* and *D*). The experiments were performed in DMEM for 2 h at 37 °C. The effects of $\alpha_v\beta_3$ mAb LM609 and cilengitide on bacterial adherence are also reported. The inocula and adherent and internalized bacteria were quantified by viable counting. Error bars show S.D. of the means from three independent determinations performed in triplicate with similar results (Student's *t* test; *, $p < 0.05$).

activity, other Isd proteins could exhibit Vn-binding activity. The presence of additional Vn receptors on the staphylococcal surface is consistent with the finding that the *isdB* mutant is capable of capturing Vn from human plasma and by the observation that other non-Isd surface proteins of *S. aureus*, such as Atl, have Vn-binding activity (26, 27). In apparent contradiction with these observations, IsdB seems to be the major Vn receptor when material released from bacterial cells was tested by far Western blotting (Fig. 2). This could be due to a higher level of expression of IsdB and/or to a higher affinity of IsdB for Vn compared with that of other potential Vn binders.

In this context, it will be worth investigating the activity of IsdB from *Staphylococcus lugdunensis*, which contains $NEAT_1$ and $NEAT_2$, 60 and 56% identical to *S. aureus* IsdB $NEAT_1$ and $NEAT_2$ domains, respectively (40), and the Vn-binding by other bacterial species expressing Isd proteins, such as *Listeria monocytogenes* and *Bacillus anthracis*.

Increasing the ionic strength had a dramatic effect on Vn binding to IsdB, indicating that Vn/IsdB complex formation is mainly driven by electrostatic interactions. Furthermore, the negatively charged heparin efficiently blocked the IsdB–Vn interaction, suggesting that the IsdB-binding region is located in the heparin-binding domain(s) of Vn. The inhibitory effect of heparin but not of heparan sulfate or chondroitin sulfate is in line with heparin possessing the highest negative charge density of any known biological macromolecule. In fact, although heparin and heparan sulfate are built up of linear chains of repeating disaccharide units, the average heparin disaccharide contains approximately 2.7 sulfate groups, whereas heparan sulfate contains $\geq$1 sulfate group per disaccharide (54).

Related to the finding that electrostatic bonds could be involved in Vn–IsdB interaction is the question of whether Vn and heme compete for the same binding site or have a different location on IsdB. The indication that IsdB uses only a hydrophobic pocket in the $NEAT_2$ domain to bind and extract heme (38) and our observation that Vn binds to both $NEAT_1$ and $NEAT_2$ domains suggest that the binding sites in IsdB for heme and Vn are separate.

Binding of *S. aureus* to Vn contributes to bacterial adhesion to mammalian cells, as demonstrated by attachment of IsdB-expressing staphylococci to HeLa and HUVEC monolayers. The inhibition of the process by an $\alpha_v\beta_3$ mAb and cilengitide strongly suggests that adhesion involves the formation of a Vn bridged complex between IsdB and the integrin. Vn also mediated the internalization of staphylococci into epithelial and endothelial cells. However, due to the modest contribution of Vn to the process, it is possible that Vn-dependent invasion could act as a backup mechanism that becomes operational in the context of tissues where Fn is poorly expressed or under conditions (specific growth medium and/or phase of growth) where bacteria express reduced levels of Fn-binding proteins FnBPA and FnBPB (55, 56).

Binding to Fn by FnBPs allows the formation of a bridge between bacterial cells and the $\alpha_5\beta_1$ integrin on host cells, and this is sufficient to trigger the bacterial uptake. This mechanism is widely acknowledged to be the main internalization process (57). Additional secondary invasion mechanisms have been reported, including, among others, the internalization mediated by EAP (58), Atl (31), and Lpl (59) proteins. Of note, the invasion assays performed in these studies have been carried out with experimental approaches and conditions (different cell lines and strains, absence/presence of serum) that significantly differ from the invasion pathway described in the present investigation. Thus, for an accurate analysis of the contribution of each mechanism to this multifactorial event, individual internalization processes should be evaluated and compared under identical standardized conditions.

It is unclear why the *isdB* deletion mutant, although it can express several Vn receptors (Fig. 6), does not adhere to and invade host cells (Fig. 7). If we hypothesize that non-IsdB receptors bind to Vn in a way that differs from IsdB, we can speculate that these receptors play a role other than adhesin/invasin in bacterial pathogenesis. For example, capture of Vn mediated by receptors could inhibit both assembly and deposition of the terminal complement complex on the bacterial surface. Alternatively, due to the plasminogen (PLG) binding ability of Vn (60), receptor-bound Vn could enhance plasminogen activation to plasmin, thereby contributing to the degradation of fibrin clots and bacterial spreading into the tissues.

IsdB binds directly to β3-containing integrins and promotes platelet activation and invasion of mammalian cells (48, 61). Consistent with this, we found a low level of invasion of both cell lines by bacteria grown in RPMI in the absence of Vn, suggesting that under these conditions the process can be driven by IsdB binding directly to integrins (48). As with many other MSCRAMMs, IsdB is a multivalent virulence factor and contributes in various ways to the pathogenesis of *S. aureus*. Examples of MSCRAMMs that bind to two or more ligands are clumping factor A (ClfA) that, in addition to binding to fibrinogen (62, 63), binds to complement factor I (64, 65), and clumping factor B (ClfB), another CWA protein that interacts with fibrinogen (66, 67), keratin 10 (68, 69), and loricrin (70, 71). These CWA proteins share similar mechanisms of binding (5). In parallel with this, the structural basis of Hb binding to IsdB NEAT motifs has been elucidated (72, 73). From this perspective, X-ray crystal structure analysis of the recombinant IsdB-binding domain of Vn in complex with NEAT motifs could provide clues about the mechanism and function of this important CWA protein in bacterial colonization of and survival within the host. Purified IsdB elicits antibodies that block heme iron scavenging, provide partial protection against *S. aureus* bacteremia in animal models (74–76), and promote opsonophagocytosis of *S. aureus* (75, 77). Although vaccination of humans with IsdB resulted in failure (78, 79), in light of these new findings, the use of IsdB as a vaccine component warrants further investigation.

Experimental procedures

Bacterial strains and culture conditions

All strains used in this study are listed in Table 1. *S. aureus* cells (48, 80–84) were grown overnight in BHI (VWR International Srl, Milan Italy) or in RPMI 1640 (Sigma-Aldrich, MO, USA) medium at 37 °C with shaking. *L. lactis* cells carrying the expression vector alone (pNZ8037) (85) or harboring the *isdB* gene (pNZ8037::*isdB*) (48) were grown overnight in BHI medium supplemented with chloramphenicol (10 μg/ml) at 30 °C without shaking. Cultures of *L. lactis* were diluted 1:100 in the same medium and allowed to reach exponential phase. Nisin (6.4 ng/ml) was added, and cultures were allowed to grow overnight as described above. In experiments where a defined number of cells were used, bacteria were harvested from the cultures by centrifugation, washed, and suspended in PBS at an optical density at 600 nm (OD_{600}) of 1.0. *Escherichia coli* strain XL1-Blue (Agilent Technologies, CA, USA) transformed with vector pQE30 (Stratagene, La Jolla, CA) or derivatives were grown in Luria agar and Luria broth (VWR) containing 100 μg/ml ampicillin at 37 °C with shaking.

Construction of S. aureus isdB deletion mutant and L. lactis expressing IsdB

Construction of *Lactococcus lactis* expressing IsdB and construction of the *S. aureus isdB* deletion mutant were performed as reported in Table 1.

Plasmid and DNA manipulation

Plasmid DNA (Table 2) was isolated using the WizardPlus SV miniprep kit (Promega, WI, USA), according to the manufacturer's instructions, and transformed into *E. coli* XL1-Blue cells using standard procedures (86). Transformants were screened by restriction analysis and verified by DNA sequencing (Eurofins Genomics, Milan, Italy). Chromosomal DNA was extracted using the bacterial genomic DNA purification kit (Edge Biosystems, MD, USA). Cloning of IsdB $NEAT_1$-$NEAT_2$ (aa residues 48–480) was performed as reported by Miajlovic *et al.* (61). Cloning of IsdB $NEAT_1$ (aa residues 144–270) and IsdB $NEAT_2$ (aa residues 334–458) domains was performed following the NEBuilder® HiFi DNA assembly according to the manufacturer's instructions (New England Biolabs, MA, USA). The primers used to amplify IsdB $NEAT_1$ and IsdB $NEAT_2$ domains and the pQE30 vector (Table S1) were purchased from Integrated DNA Technologies (Leuven, Belgium). DNA

Table 1
Bacterial strains

Bacterial strain	Relevant properties[a]	Reference or source
S. aureus		
LAC *spa*	Strain derivative of LAC* deficient in protein A; constructed by transduction of *spa*::Kan^r by phage 85 into strain LAC*	80
Newman *spa*	Strain containing a null mutation in protein A obtained through transduction from *S. aureus* 8325-4 spa::Kan^r (81) by generalized phage transduction using phage 85	82
8325-4 *spa*	*spa* gene inactivated by substituting part of the *spa* coding sequence for a DNA fragment specifying resistance to ethidium bromide. *In vitro*-constructed *spa*::EtBrr substitution mutation was introduced into the *S. aureus* chromosome by recombinational allele replacement	81
SH1000	Laboratory strain. *rsbU* + derivative of *S. aureus* 8325-4 *rsbU* + derivative of *S. aureus* 8325-4	83
SH1000 *spa*	*spa*::Tc^r transduced from 8325-4 *spa*::Tc^r	84
SH1000 *isdB*	*isdB* gene deleted by allelic exchange	48
L. lactis		
NZ9800 (pNZ8037)	Expression vector with nisin-inducible promoter, Cm^r	85
NZ9800 (pNZ8037::*isdB*)	*isdB* gene cloned in pNZ8037, Cm^r	48
E. coli		
XL1-Blue	*E. coli* cloning host	Stratagene

[a] Cm^r, chloramphenicol resistance; Kan^r, kanamycin resistance; Tc^r, tetracycline resistance.

purification was carried out using the WizardSV gel and PCR clean-up system (Promega).

Expression and purification of recombinant proteins

Recombinant proteins IsdB $NEAT_1$-$NEAT_2$, IsdB-$NEAT_1$, and IsdB-$NEAT_2$ were expressed from pQE30 (Qiagen, Hilden, Germany) in *E. coli* XL1-Blue (Agilent Technologies, CA, USA). Overnight starter cultures were diluted 1:40 in Luria broth containing ampicillin (100 μg/ml) and incubated with shaking until the culture reached the exponential phase (optical density at 600 nm of 0.4–0.6). Recombinant protein expression was induced by the addition of 1 mM (final concentration) isopropyl 1-thio-β-D-galactopyranoside (IPTG) (Inalco, Milan, Italy) to the culture. After 4 h, bacterial cells were harvested by centrifugation and frozen at −80 °C. Cells were resuspended in lysis buffer (50 mM NaH_2PO_4, 300 mM NaCl, pH 8.0) containing 1 mM PMSF (Sigma-Aldrich) as the protease inhibitor and 20 μg/ml DNase (Sigma-Aldrich) and lysed by freezing with liquid nitrogen and subsequent defrosting with warm water. The lysis procedure was repeated twice. The cell debris was removed by centrifugation, and proteins were purified from the supernatants by Ni^{+2}-affinity chromatography on a HiTrap chelating column (GE Healthcare, Buckinghamshire, UK).

Protein purity was assessed by 15% SDS-PAGE and Coomassie brilliant blue staining (Fig. S4*A*). A bicinchoninic acid protein assay (Pierce, Rockford, IL, USA) was used to measure the concentration of purified proteins.

Reagents, proteins, and antibodies

BSA, hemoglobin, protease-free DNase I, skim milk, heparin, chondroitin sulfate, heparan sulfate, cilengitide, lysostaphin, trypsin, sheep anti-Vn polyclonal IgG, and HRP-conjugated rabbit anti-sheep IgG were purchased from Sigma-Aldrich. Human fibronectin (Fn) was purified from plasma by a combination of gelatin- and arginine-Sepharose affinity chromatography (87). The human Fn rabbit antibody was purchased from Pierce. Human fibrinogen (Fbg) was obtained from Calbiochem (Darmstadt, Germany). Collagen (Coll) type I was a generous gift of Professor R. Tenni (Department of Molecular Medicine, Pavia, Italy). Coll type I rabbit antibody was from Merck (Rome, Italy). $\alpha_v\beta_3$ integrin mAb LM609 was from Abcam (Cambridge, UK). Vn mAb 8E6 was purchased from Merck. IsdB and Fbg antibodies were raised in mice by a routine immunization procedure using purified IsdB $NEAT_1$-$NEAT_2$ and Fbg as the antigen, respectively. Rabbit anti-mouse HRP-conjugated secondary antibody was purchased from Dako Cytomation (Glostrup, Denmark).

Human plasma

Normal human plasma was prepared from freshly drawn blood obtained from healthy volunteers with informed consent and permission of the ethical board of the University of Pavia (permit no. 19092013). The study also abides by the Declaration of Helsinki principles. After centrifugation, the plasma fraction was frozen in aliquots and stored at −20 °C.

Isolation of Vn from human plasma

Human Vn was purified from human plasma on a heparin-Sepharose Hi-Trap™ column (GE Healthcare) by following the protocol described by Akiyama (88). The method takes advantage of the observation that the monomeric plasma Vn must be activated or "opened" with 8 M urea before it can bind well to heparin. Thus, the plasma is first depleted of compounds such as fibronectin that bind specifically or nonspecifically to heparin-Sepharose and then treated with 8 M urea to activate the heparin-binding activity of Vn, which is subsequently bound to a heparin affinity column and eluted in a multimeric conformation.

The purity of the isolated Vn was checked with 12.5% (w/v) SDS-PAGE under reducing conditions and Coomassie brilliant blue staining (Fig. S4*B*, *lane 1*) and its concentration quantified with the BCA assay. The multimeric conformation of the isolated Vn was assessed by 12.5% PAGE performed in the absence of SDS (Fig. S4*B*, *lane 2*) and by determination of the reactivity with the mAb 8E6, which preferentially recognizes the multimeric, activated form of Vn (data not shown).

Vn binding to S. aureus

To test binding of Vn, microtiter wells were coated overnight at 37 °C with 100 µl/well of stationary-phase *S. aureus* cells

Table 2
Plasmids

Plasmid	Feature	Marker[a]	Source or reference
pQE30	*E. coli* vector for the expression of hexa-His-tagged recombinant proteins	Amp^r	Qiagen
pQE30::*isdB* $NEAT_1$-$NEAT_2$	pQE30 encoding residues 48–480 of IsdB $NEAT_1$-$NEAT_2$ protein	Amp^r	61
pQE30::rIsdB-NEAT1 (144–270)	pQE30 derivative encoding the NEAT1 domain of IsdB $NEAT_1$-$NEAT_2$ protein from *S. aureus* SH1000	Amp^r	This study
pQE30::rIsdB-NEAT2 (334–458)	pQE30 derivative encoding the NEAT2 domain of IsdB protein from *S. aureus* SH1000	Amp^r	This study

[a] Amp^r, ampicillin resistance.

(OD_{600} of 1) in PBS. The plates were washed with PBS. To block free protein binding sites, the wells were treated for 1 h at 22 °C with BSA (2%, v/v) in PBS. The plates were then incubated for 1 h with increasing concentrations of Vn (up to 250 ng/well). After several washings with PBS, 0.5 μg of anti-Vn sheep IgG in BSA (1%, v/v) was added to the wells and incubated for 90 min.

The plates were washed and then incubated for 1 h with rabbit HRP-conjugated anti-sheep IgG diluted 1:1000. After washing, *o*-phenylenediamine dihydrochloride was added, and the absorbance at 490 nm was determined using an ELISA plate reader (Bio-Rad, CA USA).

Release of cell wall-anchored proteins from S. aureus and detection of Vn-binding activity

Lysostaphin digestion—To release cell wall-anchored proteins from *S. aureus*, bacteria were grown at 37 °C to exponential phase (OD_{600} of 0.4–0.6) or stationary phase, either in RPMI or BHI medium. Cells were harvested by centrifugation at 7000 × *g* at 4 °C for 15 min, washed three times with PBS, and resuspended to an A_{600} of 2.0 in lysis buffer (50 mM Tris-HCl, 20 mM $MgCl_2$, pH 7.5) supplemented with 30% raffinose. Cell wall proteins were solubilized from *S. aureus* by incubation with lysostaphin (200 μg/ml) at 37 °C for 20 min in the presence of protease inhibitors (Complete Mini; Sigma-Aldrich). Protoplasts were recovered by centrifugation at 6000 × *g* for 20 min, and the supernatants were taken as the wall fraction. The supernatant was concentrated by treatment with 20% (v/v) TCA at 4 °C for 30 min. The precipitated proteins were washed twice with ice-cold acetone and dried overnight.

SDS-PAGE and far Western blotting—Proteins released by lysostaphin digestion were boiled for 10 min in sample buffer (0.125 M Tris-HCl, 4% [w/v] SDS, 20% [v/v] glycerol, 10% [v/v] β-mercaptoethanol, 0.002% [w/v] bromphenol blue) and separated by 12.5% (w/v) SDS-PAGE. The gels were stained with Coomassie brilliant blue (Bio-Rad). For Western blotting, proteins were subjected to SDS-PAGE and electroblotted onto a nitrocellulose membrane (GE Healthcare). After blocking with 5% (w/v) skim milk (Sigma-Aldrich) in PBS overnight at 4 °C, the membrane was probed with 2 μg/ml of Vn in PBS for 1 h at 22 °C followed by anti-Vn sheep IgG (1:10,000) and with rabbit HRP-conjugated anti-sheep IgG (1:100). Finally, blots were developed using the ECL Advance Western blotting detection kit (GE Healthcare), and images of the bands were captured by an ImageQuantTM LAS 4000 mini-biomolecular imager (GE Healthcare).

MS analysis

Proteins released by lysostaphin digestion of bacterial cells were separated by 12.5% SDS-PAGE and stained with GelCode blue stain reagent (Thermo Fisher Scientific, Waltham, MA, USA). The band marked by the *red arrow* (Fig. 2) was excised from the gel using a sterile scalpel and protein contained in the gel digested with sequencing grade trypsin (Sigma-Aldrich). Tryptic peptides were mixed with CHCA (alpha-cyano-4-hydroxycinnamic acid) and spotted onto the target plate. The spectra were acquired with a TOF/TOF 5800 system (AB SCIEX, Framingham, MT) using TOF/TOF Series Explorer acquisition software version 4.1.0. MS spectra were recorded in Reflecton positive mode (settings: fixed laser intensity, 3200 units; pulse rate, 400 Hz; total shots/spectrum, 1000; mass range (Da), 1000–4000 *m/z*). Calibration was performed using Peptide calibration Mix4 (LaserBio Laboratory, Sophia-Antipolis Cedex, France). MS-MS spectra of the most intensive MS signals were recorded in MS-MS positive mode (settings: fixed laser intensity, 3500 units; laser pulse rate, 1000 Hz; total shots/spectrum, 5000). MS-MS spectra were analyzed with ProteinPilot™ 5.0 software (AB SCIEX, Framingham, MT, USA) against the UniProtKB database updated 2 August 2016 using the following analysis parameters: (*a*) sample type, identification; (*b*) digestion, trypsin; (*c*) detected protein threshold [unused Protscore (Conf)], >0.05 (10%); (*d*) cysteine alkylation, iodoacetamide; (*e*) ID focus, biological modifications, amino acid substitutions; (*f*) FDR analysis, no; (*g*) taxonomy, no species.

Determination of isdB gene expression by qRT-PCR

Total RNA was extracted from *S. aureus* SH1000 *spa* cells during the exponential (OD_{600} of 0.4–0.6) and stationary phases of growth in BHI and RPMI media. Cells were harvested and total RNA was stabilized with RNeasy Protect bacterial reagent (Qiagen, Hilden, Germany) according to the manufacturer's instructions. Total RNA was extracted using the QuickRNA fungal/bacterial miniprep kit (Zymo Research, CA, USA) by following the manufacturer's recommendations. DNA was removed by DNase I treatment by using the TURBO DNA-free kit (Invitrogen, CA, USA). The RNA concentration was >100 ng/μl, and the A_{260}/A_{280} ratio was >1.8. qRT-PCR was performed with an iTAq Universal SYBR Green one-step kit (Bio-Rad) using 4 ng of RNA in 20-μl volumes carried out on three replicates, and all reactions were performed in 20-μl volumes according to the manufacturer's protocol. The cDNA was analyzed using primers relative to the *isdB* coding sequence (Table S1). The conditions for thermal cycling were 50 °C for 10 min and 95 °C for 1 min, 35–40 cycles with 95 °C for 10 s, and then 60 °C for 10–30 s, followed by a slow increase of temperature by 0.5 °C per cycle to 95 °C, with a continuous measurement of the fluorescence. 4 ng of total RNA from each sample was used in a qRT-PCR experiment performed using a CFX Connect real-

time PCR detection system (Bio-Rad) and an iTAq Universal SYBR Green one-step kit (Bio-Rad). Expression of *isdB* was analyzed using primers isdBF (GCAGGCGTTTTGTCTTTACC) and isdBR (GCCTAGCAAACCAACACCAT). Target gene expression was normalized using the reference gene *rpoC*, which was amplified using primers SAurpoCF (CCGCACCATCTGGTAAGATTAT) and SAurpoCR (GCTGTATCGGCAAGACCTTTA). No-template and no-RT controls were run for each assay, and the specificity of each amplification product was verified using dissociation curve analysis. Standard curves were generated from serial dilutions of chromosomal DNA spanning at least six orders of magnitude. All reactions proceeded with 90% to 110% efficiency. Gene expression analysis was performed using the CFX Manager software (Bio-Rad). Three technical replicates were performed for each experiment.

Determination of expression level of IsdB by Western immunoblotting

Material released by lysostaphin digestion of SH1000 *spa* grown either in BHI and RPMI media to both mid-exponential and stationary phases was subjected to SDS-PAGE and electroblotted onto nitrocellulose membrane, as reported above. After blocking with skim milk, the membrane was sequentially incubated with mouse IsdB antibody (1:5000) and HRP-conjugated rabbit anti-mouse IgG (1:10,000) and developed as described above.

Detection of the Vn-binding activity of IsdB-expressing L. lactis

Release of cell wall-anchored proteins from L. lactis transformants by mutanolysin/lysozyme digestion and far Western blotting—L. lactis was grown to late-exponential phase in BHI broth, washed twice in PBS, and concentrated to an A_{600} of 40 in 1 ml 26% raffinose (Sigma-Aldrich) in 20 mM Tris-HCl, pH 8, 10 mM $MgCl_2$. Cell wall-associated proteins were released by incubation at 37 °C with occasional shaking with 500 U mutanolysin/ml and 200 μg lysozyme/ml in the presence of protease inhibitors (Complete Mini; Sigma-Aldrich). Protoplasts were removed by centrifugation at 6000 × *g* for 20 min, and the supernatant was concentrated as reported above. The interaction of Vn with IsdB was detected by SDS-PAGE followed by far Western blotting as reported above.

Vn binding to L. lactis by ELISA—To investigate the binding of Vn to *L. lactis*, microtiter wells were coated overnight at 37 °C with 100 μl/well of bacterial cell suspensions (OD_{600} of 1) in PBS. After treating with BSA, the plates were incubated with 10 μg/well Vn. Proteins bound to the bacterial cells were detected as described above.

Binding of Vn to IsdB by ELISA

The ability of immobilized recombinant IsdB proteins to bind to soluble Vn was determined using ELISA. Microtiter wells were coated overnight at 4 °C with 0.2 μg/well of the appropriate IsdB protein in 0.1 M sodium carbonate, pH 9.5. The plates were washed with 0.5% (v/v) Tween 20 in PBS (PBST) and then treated for 1 h at 22 °C with BSA (2%, v/v) in PBS. The plates were incubated for 1 h with increasing concentrations of soluble Vn in PBS. Bound Vn was detected by sheep anti-Vn IgG followed by rabbit HRP-conjugated anti-sheep IgG.

To determine the effect of ionic strength on the Vn-IsdB interaction, microtiter wells coated with 200 ng of IsdB $NEAT_1$-$NEAT_2$ were incubated with 500 ng/well of Vn in PBS containing increasing concentrations of NaCl. Complex formation was detected by incubation of the wells with antibodies as described above.

The effect of heparin, chondroitin sulfate, and heparan sulfate on the IsdB $NEAT_1$-$NEAT_2$–Vn interaction was examined by incubating IsdB $NEAT_1$-$NEAT_2$ immobilized onto microtiter plates (0.2 μg/well) with 0.5 μg/well of purified Vn in the presence of increasing concentrations of heparin, chondroitin sulfate, or heparan sulfate. Vn bound to IsdB $NEAT_1$-$NEAT_2$ was detected with antibodies as reported above.

SPR

To estimate the affinity of the interaction between Vn and IsdB $NEAT_1$-$NEAT_2$ or its domain $NEAT_1$ or $NEAT_2$, surface plasmon resonance (SPR) analyses were carried out using a multicycle injection strategy on a multiple flow cell Biacore X100 instrument (GE-Healthcare). IsdB $NEAT_1$-$NEAT_2$, $NEAT_1$, or $NEAT_2$ was covalently immobilized on a dextran matrix CM5 sensor chip surface in three different flow cells by using a protein solution (50 μg/ml in 50 mM sodium acetate buffer, pH 4.5) in a 1:1 dilution with *N*-hydroxysuccinimide and 1-ethyl-3-(3-dimethylaminopropyl) carbodiimide hydrochloride. The excess of the active groups on the dextran matrix was blocked using 1 M ethanolamine, pH 8.5. On the fourth flow cell, the dextran matrix was treated as described above but without any ligand to provide an uncoated reference flow cell. The running buffer used was PBS containing 0.005%, v/v, Tween 20. A 2-fold linear dilution series of Vn, in running buffer, was passed over the ligand at a flow rate of 30 μl/min, and all the sensorgrams were recorded at 22 °C. Assay channel data were subtracted from reference flow cell data. The response units at the steady state were plotted as a function of Vn concentration and fitted to the Langmuir equation to yield the K_D values.

Capture of Vn by S. aureus cells

Stationary *S. aureus* strain SH1000 or the *isdB* mutant (10^8 cells/ml) were mixed with 1 ml of fresh human plasma for 30 min. Bacteria were then harvested by centrifugation, washed with PBS, and treated with the extraction buffer (125 mM Tris-HCl, pH 7.0, containing 2% SDS) for 3 min at 95 °C and then centrifuged at 10,000 × *g* for 3 min. The supernatants were subjected to SDS-PAGE under reducing conditions, and the proteins were transferred to a nitrocellulose membrane. The membrane was sequentially probed for bound Vn with antibodies as described above. The band intensities were quantified with Quantity One software (Bio-Rad).

To analyze the capture of purified Vn by *S. aureus* SH1000 and its *spa* mutant, bacteria (1×10^8cells/ml) were grown either in BHI or RPMI medium in the absence/presence of 1 mM

$FeCl_3$ and then incubated with purified Vn for 60 min. Bacterium-bound proteins were released from the bacterial surface by extraction buffer and subjected to SDS-PAGE and far Western blotting as reported above.

Cell culture infection with staphylococci and blocking experiments

HeLa cells were cultured in 24-well plates until reaching confluence in DMEM supplemented with 10% FBS. HUVECs were cultured as previously reported (89).

24 h before adherence or invasion assays, the medium was removed from each culture and replaced with serum-free medium. Overnight cultures of *S. aureus* SH1000 WT or the *isdB* mutant grown either in BHI or RPMI medium were suspended in DMEM without antibiotics and FBS to 1×10^7 cells/ml and added to the monolayers for 2 h at 37 °C in 5% CO_2. The effect of Vn on bacterial adhesion/invasion to monolayers was tested by pretreating the cells with 25 μg/ml of the protein 1 h prior to addition of the bacteria. To evaluate the role of $\alpha_v\beta_3$ integrin antibody and cilengitide on adhesion, monolayers were pretreated with Vn and then incubated with *S. aureus* SH1000 WT in the presence of 1 μg/ml of $\alpha_v\beta_3$ integrin LM609 mAb or 0.05 μM cilengitide. To determine bacterial adhesion, the infected cells were washed three times with Dulbecco's PBS, lysed, and plated on BHI agar for CFU counts. To enumerate internalized bacteria, the monolayers were further incubated for 2 h before cell lysis in medium supplemented with 100 μg/ml gentamicin to kill extracellular bacteria. Bacterial adherence and invasion are represented as recovered CFU/ml.

Statistical methods

Two group comparisons were performed by Student's *t test*. One-way analysis of variance, followed by Bonferroni's post hoc tests, was exploited for comparison of three or more groups. Analyses were performed using Prism 4.0 (GraphPad). Two-tailed *P* values of 0.05 were considered statistically significant.

Data availability

The MS proteomics data are available via ProteomeXchange with identifier PXD019371 (90). All other data supporting the findings of this study are available within the article and its supporting data.

Acknowledgments—We thank Giulia Barbieri, Department of Biology and Biotechnology, Pavia, Italy, for help with validation of *isdB* gene expression by qRT-PCR and cloning of recombinant fragments of IsdB. We thank PTS (Parco Tecnico Scientifico) of the University of Pavia and Polymerix srl, Pavia, Italy, for technical support with mass spectrometry.

Author contributions—G. P. conceptualization; G. P. resources; G. P., A. P., and M. J. A. data curation; G. P., A. P., and M. J. A. formal analysis; G. P., L. M., T. J. F., and P. S. supervision; G. P. funding acquisition; G. P., A. P., M. J. A., L. M., and P. S. validation; G. P., L. M., and P. S. visualization; G. P., A. P., M. J. A., L. M., and P. S. methodology; G. P., T. J. F., and P. S. writing-original draft; G. P. project administration; G. P., L. M., T. J. F., and P. S. writing-review and editing; A. P. and M. J. A. investigation; L. M. and P. S. software.

Funding and additional information—This research was funded by FFABR 2018, "Fondo di finanziamento per le attività base di ricerca," Ministero dell'Istruzione, dell'Università e della Ricerca (MIUR) to G. P.

Conflict of interest—The authors declare that they have no conflicts of interest with the contents of this article.

Abbreviations—The abbreviations used are: ECM, extracellular matrix; Aaa, autolysin/adhesin from S. aureus; Atl, autolysin; coll, collagen; EAP, extracellular adherence protein; Fn, fibronectin; Fbg, fibrinogen; Isd, iron-regulated surface determinant; Lpl, lipoprotein-like lipoprotein; NEAT, near iron transporter; MSCRAMM, microbial surface component recognizing adhesive matrix molecule; PLG, plasminogen; RU, response unit; SPR, surface plasmon resonance; Vn, vitronectin; OD, optical density; qRT-PCR, , quantitative RT-PCR; CWA, cell wall-anchored; BHI, brain heart infusion; RPMI, Roswell Park Memorial Institute; HUVEC, human umbilical vein endothelial cell.

References

1. Tong, S. Y., Davis, J. S., Eichenberger, E., Holland, T. L., and Fowler, V. G., Jr. (2015) *Staphylococcus aureus* infections: epidemiology, pathophysiology, clinical manifestations, and management. *Clin. Microbiol. Rev.* **28,** 603–661 CrossRef Medline
2. Hynes, R. O., and Naba, A. (2012) Overview of the matrisome—an inventory of extracellular matrix constituents and functions. *Cold Spring Harb. Perspect. Biol.* **4,** a004903 CrossRef Medline
3. Naba, A., Clauser, K. R., Ding, H., Whittaker, C. A., Carr, S. A., and Hynes, R. O. (2016) The extracellular matrix: tools and insights for the "omics" era. *Matrix Biol.* **49,** 10–24 CrossRef Medline
4. Foster, T. J., Geoghegan, J. A., Ganesh, V. K., and Höök, M. (2014) Adhesion, invasion and evasion: the many functions of the surface proteins of *Staphylococcus aureus*. *Nat. Rev. Microbiol.* **12,** 49–62 CrossRef Medline
5. Foster, T. J. (2019) The MSCRAMM family of cell-wall-anchored surface proteins of gram-positive cocci. *Trends Microbiol.* **27,** 927–941 CrossRef Medline
6. Preissner, K. T., and Seiffert, D. (1998) Role of vitronectin and its receptors in haemostasis and vascular remodeling. *Thromb Res.* **89,** 1–21 CrossRef Medline
7. Leavesley, D. I., Kashyap, A. S., Croll, T., Sivaramakrishnan, M., Shokoohmand, A., Hollier, B. G., and Upton, Z. (2013) Vitronectin—master controller or micromanager? *IUBMB Life* **65,** 807–818 CrossRef Medline
8. Boyd, N. A., Bradwell, A. R., and Thompson, R. A. (1993) Quantitation of vitronectin in serum: evaluation of its usefulness in routine clinical practice. *J. Clin. Pathol.* **46,** 1042–1045 CrossRef Medline
9. Chauhan, A. K., and Moore, T. L. (2006) Presence of plasma complement regulatory proteins clusterin (Apo J) and vitronectin (S40) on circulating immune complexes (CIC). *Clin. Exp. Immunol.* **145,** 398–406 CrossRef Medline
10. Berglund, L., Björling, E., Oksvold, P., Fagerberg, L., Asplund, A., Szigyarto, C. A., Persson, A., Ottosson, J., Wernérus, H., Nilsson, P., Lundberg, E., Sivertsson, A., Navani, S., Wester, K., Kampf, C., *et al.* (2008) A genecentric Human Protein Atlas for expression profiles based on antibodies. *Mol. Cell. Proteomics* **7,** 2019–2027 CrossRef Medline
11. Felding-Habermann, B., and Cheresh, D. A. (1993) Vitronectin and its receptors. *Curr. Opin. Cell Biol.* **5,** 864–868 CrossRef Medline

Vitronectin binding to Staphylococcus aureus

12. Schvartz, I., Seger, D., and Shaltiel, S. (1999) Vitronectin. *Int. J. Biochem. Cell Biol.* **31,** 539–544 CrossRef Medline
13. Stanley, K. K. (1986) Homology with hemopexin suggests a possible scavenging function for S-protein/vitronectin. *FEBS Lett.* **199,** 249–253 CrossRef Medline
14. Liang, O. D., Rosenblatt, S., Chhatwal, G. S., and Preissner, K. T. (1997) Identification of novel heparin-binding domains of vitronectin. *FEBS Lett.* **407,** 169–172 CrossRef Medline
15. Seiffert, D. (1995) Evidence that conformational changes upon the transition of the native to the modified form of vitronectin are not limited to the heparin binding domain. *FEBS Lett.* **368,** 155–159 CrossRef
16. Izumi, M., Yamada, K. M., and Hayashi, M. (1989) Vitronectin exists in two structurally and functionally distinct forms in human plasma. *Biochim. Biophys. Acta* **990,** 101–108 CrossRef Medline
17. Stockmann, A., Hess, S., Declerck, P., Timpl, R., and Preissner, K. T. (1993) Multimeric vitronectin. Identification and characterization of conformation-dependent self-association of the adhesive protein. *J. Biol. Chem.* **268,** 22874–22882 Medline
18. Zhuang, P., Li, H., Williams, J. G., Wagner, N. V., Seiffert, D., and Peterson, C. B. (1996) Characterization of the denaturation and renaturation of human plasma vitronectin. II. Investigation into the mechanism of formation of multimers. *J. Biol. Chem.* **271,** 14333–14343 CrossRef Medline
19. Lynn, G. W., Heller, W. T., Mayasundari, A., Minor, K. H., and Peterson, C. B. (2005) A model for the three-dimensional structure of human plasma vitronectin from small-angle scattering measurements. *Biochemistry* **44,** 565–574 CrossRef Medline
20. Seiffert, D., and Smith, J. W. (1997) The cell adhesion domain in plasma vitronectin is cryptic. *J. Biol. Chem.* **272,** 13705–13710 CrossRef Medline
21. Milis, L., Morris, C. A., Sheehan, M. C., Charlesworth, J. A., and Pussell, B. A. (1993) Vitronectin-mediated inhibition of complement: evidence for different binding sites for C5b-7 and C9. *Clin. Exp. Immunol.* **92,** 114–119 CrossRef Medline
22. Attia, A. S., Ram, S., Rice, P. A., and Hansen, E. J. (2006) Binding of vitronectin by the *Moraxella catarrhalis* UspA2 protein interferes with late stages of the complement cascade. *Infect. Immun.* **74,** 1597–1611 CrossRef Medline
23. Singh, B., Su, Y.-C., and Riesbeck, K. (2010) Vitronectin in bacterial pathogenesis: a host protein used in complement escape and cellular invasion. *Mol. Microbiol.* **78,** 545–560 CrossRef Medline
24. Bergmann, S., Lang, A., Rohde, M., Agarwal, V., Rennemeier, C., Grashoff, C., Preissner, K. T., and Hammerschmidt, S. (2009) Integrin-linked kinase is required for vitronectin-mediated internalization of *Streptococcus pneumoniae* by host cells. *J. Cell Sci.* **122,** 256–267 CrossRef Medline
25. Buommino, E., Di Domenico, M., Paoletti, I., Fusco, A., De Gregorio, V., Cozza, V., Rizzo, A., Tufano, M. A., and Donnarumma, G. (2014) AlphaV-Beta5 integrins mediates *Pseudomonas fluorescens* interaction with A549 cells. *Front. Biosci.* **19,** 408–415 CrossRef Medline
26. Heilmann, C., Hussain, M., Peters, G., and Götz, F. (1997) Evidence for autolysin-mediated primary attachment of *Staphylococcus epidermidis* to a polystyrene surface. *Mol. Microbiol.* **24,** 1013–1024 CrossRef Medline
27. Heilmann, C., Thumm, G., Chhatwal, G. S., Hartleib, J., Uekötter, A., and Peters, G. (2003) Identification and characterization of a novel autolysin (Aae) with adhesive properties from *Staphylococcus epidermidis*. *Microbiology* **149,** 2769–2778 CrossRef Medline
28. Hussain, M., Steinbacher, T., Peters, G., Heilmann, C., and Becker, K. (2015) The adhesive properties of the *Staphylococcus lugdunensis* multifunctional autolysin AtlL and its role in biofilm formation and internalization. *Int. J. Med. Microbiol.* **305,** 129–139 CrossRef Medline
29. Zoll, S., Schlag, M., Shkumatov, A. V., Rautenberg, M., Svergun, D. I., Götz, F., and Stehle, T. (2012) Ligand-binding properties and conformational dynamics of autolysin repeat domains in staphylococcal cell wall recognition. *J. Bacteriol.* **194,** 3789–3802 CrossRef Medline
30. Kohler, T. P., Gisch, N., Binsker, U., Schlag, M., Darm, K., Völker, U., Zähringer, U., and Hammerschmidt, S. (2014) Repeating structures of the major staphylococcal autolysin are essential for the interaction with human thrombospondin 1 and vitronectin. *J. Biol. Chem.* **289,** 4070–4082 CrossRef Medline
31. Hirschhausen, N., Schlesier, T., Schmidt, M. A., Götz, F., Peters, G., and Heilmann, C. (2010) A novel staphylococcal internalization mechanism involves the major autolysin Atl and heat shock cognate protein Hsc70 as host cell receptor. *Cell. Microbiol.* **12,** 1746–1764 CrossRef Medline
32. Hammer, N. D., and Skaar, E. P. (2011) Molecular mechanisms of *Staphylococcus aureus* iron acquisition. *Annu. Rev. Microbiol.* **65,** 129–147 CrossRef Medline
33. Mazmanian, S. K., Skaar, E. P., Gaspar, A. H., Humayun, M., Gornicki, P., Jelenska, J., Joachmiak, A., Missiakas, D. A., and Schneewind, O. (2003) Passage of heme-iron across the envelope of *Staphylococcus aureus*. *Science* **299,** 906–909 CrossRef Medline
34. Skaar, E. P., and Schneewind, O. (2004) Iron-regulated surface determinants (Isd) of *Staphylococcus aureus*: stealing iron from heme. *Microbes Infect.* **6,** 390–397 CrossRef Medline
35. Dryla, A., Gelbmann, D., Von Gabain, A., and Nagy, E. (2003) Identification of a novel iron regulated staphylococcal surface protein with haptoglobin-haemoglobin binding activity. *Mol. Microbiol.* **49,** 37–53 CrossRef Medline
36. Clarke, S. R., Wiltshire, M. D., and Foster, S. J. (2004) IsdA of *Staphylococcus aureus* is a broad spectrum, iron-regulated adhesin. *Mol. Microbiol.* **51,** 1509–1519 CrossRef Medline
37. Maresso, A. W., and Schneewind, O. (2006) Iron acquisition and transport in *Staphylococcus aureus*. *Biometals* **19,** 193–203 CrossRef Medline
38. Grigg, J. C., Ukpabi, G., Gaudin, C. F., and Murphy, M. E. (2010) Structural biology of heme binding in the *Staphylococcus aureus* Isd system. *J. Inorg. Biochem.* **104,** 341–348 CrossRef Medline
39. Pilpa, R. M., Fadeev, E. A., Villareal, V. A., Wong, M. L., Phillips, M., and Clubb, R. T. (2006) Solution structure of the NEAT (NEAr Transporter) domain from IsdH/HarA: the human hemoglobin receptor in *Staphylococcus aureus*. *J. Mol. Biol.* **360,** 435–447 CrossRef Medline
40. Zapotoczna, M., Heilbronner, S., Speziale, P., and Foster, T. J. (2012) Iron-regulated surface determinant (Isd) proteins of *Staphylococcus lugdunensis*. *J. Bacteriol.* **194,** 6453–6467 CrossRef Medline
41. Farrand, A. J., Haley, K. P., Lareau, N. M., Heilbronner, S., McLean, J. A., Foster, T., and Skaar, E. P. (2015) An iron-regulated autolysin remodels the cell wall to facilitate heme acquisition in *Staphylococcus lugdunensis*. *Infect. Immun.* **83,** 3578–3589 CrossRef Medline
42. Heilbronner, S., Monk, I. R., Brozyna, J. R., Heinrichs, D. E., Skaar, E. P., Peschel, A., and Foster, T. J. (2016) Competing for iron: duplication and amplification of the isd locus in *Staphylococcus lugdunensis* HKU09-01 provides a competitive advantage to overcome nutritional limitation. *PLoS Genet.* **12,** e1006246 CrossRef
43. Newton, S. M., Klebba, P. E., Raynaud, C., Shao, Y., Jiang, X., Dubail, I., Archer, C., Frehel, C., and Charbit, A. (2005) The svpA-srtB locus of *Listeria monocytogenes*: Fur-mediated iron regulation and effect on virulence. *Mol. Microbiol.* **55,** 927–940 CrossRef Medline
44. Skaar, E. P., Gaspar, A. H., and Schneewind, O. (2006) *Bacillus anthracis* IsdG, a heme-degrading monooxygenase. *J. Bacteriol.* **188,** 1071–1080 CrossRef Medline
45. Andrade, M. A., Ciccarelli, F. D., Perez-Iratxeta, C., and Bork, P. (2002) NEAT: a domain duplicated in genes near the components of a putative Fe^{3+} siderophore transporter from Gram-positive pathogenic bacteria. *Genome Biol.* **3,** research0047-1 CrossRef Medline
46. Clarke, S. R., Mohamed, R., Bian, L., Routh, A. F., Kokai-Kun, J. F., Mond, J. J., Tarkowski, A., and Foster, S. J. (2007) The *Staphylococcus aureus* surface protein IsdA mediates resistance to innate defenses of human skin. *Cell. Host Microbe* **1,** 199–212 CrossRef Medline
47. Visai, L., Yanagisawa, N., Josefsson, E., Tarkowski, A., Pezzali, I., Rooijakkers, S. H. M., Foster, T. J., and Speziale, P. (2009) Immune evasion by *Staphylococcus aureus* conferred by iron-regulated surface determinant protein IsdH. *Microbiology* **155,** 667–679 CrossRef
48. Zapotoczna, M., Jevnikar, Z., Miajlovic, H., Kos, J., and Foster, T. J. (2013) Iron-regulated surface determinant B (IsdB) promotes *Staphylococcus aureus* adherence to and internalization by non-phagocytic human cells. *Cell Microbiol.* **15,** 1026–1041 CrossRef Medline
49. Meenan, N. A., Visai, L., Valtulina, V., Schwarz-Linek, U., Norris, N. C., Gurusiddappa, S., Höök, M., Speziale, P., and Potts, J. R. (2007) The tandem β-zipper model defines high affinity fibronectin-binding repeats

within *Staphylococcus aureus* FnBPA. *J. Biol. Chem.* **282,** 25893–25902 CrossRef Medline

50. Geoghegan, J. A., Ganesh, V. K., Smeds, E., Liang, X., Höök, M., and Foster, T. J. (2010) Molecular characterization of the interaction of staphylococcal microbial surface components recognizing adhesive matrix molecules (MSCRAMM) ClfA and Fbl with fibrinogen. *J. Biol. Chem.* 285, 6208–6216 CrossRef Medline
51. Vazquez, V., Liang, X., Horndahl, J. K., Ganesh, V. K., Smeds, E., Foster, T. J., and Höök, M. (2011) Fibrinogen is a ligand for the *Staphylococcus aureus* microbial surface components recognizing adhesive matrix molecules (MSCRAMM) bone sialoprotein-binding protein (Bbp). *J. Biol. Chem.* 286, 29797–29805 CrossRef Medline
52. Ross, C. L., Liang, X., Liu, Q., Murray, B. E., Höök, M., and Ganesh, V. K. (2012) Targeted protein engineering provides insights into binding mechanism and affinities of bacterial collagen adhesins. *J. Biol. Chem.* **287,** 34856–34865 CrossRef Medline
53. Hare, S. A. (2017) Diverse structural approaches to haem appropriation by pathogenic bacteria. *Biochim. Biophys. Acta Proteins Proteom.* **1865,** 422–433 CrossRef Medline
54. Toida, T., Yoshida, H., Toyoda, H., Koshiishi, I., Imanari, T., Hileman, R. E., Fromm, J. R., and Linhardt, R. J. (1997) Structural differences and the presence of unsubstituted amino groups in heparan sulphates from different tissues and species. *Biochem. J.* **322,** 499–506 CrossRef
55. Johnson, M. B., Pang, B., Gardner, D. J., Niknam-Benia, S., Soundarajan, V., Bramos, A., Perrault, D. P., Banks, K., Lee, G. K., Baker, R. Y., Kim, G. H., Lee, S., Chai, Y., Chen, M., Li, W., Young-Kwong, H., *et al.* (2017) Topical fibronectin improves wound healing of irradiated skin. *Sci. Rep.* **7,** 1–10 CrossRef
56. Saravia-Otten, P., Müller, H. P., and Arvidson, S. (1997) Transcription of Staphylococcus aureus fibronectin-binding protein genes is negatively regulated by agr and an agr-independent mechanism. *J. Bacteriol.* **179,** 5259–5263 CrossRef Medline
57. Josse, J., Laurent, F., and Diot, A. (2017) Staphylococcal adhesion and host cell invasion: fibronectin-binding and other mechanisms. *Front. Microbiol.* **8,** 2433 CrossRef Medline
58. Bur, S., Preissner, K. T., Herrmann, M., and Bischoff, M. (2013) The *Staphylococcus aureus* extracellular adherence protein promotes bacterial internalization by keratinocytes independent of fibronectin-binding proteins. *J. Invest. Dermatol.* **133,** 2004–2012 CrossRef Medline
59. Tribelli, P. M., Luqman, A., Nguyen, M. T., Madlung, J., Fan, S. H., Macek, B., Sass, P., Bitschar, K., Schittek, B., Kretschmer, D., and Götz, F. (2020) *Staphylococcus aureus* Lpl protein triggers human host cell invasion via activation of Hsp90 receptor. *Cell. Microbiol.* **22,** e13111 CrossRef Medline
60. Kost, C., Stüber, W., Ehrlich, H. J., Pannekoek, H., and Preissner, K. T. (1992) Mapping of binding sites for heparin, plasminogen activator inhibitor-1, and plasminogen to vitronectin's heparin-binding region reveals a novel vitronectin-dependent feedback mechanism for the control of plasmin formation. *J. Biol. Chem.* **267,** 12098–12105 Medline
61. Miajlovic, H., Zapotoczna, M., Geoghegan, J. A., Kerrigan, S. W., Speziale, P., and Foster, T. J. (2010) Direct interaction of iron-regulated surface determinant IsdB of *Staphylococcus aureus* with the GPIIb/IIIa receptor on platelets. *Microbiology* **156,** 920–928 CrossRef Medline
62. McDevitt, D., Nanavaty, T., House-Pompeo, K., Bell, E., Turner, N., Mcintire, L., Foster, T., and Höök, M. (1997) Characterization of the interaction between the *Staphylococcus Aureus* clumping factor (ClfA) and fibrinogen. *Eur. J. Biochem.* **247,** 416–424 CrossRef Medline
63. Ganesh, V. K., Rivera, J. J., Smeds, E., Ko, Y. P., Bowden, M. G., Wann, E. R., Gurusiddappa, S., Fitzgerald, J. R., and Höök, M. (2008) A structural model of the *Staphylococcus aureus* ClfA-fibrinogen interaction opens new avenues for the design of anti-staphylococcal therapeutics. *PLoS Pathog.* 4, e1000226 CrossRef Medline
64. Hair, P. S., Ward, M. D., Semmes, O. J., Foster, T. J., and Cunnion, K. M. (2008) *Staphylococcus aureus* clumping factor A binds to complement regulator factor I and increases factor I cleavage of C3b. *J. Infect. Dis.* **198,** 125–133 CrossRef Medline
65. Hair, P. S., Echague, C. G., Sholl, A. M., Watkins, J. A., Geoghegan, J. A., Foster, T. J., and Cunnion, K. M. (2010) Clumping factor A interaction with complement factor I increases C3b cleavage on the bacterial surface of *Staphylococcus aureus* and decreases complement-mediated phagocytosis. *Infect. Immun.* **78,** 1717–1727 CrossRef Medline
66. Ní Eidhin, D., Perkins, S., Francois, P., Vaudaux, P., Höök, M., and Foster, T. J. (1998) Clumping factor B (ClfB), a new surface-located fibrinogen-binding adhesin of *Staphylococcus aureus*. *Mol. Microbiol.* **30,** 245–257 CrossRef Medline
67. Perkins, S., Walsh, E. J., Deivanayagam, C. C., Narayana, S. V., Foster, T. J., and Höök, M. (2001) Structural organization of the fibrinogen-binding region of the clumping factor B MSCRAMM of *Staphylococcus aureus*. *J. Biol. Chem.* **276,** 44721–44728 CrossRef Medline
68. O'Brien, L. M., Walsh, E. J., Massey, R. C., Peacock, S. J., and Foster, T. J. (2002) *Staphylococcus aureus* clumping factor B (ClfB) promotes adherence to human type I cytokeratin 10: implications for nasal colonization. *Cell. Microbiol.* **4,** 759–770 CrossRef Medline
69. Walsh, E. J., O'Brien, L. M., Liang, X., Hook, M., and Foster, T. J. (2004) Clumping factor B, a fibrinogen-binding MSCRAMM (microbial surface components recognizing adhesive matrix molecules) adhesin of *Staphylococcus aureus*, also binds to the tail region of type I cytokeratin 10. *J. Biol. Chem.* **279,** 50691–50699 CrossRef Medline
70. Mulcahy, M. E., Geoghegan, J. A., Monk, I. R., O'Keeffe, K. M., Walsh, E. J., Foster, T. J., and McLoughlin, R. M. (2012) Nasal colonisation by *Staphylococcus aureus* depends upon clumping factor B binding to the squamous epithelial cell envelope protein loricrin. *PLoS Pathog.* **8,** e1003092 CrossRef Medline
71. Vitry, P., Valotteau, C., Feuillie, C., Bernard, S., Alsteens, D., Geoghegan, J. A., and Dufrêne, Y. F. (2017) Force-induced strengthening of the interaction between Staphylococcus aureus clumping factor B and loricrin. *mBio* **8,** e01748-17 CrossRef
72. Bowden, C., Chan, A., Li, E., Arrieta, A. L., Eltis, L. D., and Murphy, M. (2018) Structure-function analyses reveal key features in *Staphylococcus aureus* IsdB-associated unfolding of the heme-binding pocket of human hemoglobin. *J. Biol. Chem.* **293,** 177–190 CrossRef Medline
73. Gianquinto, E., Moscetti, I., De Bei, O., Campanini, B., Marchetti, M., Luque, F. J., Cannistraro, S., Ronda, L., Bizzarri, A. R., Spyrakis, F., and Bettati, S. (2019) Interaction of human hemoglobin and semi-hemoglobins with the *Staphylococcus aureus* hemophore IsdB: a kinetic and mechanistic insight. *Sci. Rep.* **9,** 18629 CrossRef Medline
74. Stranger-Jones, Y. K., Bae, T., and Schneewind, O. (2006) Vaccine assembly from surface proteins of *Staphylococcus aureus*. *Proc. Natl. Acad. Sci. USA* **103,** 16942–16947 CrossRef Medline
75. Kuklin, N. A., Clark, D. J., Secore, S., Cook, J., Cope, L. D., McNeely, T., Noble, L., Brown, M. J., Zorman, J. K., Wang, X. M., Pancari, G., Fan, H., Isett, K., Burgess, B., Bryan, J., *et al.* (2006) A novel *Staphylococcus aureus* vaccine: iron surface determinant B induces rapid antibody responses in rhesus macaques and specific increased survival in a murine *S. aureus* sepsis model. *Infect. Immun.* **74,** 2215–2223 CrossRef Medline
76. Kim, H. K., DeDent, A., Cheng, A. G., McAdow, M., Bagnoli, F., Missiakas, D. M., and Schneewind, O. (2010) IsdA and IsdB antibodies protect mice against *Staphylococcus aureus* abscess formation and lethal challenge. *Vaccine* **28,** 6382–6392 CrossRef Medline
77. Brown, M., Kowalski, R., Zorman, J., Wang, X. M., Towne, V., Zhao, Q., Secore, S., Finnefrock, A. C., Ebert, T., Pancari, G., Isett, K., Zhang, Y., Anderson, A. S., Montgomery, D., Cope, L., *et al.* (2009) Selection and characterization of murine monoclonal antibodies to *Staphylococcus aureus* iron-regulated surface determinant B with functional activity in vitro and in vivo. *Clin. Vaccine Immunol.* **16,** 1095–1104 CrossRef
78. Fowler, V. G., Allen, K. B., Moreira, E. D., Moustafa, M., Isgro, F., Boucher, H. W., Corey, G. R., Carmeli, Y., Betts, R., Hartzel, J. S., Chan, I. S., McNeely, T. B., Kartsonis, N. A., Guris, D., Onorato, M. T., *et al.* (2013) Effect of an investigational vaccine for preventing *Staphylococcus aureus* infections after cardiothoracic surgery: a randomized trial. *JAMA* **309,** 1368–1378 CrossRef Medline
79. Bagnoli, F., Bertholet, S., and Grandi, G. (2012) Inferring reasons for the failure of *Staphylococcus aureus* vaccines in clinical trials. *Front. Cell. Infect. Microbiol.* **2,** 16 CrossRef Medline
80. O'Halloran, D. P., Wynne, K., and Geoghegan, J. A. (2015) Protein A is released into the *Staphylococcus aureus* culture supernatant with an

unprocessed sorting signal. *Infect. Immun.* **83,** 1598–1609 CrossRef Medline

81. Patel, A. H., Nowlan, P., Weavers, E. D., and Foster, T. (1987) Virulence of protein A-deficient and alpha-toxin-deficient mutants of *Staphylococcus aureus* isolated by allele replacement. *Infect. Immun.* **55,** 3103–3110 CrossRef Medline
82. Higgins, J., Loughman, A., Van Kessel, K. P., Van Strijp, J. A., and Foster, T. J. (2006) Clumping factor A of *Staphylococcus aureus* inhibits phagocytosis by human polymorphonuclear leucocytes. *FEMS Microbiol. Lett.* **258,** 290–296 CrossRef Medline
83. Horsburgh, M. J., Aish, J. L., White, I. J., Shaw, L., Lithgow, J. K., and Foster, S. J. (2002) σB modulates virulence determinant expression and stress resistance: characterization of a functional rsbU strain derived from *Staphylococcus aureus* 8325-4. *J. Bacteriol.* **184,** 5457–5467 CrossRef Medline
84. Claro, T., Widaa, A., O'Seaghdha, M., Miajlovic, H., Foster, T. J., O'Brien, F. J., and Kerrigan, S. W. (2011) *Staphylococcus aureus* Protein A Binds to Osteoblasts and Triggers Signals That Weaken Bone in Osteomyelitis. *PLoS ONE* **6,** e18748 CrossRef Medline
85. De Ruyter, P. G., Kuipers, O. P., and De Vos, W. M. (1996) Controlled gene expression systems for *Lactococcus lactis* with the food-grade inducer nisin. *Appl. Environ. Microbiol.* **62,** 3662–3667 CrossRef Medline
86. Sambrook, J., Fritsch, E. F., and Maniatis, T. (1989) *Molecular cloning: a laboratory manual*, 2nd ed. Cold Spring Harbor Laboratory, Cold Spring Harbor, NY
87. Speziale, P., Visai, L., Rindi, S., and Di Poto, A. (2008) Purification of human plasma fibronectin using immobilized gelatin and Arg affinity chromatography. *Nat. Protoc.* **3,** 525–533 CrossRef Medline
88. Akiyama, S. K. (2013) Purification of vitronectin. *Curr. Protoc. Cell Biol.* **60,** Unit 10.6 CrossRef Medline
89. Viela, F., Prystopiuk, V., Leprince, A., Mahillon, J., Speziale, P., Pietrocola, G., and Dufrêne, Y. F. (2019) Binding of *Staphylococcus aureus* protein A to von Willebrand factor is regulated by mechanical force. *mBio* **10,** e00555-19 CrossRef
90. Perez-Riverol, Y., Csordas, A., Bai, J., Bernal-Llinares, M., Hewapathirana, S., Kundu, D. J., Inuganti, A., Griss, J., Mayer, G., Eisenacher, M., Pérez, E., Uszkoreit, J., Pfeuffer, J., Sachsenberg, T., Yilmaz, S., *et al.* (2019) The PRIDE database and related tools and resources in 2019: improving support for quantification data. *Nucleic Acids Res.* **47,** D442–D450 CrossRef Medline